Global Journal of Pure and Applied Mathematics (GJPAM) ISSN 0973-1768 Volume 12,Number 4 (2016)

Detecting misbehaving nodes in MANET using EA3ACK algorithm

K. Prabu
Department of Computer Science,
Thiruvalluvar University Constituent College,
Tittagudi, Tamilnadu, India – 606 106,
E-mail: kprabu.phd@gmail.com

*K. Thamizhmaran**
Department of Electrical Engineering,
Annamalai University,
Chidambaram, Tamilnadu, India - 608 002,
E-mail: tamil10_happy@rediff.com

Abstract **— Wireless networking is an emerging technology that allows users to access information and services anywhere regardless of their geographic areas over the past few years, with the trend of mobile computing. Mobile Adhoc Network (MANET) has become one of the most important wireless communication mechanisms among all, unlike traditional network. MANET does not have a fixed infrastructure. Every single node in the MANET works as both receiver and transmitter. Each node directly communicates with others when they are both within their communication ranges. All nodes work as routers and take path in discovery and maintenance of routes to other nodes in the network. In this paper proposed a new routing algorithm named Enhanced Adaptive 3 Acknowledgement (EA3ACK) using EAACK with hybrid cryptography is (MARS4) specially designed for MANET. This hybrid cryptography a two key method namely MARS4 which is a combination of RSA and MAJE4 employed to reduce the routing overhead. The proposed EA3ACK algorithm provides efficient secured transmission compare to existing EAACK algorithm.**

Keywords: EA3ACK, IDS, MARS4, Cryptography, Security, MANET, Throughput.

I. INTRODUCTION

Mobile Ad-hoc Networks (MANET) represent a new form of communication consisting of mobile wireless terminals where it is an infrastructure less IP based network of mobile and wireless machine nodes connected with radio. As shown in the fig.1.1 nodes of a MANET do not have a centralized administration mechanism. It is known for its routable network properties where each node act as a “router” to forward the traffic to other specified node in the network. MANET were wireless multi-hop networks without any fixed infrastructure and centralized administration, in contrast to today’s wireless communications, which is based on fixed, pre-established infrastructure.

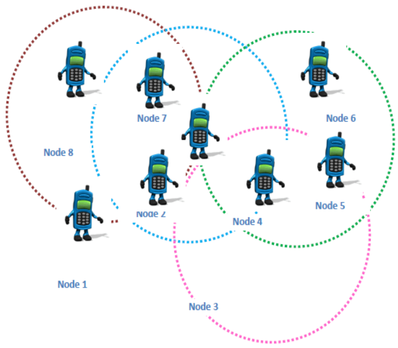

Figure 1.1 Mobile Adhoc Networks

All networking functions, such as determining the network topology, multiple accesses, and routing of data over the most appropriate paths, must be performed in a distributed way. These tasks are particularly challenging due to the limited communication bandwidth available in the wireless channel.

II. BACKGROUND

2.1 Routing Protocol

A routing protocol specifies how routers communicate with each other, disseminating information that enables them to select routes between any two nodes on a computer network. Routing algorithms determine the specific choice of route. Each router has a priori knowledge only of networks attached to it directly. A routing protocol shares this information first among immediate neighbors, and then throughout the network. The two main types of routing: Static routing and dynamic routing.

Generally, there are two different stages in routing; they are route discovery and data forwarding. In route discovery, route to a destination will be discovered by broadcasting the query. Then, once the route has been established, data forwarding will be initiated and sent via the routes that have been determined. The power consumption, route relaying load, battery life, and

*Corresponding author.
This paper was presented by the second author in the National Conference on AMASE-2016 conducted in Department of Mathematics, University College of Engineering Pattukkottai, Thanjavur, Tamil Nadu, India, on 22nd January 2016.

reduction in the frequency of sending control messages, optimization of size of control headers and efficient route reconfiguration should be considered when developing a routing protocol.

Proactive approach every node generates routing information periodically to maintain and construct routing tables even if there is no data traffic to deliver. Information contained in routing tables, is updated when the topology changes. Thus, every node maintains routing information to every other node in the network. Proactive routing protocols may use either hop-by-hop or source routing strategies to forward data traffic. The performance of the network degrades due to the exchange of control traffic messages, but the packets experience less latency because the routes are always constructed and maintained for eventual data traffic. Proactive protocols work better in networks with low mobility.

Reactive routing protocols discovery and maintenance of routes are delayed until necessary. When a given node needs to send a packet to any other node in the network, the sender node initiates the process to construct a path to reach the destination. To discover a route, a node floods the route request messages through the network. When a node with a route to the destination (or the destination itself) is reached, a route replay message is sent back to the source node. Reactive protocols can be classified into two categories: source routing and hop-by-hop routing.

Hybrid routing protocol is a combination of proactive and reactive routing protocol. Zone-based Hierarchical Link State (ZHLS) is a typical example. According to ZHLS routing protocol, the entire network is divided into several non-overlapping zones. If the source and destination nodes are within the same zone, ZHLS works as a passive routing protocol.

2.2 Cryptography

Cryptography technique has a long and fascinating history. Completed in 1963, the Kahn's book covers the most important history of cryptography technique. From 4,000 years ago by the Egyptians, to the two world wars in the twentieth century, the cryptography technique has been widely served as a tool to protect secrets. With the development of Internet, the security of communication has become more important than ever. Many researchers and scientists have contributed their countless time and efforts in this area since then. Among all of them, it is believed the most significant development was in 1976 when Diffie and Hellman published the paper "New Directions in Cryptography", in which they first introduced the concept of public-key cryptography. Although no practical implementation was provided along with the paper, the idea had since then attracted various attentions and interests. Two years later, in 1978, Rivest, Shamir and Adleman proposed the first practical public-key encryption and signature scheme, which we now referred to as RSA. Later after that, the 1980s has witnessed much more advancement in this area but none of them rendered RSA as insecure. EIGamal in 1985, found another class of powerful and practical public-key schemes. These are also based on the discrete logarithm problem. The Digital Signature Standard (DSA) scheme announced in 1994 was developed based on the EIGamal public key scheme. Cryptographic techniques are typically divided into two generic types: symmetric-key and public-key.

III. PROPOSED SYSTEM

A) RSA

RSA is computationally easy for a party B to generate the key pair (Public key KSb, Private key KRb). It is computationally easy for a sender A, knowing the public key KSb and the message to be encrypted M, to generate the cipher text C=EKSb (M). It is computationally easy for the receiver B, to decrypt the resulting cipher text using the private key to recover the original message *M=DKRb(C) =DKRb [EKSb (M)]*. It is also computationally infeasible for an opponent, knowing the public key KSb, and a cipher text C, to recover the original message M. The encryption and decryption functions can be applied in either order. M=DKRb [EKSb(M)]= DKSb[EKRb(M)]

- Choose two higher prime numbers P and Q, and find N=P*Q.
- Select the encryption (public key) E & Select the decryption (private key) D. the following equation is true: (D*E) mod (P-1) * (Q-1) = 1
- Encrypt the PT to CT = PTE mod N
- Send CT to the receiver.

B) MAJE4

The same as that for a One-time-Pad cipher, which encrypts by XOR' of the plain text with a random key. But for a One-Time-Pad Cipher it is required to have a key of the same size as the plain text, which makes it impractical for most applications. While the stream ciphers require only a short random key.

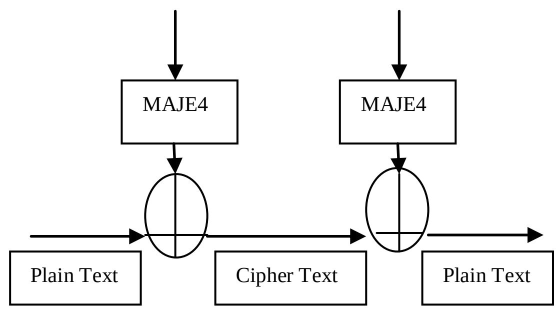

Figure 3.1 MAJE4

C) MARS4

Now MAJE4 and RSA can be combined to have MARS4 as a very efficient security solution. Assume that A is the sender of a message and B is the receiver. MARS4 is designed to work as follows.

1) A encrypts the original message (PT) with the help of MAJE4 and the symmetric key (K1) and forms the cipher text (CT).
2) Encrypt K1 (CT) to (K2) of B using RSA.
3) B now uses the RSA algorithm and its private key (K3) to decrypt K1.
4) Then B uses K1 and the MAJE4 algorithm to decrypt the CT for the original plain text (PT).

IV. METHODOLOGY

FLOW DIAGRAM

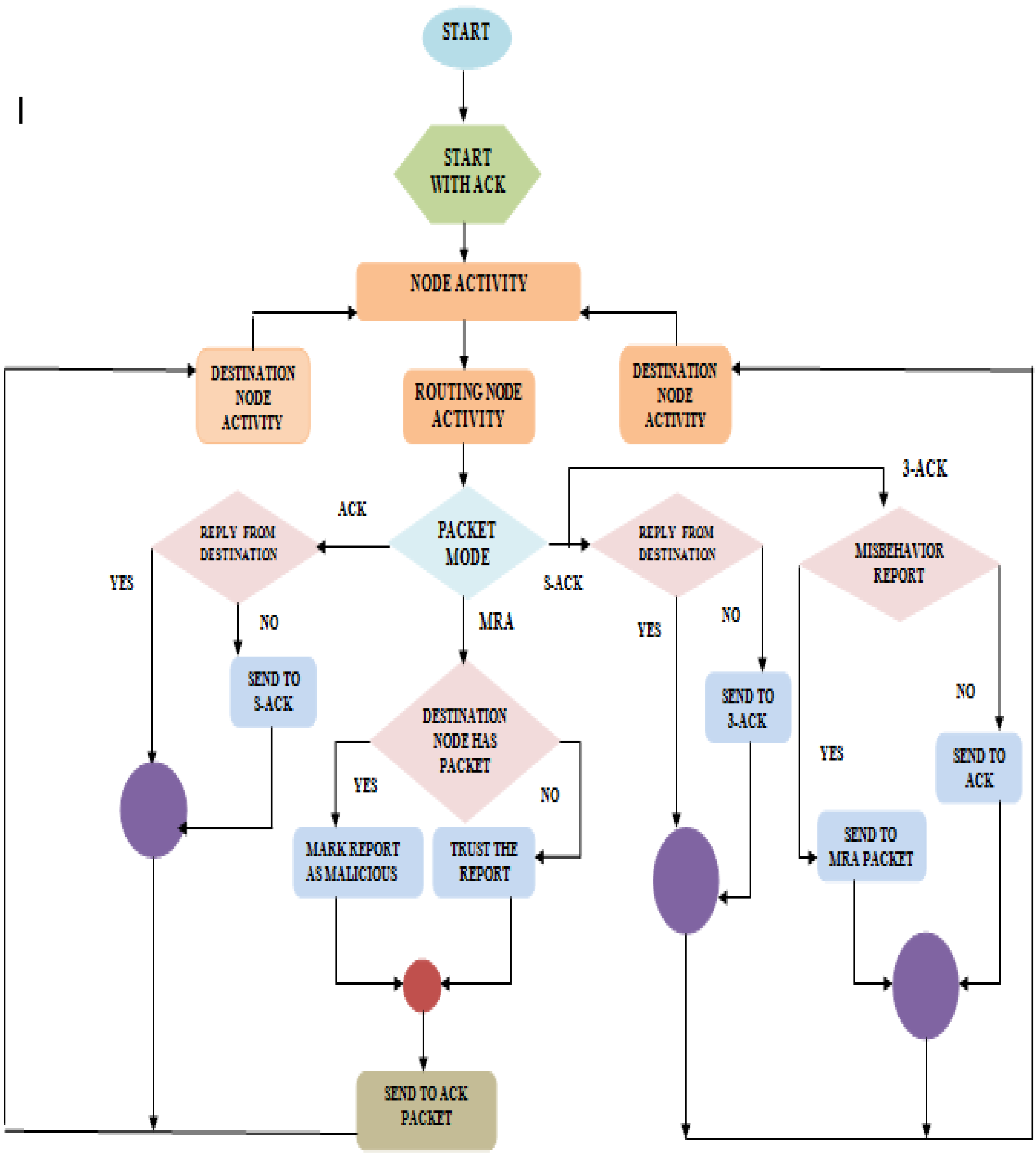

Figure 4.1 Flow diagrams for EA3ACK

In this section, we describe our proposed EA3ACK scheme in detail. The approach described in this research paper is based on previous work (2), where the backbone of EA3ACK was proposed and evaluated through implementation. We extend it with the introduction of MARS4 Hybrid cryptography to prevent the attacker from forging acknowledgment packets. EA3ACK is consisted of four major parts, namely, ACK, secure ACK (S-ACK), 3-ACK and misbehaviour report authentication (MRA). In order to distinguish different packet types in different schemes In EA3ACK, we use 3 b of the different types of packets. Details are listed in Table 5.1 Fig. 5.1presents a flowchart describing the EA3ACK scheme. Please note that, in our proposed scheme, we assume that the link between each node in the network is bidirectional. Furthermore, for each communication process, both the source node and the destination node are not malicious. Unless specified, all acknowledgment packets described in this research are required to two different keys (public and private) by its one key for sender and verified another key by its receiver.

V. RESULT AND DISSCUSSION

Simulation Configurations

In this section, we evaluate the performance of routing protocol of MANETs in an open environment. The simulations were carried out using network simulator (NS 2.34). We are simulating the mobile ad hoc routing protocols using this simulator by varying the number of nodes. The IEEE 802.11 distributed coordination function (DCF) is used as the medium access control protocol. The traffic sources are UDP. Initially nodes were placed at certain specific locations. The simulation parameters are specified in Table 5.1.

Parameters	Values
Simulation area	1,000 m * 1,000 m
Number of nodes	60
Average speed of nodes	0–25 meter/second
Mobility model	Random waypoint
Number of packet senders	40
Transmission range	250 m
Constant bit rate	2 (packets/second)
Packet size	512 bytes
Node beacon interval	0.5 (seconds)
MAC protocol	802.11 DCF
Initial energy/node	100 joules
Antenna model	Omni directional
Simulation time	500 sec

Table 5.1 Simulation parameters

In this section, malicious nodes drop all the packets that pass through it. Fig 5.1 and Table 5.1 shows the simulation results that are based on PDR.

Packet Delivery Ratio					
Routing / Malicious Node	**0%**	**10%**	**20%**	**30%**	**40%**
DSR	1	0.82	0.73	0.68	0.66
WATCHDOG	1	0.83	0.77	0.70	0.67
AACK	1	0.96	0.96	0.93	0.92
TWOACK	1	0.97	0.96	0.92	0.92
THREEACK	1	0.96.5	0.96	0.91	0.92
EAACK(RSA)	1	0.96	0.97	0.92	0.92
EEACK(DSA)	1	0.96	0.97	0.93	0.91
EA3ACK	1	0.97	0.97	0.96	0.95
Routing Overhead					
Routing / Malicious Node	**0%**	**10%**	**20%**	**30%**	**40%**
DSR	0.02	0.023	0.023	0.022	0.02
WATCHDOG	0.02	0.025	0.025	0.023	0.023
AACK	0.03	0.23	0.32	0.33	0.39
TWOACK	0.18	0.4	0.43	0.42	0.51
THREEACK	0.19	0.43	0.45	0.42	0.50
EAACK(RSA)	0.16	0.3	0.37	0.47	0.61
EEACK(DSA)	0.15	0.28	0.35	0.44	0.58
EA3ACK	0.14	0.26.5	0.32	0.40	0.55
Throughput					
Routing / Malicious Node	**0%**	**10%**	**20%**	**30%**	**40%**
EAACK(RSA)	0	0.25	0.38	0.50	0.54
EEACK(DSA)	0	0.27	0.40	0.53	0.57
EA3ACK	0	0.37	0.50	0.63	0.58
Energy					
Routing / Malicious Node	**0%**	**10%**	**20%**	**30%**	**40%**
EEACK	1	0.95	0.89	0.80	0.76
EA3ACK	1	0.92	0.84	0.76	0.72

Table 5.2 Performance Comparison.

In Fig. 5.1 and Table 5.2 we observe that all acknowledgment-based IDSs our proposed scheme EA3ACK surpassed EAACK performance by above 95% when there are 30% and 40% of malicious nodes in the network. From the results, we conclude that acknowledgment-based schemes, EA3ACK, are able to detect misbehaviors with the presence of receiver collision, limited transmission power and partial dropping.

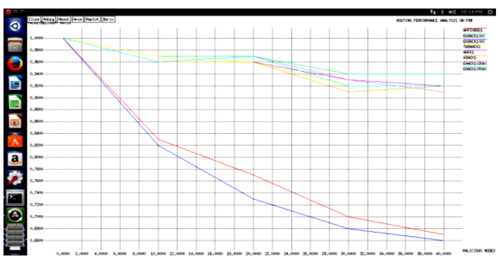

Figure 5.1 PDR vs. Malicious Nodes

Simulation results are shows that fig.5.2 and table 5.2. We observe that DSR scheme achieve the best performance, as they do not require acknowledgment scheme to detect misbehaviors. For the rest of the IDSs, EA3ACK has the lowest overhead when there are 10% to 30%. Although EA3ACK requires public and private key at all acknowledgment process.

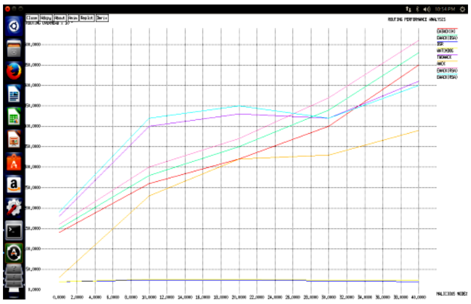

Figure 5.2 Routing Performance vs. Malicious Nodes

Simulation results are shows that fig 5.3 and table 5.2 shows that comparison of the EAACK with corresponding RSA and DSA algorithm since on along with EA3ACK where it shows the throughput is increase with increase in the number of malicious nodes on while 30% and 40%.

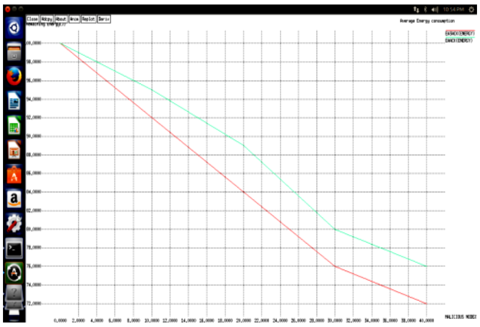

Figure 5.3 Average Energy Consumption vs. Malicious Nodes

Simulation results are shows that fig 5.4 and table 5.2 shows that our proposed EA3ACK deceasing the remaining energy with increasing malicious nodes compare to the existing algorithm.

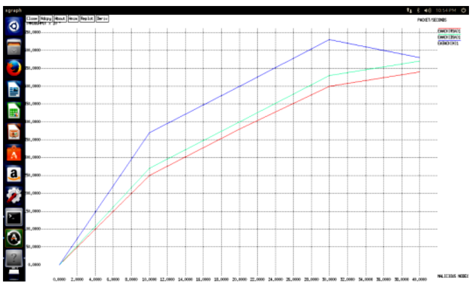

Figure 5.4 Packer per/sec vs. Malicious Nodes

Simulation results are shows that the all above figure and Table shows that the comparison of the EAACK with corresponding RSA and DSA algorithm since on along with EA3ACK with hybrid cryptography where it shows the throughput is increase with increase in the number of malicious nodes on while.

VI. CONCLUSION

In the recent research year there has been a lot of interest within the field of cryptography in MANET. Because during the transmission drop (or) attack the packet without the acknowledgement. So acknowledge based transmission is very safe and high security. The motivation for our work is to develop an Intrusion Detection System (IDS) scheme able to detect misbehaving node in case of collision, limited transmission power and false misbehavior report. We demonstrated the performance of our proposed scheme named EA3ACK with hybrid cryptography using EAACK through an evaluation in the network simulator environment. This EA3ACK provide better performance compare to existing EAACK routing protocol and also improved packet delivery ration, improved throughput, and reduced routing overhead compare to existing EAACK routing protocol. Finally EA3ACK shows that the result of proposed scheme is effective in detecting misbehaving nodes in MANET.

REFERENCES

[1] Nan Kang, Elhadi et.al "Detecting Misbehaving Nodes in MANETs", International conference on Advanced Information Networking and Applications, pp.488-494, 2010.

[2] Prabu, K. and Subramani, A. (2012) 'Performance comparison of routing protocol in MANET', Int. J. of Adv. Research in Com. Sci. and Soft Engg. (IJARCSSE), Vol. 2, No. 9, pp.388–392, 2012.

[3] Elhadi, M. Shakshuki, Nan Kang and Tarek R. Sheltami "EAACK—A Secure Intrusion-Detection System for MANETs", IEEE Trans on industrial electronics, vol. 60, no. 3, pp.1089-1098, 2013.

[4] Abdulsalam Basabaaa, et al, "Implementation of A3ACKs intrusion detection system under various mobility speeds", 5th International Conf. on Ambient Systems, Networks and Technologies, pp.571-578, 2014.

[5] Sheena Mathew and K.Paulose Jacob "A Novel Fast Hybrid Cryptographic System: MARS4", IEEE, vol.2, no.4, 2006.

[6] S. Subasree and N. K. Sakthivel "Design Of a New Security Protocol Using Hybrid Cryptography Algorithms", IJRRAS vol.2 no.2, pp., 2010.

[7] Nidal Nasser and Yunfeng Chen "Enhanced Intrusion Detection System for Discovering Malicious Nodes n in Mobile Ad hoc Networks", IEEE Comm Society, 2007.

[8] K. Liu, J. Deng, P. K. Varshney et al, "An acknowledgment-based approach for the detection of routing misbehaviour in MANETs," IEEE Trans. Mobile Comput., vol.6, no.5, pp.536–550, 2007.

[9] Balakrishnan, K.; Jing Deng; Varshney, V.K., "TWOACK: preventing selfishness in mobile ad hoc networks," Wireless Communications and Networking Conference, vol.4, no.10, pp. 2137-2142, 2005.

[10] Al-Roubaiey, A.; Sheltami, T.; et al "AACK: Adaptive Acknowledgment Intrusion Detection for MANET with

Node Detection Enhancement," 24th IEEE Conf. on AINA, pp.634-640, 2010.

[11] D. Johnson, D.A. Maltz and J. Broch, "The dynamic source routing protocol for mobile ad hoc networks", Internet Draft, Mobile Ad Hoc Network (MANET) Working Group, IETF, 1998.

[12] Hao Yang, Haiyun Luo, Fan Ye, Songwu Lu, Lixia Zhang, "Security in Mobile Ad hoc Networks: Challenges and Solutions", UCLA Computer Science Department, 2010.

[13] Jongoh Choi, Si-Ho Cha, GunWoo Park, and JooSeok Song. "Malicious Nodes Detection in AODV-Based Mobile Ad Hoc Networks", GESTS Trans. Comp. Science and Engr., Vol.18, No.1 pp.49-55, 2005.

[14] A Rajaram, and S. Palaniswami, "Detecting Malicious Node in MANET Using Trust Based Cross-Layer Security Protocol" (IJCSIT) Int. Journal of Com Sci and Information Technologies, Vol.1, no.2, pp., 2010.

[15] Aishwarya Sagar Anand Ukey, Meenu Chawla, "Detection of Packet Dropping Attack Using Improved Acknowledgement Based Scheme in MANET", IJCSI, Vol.7, No.4 (1), 2010.

Global Journal of Pure and Applied Mathematics (GJPAM) ISSN 0973-1768 Volume 12,Number 4 (2016)

Analytical solutions of coupled non-linear reaction diffusion equations for substrate and Hydrogen ion concentrations in immobilized enzyme system

*M. Veeramuni**, [1]
Department of Mathematics,
The Madura College,
Madurai 625 011, Tamilnadu, India.
Email: mmv.muni@gmail.com

N. Mehala[2]
Department of Mathematics,
Kamaraj College of Engineering & Technology,
Madurai, Tamilnadu, India.
Email: mehalapaviammu@gmail.com

D. Pandiaraja[3],
National Centre of Excellence,
Statistical and Mathematical modeling on
Bio-Resource management,
PG and Research Department of Mathematics,
Thiagarajar College,
Madurai, Tamilnadu, India
Email: pandiaraja.d@gmail.com

L. Rajendran[4]
Department of Mathematics,
Sethu Institute of Technology,
Kariapatti, Tamil Nadu, India.
Email: dr.rajendran.l@gmail.com

***Abstract*—A mathematical model describing the effects of electrostatic interaction with reaction generated pH change on the kinetics of immobilized enzyme has been discussed for both large and small pore cases. This model contains the system of non-linear reaction diffusion equations. Approximate analytical solutions of non-linear reaction diffusion equations containing non-linear terms related to rate of reaction mechanism are solved using Adomian decomposition method. The relevant analytical expressions for the substrate and hydrogen ion concentration profiles are discussed in terms of dimensionless reaction diffusion parameters α, β and γ. The numerical solutions are also obtained using MATLAB program. While comparing our analytical solutions with the numerical estimation a good agreement is noted.**

Keywords*— Mathematical modeling; non-linear reaction diffusion equations; immobilized enzyme system; hydrogen ion; electrostatic interaction.

I. INTRODUCTION

Immobilization is one of the efficient methods to improve enzyme stability [1]. The main aim of immobilization is to obtain stable and reusable enzymes with resistance to different environmental factors [2, 3].The main objective of the immobilization of enzymes is to enhance the economics of bio catalytic processes. Immobilization allows one to re-use the enzyme for an extended period of time and enables easier separation of the catalyst from the product. Additionally, immobilization improves many properties of enzymes such as performance in organic solvents, pH tolerance, heat stability or the functional stability. Many enzyme-catalyzed reactions involve the production or consumption of hydrogen ions and this is expressed by the change in the binding of hydrogen ions in the biochemical reactions as written in terms of reactants [4]. The change in the binding of hydrogen ions in an enzyme catalyzed reaction is noteworthy as it determines the effect of pH on the thermodynamics of the reaction which has been catalyzed [5]. In many biochemical reactions the produced hydrogen ions can alter the micro environment considerably [6].

A mathematical model based on immobilized enzyme catalysis with reaction-generated pH change was investigated by Bailey and Chow [7] and their study is restricted mainly to the large pore case. The electrostatic effects in immobilized enzyme system in terms of apparent Michaaelis-Menten constants were first discussed by Goldstein et al. [8]. A mathematical frame work was established by Bhalla and Deen [9] to evaluate the electrostatic interaction energy between a charged sphere and a charged pore by solving the nonlinear Poisson Boltzmann equations. Gupta and Ramachandran[10] have analyzed the effect of both internal and external diffusion resistances together with electrostatic interaction not only for the small pore case and also for large pore case .

In this study, the effect of interactions between the charged carrier and the hydrogen ion has been analyzed analytically for both small and large pore cases. The nonlinear equations depicted by the mathematical model discussed here have been solved by Adomian decomposition method [10-15] and the analytical expressions corresponding to the steady state concentrations of the substrate and hydrogen ion, have been derived. These analytical results are useful to understand and optimize the behavior of electrostatic interaction in the kinetics of immobilized enzymes. The information gathered from the theoretical modeling is fruitful in experimental design, optimization and prediction of the enzyme kinetics.

II. MATHEMATICAL FORMULATION OF THE PROBLEM

The system under consideration consists of enzyme immobilized on a plain porous charge support. The enzyme catalyses the reaction

*Corresponding author.

This paper was presented by the first author in the National Conference on AMASE-2016 conducted in Department of Mathematics, University College of Engineering Pattukkottai, Thanjavur, Tamil Nadu, India, on 22nd January 2016.

$$E + S \rightarrow P^- + H^+ + E \quad (1)$$

The rate expression for the above enzyme catalyzed reaction based on the effect of hydrogen ion concentration is given by

$$r(s,h)=\left[\frac{V_m s}{s+K_m}\right]\left[\frac{1}{1+h/K_1+K_2/h}\right]$$

Small pore case:

In this small pore case the analysis is done for supports having pores of very small diameter of the order of the characteristic dimensions of the electrostatic double layer and the electrostatic potential due to charged support will be uniform within the pore. The transport of hydrogen ion from the pore mouth to the exterior of the bulk will be affected by the electrostatic interaction.

In the small pore case the potential is uniform within the pore and the flux within the pore due to electrostatic effect becomes zero. Hence for such system the mass balance equations for the substrate and the hydrogen ion for the reaction following the kinetics given by equation can be written by the following equations [6]:

$$D_{es}\frac{d^2 s}{dx^2}=\left[\frac{V_m s}{s+K_m}\right]\left[\frac{1}{1+h/K_1+K_2/h}\right] \quad (2)$$

$$D_{eh}\frac{d^2 h}{dx^2}=\left[\frac{-V_m s}{s+K_m}\right]\left[\frac{1}{1+h/K_1+K_2/h}\right] \quad (3)$$

The corresponding boundary conditions are given by

$$\frac{ds}{dx}=0,\ \frac{dh}{dx}=0 \text{ at } x=0 \quad (4)$$

$$D_{es}\frac{ds}{dx}=k_s(s_o-s),\quad D_{eh}\frac{dh}{dx}=Mk_h\left(h_0-\frac{h}{P}\right) \quad (5)$$

at $x = L$, where s and h denote the concentration of substrate and hydrogen ion, V_m is the maximum rate of reaction, k_1 and k_2 are equilibrium constants, K_m is the Michaelis - Menten constant, h is the external mass transfer coefficient, x represents the distance from the center of the pore and P is the partition coefficient defined by $P=e^{-\lambda}$.

III. Dimensionless Form of the Problem

To compare the analytical results with simulation results, we make the above non-linear partial differential equations (3) and (4) in dimensionless form by defining the following parameters.

$$X=\frac{x}{L},\ S=\frac{s}{s_o},\ H=\frac{h}{h_o},\ \varphi=\frac{V_m L^2}{D_{es}K_m},$$
$$\alpha_1=\frac{h_o}{K_1},\ \alpha_2=\frac{h_0}{K_2},\ \gamma=\frac{s_0}{K_M},\ \beta_S=\frac{Lk_S}{D_{es}} \quad (6)$$

The dimensionless form of the equations (2) and (3) in terms of dimensionless quantities described in equation (6) can be written as

$$\frac{d^2 S}{dX^2}=\frac{\varphi S}{1+\gamma S}\left(\frac{1}{1+\alpha_1 H+1/\alpha_2 H}\right) \quad (7)$$

$$\frac{d^2 H}{dX^2}=-\frac{D_{es}}{D_{eh}}\frac{s_0}{h_0}\frac{\varphi S}{1+\gamma S}\left(\frac{1}{1+\alpha_1 H+1/\alpha_2 H}\right)$$

The boundary conditions in dimensionless form will be as follows:

$$\frac{dS}{dX}=\frac{dH}{dX}=0 \quad \text{at} \quad X=0$$

$$\frac{dS}{dX}=\beta_s(1-S) \quad \text{at} \quad X=1$$

$$\frac{dH}{dX}=M\beta_s\frac{D_{es}}{D_{eh}}\frac{k_h}{k_s}\left(1-\frac{H}{P}\right) \quad \text{at} \quad X=1$$

Using the Adomian decomposition method (Appendix B) the non-linear equations (7) and (8) can be solved and the analytical expressions of substrate and hydrogen ion concentrations are given by

$$S(X)=1+\left(\frac{\varphi}{1+\gamma}\right)\left(\frac{1}{1+\alpha_1 P+1/\alpha_2 P}\right)\left(\frac{X^2}{2}-\frac{1}{2}-\frac{1}{\beta_s}\right) \quad (12)$$

$$H(X)=P-\left(\frac{\beta_s PD}{M_h}\right)\left[\left(\frac{\varphi}{1+\gamma}\right)\left(\frac{1}{1+\alpha_1 P+1/\alpha_2 P}\right)\left(\frac{X^2}{2}-\frac{1}{2}-\frac{1}{\beta_s}\right)\right] \quad (13)$$

The basic concepts of Adomian decomposition method are given in Appendix A

The Thiele module is defined as

$$\varphi=\frac{V_m L^2}{D_{es}K_M} \quad (14)$$

The effectiveness factor η, which is defined as the ratio of the actual reaction rate and Thiele modulus if the reaction took place at the bulk concentrations without the electrostatic effect in dimensionless form and its corresponding analytical expression are given below

$$\eta=\frac{1}{\varphi}(1+\gamma)(1+\alpha_1+1/\alpha_2)\left(\frac{dS}{dX}\right)_{X=1} \quad (15)$$

$$\eta=(1+\alpha_1+1/\alpha_2)\left(\frac{1}{1+\alpha_1 P+1/\alpha_2 P}\right) \quad (16)$$

The dimensionless reaction rate and its corresponding analytical solution are given by

$$V=\left(\frac{dS}{dX}\right)_{X=1}=\left(\frac{\varphi}{1+\gamma}\right)\left(\frac{1}{1+\alpha_1 P+1/\alpha_2 P}\right) \quad (17)$$

Large pore case:

In artificial immobilized enzyme systems, the pores can be significantly larger than the electrostatic double layer thickness. For these cases, the effects can be taken into account by lumping them into the partitioning coefficient *P*. For this case the mass balance equation for substrate and hydrogen ion can be obtained by replacing H by PH and defining the partition coefficient as $P = e^{\lambda}$. Hence the boundary condition for hydrogen ion becomes

$$\frac{dH}{dX} = M\beta_s \frac{D_{es}}{D_{eh}} \frac{k_h}{k_s}(1-H) \ at \ X = 1 \quad (18)$$

Hence the analytical expression for hydrogen ion in large pore case is given by

$$H = P - \left(\frac{\beta_s PD}{M_h}\right)\left[\left(\frac{\varphi}{1+\gamma}\right)\left(\frac{1}{1+\alpha_1 P + 1/\alpha_2 P}\right)\left(\frac{x^2}{2} - \frac{1}{2} - \frac{1}{\beta_s}\right)\right] \quad (19)$$

Table: 1 Parameters used in this work and Ramachandran et. al work

Para meter	Values used in this work	Parameter	Values used in previous work
$K1$	5x10^{-5} M	$\alpha_1 = \frac{h_o}{K_1}$	0.01 - 0.5
K_2	10^{-5} M	$\alpha_2 = \frac{h_0}{K_2}$	0.01-0.5
K_M	10^{-5} M	$\gamma = \frac{s_0}{K_M}$	1
k_h / k_s	1	$\beta_s = \frac{Lk_s}{D_{es}}$	100
D_{es} / D_{eh}	0.25	$X = \frac{x}{L}$	0 - 1
$s0$	10^{-4} M, 10^{-6}M	s_0	10^{-4} M, 10^{-6}M
h_0	10^{-4} M, 10^{-7}M	h_0	10^{-4} M, 10^{-7}M
λ	-1, 0, 1	λ	-1,0,1
β	10,100, 1000	β	10,100,1000

IV. NUMERTICAL SIMULATION

The non-linear differential equations (4) and (12) for the given initial – boundary conditions are being solved numerically. The function pdex, in MATLAB software which is a function of solving the initial – boundary value problems for non-linear ordinary differential equations is used to solve these equations. The numerical solutions are compared with analytical results using Adomian decomposition method as shown in figures 1, 2 and 3 and it gives a satisfactory result. The MATLAB program is also given in Appendix C.

V. RESULTS AND DISCUSSION

The proposed mathematical model for small pore and large pore cases consists of coupled non - linear equations for substrate and hydrogen ion concentrations. They are solved by adomian decomposition method to obtain analytical solutions for the both concentrations as well as for Thiele module and effectiveness factors. These analytical results are discussed graphically as shown in figures. Fig. 1 shows the time independent evolution of normalized concentration profiles for the substrate. Fig. 1(a) - 1(d) shows the dimensionless concentration S versus the dimensionless Length L. Fig. 1(a) indicates that the value of the concentration increases when then value of the Thiele modulus is being decreased and from Fig. 1(b) it is evident that as the value of the equilibrium constant α_1 increases the concentration also increases. Fig. 1 (c) denotes the concentration increases with the increase in the value of reaction diffusion parameter γ. From Fig. 1(d) it is obvious that the Sherwood number β does not play a significant role in the concentration of the substrate as there is no change when the number is being increased. Fig. 2 demonstrates steady state normalized profiles of hydrogen ion concentration. In Fig. 2(b) and (c), it is understood there is remarkable increase in the concentration when the Sherwood number β as well as the Thiele modulus are being increased. Fig. 2(a) and (d) exhibits that the concentration increases when the parameter M_h and reaction diffusion parameter γ are being decreased. Fig.3 indicates the concentration profiles of hydrogen ion for large pore case. It is noteworthy that same results are obtained in both the cases for varying the parameters β and γ. Fig.4 illustrates that there is a linear relationship between the reaction rate and Thiele modulus for various values of the parameters.

VI. SENSITIVITY ANALYSIS

Equation (12) represents the analytical expression for the concentration of the substrate in dimensionless form in terms of the parameters $\alpha_1, \alpha_2, \beta, \gamma,$ and P. From the spread sheet analysis given in Figure 5 it is understood that the parameter α_1 has the greater impact than all other factors. The parameters α_2, γ and the Thiele modulus φ, partition coefficient P have more or less equal impact whereas the parameter β has very less impact in the substrate concentration. It is evident from the spread sheet analysis exhibited in Figure 6, the influence of the partition coefficient P is very high whereas influence of the diffusion coefficient D is very low in the hydrogen ion concentration H . It is noteworthy that the Thiele modulus φ as well as the diffusion parameter β have similar impact .The parameter M_h also has significant impact in H whereas the influence of other parameters such as α_1, α_2 and γ are comparatively less. On the whole, the sensitivity analysis described in this paper will be fruitful to evaluate the significance of each parameter to the simulation's accuracy.

VII. CONCLUSION

A mathematical model based on the effects of electrostatic interaction with reaction generated pH change on the kinetics of immobilized enzymes has been discussed here. The analytical expressions for the concentrations of the substrate and hydrogen ion concentration have been derived by making use of Adomian Decomposition Method. It is noteworthy that there is a good agreement between the analytical and numerical simulations. The analytical results derived by making use of this described model are used to determine the influence of effectiveness factor as well as Thiele modulus in the electrostatic interaction without using any experimental techniques. The importance of partition coefficient in selecting a carrier for enzyme immobilization is also shown graphically. This theoretical model can also be used to optimize the performance of the electrodes.

REFERENCES

[1] Liao M. H, Chen D. H. Immobilization of yeast alcohol dehydrogenase on magnetic Nano particles for improving its stability J Biotechnol Lett., 2001; 23: 1723–1727.

[2] Lei, Z., Bi S., Yang, H. Chitosan-tethered the silica particle from a layer-by-layer approach for pectinase immobilization. Food.Chem. 2007; *104*: 577–584.

[3] Mateo, C. Palomo, J.M., Fernandez-Lorente, G., Guisan, J.M., Fernandez-Lafuente, R, Improvement of enzyme activity, stability and selectivity via immobilization techniques. Enzyme Microb. Technol., 2007, 40: 1451–1463.

[4] Alberty R.A., Degrees of freedom in biochemical reaction systems at specified pH and pMg, J. Phys. Chem. 1992; 96: 9614–9621.

[5] Alberty R.A. Changes in binding of hydrogen ions in enzyme-catalyzed reactionsBio physical Chemistry 2007; 125: 328–333.

[6] Ramachandran K.B., Rathore, A.S., Gupta S.K. Modeling the effects of electrostatic interaction with reaction-generated pH change on the kinetics of immobilized enzyme. The chemical Engineering Journal, 1995; 57: B15-B21.

[7] Bailey J.E, Chow M.T.C. Immobilized enzyme catalysis with reaction generated pH change Biotechnol. Bioeng., 1974; 16: 1345-.1357.

[8] Goldstein L., Levin L. Katchalski E. A water- insoluble polyanionic derivative of trypsin. II. Effect of the poly electrolyte carrier on the kinetic behavior of the bound trypsin. Biochemistry.1964; 3: 1913-1919.

[9] Bhalla, G.J., Deen W.M. Effects of charge on osmotic reflection coefficients of macromolecules in porous membranes. J. Colloid Interface Sci. 2009; 333: 363-372.

[10] Gupta A., Ramachandran K.B. Diffusional and electrostatic effects on the kinetics of immobilized enzymes. J. Ferment. Technol., 1983; 61: 319-323

[11] Bernstein Polynomial methods, British Journal of Mathematics & Computer science. 2015; 9: 498-515.

[12] Q.H. Yahya, M.Z. Liu. Modified Adomian decomposition method for singular initial value problems in the second -order ordinary differential equations. Sur v. Math. Appl. 2003; 3:183-193.

[13] Ine M, Evans D. J. The decomposition method for solving of a class of singular two-point boundary value problems. Int. J. Comp. Math. 2003; 80: 869-882.

[14] Praveen T., Rajendran L., Mathematical model for multi-phase micro channel bioreactors International Journal of Mathematical Archive, 2011; 2: 2270-2280.

[15] Saravanakumar K., Rajendran L., Analytical solution of the concentration of substrate and effectiveness factor for acetophenone in packed bed reactor. International Journal of Mathematical Archive.2011; 2: 2347-2357.

APPENDIX - A

Basic concepts of the modified Adomian decomposition method

The modified Adomian decomposition method consists of decomposing the nonlinear differential equation.

$$F[x, y(x)] = 0 \qquad \text{(A.1)}$$

into two components

$$L[y(x)] + N[y(x)] = 0 \qquad \text{(A.2)}$$

Where L and N are the linear and the nonlinear parts of F respectively. The operator L is assumed to be an invertible operator. Solving for $L(y)$ leads to

$$L[y(x)] = -N[y(x)] \qquad \text{(A.3)}$$

Applying the inverse operator L to both sides of Eq. (A.3) yields $y(x) = -L^{-1}[N(y)] + \varphi(x)$ (A.4)

Where $\varphi(x)$ is the function that satisfies the condition $L(\varphi)$ =0. Now suppose that the solution y can be represented as an infinite series of the form

$$y(x) = \sum_{n=0}^{\infty} y_n \qquad \text{(A.5)}$$

The modified Adomian decomposition method assumes that the nonlinear term $N(y)$ can be written as an infinite series in terms of the Adomian polynomials A_n :

$$N(y) = \sum_{n=0}^{\infty} A_n \qquad \text{(A.6)}$$

where the Adomian polynomials A_n of $N(y)$ are evaluated using the formula

$$A_n(x) = \frac{1}{n!} \frac{d^n}{d\lambda^n} N\left(\sum_{n=0}^{\infty} \lambda^n y_n\right)\Bigg|_{\lambda=0} \qquad \text{(A.7)}$$

where $\lambda \in [0, 1]$ is a hypothetical parameter (28).
Substituting Eqs.(A.5) and (A.6) in (A.4) gives

$$\sum_{n=0}^{\infty} y_n(x) = \varphi(x) - L^{-1}\left(\sum_{n=0}^{\infty} A_n\right) \qquad \text{(A.8)}$$

By equating the terms in the linear system of Eq. (A.8) one obtains the recurrence formula:

$$y_0(x) = \varphi(x), \; y_{n+1}(x) = -L^{-1}(A_n) \qquad n \geq 0 \qquad \text{(A.9)\}$$

However, in practice all terms of the series (A.6) cannot be determined, and the solution is approximated by the truncated series $\sum_{n=0}^{N} y_n$.

APPENDIX - B

Approximate analytical solution of Eqn. (7) using ADM method

In this appendix, we indicate how Eq. (12) in this paper has been derived. Furthermore, an ADM was constructed to determine the solution of Eq. (7) for $(a=1)$ in the operator form,

$$Ls = \frac{\varphi S}{1+\gamma S}\left(\frac{1}{1+\alpha_1 P+1/\alpha_2 P}\right) \quad \text{(B.1)}$$

where $L = \frac{d^2}{dx^2}$, Applying the inverse operator L^{-1} on both sides of Eq. (B.1) yields

$$s(x) = Ax + B + \frac{\varphi S}{1+\gamma S}\left(\frac{1}{1+\alpha_1 P+1/\alpha_2 P}\right) \quad \text{(B.2)}$$

Where A and B are the constants of integration. We let,

$$s(x) = \sum_{n=0}^{\infty} s_n \quad \text{(B.3)}$$

$$N[s(x)] = \sum_{n=0}^{\infty} A_n \quad \text{(B.4)}$$

where $N[s(x)] = \frac{\varphi S}{1+\gamma S}\left(\frac{1}{1+\alpha_1 P+1/\alpha_2 P}\right)$ (B.5)

From the Eqns (B.3), (B.4) and (B.5), Eq. (B.2) gives

$$\sum_{n=0}^{\infty} s_n(x) = Ax + B + \frac{S}{1+\gamma S}\left(\frac{1}{1+\alpha_1 P+1/\alpha_2 P}\right) \quad \text{(B.6)}$$

We identify the zeroth component as

$$s_0(x) = Ax + B \quad \text{(B.7)}$$

And the remaining components as the recurrence relation

$$s_{n+1} = \varphi L^{-1} A_n \,;\, n \ge 0 \quad \text{(B.8)}$$

where A_n are the Adomian polynomials of $s_0, s_1, \ldots, s_n$. We can find the first few A_n as follows:

$$s_0(x) = 1 \quad \text{(B.9)}$$

$$s_1(x) = \left(\frac{\varphi S}{1+\gamma S}\right)\left(\frac{1}{1+\alpha_1 P+1/\alpha_2 P}\right)\left(\frac{x^2}{2}-\frac{1}{2}-\frac{1}{\beta_s}\right) \quad \text{(B.10)}$$

Adding (B.9) and (B.10), we get the concentration substrate Eqn.(12). Similarly, we can obtain the concentration of hydrogen ion (13) by solving Eqns. (8), (9) and (11).

APPENDIX - C

Scilab/Matlab program for the numerical solution of equation (4)

```
function pdex4
m = 0;
x = linspace(0,1);
t = linspace(0,100000);
sol = pdepe(m,@pdex4pde,@pdex4ic,@pdex4bc,x,t);
u1 = sol(:,:,1);
%————————————————————————
Figure
plot(x,u1(end,:))
title('u1(x,t)')
xlabel('Distance x')
ylabel('u1(x,1)')
function [c,f,s] = pdex4pde(x,t,u,DuDx)
c =1;
f =1.* DuDx;
e=0.3;alpha=2;
F =-(e*u(1))/((1+(alpha*u(1))));
s =F;
% ————————————————————————
function u0 = pdex4ic(x);
  u0 = [0];
% ————————————————————————
function [pl,ql,pr,qr] = pdex4bc(xl,ul,xr,ur,t)
j=10;
pl = [0];
ql = [1];
pr = [-j*(1-ur(1))];
qr = [1];
```

APPENDIX - D

Nomenclature

D_{es}	Effective diffusivity of substrate concentration
D_{eh}	Effective diffusivity of hydrogen ion concentration
e	Euler's Constant
h	Hydrogen ion Concentration
H	Dimensionless Hydrogen ion Concentration
K_1, K_2	Equilibrium constants
K_M	Michael-Menten Constant
L	Length of the pore
M	Dimensionless electro static potential modifier
P	Partition coefficient
s	Substrate Concentration
S	Dimensionless Substrate Concentration
V_m	Maximum rate of reaction
x	Distance from the center of the pore
X	Dimensionless Length

Greek symbols

α_1, α_2	Reduced equilibrium constant
β	Sherwood number
γ	Dimensionless Michaelis - Menten constant
η	Effectiveness factor
λ	Dimensionless surface potential
φ	Thiele modulus

Fig.1

(a)

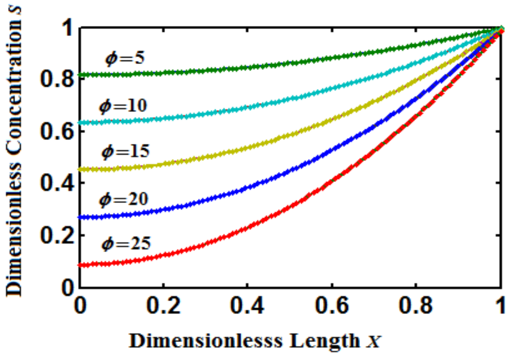

(b)

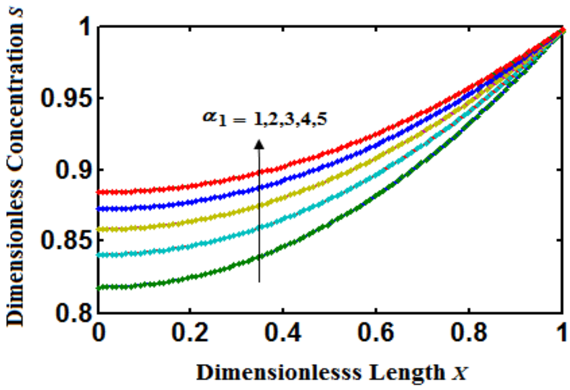

(c)

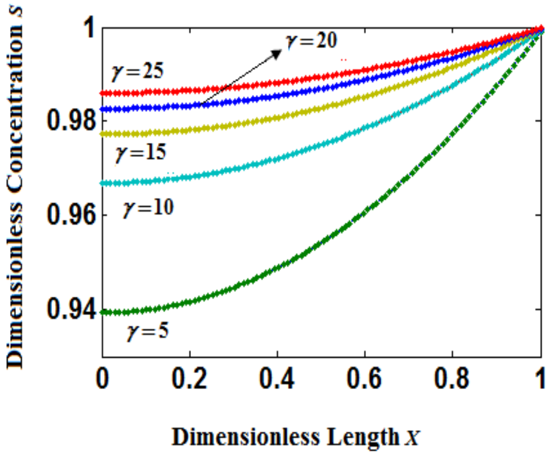

(d)

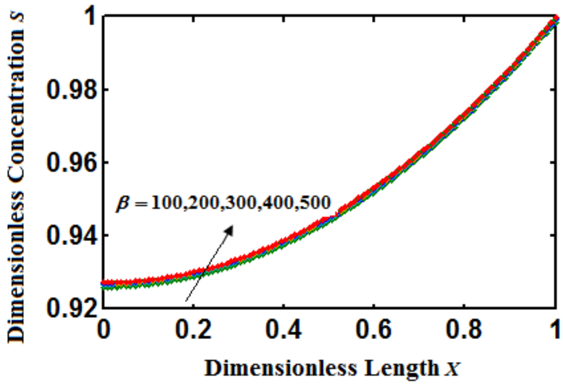

Fig.1. Plot of dimensionless concentration S versus dimensionless length X for various values of the parameters

a) $\alpha_1 = 1, \alpha_2 = 0.2, P = 1, \beta = 100$ *and* $\gamma = 1$

b) $\varphi = 5, \alpha_2 = 0.2, P = 1, \beta = 100$ *and* $\gamma = 1$

(c) $\alpha_1 = 1, \alpha_2 = 0.2, P = 1, \beta = 100$ *and* $\varphi = 5$

(d) $\alpha_1 = 1, \alpha_2 = 0.2, P = 1, \quad = 10$ *and* $\gamma = 5$

Solid lines represent numerical solutions whereas the dotted line represents analytical solutions.

Fig.2

(a)

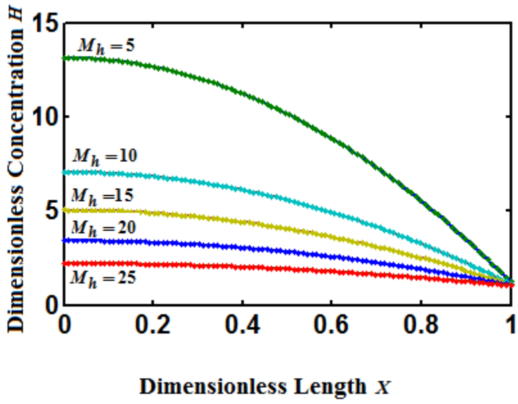

(b)

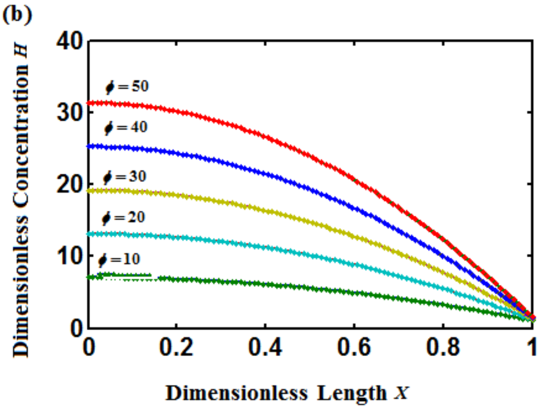

(c)

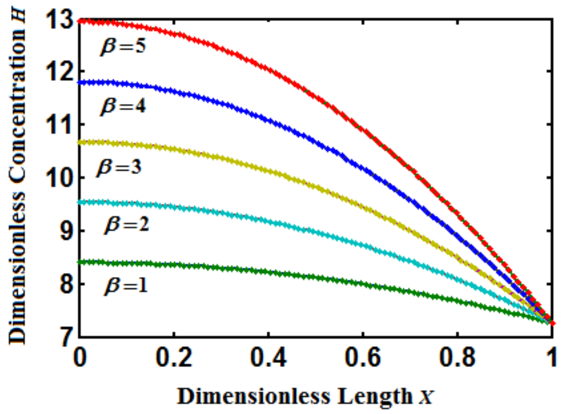

(d)

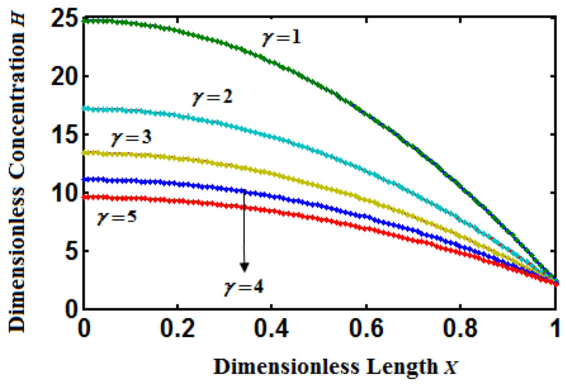

Fig.2. Plot of dimensionless concentration H versus dimensionless length X for various values of the other parameters

a) $\alpha_1 = 0.01, \alpha_2 = 0.05, P = 1, \beta = 100, \varphi = 10, D = 5$ and $\gamma = 1$

b) $\alpha_1 = 1, \alpha_2 = 5, P = 5, \beta = 100, M_h = 10, D = 5$ and $\gamma = 1$

c) $\alpha_1 = 0.01, \alpha_2 = 0.05, P = 5, M_h = 10, \varphi = 10, D = 5$ and $\gamma = 1$

d) $\alpha_1 = 0.01, \alpha_2 = 0.05, P = 5, M_h = 10, \varphi = 10, D = 5$ and $\beta = 100$

Solid lines represent numerical solutions whereas the dotted line represents analytical solutions.

Fig.3

(a)

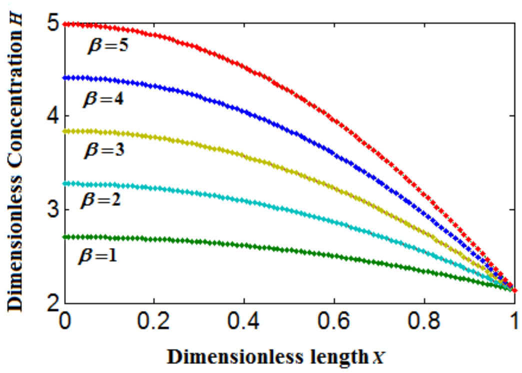

(b)

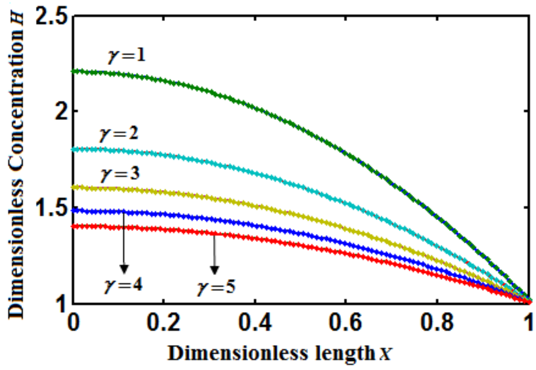

Fig.3. Plot of dimensionless concentration H versus dimensionless length X for various values of the parameters

a) $\alpha_1 = 1, \alpha_2 = 5, P = 1, M_h = 10, \varphi = 10, D = 5$ and $\gamma = 1$

b) $\alpha_1 = 1, \alpha_2 = 5, P = 1, M_h = 10, \varphi = 10, D = 5$ and $\beta = 100$

For large pore case

(a)

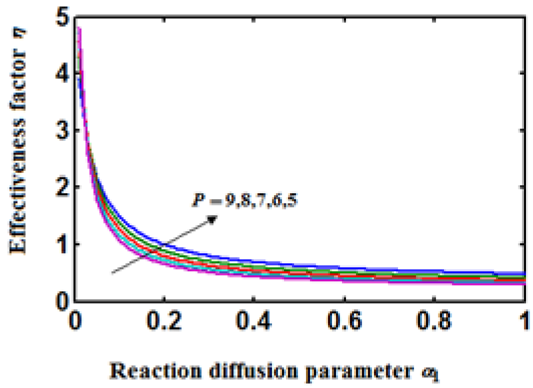

(b)

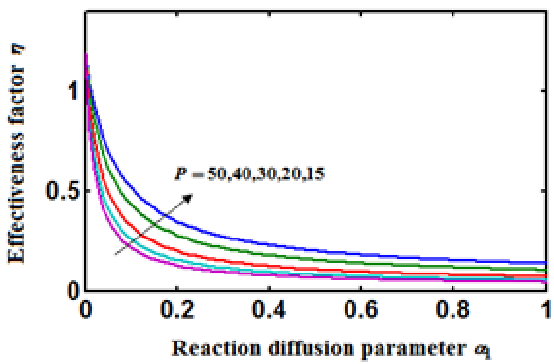

Fig.4. Plot of dimensionless effectiveness factor η versus dimensionless reaction diffusion parameter α_1 for various values of the other parameters.

Global Journal of Pure and Applied Mathematics (GJPAM) ISSN 0973-1768 Volume 12,Number 4 (2016)

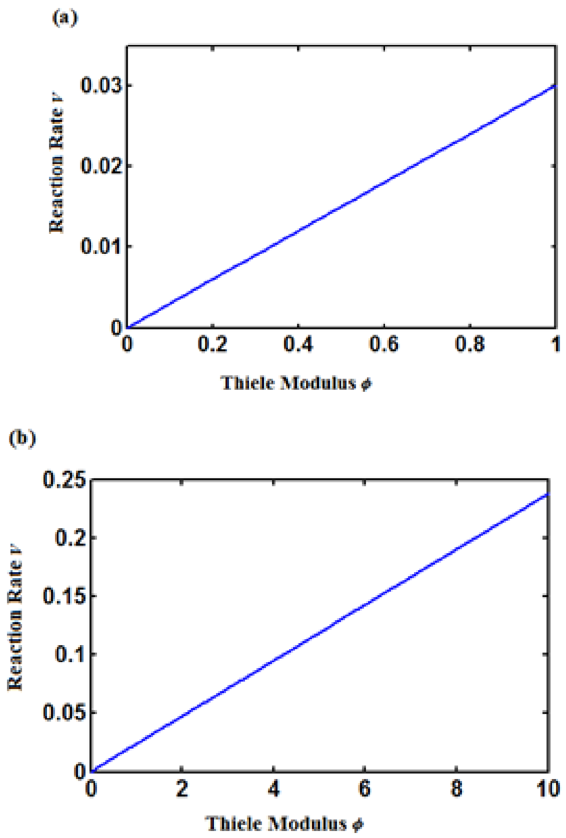

Fig.5.Plot of dimensionless reaction rate v versus dimensionless thiele modulus for various values of the parameters a) $\alpha_1 = 0.01, \alpha_2 = 0.05, P = 1$ *and* $\gamma = 1$
b) $\alpha_1 = 0.01, \alpha_2 = 0.05, P = 5$ and $\gamma = 10$

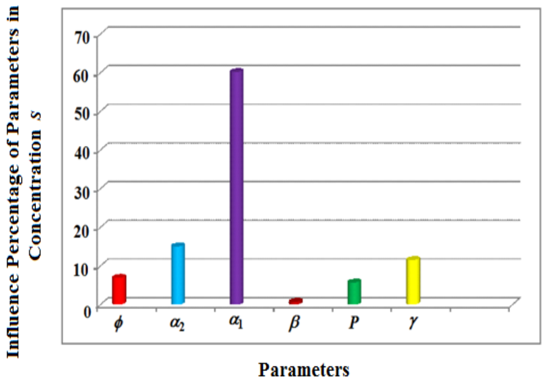

Fig.5. Sensitivity Analysis for evaluating the influence of parameters in Concentration S using equation (12)

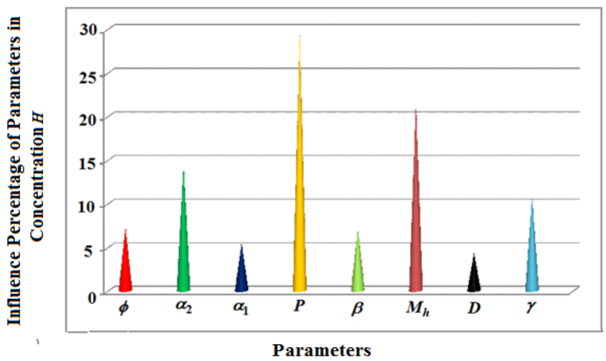

Fig.6. Sensitivity Analysis for evaluating the influence of parameters in Concentration H using equation (13).

Empirical and finite element prediction and validation of weld bead profile generated during TIG welding process

S. Renold Elsen
Department of Mechanical Engineering,
MIET Engineering College, Trichy.
Email:renoldelsen@gmail.com

*K. Jegadeesan**
Department of Mechanical Engineering,
SRM University, Kattankulathur–Chennai.
Email:mechjegadeesan@gmail.com

Abstract—**Welding is a permanent type fastening method used to join to two metal plates together. Tungsten Inert Gas (TIG) welding is a special type of welding technique developed to join metals which are hard to weld. For better weld quality TIG welding is employed to weld ferrous alloys with low weldability used in various engineering applications. The double ellipsoidal heat source is selected to simulate the welding process as it is a suitable heat source for simulating a more realistic welding process. The welding process is simulated mathematically by using empirical relations developed for the double ellipsoidal heat. Further, a code was developed using C Program and the temperature distribution plots were obtained. The weld bead profile is predicted from the plot using the extrapolation method. Further using SYSWELD, Finite Element Analysis software the temperature distribution in the plate is obtained and the bead width and bead depth were found. To validate the empirical and Finite Element prediction and experiment was conducted. In the experimental studies SA 516 Grade 70 steel alloy plate is welded by TIG welding using similar welding parameters as the earlier mathematical studies used for prediction. The weld bead profile from the predicted and experimental results was found to validate each other.**

Keywords- TIG welding; weld quality; Double Ellipsoidal Heat Source; Extrapolation method; Weld Bead Profile and SYSWELD.

I. INTRODUCTION

Welding has been for many years a big part of the manufacturing process in many industries around the world. Welding, among all mechanical joining processes, has been employed at an increasing rate for its advantages in design flexibility, cost savings, reduced overall weight and enhanced structural performance. The advantages of welding do not need further exemplification. Unfortunately the welding process induces also few problems that need to be more accurately identified and after that minimized as much as possible. Among the welding typical problems and most important are the residual stress/strain and the induced distortions in structures. In order to better understand the welding process and its effects on structures, engineers and researchers around the world, covering a large number of industries, have been trying to create algorithms and methodologies to simulate the complete process or just individual phases (e.g. the cooling phase). In recent years, due to the high expansion of computers computations possibilities, many researchers identified the Finite Element Analysis (FEA) as a reliable method for this purpose [1].Gas tungsten arc welding formerly known as tungsten inert gas (TIG) welding is a process that relies upon the formation of an arc between a non-consumable tungsten electrode and the work piece [2].The arc is generally initiated by a high-frequency unit and protected by an inert-gas shroud. The electrode-tip angle determines the spread of the welding arc contained within an envelope of the protective (argon) gas. The gas generates a plasma arc and also protects the molten pool from undesirable oxidation effects from surrounding atmosphere .The GTAW process is one of the most versatile welding processes but it requires a high level of welder skill for manual application. It can be used at current less than 1 A for components up to 0.1 mm thick as well as at higher current for thicker section. GTAW offers great potential in applications where there are arc high demands on weld integrity. Its relatively low deposition rate makes it uneconomic. The Deposition rates can be improved by using hot-wires techniques and narrow-gap preparation.

IV.SELECTION OF HEAT SOURCE MODELS FOR TIG WELDING SIMULATION

The temperature vs. time relationship of welded components and structures can be theoretically obtained by carrying out a heat-transfer analysis of the welding process. This involves many complicated heat-flow phenomena including heat radiation, convection, heat conduction as well as fluid flow of melting weld metal [3]. This process would require solving many constitutive differential equations using finite element or finite difference methods that are time consuming despite the fact that the computing power continues to improve. Therefore, from practical point of view, analytical solutions for the heat-transfer problem in welding are preferable despite their limitations. Their major advantage is that they are given in the closed form equation that could provide the temperature-time information for the welding thermal problems in a rapid and convenient way.Lower-current welding arcs can be treated as a moving-point heat source. Welding heat sources that produce a key hole during the welding, such as electronic beam welding (EBW), laser beam welding (LBW) and plasma arc welding (PAW), should be treated like line heat source. For broad heat sources that envelope an area on a surface (e.g. a large oxygen-acetylene flame) can be considered as a plane heat

*Corresponding author.

This paper was presented by the second author in the National Conference on AMASE-2016 conducted in Department of Mathematics, University College of Engineering Pattukkottai, Thanjavur, Tamil Nadu, India, on 22nd January 2016.

source.Heat source used for welding processes such as electric resistance spot welding, electrical meat explosion welding, arc stud welding and rotational friction welding, where the heat quantity released for welding at fixed location over a relatively short period of time, can be considered as instantaneous heat sources. However, when the heat sources are maintained over a longer period of time such as found in the electric arc or flame welding processes, these are considered to be continuous heat sources [4].Periodic heat sources are those used in pulse arc welding or in resistance seam welding with on-and-off current. In most welding process performed on thick plates, the heat flow is three-dimensional (3D). In order to simulate 3D heat flow, it is necessary to make use of 3D heat source such as spherical or ellipsoidal density heat source [5,6, 7]. In case of welding of relatively thin plates, where a single weld pass is sufficient to penetrate the plate thickness, then two-dimensional (2D) heat flow equation can be used for the analysis using 2 D heat sources. For cases of high power or fast-moving heat sources, the heat flow along the travel direction of the heat source can be neglected, hence, the one-dimensional heat flow can be used to model this situation.For different heat source an analytical approach has been derived by ignoring the complexity of radiation and convection in the thermal analysis of welding process. The temperature-time distribution is obtained by considering the classical heat-conduction equations in solid medium [8].

A. Double Ellipsoidal Heat Source

The double-ellipsoidal heat source is considered to be a more advanced heat source than the single-ellipsoidal source due to its greater flexibility to model realistic shapes of the moving heat source. The double-ellipsoidal heat source is also known in literature [9,10] as Goldak's heat source.John Goldak et al. studied the mathematical models for weld heat sources based on Gaussian distributed of power density in space.

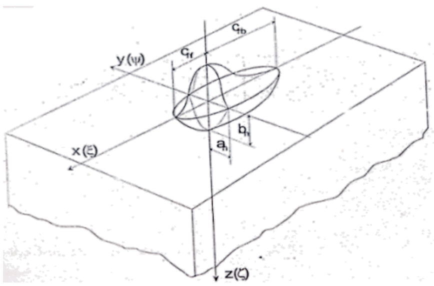

Figure 1 Double-ellipsoidal power density distribution heat sources

The double-ellipsoidal heat source consist of two different semi-ellipsoids, hence, the density within each semi-ellipsoid is described by a different separate equation. The heat density at any arbitrary point (x, y, z) within the double-ellipsoid heat source is shown in Figure 1. The heat density equation for a point (x, y, z) within the front and the rear semi-ellipsoid heat source is described by the two equations below, respectively

$$Q(x, y, z) = \frac{6\sqrt{3} r_f Q}{a_h b_h c_{hf} \pi \sqrt{\pi}} \exp\left(-\frac{3x^2}{{c_{hf}}^2} - \frac{3y^2}{{a_h}^2} \frac{3y^2}{{b_h}^2} \right) \quad (1)$$

$$Q(x, y, z) = \frac{6\sqrt{3} r_b Q}{a_h b_h c_{hb} \pi \sqrt{\pi}} \exp\left(-\frac{3x^2}{{c_{hb}}^2} - \frac{3y^2}{{a_h}^2} \frac{3y^2}{{b_h}^2} \right) \quad (2)$$

where a_h, b_h, c_{hf}, c_{hb} – ellipsoidal heat source parameters

Q – arc heat input ($Q = \eta IU$ where I and U are arc voltage, respectively)

r_f, r_b – proportional co-efficient at front and back of heat source, respectively

TABLE 1HEAT SOURCE PARAMETER OF DOUBLE-ELLIPSOIDAL HEAT SOURCE

Sl. No	Welding Parameter	Dimensions (mm)
1.	a_h	7
2.	b_h	2
3.	c_{hf}	8
4.	c_{hb}	16

A program in C was developed and executed to obtain the temperature distribution and from the repeated analysis, temperature history is also obtained at the desired location [11]. Similar logic is used for other moving heat source models. Figure 3.10 shows the temperature distribution along the line y = 0 to 50 at x = 25, at different times. It can be observed that the temperature at point (25, 0) is increasing to infinity as the source approaches to the point. The Heat Source Parameter of double-ellipsoidal heat source given in Table 1 is used for the complete analysis.

I. Finite Element Weld Analysis and Simulation Using SYSWELD

The nonlinear element solver, SYSWELD, is employed to solve the transient analysis of the problem [12]. The peak temperature reached is more than the boiling point of the material and hence the phase change is to be considered while performing the analysis. SA 516 Grade 70 steel alloy plate of length 100 mm, width 90 mm and thickness 10 mm is taken. The heat-affected zone is smaller than the domain of the material. Very fine mesh is created to resolve the temperature distribution in the weld region. The whole domain is discredited into uniform 8-node hexahedrons, consisting of 14927 nodes 18362 and elements. The convection and radiation loads are simulated as surface loads on the element free face with the initial and boundary conditions, the weak formulation of heat conduction equation that describes the transient temperature distribution is obtained in the discrete domain.Also the Temperature Dependent Thermal Properties for SA 516 Grade 70 steel alloy such as thermal conductivity and specific heat is given in Table 2. The cross-sectional and isometric view of the Finite element model is given in Figure 2 and 3.

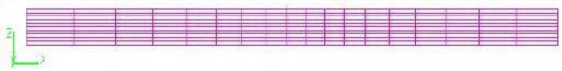

Figure 2 Cross-sectional view of the mesh

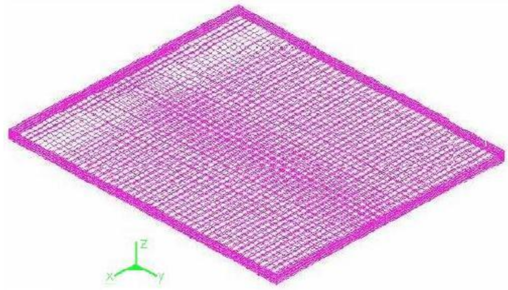

Figure 3 FEA Plate Model

TABLE 2 TEMPERATURE DEPENDENT THERMAL PROPERTIES FOR SA 516 GRADE 70 STEEL ALLOY

Sl. No	Temperature (K)	Thermal Conductivity (W/m K)	Specific heat (J/kg K)
1.	273	51.90	450
2.	373	51.10	499.2
3.	273	51.90	450
4.	373	51.10	499.2
5.	573	46.10	565.5
6.	723	41.05	630.5
7.	823	37.50	705.5
8.	873	35.60	773.3
9.	993	30.64	1080.4
10.	1073	26	931

A. Boundary Condition

- The work piece initial temperature is 30º C (or) 303 K.
- The heat source is moving while the work piece is fixed.
- All the thermo-physical properties for SA 516 Grade 70 steel alloy is considered to be temperature dependent.
- The latent heat of fusion and vaporization are247 kJ/kg and 7600 kJ/kg respectively.

II. Experimental Setup

The welding in the plate is done in such a way that linear segment of the weld bead run on the top of the plate. The experiments where run on the samplewith the welding parameter of the TIG welding process like welding current I, welding voltage U, welding speed v, Gas Flow litre/min as given in Table 3. The schematic view of experimental setup is shown in Figure 4.

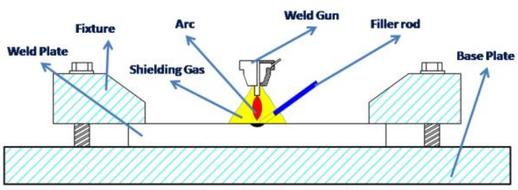

Figure 4 Schematic View of Experimental Setup

Since the welding is done manually the welding speed for each specimen is calculate form the weld length and time taken from the start to finish of the weld.

TABLE 3WELDING PARAMETERDETAILS

Current (I)	26 (Amps)
Voltage (V)	230 (volts)
Arc Efficiency (ή)	0.8
Heat Input (q)	4784 J/s (or) W
Melting Point	1400ºC

III. Results and Discussion

The empirical, finite element method and experimental analysis were done and based on the results the weld bead profile is calculated.

A. Weld bead prediction using Double Ellipsoidal heat Source

The double ellipsoidal heat source was found to be the best suited heat source and the mathematical simulation was done and is presented in Table 4. The temperature distribution from the simulation is obtained along the width and depth of the plate after 5 seconds. The temperature distribution plot along the plate width and depth is plotted as given in Figure 5 and 6.

TABLE 4 TEMPERATURE PROFILE AT 5 SEC.

Sl. NO	Bead Width		Bead Depth	
	Plate Width (mm)	Temperature (K)	Plate Depth (mm)	Temperature (K)
1.	0	2354.1113	0	2354.1113
2.	2	1897.8617	2	1809.0486
3.	4	1164.9642	4	1067.7036
4.	6	737.21039	6	696.52228
5.	8	537.11957	8	520.55444
6.	10	435.86737	10	428.0513
7.	12	380.61707	12	376.60254
8.	14	349.10657	14	346.92459
9.	16	330.62973	16	329.39682
10.	18	319.60815	18	318.89261
11.	20	312.97025	20	312.54742
12.	22	308.95688	22	308.70429
13.	24	306.53201	24	306.38031
14.	26	305.07336	26	304.98221
15.	28	304.20255	28	304.14795
16.	30	303.68796	30	303.65549
17.	32	303.3876	32	303.36847
18.	34	303.21478	34	303.20367
19.	36	303.11694	36	303.11057
20.	38	303.0625	38	303.0589
21.	40	303.03275	40	303.03076
22.	42	303.01682	42	303.01575
23.	44	303.00845	44	303.0079
24.	46	303.00418	46	303.00388
25.	48	303.00201	48	303.00186
26.	50	303.00095	50	303.00089

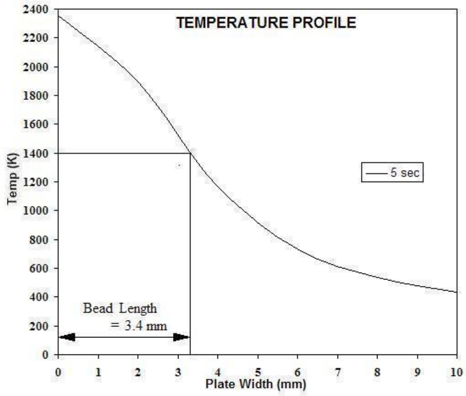

Figure 5 Calculation of Bead Length from Temperature Profile Plot

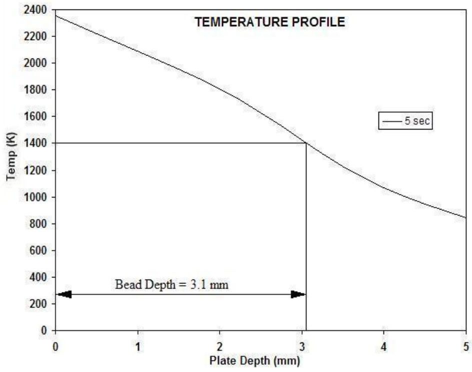

Figure 6 Calculation of Bead Depth from Temperature Profile Plot

Using the extrapolation method [13] and keeping the melting point temperature of the plate is kept as 1400 K the weld bead with and depth of penetration can be estimated. It is found that both matches nearer to the measured bead profile.

B. Weld bead prediction using Finite Element Method

The temperature contour for the simulated TIG welding is found by using the SYSWELD software and the plot of the temperature profile is obtained along the surface and the depth of plate. By the same welding parameters the simulation is done the different temperature profile is obtained. These data can be used for other welding related studies like stress prediction after welding, distortion and weld pool profile. In Figure 7 the four stages of the welding source movement aredepicted and the temperature values are given.

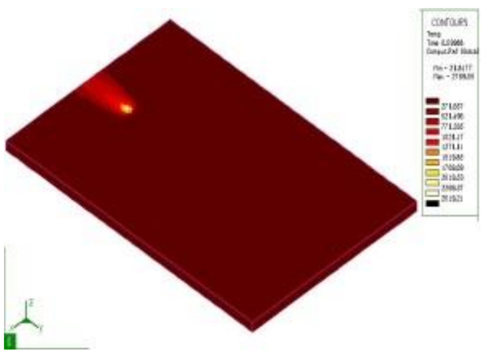

a) Heat Source at Time 0.5 sec

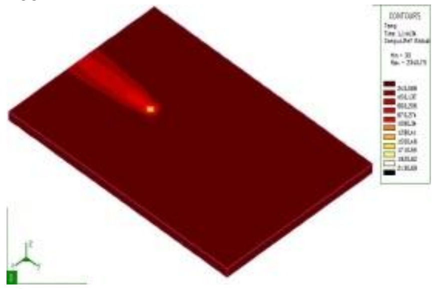

b) Heat Source at Time 1 sec

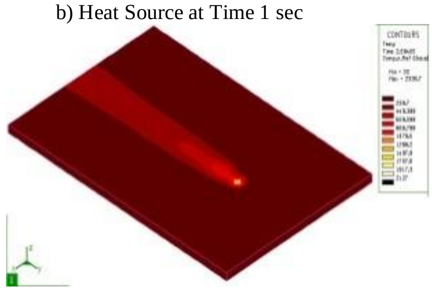

c) Heat Source at Time 2.5 sec

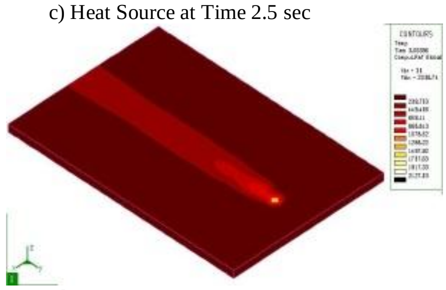

d) Heat Source at Time 3 sec

Figure 7 Stages of the heat source and temperature distribution in the plate

In this case 23 nodes are selected in the FEA model and the temperature distribution plot along the plate width is obtained. After the welding simulation is over the nodes along the depth of the plate is taken at fixed distance from the edges of the plate. And the temperature distribution on each node is obtained. Using the interpolation method and taking the melting point temperature of metal as 1400º C the bead profile is obtained. The width of the bead profile and the depth of the bead profile are found to be 7.2 mm and 3.2mm as shown in Figure 8 and 9.

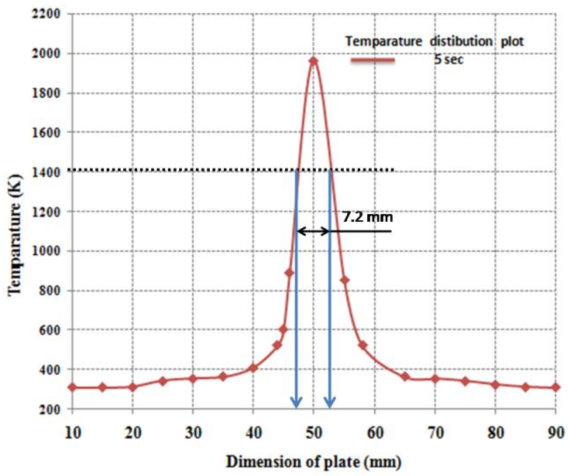

Figure 8 Temperature Profile Plot along the surface of the Plate

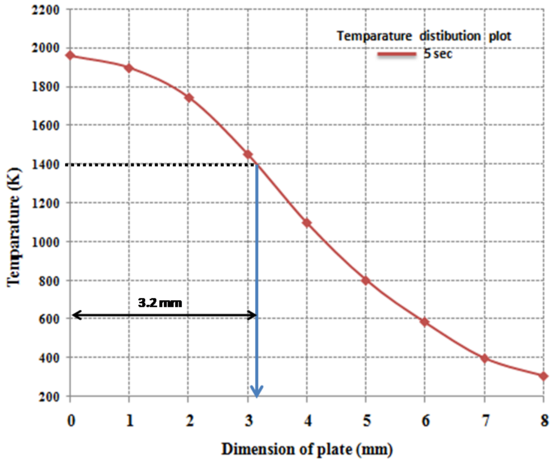

Figure 9 Temperature Profile along the depth of the plate

And the nodes are taken in such a sequence that they lay perpendicular to the weld direction. In this case 23 nodes are selected in the FEA model and the temperature distribution plot along the plate with is obtained. Using the interpolation method and taking the melting point temperature of metal as 1400° C the bead profile is obtained.

C. *Weld Bead Profile Measurement on welded plates*

The geometry of the weld bead was measured from the bead-on-plate specimen by means of digital photos taken for the top view of the weld-pool shape for welded specimens as shown in Figure 10and transverse cross sectional view of the weld-pool shape for the welded specimens is shown in Figure 11.

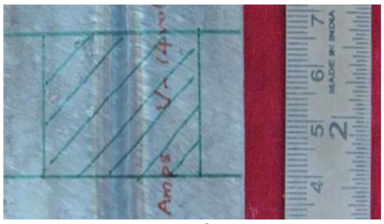

Figure 10 Top views of the welded pieces.

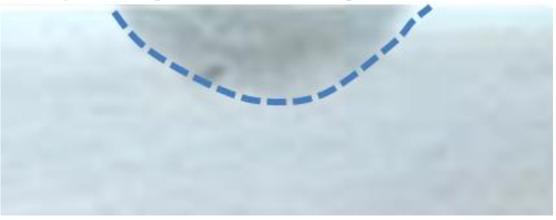

Figure 11 Cross-sectional views of the welded pieces

The experimentally obtained weld pool profile is compared with the Finite Element results and is found to match to a good extent in the Figure 12. The dimensions weld width and weld depth match well with the FEA results.

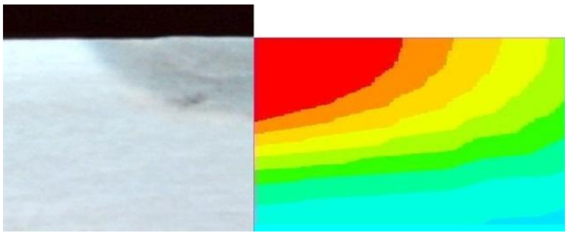

Figure 12 Comparison of Experimental and FEA results

D. *Validation of weld bead profile*

Initially the double ellipsoidal heat source model was used to develop the temperature profile plot for plate width and plate depth. The weld bead profile such as bead width and depth is predicted using extrapolation method. The finite element method studies were developed with the temperature dependent material properties [14] for better prediction and the welding simulation were carried out. The developed temperature profile from the simulation is used to predict the weld bead width and depth by extrapolation method.

TABLE 5 COMPARISON OF BEAD PROFILES FOR THE THREE METHODS

Sl. No	Methods	Bead width (mm)		Bead depth (mm)	
			Error %		Error %
1.	Experimental	7.3		3.3	
2.	Empirical	6.8	6.84	3.1	6.06
3.	Finite Element Analysis	7.2	1.36	3.2	3.03

The weld bead profile of the experimental investigation is also obtained by using image processing software. The comparison of the three methods were tabulated (Table 5) with experimental method as the reference which was found to have acceptable error percentage.

IV. Conclusion

The prediction of weld bead profile was done by using both the empirical and finite element method. To validate the predicted result an experimental investigation was done. The results obtained had acceptable error percentage.The work can be extended to residual stress distribution in a welded joint. Crack developed after welding can also be analyzed by FEA method. In various sections like T-section, I-section, cylindrical shape etc., can be modelled and simulated. Knowledge of residual stress distribution is further helpful in the assessment of failure of the component.The analysis results help us understand the phenomena governing the welding of a joint, offering insight on the mechanisms and mechanical aspect particular to the welding process. Having understood the welding mechanism, the effects of the welding can be better quantified and therefore can be better addressed in the early stages of the design.

REFERENCES

[1]. Bonifaz E.A., “Finite element Analysis of Heat Flow in Single Pass arc Welds”, Welding journal, pp 121-125, 2000.

[2]. Parmer. R.S., “Welding Process and Technology”, 2nd edition, 2001 (Khanna Publishers, New Delhi).

[3]. N.T.Nguyen, “Thermal Analysis of welds – series : Developments in Heat Transfer” ETRS Pvt Ltd, WIT Press, Australia

[4]. Zacharia, T., Vitek, J.M., &Rapaz, M., “Modeling of fundamental phenomena in welds”, Modeling Simulation Material, Sci.Engg., pp 265-288, 1995.

[5]. Nguyen, N.T., Ohata, A., Matsuoka, K., Sukuki, N. & Maeda, Y., Transient Temperature of Bead-on-Plate Predicted by Double-Ellipsoidal Power Density Moving Heat Source. Paper No. 107, Proc. Of the National Meeting of Japanese Welding Society, No 64, pp. 16-17, 21-23 April, 1999.

[6]. Nguyen, N.T., Analytical Solution for Semi-Infinite Boby Subjected to 3-D Moving Heat Source and Its Application in Weld Pool Simulation. Proc. Of IMPLAST'2000, the 7th International Symposium on Structural Failure and Plasticity, Melbourne, Australia, Eds. X.L. Zhao & G.H. Grzebieta, pp. 819-826, 4-6 October 2000.

[7]. Nguyen, N.T., Mai Y-W., Simpson, S. &Ohta, A., Approximate Analytical Solution for Double-Ellipsoidal Heat Source in Finite Thick Plate, 2002, Welding Journal, 2004.

[8]. Carslaw, H.S. & Jaeger, J.C., "Conduction of Heat in Solid", Oxford University Press, pp. 255, 1967.

[9]. Goldak. J., Chakravarti. A., &Bibby. M., "A Double Ellipsoidal Finite Element Model for Welding Heat Sources, IIW Doc. No. 212-603-85. 1985.

[10]. Pavelic, V., Tanbakuchi, R., Uyehara, R., &Myera, P.S., "Experimental and computed temperature histories in GTAW of thin plates", Welding Journal, V 48, pp 2955-3053, 1969.

[11]. Jeong, S.K. & Cho, H.S., An Analytical Solution to Predict the Transient Temperature Distribution in Fillet Arc Welds. Welding Journals, 76(6), pp. 223s-232s, 1997.

[12]. Mahapatra. M.M., "Three-dimensional finite element analysis to predict the effects of shielded metal arc welding process parameters on temperature distributions and weldment zones in butt and one-sided fillet welds", Journal of Engineering Manufacture, pp 837-845,2005.

[13]. Rayes, M.E.I., Walz, C., &Sepold, G., "The Influence of Various Welding Parameters on Bead Geometry", Supplement to the Welding Journal, pp 147-153, May 2004.

[14]. Chao. Y.J, "Effects of Temperature Dependent Material Properties on Welding Simulation", Journal of Computers and Structures, Vol 80, pp 967-976.2002.

Global Journal of Pure and Applied Mathematics (GJPAM) ISSN 0973-1768 Volume 12,Number 4 (2016)

Optimization of friction stir spot welding parameters on dissimilar joints using response surface methodology

*S. Siddharth**
Department of Mechanical Engineering,
University College of Engineering,
BIT Campus, Anna University Tiruchirappalli,
Tiruchirappalli, Tamil Nadu, India.

Email: sksmsiddharth1@yahoo.in

T. Senthilkumar
Department of Mechanical Engineering,
University College of Engineering,
BIT Campus, Anna University Tiruchirappalli,
Tiruchirappalli, Tamil Nadu, India.

***Abstract*— Joining of dissimilar materials pose a challenge due to differences in mechanical and chemical properties of the materials. For these types of requirements, solid state joining process like friction welding are used. A variant of linear friction stir welding called as friction stir spot welding process is used for spot joining in lap configurations. In this paper optimization of friction stir spot welding process parameters of dissimilar Aluminium/ Copper joints, such as tool rotational speed, axial plunge depth and dwell time is done using response surface methodology. The effect of the process parameters on strength of the dissimilar joints are ascertained. Optimum parameters for maximum weld strength is obtained.**

Keywords*— *Friction stir spot welding; dissimilar materials; optimization; Response Surface Methodology

I. INTRODUCTION

Response surface methodology (RSM) is a statistical tool used to explore relationships between many explanatory variables and one or more response variables, which was introduced by G. E. P. Box and K. B. Wilson in 1951 [1]. An optimal response is obtained, by using sequentially designed set of experiments [2].

For the purpose of elimination of copper (II) ions from watery solution, the utilization of waste flax meal was explored. A feed-forward neural network with a proper framework, which was properly optimized by using RSM, was applied for appropriate prediction of the bio sorption performance for the effective removal of Cu^{2+} ions by waste flax meal [3].

Using a fully developed three dimensional heat transfer and flow model, the geometric design for double tube heat exchangers with inner corrugated tube was investigated using response surface methodology [4].

Modelling of experimental data of surface roughness of $Co_{28}Cr_6Mo$ medical alloy machined using a completely computer numerically controlled lathe using optimized cutting conditions (spindle speed of circular rotation, feed rate, depth of cut and tool tip radius) were done and evaluated using response surface methodology [5].

Friction stir spot welding (FSSW), a linear variant of friction stir welding (FSW), is a novel method of joining dissimilar materials with different melting, boiling point, density differences etc. [6]. Friction stir spot welding of high-Mn twinning-induced plasticity steel has been studied and its microstructural characteristics and physical aspects were evaluated [7].

II. EXPERIMENTAL INVESTIGATIONS

A. Materials and Methods

For the present investigation, two different dissimilar combination of material were chosen. Alloy plates of Aluminum and Copper were chosen with a thickness of 1.5 mm. The process parameters which determine the output quality of friction stir spot dissimilar joints are

- Tool Penetration Depth in mm
- Tool rotation rate in rpm
- Tool shoulder plunge depth in mm
- Dwell time – Operation duration in seconds
- Tool plunge speed in mm/min
- Axial force of the rotating tool in N

From these three most important process parameters are chosen and listed in Table 1

TABLE 1 - Process parameters of FSSW

S No	**Parameters**	**Notation**
1	Tool rotational speed (rpm)	R
2	Dwell time in seconds	T
3	Plunge depth in mm	D

B. Identification of feasible process parameters

Initial sets of experiments were conducted by trial and error method and with reference from previous literatures and

*Corresponding author.

This paper was presented by the first author in the National Conference on AMASE-2016 conducted in Department of Mathematics, University College of Engineering Pattukkottai, Thanjavur, Tamil Nadu, India, on 22nd January 2016.

the feasible limits of the process parameters for proper joining of dissimilar materials are obtained. The lower limit is set below which the material does not weld together and the upper limit is set beyond which there is excess heat generation.

Experiments were conducted to attain the feasible working parameters for the tool rotational speed RS in rpm, Dwell time DT in seconds and Plunge depth PD in millimeters.

For RS, DT and PD the mean values were taken as 950, 6, 1 whereas low and high values were taken as 900, 5, 0.8 and 1000, 7, 1.2 respectively.

A 3 factor three level central composite design is chosen as shown in Table 2.

TABLE 2. 3 factor 3 levels of FSSW

S No	Name	Unit	Level		Alpha	
			Low	High	Low	High
1	R	rpm	-1	1	-1.68	1.68
2	T	sec	-1	1	-1.68	1.68
3	D	mm	-1	1	-1.68	1.68

The total number of runs = 20

No of not center points = 14

No of center points = 6

The response is two

1. Hardness of Al material
2. Hardness of Cu material

The central composite design matrix is given in Table 3

TABLE 3. Design Matrix

S No	Std	Run	R	T	D
1	7	1	-1	1	1
2	16	2	0	0	0
3	9	3	-1.68	0	0
4	3	4	-1	1	-1
5	1	5	-1	-1	-1
6	18	6	0	0	0
7	6	7	1	-1	1
8	4	8	1	1	-1
9	14	9	0	0	1.68
10	20	10	0	0	0
11	2	11	1	-1	-1
12	10	12	1.68	0	0
13	12	13	0	1.68	0
14	19	14	0	0	0
15	13	15	0	0	-1.68
16	11	16	0	-1.68	0
17	15	17	0	0	0
18	17	18	0	0	0
19	8	19	1	1	1
20	5	20	-1	-1	1

The design summary of the response surface study, with initial central composite design, of the quadratic model is given in Table 4. The correlation at 0.068 for Al hardness and at 0.067 for Cu hardness are given in Fig. 1 and Fig. 2.

TABLE 4. Design summary

Study Type	Response Surface		Runs	20							
Initial Design	Central Composite		Blocks	No Blocks							
Design Model	Quadratic										
Factor	Name	Units	Type	Low Actual	High Actual	Low Coded	High Coded	Mean	Std. Dev.		
A	R	rpm	Numeric	-1	1	-1	1	0	0.826343		
B	T	seconds	Numeric	-1	1	-1	1	0	0.826343		
C	D	millimeter	Numeric	-1	1	-1	1	0	0.826343		
Response	Name	Units	Obs	Analysis	Minimum	Maximum	Mean	Std. Dev.	Ratio	Trans	Model
Y1	Al hardness	HV	20	Polynomial	83	105	92.65	6.51364	1.26506	None	No model chosen
Y2	Cu hardness	HV	20	Polynomial	69	93	79.95	6.917189	1.347826	None	No model chosen

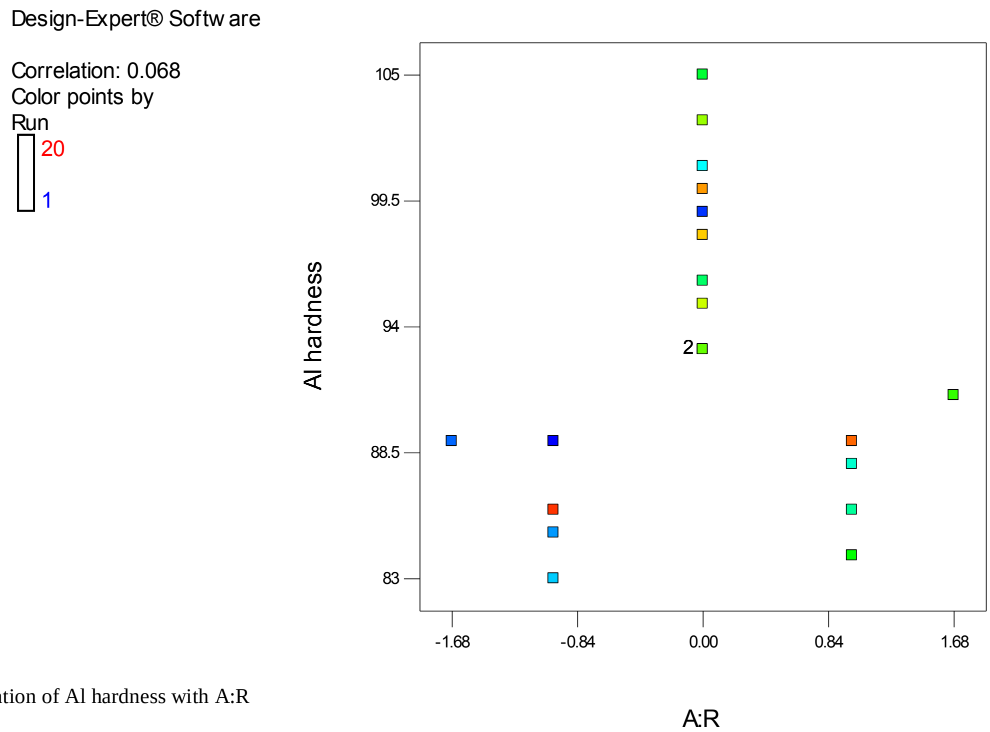

Fig 1. Correlation of Al hardness with A:R

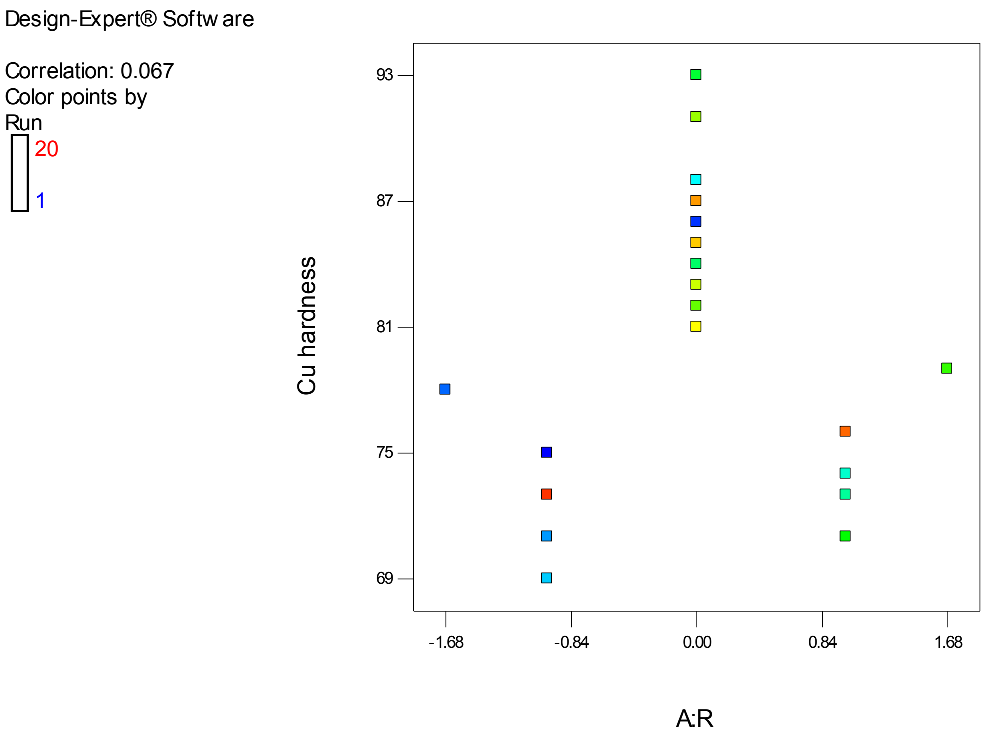

Fig. 2. Correlation of Cu hardness with A:R

Design Matrix Evaluation for Response Surface Quadratic Model is given in

Degrees of Freedom for Evaluation

Model	9
Residuals	10
Lack 0f Fit	5
Pure Error	5
Corr Total	19

TABLE – 5. Design evaluation response model

Power at 5 % alpha level for effect of						
Term	StdErr**	VIF	Ri-Squared	0.5 Std. Dev.	1 Std. Dev.	2 Std. Dev.
A	0.270598	1	0	13.3 %	38.6 %	91.4 %
B	0.270598	1	0	13.3 %	38.6 %	91.4 %
C	0.270598	1	0	13.3 %	38.6 %	91.4 %
AB	0.353553	1	0	9.8 %	24.9 %	72.2 %
AC	0.353553	1	0	9.8 %	24.9 %	72.2 %
BC	0.353553	1	0	9.8 %	24.9 %	72.2 %
A^2	0.26342	1.018265	0.017938	40.4 %	92.7 %	99.9 %
B^2	0.26342	1.018265	0.017938	40.4 %	92.7 %	99.9 %
C^2	0.26342	1.018265	0.017938	40.4 %	92.7 %	99.9 %
**Basis Std. Dev. = 1.0						

TABLE – 6. Measures derived

Measures Derived From the (X'X)^-1 Matrix			
S No	Std	Leverage	Point Type
1	1	0.669768	Fact
2	2	0.669768	Fact
3	3	0.669768	Fact
4	4	0.669768	Fact
5	5	0.669768	Fact
6	6	0.669768	Fact
7	7	0.669768	Fact
8	8	0.669768	Fact
9	9	0.607303	Axial
10	10	0.607303	Axial
11	11	0.607303	Axial
12	12	0.607303	Axial
13	13	0.607303	Axial
14	14	0.607303	Axial
15	15	0.16634	Center
16	16	0.16634	Center
17	17	0.16634	Center
18	18	0.16634	Center
19	19	0.16634	Center
20	20	0.16634	Center
	Average =	0.5	

The standard error of the design in represented in Fig. 3. Vickers micro hardness testing equipment was used for testing the interface micro-hardness of the joints. For one particular specification of the process parameters, three sets of values of micro-hardness were measured and the average of the three is taken.

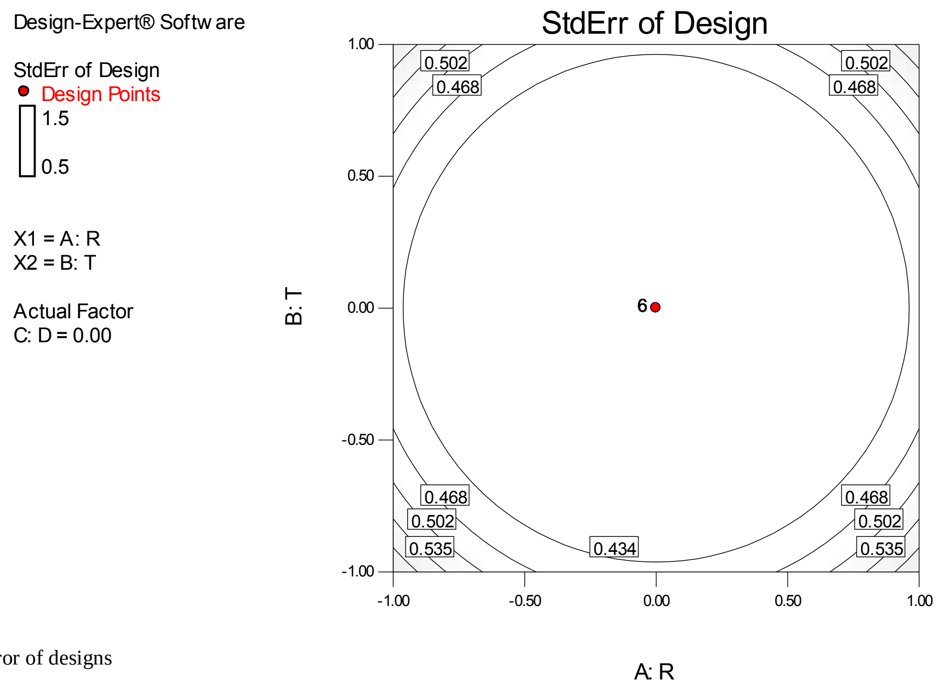

Fig. 3. Standard error of designs

TABLE – 7 ANNOVA response for surface quadratic model for Al micro hardness

Response	1	Al hardness				
	Sum of		Mean	F	p-value	
Source	Squares	df	Square	Value	Prob > F	
Model	685.3442	9	76.14935	4.665848	0.0123	significant
A-R	3.970343	1	3.970343	0.243272	0.6325	
B-T	4.686292	1	4.686292	0.28714	0.6038	
C-D	18.00697	1	18.00697	1.103329	0.3183	
AB	0.5	1	0.5	0.030636	0.8645	
AC	0	1	0	0	1.0000	
BC	0	1	0	0	1.0000	
A^2	385.7628	1	385.7628	23.63659	0.0007	
B^2	243.8078	1	243.8078	14.93867	0.0031	
C^2	150.2814	1	150.2814	9.208088	0.0126	
Residual	163.2058	10	16.32058			
Lack of Fit	129.2058	5	25.84116	3.800171	0.0846	not significant
Pure Error	34	5	6.8			
Cor Total	848.55	19				

TABLE – 8 ANNOVA response for surface quadratic model for Cu micro hardness

Response	1	Cu hardness				
ANOVA for Response Surface Quadratic Model						
Analysis of variance table [Partial sum of squares - Type III]						
	Sum of		Mean	F	p-value	
Source	Squares	df	Square	Value	Prob > F	
Model	696.8315	9	77.42572	2.976555	0.0522	not significant
A-R	4.320903	1	4.320903	0.166113	0.6922	
B-T	6.863741	1	6.863741	0.26387	0.6186	
C-D	18.00697	1	18.00697	0.69226	0.4248	
AB	0	1	0	0	1.0000	
AC	0.5	1	0.5	0.019222	0.8925	
BC	0	1	0	0	1.0000	
A^2	383.8563	1	383.8563	14.75698	0.0033	
B^2	242.2926	1	242.2926	9.314701	0.0122	
C^2	165.9309	1	165.9309	6.379051	0.0301	
Residual	260.1185	10	26.01185			
Lack of Fit	212.7852	5	42.55704	4.495462	0.0623	not significant
Pure Error	47.33333	5	9.466667			
Cor Total	956.95	19				

The "Deficit of Fit F-value" of 3.80 implies there is 8.46% chance that a "Deficit of Fit F-value" this large could occur due to noise.

III. RESULTS AND ANALYSIS

Analysis of variance (ANOVA) is an assemblage statistically built up models used to analyze the changes and the dissimilarities among the group means with their associated rules and regulations (such as "variation" among and between groups).

Using response surface methodology, ANOVA regression analysis is done and the results are tabulated. In Table 7, ANOVA response for surface quadratic model for Al micro hardness is given and in table 8, ANOVA response for surface quadratic model for Cu micro hardness is given.

In Al regression analysis, The Model F-value of 4.67 implies the model is significant. There is only a 1.23% chance that a "Model F-Value" this large could occur due to noise. Values of "Prob > F" less than 0.0500 is an absolute explanation that the terms in the models are significant. In this case A2, B2, C2 are significant model terms. Values greater than 0.1000 suggests that the model expressions are insignificant.

In Cu regression analysis, the Model F-value of 2.98 implies there is a 5.22% chance that a "Model F-Value" this large could occur due to noise.

Values of "Prob > F" less than 0.0500 shows that model terms values are of significance.

In this case A^2, B^2, C^2 are significant model terms. Values more than 0.1000 shows that the model term values are not valid values. If there are many insignificant model terms (not counting those required to support hierarchy), model reduction may improve your model.

The "Lack of Fit F-value" of four and a half clearly determines that there is a 6.23 percent chance that a "Deficit of Fit F-value" this large could occur due to noise. Deficit (Lack) of fit is bad -- we want the model to fit.

In Fig. 4 and Fig. 5 normal and design plots for Cu micro hardness are given.

In Fig. 6 and Fig. 7 normal and design plots for Al micro hardness are given.

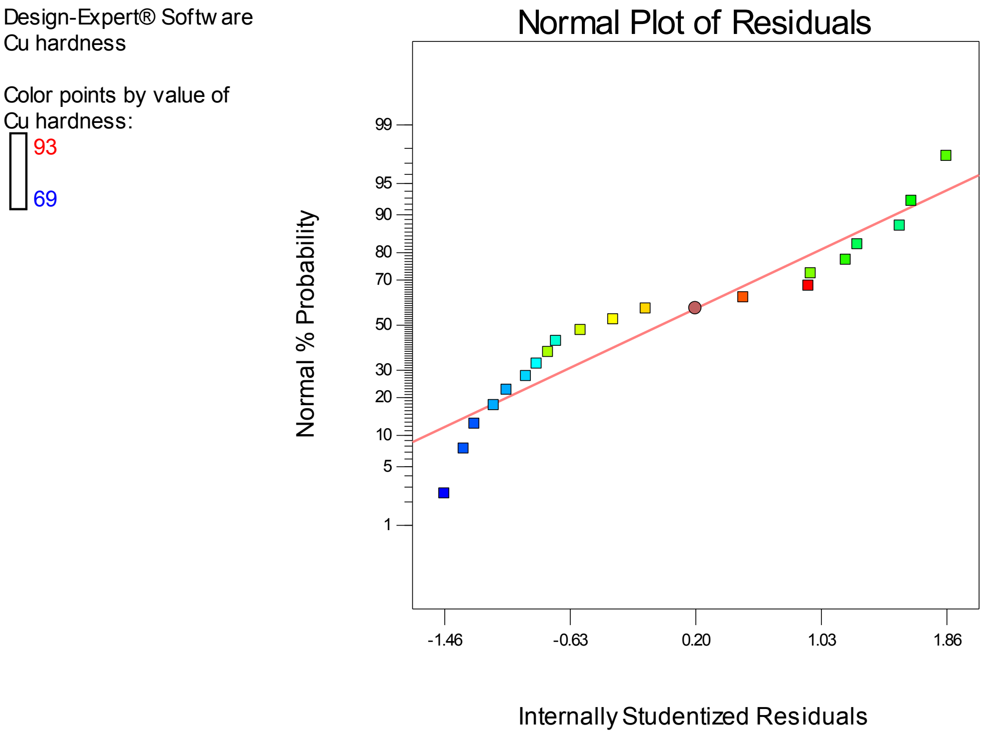

Fig. 4. Normal plots of residuals of Cu micro hardness

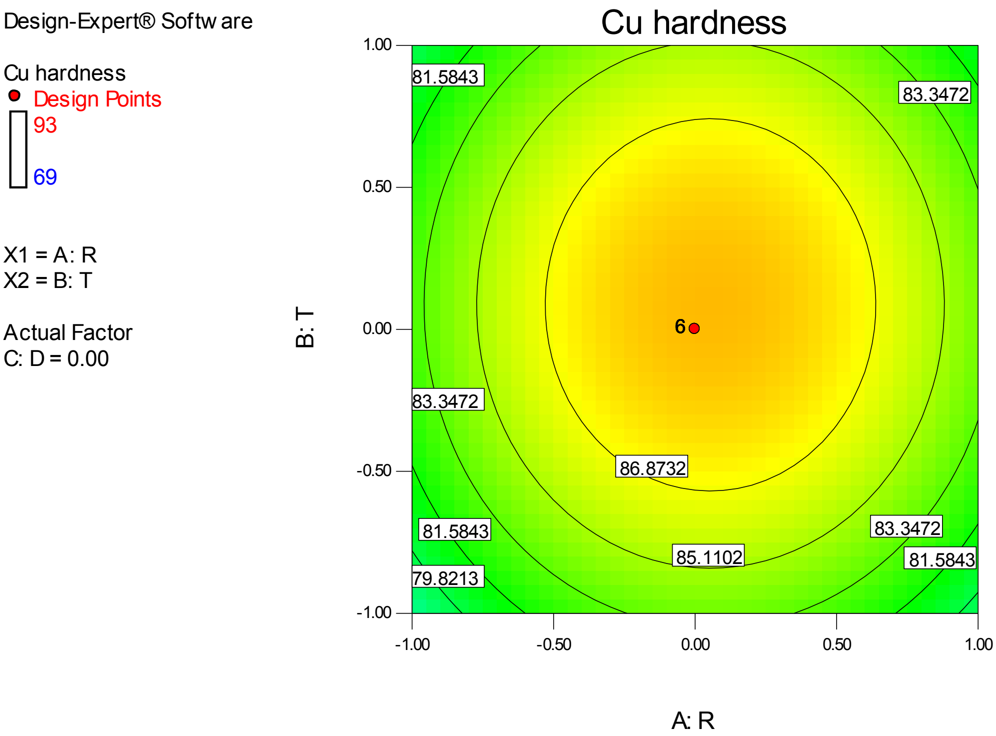

Fig. 5. Design plots of Cu micro hardness

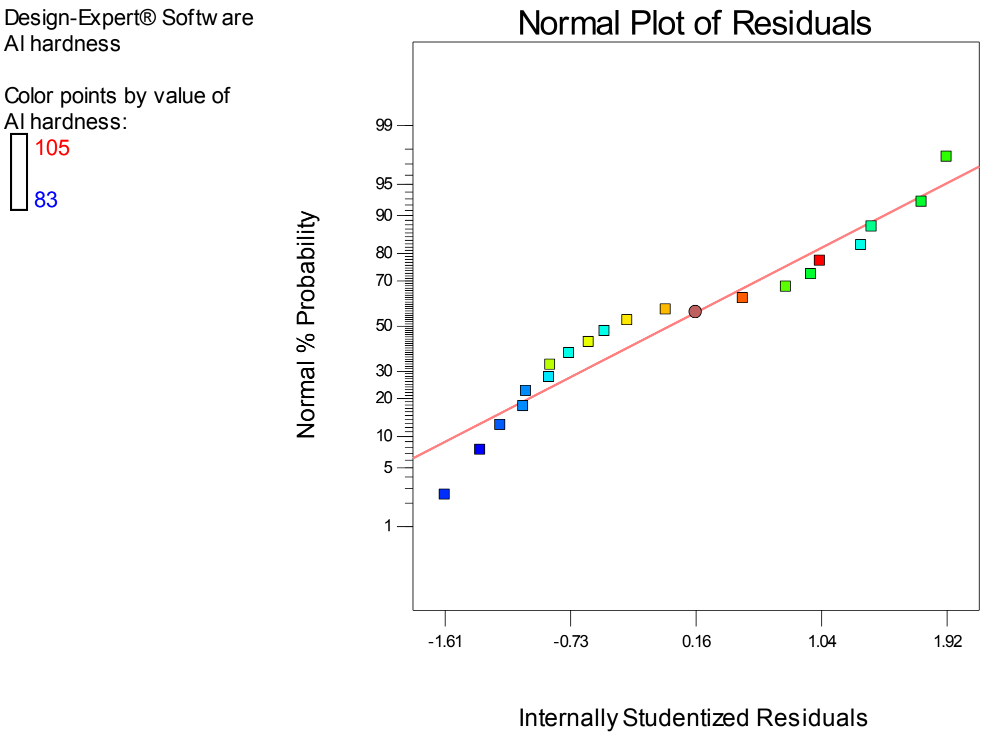

Fig. 6. Normal plots of residuals of Al micro hardness

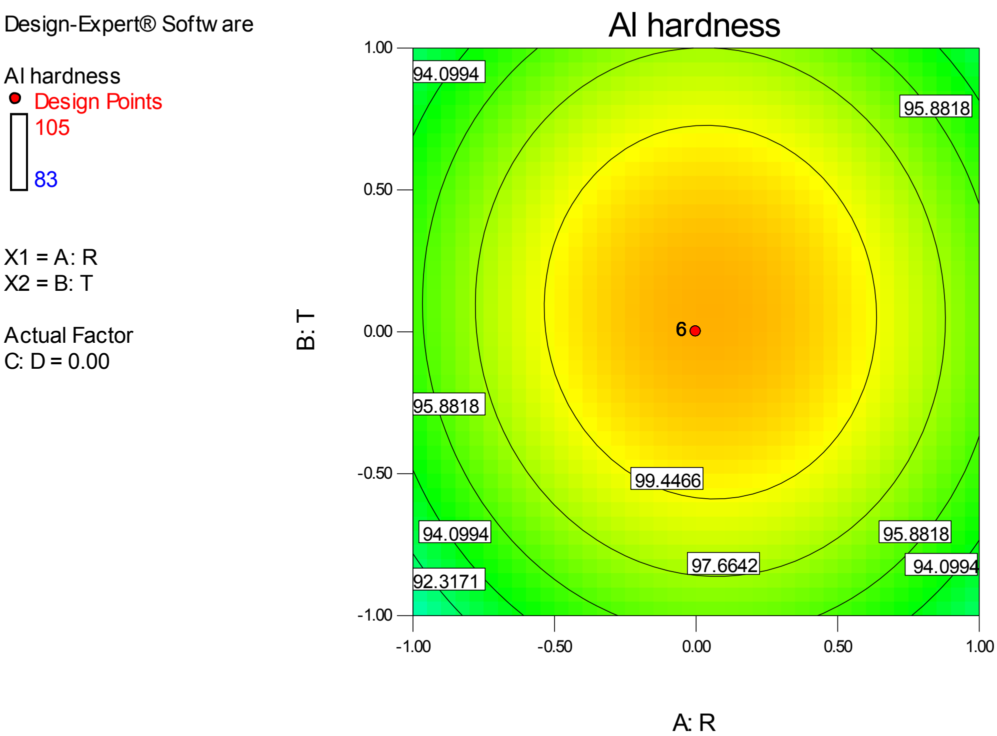

Fig. 7. Design plots of Al micro hardness

IV. CONCLUSION

Thus using response surface methodology, optimization of friction stir spot welding process parameters of dissimilar joints of Al and Cu have been done.

Using three factor three level central composite design, the parameter values were taken for the experiments.

Using ANOVA analysis, the significance of the developed model were analyzed.

The design and normal plots generated gives the relationship between the material micro hardness with important process parameters such as dwell time, plunge depth and tool rotational speed.

ACKNOWLEDGEMENT

The authors wish to extend their thanks to Mr. Murali Lakshmi Narayanan, Managing Director, M/S. Omega Techniks India (P) Ltd, SIDCO Estate, Ambattur, Chennai, India for assistance in fabrication of FSSW joints.

REFERENCES

[1] C.B. Smith, J.F. Hinrichs, P.C. Ruehl, "Friction Stir and Friction Stir Spot Welding - Lean, Mean and Green" - Friction Stir Link, Inc. W227 N546 Westmound Dr., Waukesha, WI 53186.

[2] R.S. Mishra, Z.Y. Ma, "Friction stir welding and processing", Materials Science and Engineering: R: Reports, vol. 50, Issues 1–2, 31, 2005, pp.1–78.

[3] Daria Podstawczyk, Anna Witek-Krowiak, Anna Dawiec, Amit Bhatnagar, "Biosorption of copper (II) ions by flax meal: Empirical modeling and process optimization by response surface methodology (RSM) and artificial neural network (ANN) simulation", Ecological Engineering, vol. 83, 2015, pp 364-379.

[4] Huai-Zhi Han, Bing-Xi Li, Hao Wu, Wei Shao "Multi-objective shape optimization of double pipe heat exchanger with inner corrugated tube using RSM method", International Journal of Thermal Sciences, vol. 90, 2015, pp 173-186.

[5] İlhan Asilturk, Suleyman Neşeli, Mehmet Alper Ince "Optimization of parameters affecting surface roughness of $Co_{28}Cr_6Mo$ medical material during CNC lathe machining by using the Taguchi and RSM methods", Measurement, vol. 78, 2016, pp 120-128.

[6] S. Siddharth, T. Senthilkumar, M. Joseph Fernandus, "Study of Friction Stir Spot Welding Process and its Parameters for Increasing Strength of Dissimilar Joints", Proceedings of International Conference on Advances in Mechanical Engineering, ICAME 2015, 15th& 16th of October 2015, ISBN 978-93-85477-29-4, pp 900-906

[7] M.M.Z. Ahmed, Essam Ahmed, A.S. Hamada, S.A. Khodir, M.M. El-Sayed Seleman, B.P. Wynne, "Microstructure and mechanical properties evolution of friction stir spot welded high-Mn twinning-induced plasticity steel", Materials & Design, Vol. 91, 2016, pp. 378–387

Global Journal of Pure and Applied Mathematics (GJPAM) ISSN 0973-1768 Volume 12,Number 4 (2016)

M/M/1/K/N interdependent retrial queueing model with controllable arrival rates, balking and retention of reneged customers

*B. Antline Nisha**
P.G and Research Department of Mathematics,
St.Joseph's College (Autonomous),Tiruchirappalli,
Tamilnadu, India.
Email: antlinenisha@gmail.com

M. Thiagarajan
P.G and Research Department of Mathematics,
St.Joseph's College (Autonomous),Tiruchirappalli,
Tamilnadu, India

***Abstract*—In this paper, a finite capacity single server finite population interdependent retrial queueing model with controllable arrival rates, balking and retention of reneged customers is considered. The steady state solutions and the system characteristics are derived and analyzed for this model. Some particular cases of the model have been discussed. This model may be of great importance to the business facing the serious problem of customer impatience. Numerical results are given for better understanding and relevant conclusion is presented**

***Keywords*— retrial queue; reneging; customer retention; balking; interdependent primary arrival and service processes; finite capacity.**

I. INTRODUCTION

Retrial queues have been widely used to model many problems in telephone switching systems, telecommunication networks and computer systems for competing to gain service from a central processing unit and so on. Moreover, retrial queues are also used as mathematical models for several computer systems: packet switching networks, shared bus local area networks operating under the carrier-sense multiple access protocol and collision avoidance star local area networks, etc. Retrial queueing systems are characterized by the feature that a blocked customer (a customer who finds the server unavailable) may leave the service area temporarily and join a retrial group in order to retry his request after some random time. Abandonment happens when a subscriber's call becomes rejected and the subscriber gets impatient and gives up after a certain time without getting service. The model studied in this paper not only takes into account retrials due to congestion but also considers the effects of balking and retention of reneged customers discipline.

The detailed account on retrial queues can be found in the book on retrial queues by Falin and Templeton [10]. Artalejo [2] analyzed queueing system with returning customers and waiting line. Artalejo [3] studied retrial queues with a finite number of sources. An extensive survey on retrial queues can be found in notable survey articles by Artalejo [4-6] and Kumar and Kumar Sharma [12-15] have studied the M/M/1/N queue with the concept of retention of reneged customers. Thiagarajan and Srinivasan [16] have analyzed M/M/C/K/N interdependent queueing model with controllable arrival rates balking, reneging and spares. Jain and Bhagat [11] have considered the finite population retrial queueing model with threshold recovery geometric arrivals and impatient customers. Recently Antline Nisha and Thiagarajan [17] have studied M/M/1/K/N interdependent retrial queueing model with controllable arrival rates. In general it is assumed that the arrival stream of primary calls, the service times and retrial times are mutually independent. But the primary arrival and service processes are interdependent in practical situations. Although it is natural in the real world, there are only few works taking into consideration retrial phenomena involving the interdependent controllable arrival rates.

In this paper, the M/M/1/K/N interdependent retrial queueing model with controllable arrival rates, balking and retention of reneged customers is considered. In section 2, the description of the model is given stating the relevant postulates. In section 3, the steady state equations are obtained. In section 4, the characteristics of the model are derived. In section 5, numerical results are calculated.

II. DESCRIPTION OF THE MODEL

Consider a single server finite capacity finite source retrial queueing system in which primary customers arrive according to the Poisson flow of rate λ_0 and λ_1, service times are exponentially distributed with rate μ. If a primary customer finds some server free, he instantly occupies it and leaves the system after service. Otherwise, if the server is busy, at the time of arrival of a primary call then with probability $H_1 \geq 0$ the arriving customer enters an orbit and repeats his demand after an exponential time with rate θ. Thus the Poisson flow of repeated call follow the retrial policy where the repetition times of each customer is assumed to be independent and exponentially distributed.

If an incoming repeated call finds the line free, it is served and leaves the system after service, while the source which produced this repeated call disappears. Otherwise, if the server is occupied at the time of a repeated call arrival with probability $(1\text{-}H_2)$ the source leaves the system

*Corresponding author.

This paper was presented by the first author in the National Conference on AMASE-2016 conducted in Department of Mathematics, University College of Engineering Pattukkottai, Thanjavur, Tamil Nadu, India, on 22nd January 2016.

without service. Each customer upon arriving in the queue will wait a certain length of time (reneging time) for his service to begin. If it has not begun by then, he will get impatient and may leave the queue without getting service with probability p and may remain in the queue for his service with probability (q = 1-p). The reneging times follow exponential distribution with parameter α.

It is assumed that the primary arrival process [$X_1(t)$] and the service process [$X_2(t)$] of the systems are correlated and follow a bivariate Poisson process given by

$P(X_1=x_1,X_2=x_2;t)$

$$= e^{-(\lambda_i + \mu-\varepsilon)t}\frac{\sum_{j=0}^{\min(x_1 x_2)} \varepsilon(t)^j \; (\lambda_i-\varepsilon)t^{x_1-j}\;(\mu-\varepsilon)t^{x_2-j}}{j!\,(x_1-j)!\,(x_2-j)!}$$

$x_1, x_2 = 0,1,2,\ldots,\lambda_i$, $\mu < 0$, $i = 0,1$;

with parameters λ_0, λ_1, μ_n and ε as mean faster rate of primary arrivals, mean slower rate of primary arrivals, mean service rate and mean dependence rate (covariance between the primary arrival and service processes) respectively.

At time t, let N(t) be the number of sources of repeated calls and C(t) be the number of busy servers. The system state at time t can be described by means of a bivariate process {C(t),N(t)},t ≥ 0, where C(t)=1 or 0 according as the server is busy or idle, the process will be called CN process. If the service time is exponential, then C(t),N(t) is Markovian.

The process N(t),C(t) ;t ≥ 0 forms a Markov chain with state space (n,c)|n = {0,1,2,.....r-1,r,r+1,....R-1,R,R+1....K} ,c={ 0,1}. Let C and N be the numbers of customers in the service facility and in the orbit, respectively, in steady state. The state probabilities at time t are defined as follows

III. Steady State Equation

Let $P_{0,n,0}$ denote the steady state probability that there are n customers in the queue when the system is in the faster rate of primary arrivals and the server is idle.

Let $P_{0,n,1}$ denote the steady state probability that there are n customers in the queue when the system is in the slower rate of primary arrivals and the server is idle.

Let $P_{1,n,0}$ denote the steady state probability that there are n customers in the queue when the system is in the faster rate of primary arrivals and the server is busy.

Let $P_{1,n,1}$ denote the steady state probability that there are n customers in the queue when the system is in the slower rate of primary arrivals and the server is busy.

We observe that only $P_{0,n,0}$ and $P_{1,n,0}$ exists when n=0,1,2, ……., r-1,r; $P_{0,n,0}$, $P_{1,n,0}$, $P_{0,n,1}$ and $P_{1,n,1}$ exist when n=r+1,r+2,……, R-2,R-1; $P_{0,n,1}$ and $P_{1,n,1}$ exists when n=R,R+1,….. , K. Further $P_{0,n,0}= P_{1,n,0} = P_{0,n,1} = P_{1,n,1} = 0$ if n>K.

The steady state equations are

$-N(\lambda_0-\varepsilon)P_{0,0,0}+(\mu-\varepsilon)P_{1,0,0}=0$ (1)

$-[(N-1)H_1(\lambda_0-\varepsilon)+(\mu-\varepsilon)]P_{1,0,0}+N(\lambda_0-\varepsilon)P_{0,0,0}$
$+\theta P_{0,1,0}+\theta(1-H_2)P_{1,1,0}=0$ (2)

$-[(N-n)(\lambda_0-\varepsilon)+n\theta]P_{0,n,0}+(\mu-\varepsilon)P_{1,n,0}=0$ (3)

$-[(N-n-1)H_1(\lambda_0-\varepsilon)+(\mu-\varepsilon)+n\theta(1-H_2)+$
$(n-1)\alpha p]P_{1,n,0}+[(N-n)(\lambda_0-\varepsilon)]P_{0,n,0}+$
$[(N-n)H_1(\lambda_0-\varepsilon)]P_{1,n-1,0}+(n+1)\theta P_{0,n+1,0}+$
$[(n+1)\theta(1-H_2)+n\alpha p]P_{1,n+1,0}=0,$
$n=1,2,3,\ldots,r-1$ (4)

$-[(N-r)(\lambda_0-\varepsilon)+r\theta]P_{0,r,0}+(\mu-\varepsilon)P_{1,r,0}=0$ (5)

$-[(N-r-1)H_1(\lambda_0-\varepsilon)+(\mu-\varepsilon)+r\theta(1-H_2)+$
$(r-1)\alpha p]P_{1,r,0}+[(N-r)(\lambda_0-\varepsilon)]P_{0,r,0}+$
$[(N-r)H_1(\lambda_0-\varepsilon)]P_{1,r-1,0}+(r+1)\theta P_{0,r+1,0}+$
$[(r+1)\theta(1-H_2)+r\alpha p]P_{1,r+1,0}+(r+1)\theta P_{0,r+1,1}+$
$[(r+1)\theta(1-H_2)+r\alpha p]P_{1,r+1,1}=0$ (6)

$-[(N-n)(\lambda_0-\varepsilon)+n\theta]P_{0,n,0}+(\mu-\varepsilon)P_{1,n,0}=0$ (7)

$-[(N-n-1)H_1(\lambda_0-\varepsilon)+(\mu-\varepsilon)+n\theta(1-H_2)+$
$(n-1)\alpha p]P_{1,n,0}+[(N-n)(\lambda_0-\varepsilon)]P_{0,n,0}+$
$[(N-n)H_1(\lambda_0-\varepsilon)]P_{1,n-1,0}+(n+1)\theta P_{0,n+1,0}+$
$[(n+1)\theta(1-H_2)+n\alpha p]P_{1,n+1,0}=0,$
$n=r+1,r+2,\ldots,R-2$ (8)

$-[(N-R+1)(\lambda_0-\varepsilon)+(R-1)\theta]P_{0,R-1,0}+(\mu-\varepsilon)P_{1,R-1,0}=0$ (9)

$-[(N-R)H_1(\lambda_0-\varepsilon)+(\mu-\varepsilon)+(R-1)\theta(1-H_2)]P_{1,R-1,0}+$
$[(N-R+1)(\lambda_0-\varepsilon)]P_{0,R-1,0}+$
$[(N-R+1)H_1(\lambda_0-\varepsilon)]P_{1,R-2,0}=0$ (10)

$-[(N-r-1)(\lambda_1-\varepsilon)+(r+1)\theta]P_{0,r+1,1}+(\mu-\varepsilon)P_{1,r+1,1}=0$ (11)

$-[(N-r-2)H_1(\lambda_1-\varepsilon)+(\mu-\varepsilon)+(r+1)\theta(1-H_2)+$
$(r\alpha p)]P_{1,r+1,1}+[(N-r-1)(\lambda_1-\varepsilon)]P_{0,r+1,1}+$
$[(N-n)H_1(\lambda_1-\varepsilon)]P_{0,r+1,1}+(r+2)\theta P_{0,r+2,1}+$
$[(r+2)\theta(1-H_2)+(r+1)\alpha p]P_{1,r+2,1}=0$ (12)

$-[(N-n)(\lambda_1-\varepsilon)+n\theta]P_{0,n,1}+(\mu-\varepsilon)P_{1,n,1}=0$ (13)

$-[(N-n-1)H_1(\lambda_1-\varepsilon)+(\mu-\varepsilon)+n\theta(1-H_2)+$
$(n-1)\alpha p]P_{1,n,1}+[(N-n)(\lambda_1-\varepsilon)]P_{0,n,1}+$
$[(N-n)H_1(\lambda_1-\varepsilon)]P_{1,n-1,1}+(n+1)\theta P_{0,n+1,1}+$
$[(n+1)\theta(1-H_2)+n\alpha p]P_{1,n+1,1}=0,$
$n=r+2,r+3,\ldots,R-1$ (14)

$-[(N-R)(\lambda_1-\varepsilon)+R\theta]P_{0,R,1}+(\mu-\varepsilon)P_{1,R,1}=0$ (15)

$-[(N-R-1)H_1(\lambda_1-\varepsilon)+(\mu-\varepsilon)+R\theta(1-H_2)+$
$(R-1)\alpha p]P_{1,R,1}+[(N-R)(\lambda_1-\varepsilon)]P_{0,R,1}+$
$[(N-R)H_1(\lambda_1-\varepsilon)]P_{1,R-1,1}+[(N-R)H_1(\lambda_0-\varepsilon)]P_{1,R-1,0}+$
$(R+1)\theta P_{0,R+1,1}+[(R+1)\theta(1-H_2)+R\alpha p]P_{1,R+1,1}=0$ (16)

$-[(N-n)(\lambda_1-\varepsilon)+n\theta]P_{0,n,1}+(\mu-\varepsilon)P_{1,n,1}=0$ (17)

$-[(N-n-1)H_1(\lambda_1-\varepsilon)+(\mu-\varepsilon)+n\theta(1-H_2+$
$(n-1)\alpha p)]P_{1,n,1}+[(N-n)(\lambda_1-\varepsilon)]P_{0,n,1}+$
$[(N-n)H_1(\lambda_1-\varepsilon)]P_{1,n-1,1}+(n+1)\theta P_{0,n+1,1}+$
$[(n+1)\theta(1-H_2)+n\alpha p]P_{1,n+1,1}=0,$

n = R+1, R+2, ………K-1 (18)

-[(N-K)$(\lambda_1 - \varepsilon)$+K$\theta$]$P_{0,K,1}$ + $(\mu - \varepsilon)P_{1,K,1}$=0 (19)

-$(\mu - \varepsilon)$ $P_{1,K,1}$ + [(N-K)$H_1(\lambda_1 - \varepsilon)$] $P_{1,K-1,1}$

[(N-K)$(\lambda_1 - \varepsilon)$] $P_{0,K,1}$ = 0 (20)

Write $\gamma = [H_1(\lambda_0 - \varepsilon)]$ and $\delta = [H_1(\lambda_1 - \varepsilon)]$

From (1) to (4) we get,

$$P_{0,n,0} = \frac{(N-1)_n \gamma^n \prod_{i=0}^{n-1}[(N-i)(\lambda_0-\varepsilon)+i\theta]}{\prod_{i=1}^{n} i\theta(\mu-\varepsilon)+[i\theta(1-H_2)+(i-1)\alpha p][(N-i)(\lambda_0-\varepsilon)+i\theta]} P_{0,0,0}$$

1≤n≤r (21)

$$P_{1,n,0} = \frac{(N-1)_n\gamma^n}{\mu-\varepsilon} \prod_{i=1}^{n} \frac{[(N-i)(\lambda_0-\varepsilon)+i\theta]}{i\theta(\mu-\varepsilon)+[i\theta(1-H_2)+(i-1)\alpha p][(N-i)(\lambda_0-\varepsilon)+i\theta]} P_{0,0,0}$$

(22)

From (5) to (8) we get,

$$P_{0,n,0} = \frac{(N-1)_n \gamma^n \prod_{i=0}^{n-1}[(N-i)(\lambda_0-\varepsilon)+i\theta]}{\prod_{i=1}^{n} i\theta(\mu-\varepsilon)+[i\theta(1-H_2)+(i-1)\alpha p][(N-i)(\lambda_0-\varepsilon)+i\theta]} P_{0,0,0} - \left\{\frac{A_1}{A_2}\left(\left[\sum_{m-r}^{n-2}(N-m-2)\gamma^{n-1-m} \prod_{i=m+1}^{n} \frac{[(N-i)(\lambda_0-\varepsilon)+i\theta]}{i\theta(\mu-\varepsilon)+[i\theta(1-H_2)+(i-1)\alpha p][(N-i)(\lambda_0-\varepsilon)+i\theta]}\right] + 1\right)\right\} P_{0,r+1,1}$$

(23)

$$P_{1,n,0} = \frac{(N-1)_n\gamma^n}{\mu-\varepsilon} \prod_{i=1}^{n} \frac{[(N-i)(\lambda_0-\varepsilon)+i\theta]}{i\theta(\mu-\varepsilon)+[i\theta(1-H_2)+(i-1)\alpha p][(N-i)(\lambda_0-\varepsilon)+i\theta]} P_{0,0,0}$$

$$-\left\{\frac{A_1}{A_2(\mu-\varepsilon)}\left(\left[\sum_{m-r}^{n-1}(N-m-2)\gamma^{n-1-m} \prod_{i=m+1}^{n} \frac{[(N-i)(\lambda_0-\varepsilon)+i\theta]}{i\theta(\mu-\varepsilon)+[i\theta(1-H_2)+(i-1)\alpha p][(N-i)(\lambda_0-\varepsilon)+i\theta]}\right]\right)\right\} P_{0,r+1,1}$$

n = r+1,r+2,……,R-1 (24)

where

$A_1 = (r+1)\theta(\mu-\varepsilon) + [(r+1)\theta(1-H_2) + r\alpha p]$
$[(N-r-1)(\lambda_1-\varepsilon) + (r+1)\theta]$

$A_2 = n\theta(\mu-\varepsilon) + [n\theta(1-H_2) + (n-1)\alpha p]$
$[(N-n)(\lambda_0-\varepsilon) + n\theta]$

From (9) to (10) we get,

$P_{0,r+1,1} = \frac{A_3}{A_4} p_{0,0,0}$

Where

$$A_3 = \frac{(N-1)_R\gamma^R \prod_{i=0}^{R-1}[(N-i)(\lambda_0-\varepsilon)+i\theta]}{\prod_{i=1}^{R-1} i\theta(\mu-\varepsilon)+[i\theta(1-H_2)+(i-1)\alpha p][(N-i)(\lambda_0-\varepsilon)+i\theta]} P_{0,0,0}$$

$$A_4 = -\left\{A_1\left(\left[\sum_{m-r}^{R-2}(N-m-2)\gamma^{n-1-m} \prod_{i=m+1}^{R-1} \frac{[(N-i)(\lambda_0-\varepsilon)+i\theta]}{i\theta(\mu-\varepsilon)+[i\theta(1-H_2)+(i-1)\alpha p][(N-i)(\lambda_0-\varepsilon)+i\theta]}\right]\right)\right\} P_{0,r+1,1}$$

(25)

From (11) to (14), we recursively derive,

$$P_{0,n,1} = \left\{\frac{A_1}{A_5}\left(\left[\sum_{m-r}^{n-2}(N-m-2)\delta^{n-1-m} \prod_{i=m+1}^{n-1} \frac{[(N-i)(\lambda_1-\varepsilon)+i\theta]}{i\theta(\mu-\varepsilon)+[i\theta(1-H_2)+(i-1)\alpha p][(N-i)(\lambda_0-\varepsilon)+i\theta]}\right] + 1\right)\right\} P_{0,r+1,1}$$

(26)

$$P_{1,n,1} = \left\{\frac{A_1}{\mu-\varepsilon}\left(\left[\sum_{m-r}^{n-1}(N-m-2)\delta^{n-1-m} \prod_{i=m+1}^{n} \frac{[(N-i)(\lambda_1-\varepsilon)+i\theta]}{i\theta(\mu-\varepsilon)+[i\theta(1-H_2)+(i-1)\alpha p][(N-i)(\lambda_1-\varepsilon)+i\theta]}\right]\right)\right\} P_{0,r+1,1}$$

n= r+1,r+2,……R-1,R (27)

where

$A_5 = n\theta(\mu-\varepsilon) + [n\theta(1-H_2) + (n-1)\alpha p]$
$[(N-n)(\lambda_1-\varepsilon) + n\theta]$

A_1 is given by (23) and $P_{0,r+1,1}$ is given by (25)

From (15) to (20) we recursively derive,

$$P_{0,n,1} = \left\{\frac{A_1}{A_5}\left(\left[\sum_{m-r}^{R-2}(N-m-2)\delta^{n-1-m} \prod_{i=m+1}^{n-1} \frac{[(N-i)(\lambda_1-\varepsilon)+i\theta]}{i\theta(\mu-\varepsilon)+[i\theta(1-H_2)+(i-1)\alpha p][(N-i)(\lambda_0-\varepsilon)+i\theta]}\right]\right)\right\} P_{0,r+1,1}$$

(28)

$$P_{1,n,1} = \left\{\frac{A_1}{\mu-\varepsilon}\left(\left[\sum_{m-r}^{R-1}(N-m-2)\delta^{n-1-m} \prod_{i=m+1}^{n} \frac{[(N-i)(\lambda_1-\varepsilon)+i\theta]}{i\theta(\mu-\varepsilon)+[i\theta(1-H_2)+(i-1)\alpha p][(N-i)(\lambda_1-\varepsilon)+i\theta]}\right]\right)\right\} P_{0,r+1,1}$$

n=R+1, R+2,…K-1,K (29)

where A_1, A_5 and $P_{0,r+1,1}$ are given by (23), (25), (26).

Thus from (21) to (29), we find that all the steady state probabilities are expressed in terms of $P_{0,0,0}$.

IV. Characteristics of The Model

The following system characteristics are considered and their analytical results are derived in this system.

- The probability P(0)that the system is in faster rate of primary arrivals with the server idle and busy.
- The probability P(1) that the system is in slower rate of primary arrivals with the server idle and busy.
- The probability $P_{0,0,0}$ that the system is empty.
- The expected number of customers in the system Ls_0, when the system is in faster rate of primary arrivals with the server idle and busy.
- The expected number of customers in the system Ls_1, when the system is in slower rate of primary arrivals with the server idle and busy.

The probability that the system is in faster rate of primary arrivals is

$$P(0) = \left[\sum_{n=0}^{K} P_{0,n,0} + \sum_{n=0}^{K} P_{1,n,0}\right]$$

$$= \begin{bmatrix} \sum_{n=0}^{r} P_{0,n,0} + \sum_{n=r+1}^{R-1} P_{0,n,0} \\ +\sum_{n=r+1}^{R-1} P_{0,n,0} \end{bmatrix} + \begin{bmatrix} \sum_{n=0}^{r} P_{1,n,0} + \sum_{n=r+1}^{R-1} P_{1,n,0} \\ +\sum_{n=R}^{K} P_{1,n,0} \end{bmatrix}$$

Since $P_{0,n,0}$ and $P_{1,n,0}$ exist only when n= 0,1,2,……, r-1,r,r+1,r+2,…..R-2,R-1, we get

$$P(0) = \left[\sum_{n=0}^{r} P_{0,n,0} + \sum_{n=r+1}^{R-1} P_{0,n,0}\right] + \left[\sum_{n=0}^{r} P_{1,n,0} + \sum_{n=r+1}^{R-1} P_{1,n,0}\right] \qquad (30)$$

The probability that the system is in slower rate of primary arrivals is,

$$P(1) = \left[\sum_{n=0}^{K} P_{0,n,1} + \sum_{n=0}^{K} P_{1,n,1}\right]$$

$$= \begin{bmatrix} \sum_{n=0}^{r} P_{0,n,1} + \sum_{n=r+1}^{R-1} P_{0,n,1} \\ +\sum_{n=r+1}^{R-1} P_{0,n,1} \end{bmatrix} + \begin{bmatrix} \sum_{n=0}^{r} P_{1,n,1} + \sum_{n=r+1}^{R-1} P_{1,n,1} \\ +\sum_{n=R}^{K} P_{1,n,1} \end{bmatrix}$$

Since $P_{0,n,1}$ and $P_{1,n,1}$ exist only when n= r+1,r+2,….. R-2,R-1…..K, we get

$$P(1) = \left[\sum_{n=r+1}^{R} P_{0,n,1} + \sum_{n=R+1}^{K} P_{0,n,1}\right] + \left[\sum_{n=r+1}^{R} P_{1,n,1} + \sum_{n=R+1}^{K} P_{1,n,1}\right] \qquad (31)$$

The probability $P_{0,0,0}$ that the system is empty can be calculated from the normalizing condition P(0) + P(1) =1. $P_{0,0,0}$ is calculated from (30) and (31) .

Let L_s denote the average number of customers in the system, then we have

$$L_s = L_{so} + L_{s1} \qquad (32)$$

$$L_{s_0} = \left[\sum_{n=0}^{r} nP_{0,n,0} + \sum_{n=r+1}^{R-1} nP_{0,n,0}\right] + \left[\sum_{n=0}^{r} (n+1)P_{1,n,0} + \sum_{n=r+1}^{R-1} (n+1)P_{1,n,0}\right] \qquad (33)$$

and

$$L_{s_1} = \left[\sum_{n=r+1}^{R} nP_{0,n,1} + \sum_{n=R+1}^{K} nP_{0,n,1}\right] + \left[\sum_{n=r+1}^{R} (n+1)P_{1,n,1} + \sum_{n=R+1}^{K} (n+1)P_{1,n,1}\right] \qquad (34)$$

From (21) to (29) , (33) and (34) , we can calculate the value of L_s. The expected waiting time of the customers in the orbit is calculated as $W_s = \frac{L_s}{\bar{\lambda}}$, Where $\bar{\lambda} = \lambda_0$ P(0) + λ_1P(1). W_s is calculated from (30) to (32).

This model includes the following models as particular cases. For example, when H_1 = 1, H_2 = 1 , p=0, α= 0 we get the M/M/1/K/N interdependent retrial queueing model with controllable arrival rates. When H_1 = 1, H_2 = 1, α = 0, p=0 and $\theta \to \infty$, we get the standard M/M/1/K/N interdependent queueing model with controllable arrival rates. When λ_0 tends to λ_1, p=1, ϵ = 0 and infinite source this model reduces to M/M/1/K retrial queueing model with balking and reneging customers. When λ_0 tends to λ_1, ϵ = 0, H_1 = 1 and H_2 = 1, $\theta \to \infty$, infinite source this model reduces to M/M/1/N queue with retention of reneged customers. When λ_0 tends to λ_1, ϵ = 0, H_1=1 , H_2=1, p=0, α = 0 and $\theta \to \infty$, this model reduces to standard M/M/1/K/N queueing model.

V. Numerical Illustrations

For various values λ_0, λ_1, μ, ϵ, θ, α , p, N while r, R, K, H_1, H_2 are fixed values, computed and tabulated the values of $P_{0,0,0}$,P(0), P(1), L_s and W_s.

TABLE 1

r=3,R=6,K=8,H_1=0.8, H_2=0.2								
λ_0	λ_1	μ	θ	ϵ	α	p=1-q	N	$P_{0,0,0}$
3	2	4	2	0.5	0.1	0.4	10	3.4670155×10^{-4}
4	2	4	2	0.5	0.1	0.4	10	5.2238772×10^{-5}
4	3	4	2	0.5	0.1	0.4	10	4.0896436×10^{-5}
4	3	4	3	0.5	0.1	0.4	10	1.4703411×10^{-4}
4	3	4	3	0.5	0.1	0.4	11	9.4184131×10^{-5}
4	3	5	3	0.5	0.1	0.4	10	3.2178762×10^{-4}
3	2	4	2	1	0.1	0.4	10	1.5542188×10^{-4}
4	3	4	3	0.5	0.1	1	10	2.7459791×10^{-4}
3	2	4	2	0.5	0	0	10	2.6926279×10^{-4}

TABLE 2

P(0)	P(1)	L_s	W_s
0.298036875	0.701963125	5.076481742	2.209051472
0.049843111	0.95015689	5.557583062	2.646863617
0.038787671	0.961212328	6.129769643	2.01717603
0.121727476	0.878272524	3.109381261	0.99604507
0.206467401	0.793532599	5.273733544	1.644717655
0.430291789	0.569708211	2.689848833	0.78414578
0.049264609	0.950735391	6.058771001	2.956558648
0.316152413	0.683847587	3.086583413	0.969901382
0.264762025	0.735237975	6.205176895	2.739880319

VI. CONCLUSION

It is observed from the tables 1 and 2 that when λ_0 increases keeping the other parameters fixed, $P_{0,0,0}$ and P(0) decrease but P(1), Ls and Ws increase. When λ_1 increases keeping the other parameters fixed, $P_{0,0,0}$ and P(0) decrease but P(1), Ls and Ws increase. When θ increases keeping the other parameters fixed, $P_{0,0,0}$ and P(0) increase but P(1), Ls andWs decrease. When θ increases keeping the other parameters fixed, $P_{0,0,0}$ and P(0) increase but P(1), Ls and Ws decrease. When μ increases keeping the other parameters fixed, $P_{0,0,0}$ and P(0) increase but P(1), Ls and Ws decrease. When N increases keeping the other parameters fixed, $P_{0,0,0}$ and P(0) decrease but P(1), Ls and Ws increase. When p=1 keeping the other parameters fixed, $P_{0,0,0}$ and P(0) increase but P(1), Ls and Ws decrease. When $\alpha = 0$, $p = 0$ keeping the other parameters fixed, $P_{0,0,0}$ and P(0) decrease but P(1), Ls and Ws increase.

REFERENCES

[1] A.A. Bouchentouf and F. Belarbi,F, Performance evaluation of two Markovian retrial queueing model with balking and feedback, Acta Univ. Sapientiae, Mathematica, 5, 2(2013) pp.132-146.

[2] A.A. Bouchentouf, M. Kadi and A. Rabhi, Analysis of two heterogeneous server queueing model with balking, reneging and feedback, Mathematical sciences and application E-notes, 2(2) (2013) pp.10-21.

[3] B. Antline Nisha, and M. Thiagarajan, The M/M/1/K/N interdependent retrial queueing model with controllable arrival rates, International Journal of Mathematical Sciences and Engineering Application, ISSN 0973-9424, 8, N0.VI,(2014),pp. 27-41.

[4] G.I. Falin, A survey of retrial queues, Queuing Systems, 7(1990) pp. 127-168.

[5] G.I. Falin and J.G.C. Templeton, Retrial Queues, Chapman and Hall, London, (1997).

[6] J.R. Artalejo, A queueing sysytem with returning customers and waiting line, Operations Research Letters, 17(1995) pp. 191-199.

[7] J.R. Artalejo, Retrial queues with a finite number of sources, Journal of Korean Mathematical Society, 35(1998) pp. 503-525.

[8] J.R. Artalejo, A classified bibliography of research on retrial queues: Progress in 1990-1999 Top 7 (1999a) pp. 187-211.

[9] J.R. Artalejo, Accessible bibliography on retrial queues, Mathematical and Computer Modeling, 30(1999b) pp. 223-233.

[10] J.R. Artalejo, Accessible bibliography on retrial queues progress in 2000-2009, Mathematical Computer Modeling, 51(2010) pp. 1071-1081.

[11] M. Jain and A. Bhagat, Finite population retrial queueing model with threshold recovery geometric arrivals and impatient customers, Journal of Information and Operations Management, Vol 3(1), (2012) pp. 162-165.

[12] M. Thiagarajan and A. Srinivasan, The M/M/c/K/N interdependent queueing model with controllable arrival rates balking, reneging and spares, Journal of Statistics and Applications, 2, Nos.1-2,(2007) pp. 56-65.

[13] M.O. Abou-El-Ata and Hariri, A.M.A. The M/M/c/N queue with balking and reneging, Computers Ops. Res., 19, (1992) pp. 713-716.

[14] R. Kumar and S. Kumar Sharma, M/M/1/N Queuing System with Retention of Reneged Customers, Pakistan Journal of Statistics and Operation Research, 8(4), (2012), pp. 719-735.

[15] R. Kumar and S. Kumar Sharma, M/M/1/N Queuing System with Retention of Reneged Customers and balking, American Journal of Operational Research, 2(1), (2012), pp. 1-5.

[16] R. Kumar and S. Kumar Sharma, A single server markovian queueing system with discouraged arrivals and retention of reneged customers, Yugoslav Journal of Operation Research, 24(1) (2014) pp. 199-126.

[17] S. Kumar Sharma and R. Kumar, A markovian feedback queue with retention of reneged customers and balking, Advanced Modelling and Optimization, 14(3) (2012), pp. 681-688

Global Journal of Pure and Applied Mathematics (GJPAM) ISSN 0973-1768 Volume 12,Number 4 (2016)

Redefined T-fuzzy right h-ideals of hemirings

*G. Mohanraj**
Department of Mathematics,
Annamalai University,
Tamil Nadu, India.
Email: gmohanraaj@gmail.com

E. Prabu
Department of Mathematics,
Annamalai University,
Tamil Nadu, India.
Email: ersprabumath@gmail.com

Abstract— **We redefine the concepts of T-fuzzy right ideals and T-fuzzy right h-ideals of hemirings by using T-sum and T-product. We establish various necessary and sufficient conditions for a fuzzy set to be a T-fuzzy right ideal and T-fuzzy right h-ideal. The concept of T-fuzzy h-closure is introduced. We generalize the notion of h-closure into T-fuzzy h-closure.**

Keywords— Hemirings, T-norm, T-fuzzy right ideals, T-fuzzy right h-ideals

I. INTRODUCTION

In 1965, the origin of fuzzy sets was introduced by L.A.Zadeh [14]. Latter it was applied in group theory by Rosenfeld [13]. Since then, many authors further introduced fuzzy sub-semigroups, fuzzy sub-rings, fuzzy sub-semirings, fuzzy sub-hemirings, fuzzy ideals and fuzzy sub-algebras, and so on (see, [7, 2, 5]). The notion of h-ideals in hemirings was initiated by D.R.La Torre [9] in 1965. The general properties of fuzzy h-ideals of hemirings were described in [12, 7, 15]. P.Dheena and G.Mohanraj [1] introduced T-fuzzy bi-ideal and T -fuzzy quasi ideal in a ring.

In this paper, the notions of T-fuzzy right ideals and T-fuzzy right h-ideals of hemirings are redefined by using T-sum and T-product. We establish various necessary and sufficient conditions for a fuzzy set to be a T-fuzzy right ideal and T-fuzzy right h-ideal. The concept of T-fuzzy h-closure is introduced. We generalize the notion of h-closure into T-fuzzy h-closure.

Basic definitions and mathematical facts about triangular norms can be found in [8].

II. PRELIMINARIES

Definition 2.1.[16] *An algebraic system* $(S,+,\cdot)$ *is called a semiring if* $(S,+)$ *and* $(S,\cdot)$ *are semigroups, that follows both distributive laws:*

$$x\cdot(y+z)=x\cdot y+x\cdot z \text{ and } (x+y)\cdot z=x\cdot z+y\cdot z$$

for all $x,y,z\in S$.

Definition 2.2. *An additively commutative semiring S is called a hemiring if it has an absorbing element* $0\in S$ *such that*

$$0\cdot a=0=a\cdot 0 \text{ and } 0+a=a=a+0$$

for all $a\in S$.

A hemiring $(S,+,\cdot)$ *in which "$\cdot$" is commutative is called commutative hemiring.*

Definition 2.3. *[1]* A triangular norm [T-norm] is a binary operation T on [0,1], such that for all $x,y,z\in[0,1]$ which satisfies the following conditions:

i) $T(x,y)=T(y,x)$

ii) $T(x,T(y,z))=T(T(x,y),z)$

iii) If $x\geq x^{*}$ *and* $y\geq y^{*}$ *then* $T(x,y)\geq T(x^{*},y^{*})$

iv) $T(x,1)=T(1,x)=x$

Note: *Some basic triangular norms [8] are defined as follows:*

i) Minimum T-norm: $T_M(x,y)=\min\{x,y\}$

ii) Product T-norm: $T_P(x,y)=x\cdot y$

iii) Lukasiewicz T-norm: $T_L(x,y)=\max\{x+y-1,0\}$

iv) Drastic product T-norm:

$T_D(x,y)=0$ *if* $x,y\in[0,1)$ *and*

$T_D(x,y)=\min\{x,y\}$ *is otherwise,*

(v) Hamacher T-norms: for any $\lambda\in[0,\infty]$

$$(T_\lambda^H)(x,y)=\begin{cases} T_D(x,y) & \text{if } \lambda=\infty \\ 0 & \text{if } \lambda=x=y=0 \\ \dfrac{xy}{\lambda+(1-\lambda)(x+y-xy)} & \textit{otherwise} \end{cases}$$

Definition 2.4. *A fuzzy set* η *of a hemiring S is a mapping* $\eta:S\to[0,1]$.

Definition 2.5. *A non-empty subset A of a hemiring S is called a right [left] ideal in S if (A,+) is closed and* $AS\subseteq A(SA\subseteq A)$.

Definition 2.6. *A right [left] ideal A of a hemiring S is called a right [left] h-ideal if* $a_1,b_1\in A$ *and* $x_1+a_1+z_1=b_1+z_1$ *imply* $x_1\in A$ *for* $x_1,z_1\in S$.

Definition 2.7. *Let B be a subset of a hemiring S. The h-closure of B, denoted* $\overline{B}$ *is defined as:*

$$\overline{B}=\{a\in S \mid a+b_1+z=b_1'+z\} \text{ for } b_1,b_1'\in B,\ z\in S\}.$$

---

*Corresponding author.

This paper was presented by the second author in the National Conference on AMASE-2016 conducted in Department of Mathematics, University College of Engineering Pattukkottai, Thanjavur, Tamil Nadu, India, on 22nd January 2016.

Definition 2.8. *Let η and δ be the fuzzy sets of a hemiring S and T be a triangular norm on [0, 1]. The T-sum of fuzzy sets η and δ is defined as follows:*

$$(\eta +_T \delta)(p) = \bigvee_{p=q+r} T(\eta(q), \delta(r))$$

Remark: Instead of T-norm, if we take minimum T-norm in Definition 2.8, the T-sum is referred to as a sum of fuzzy sets η and δ.

Definition 2.9. *Let η and δ be the fuzzy sets of a hemiring S and T be a triangular norm on [0, 1]. The T-product of fuzzy sets η and δ is defined as follows:*

$$(\eta \cdot_T \delta)(p) = \begin{cases} \bigvee_{p=qr} T(\eta(q), \delta(r)) & \text{if } p = qr \\ 0 & \text{if p cannot be expressible as } p = qr \end{cases}$$

Remark: Instead of T-norm, if we take minimum T-norm in Definition 2.9, the T-product is called a fuzzy product of fuzzy sets η and δ.

III. REDEFINED T-FUZZY RIGHT h-IDEALS

Throughout this paper, unless otherwise specified, S denotes a hemiring, T indicates a triangular norm on [0,1] and "1" is a fuzzy set on S defined as 1(p) = 1 for all $p \in S$.

Definition 3.1. *A fuzzy set η of S is called a T-fuzzy right [left] ideal of S if*

i) $\eta(p+q) \geq T(\eta(p), \eta(q))$

ii) $\eta(pq) \geq \eta(p)$ $[\eta(pq) \geq \eta(q)]$ *for all* $p, q \in S$.

Definition 3.2. *A fuzzy set η of S is called a fuzzy right [left] ideal of S if*

i) $\eta(p+q) \geq \min\{\eta(p), \eta(q)\}$

ii) $\eta(pq) \geq \eta(p)$ $[\eta(pq) \geq \eta(q)]$ *for all* $p, q \in S$.

Lemma 3.3. *Let η be a fuzzy set of S. Then the following conditions are equivalent*

i) $\eta(p+q) \geq T(\eta(p), \eta(q))$ *for all* $p, q \in S$.

ii) $\eta +_T \eta \subseteq \eta$.

Proof. Let $\eta(p+q) \geq T(\eta(p), \eta(q))$ for all $p, q \in S$. If $p = q + r$, then $\eta(p) = \eta(q+r) \geq T(\eta(q), \eta(r))$. Thus

$$\eta(p) \geq \bigvee_{p=q+r} T(\eta(q), \eta(r))$$
$$= (\eta +_T \eta)(p).$$

Therefore $\eta(p) \geq (\eta +_T \eta)(p)$ for all $p \in S$ implies $\eta +_T \eta \subseteq \eta$.

Conversely, let $\eta +_T \eta \subseteq \eta$ implies $\eta(p) \geq (\eta +_T \eta)(p)$. Thus

$$\eta(p+q) \geq (\eta +_T \eta)(p+q)$$
$$= \bigvee_{p+q=a+b} T(\eta(a), \eta(b))$$
$$\geq T(\eta(p), \eta(q)).$$

Therefore $\eta(p+q) \geq T(\eta(p), \eta(q))$ for all $p, q \in S$.

Theorem 3.4. *A fuzzy set η of S is a T-fuzzy right [left] ideal of S if and only if*

i) $\eta +_T \eta \subseteq \eta$

ii) $\eta \cdot_T 1 \subseteq \eta [1 \cdot_T \eta \subseteq \eta]$

Proof. Let η be a T-fuzzy right ideal of S. By Lemma 3.3, $\eta +_T \eta \subseteq \eta$. If p cannot be expressible as $p = qr$, then $(\eta \cdot_T 1)(p) = 0$. Therefore $0 = (\eta \cdot_T 1)(p) \leq \eta(p)$. If $p = qr$, then $\eta(p) = \eta(qr) \geq \eta(q) = T(\eta(q), 1(r))$. Thus

$$\eta(p) \geq \bigvee_{p=qr} T(\eta(q), 1(r))$$
$$= (\eta \cdot_T 1)(p).$$

Therefore $\eta(p) \geq (\eta \cdot_T 1)(p)$ for all $p \in S$. Hence $\eta \cdot_T 1 \subseteq \eta$. Similarly, we prove that if η is a T-fuzzy left ideal of S, then $1 \cdot_T \eta \subseteq \eta$.

Conversely, by Lemma 3.3, $\eta(p+q) \geq T(\eta(p), \eta(q))$ for all $p, q \in S$. Now, $\eta \cdot_T 1 \subseteq \eta$ implies $\eta(p) \geq (\eta \cdot_T 1)(p)$. Thus

$$\eta(pq) \geq (\eta \cdot_T 1)(pq)$$
$$= \bigvee_{pq=ab} T(\eta(a), 1(b))$$
$$\geq T(\eta(p), 1(q))$$
$$= \eta(p)$$

Therefore $\eta(pq) \geq \eta(p)$ for all $p \in S$. Hence η is a T-fuzzy right ideal of S. Similarly, we prove that if $1 \cdot_T \eta \subseteq \eta$, then η is a T-fuzzy left ideal of S,

Corollary 3.5. *A fuzzy set η of S is a fuzzy right [left] ideal of S if and only if*

i) $\eta + \eta \subseteq \eta$

ii) $\eta \cdot 1 \subseteq \eta$ $[1 \cdot \eta \subseteq \eta]$

Proof. By taking $T(a,b) = \min\{a,b\}$ for all $a, b \in S$ in Theorem 3.4, we get the result.

Definition 3.6. *Let η be a fuzzy set of S. A T-fuzzy right [left] ideal of S is called a T-fuzzy right [left] h-ideal of S if* $x_1 + a_1 + z_1 = b_1 + z_1$ *implies* $\eta(x_1) \geq T(\eta(a_1), \eta(b_1))$ *for* $x_1, a_1, b_1, z_1 \in S$.

Definition 3.7. *Let η be a fuzzy set of S. A fuzzy right [left] ideal of S is called a fuzzy right [left] h-ideal of S if*

$x_1+a_1+z_1=b_1+z_1$ *implies* $\eta(x_1)\geq\min\{\eta(a_1),\eta(b_1)\}$ *for* $x_1,a_1,b_1,z_1\in S.$

Definition 3.8. *Let* η *be a fuzzy set of S. Then the T-fuzzy h-closure denoted by* $\overline{\eta}_T$ *of S is defined as:*

$$(\overline{\eta}_T)(x_1)=\bigvee_{x_1+a_1+z_1=b_1+z_1} T(\eta(a_1),\eta(b_1))\text{ for } x_1,a_1,b_1,z_1\in S.$$

Remark: Instead of T-norm, if we take minimum T-norm in Definition 3.8, $\overline{\eta}_T$ denoted by $\overline{\eta}$ is called a fuzzy h-closure of η of S.

Theorem 3.9. *A T-fuzzy right [left] ideal* η *of S is T-fuzzy right [left] h-ideal if and only if* $\overline{\eta}_T\subseteq\eta.$

Proof. Let η be a T-fuzzy right h-ideal of S. Now, $x_1+a_1+z_1=b_1+z_1$ implies $\eta(x_1)\geq T(\eta(a_1),\eta(b_1))$. Thus

$$\eta(x_1)=\bigvee_{x_1+a_1+z_1=b_1+z_1} T(\eta(a_1),\eta(b_1))=\overline{\eta}_T(x_1).$$

Therefore $\overline{\eta}_T\subseteq\eta.$

Conversely, let $\overline{\eta}_T\subseteq\eta$ implies $\eta(x_1)\geq\overline{\eta}_T(x_1)$ for all $x_1\in S.$ Thus if $x_1+a_1+z_1=b_1+z_1$, then

$$\eta(x_1)\geq\overline{\eta}_T(x_1)\geq\bigvee_{x_1+a_1+z_1=b_1+z_1} T(\eta(a_1),\eta(b_1))\geq T(\eta(a_1),\eta(b_1)).$$

Therefore η is a T-fuzzy right h-ideal of S. Similarly, we prove that a T-fuzzy left ideal η of S is T-fuzzy left h-ideal of S if and only if $\overline{\eta}_T\subseteq\eta.$

Theorem 3.10. *A fuzzy set* η *of S is a T-fuzzy right [left] h-ideal of S if and only if*

i) $\eta+_T\eta\subseteq\eta$,

ii) $\eta\cdot_T 1\subseteq\eta[1\cdot_T\eta\subseteq\eta]$,

iii) $\overline{\eta}_T\subseteq\eta.$

Proof. The proof follows from the Theorem 3.4 and Theorem 3.9.

Corollary 3.11. *A fuzzy set* η *of S is a fuzzy right [left] h-ideal of S if and only if*

i) $\eta+\eta\subseteq\eta$,

ii) $\eta\cdot 1\subseteq\eta\ [1\cdot\eta\subseteq\eta]$,

iii) $\overline{\eta}\subseteq\eta.$

Proof. By taking $T(a,b)=\min\{a,b\}$ for all $a,b\in S$ in Theorem 3.10, we get the result.

Theorem 3.12. *Every fuzzy right [left] h-ideal is a T-fuzzy right [left] h-ideal of S for any T-norm.*

Proof. Let η be fuzzy right h-ideal of S. For any T-norm, $T(a,b)\leq T_m(a,b)=\min\{a,b\}.$ Thus, for any T-norm $\eta(p+q)\geq\min\{\eta(p),\eta(q)\}\geq T(\eta(p),\eta(q))$ and $\eta(pq)\geq\eta(p).$ Now $x_1+a_1+z_1=b_1+z_1$ implies $\eta(x_1)\geq\min\{\eta(a_1),\eta(b_1)\}\geq T(\eta(a_1),\eta(b_1))$. Therefore η is a T-fuzzy right h-ideal of S for any T-norm. Similarly, we prove that every fuzzy left h-ideal is a T-fuzzy left h-ideal of S for any T-norm.

Remark: Converse of Theorem 3.12 need not be true as shown by the following Example 3.13.

Example 3.13. *Let* $S=\{0,a_1,a_2,a_3\}$ *be a hemiring by the Cayley table as follows:*

$+$	0	a_1	a_2	a_3
0	0	a_1	a_2	a_3
a_1	a_1	0	a_3	a_2
a_2	a_2	a_3	0	a_1
a_3	a_3	a_2	a_1	0

$\cdot$	0	a_1	a_2	a_3
0	0	0	0	0
a_1	0	0	0	0
a_2	0	a_1	a_2	a_3
a_3	0	a_1	a_2	a_3

We define a fuzzy set η as follows:

$$\eta(x)=\begin{cases}0.6 & \text{if } x=a_3\\ 0.5 & \text{if } x=0\\ 0.45 & \text{if } x=a_1\\ 0.4 & \text{if } x=a_2\end{cases}$$

Clearly, η is a T_P-fuzzy right h-ideal of S for the product T-norm. But $\eta(a_3+a_3)=\eta(0)=0.5\ngeq 0.6=\min\{\eta(a_3),\eta(a_3)\}$ implies η is not fuzzy right h-ideal of S.

Definition 3.14. *Let* η *and* δ *be the fuzzy sets of a hemiring S and T be a triangular norm on [0, 1]. A T-intersection* η *and* δ *denoted by* $T(\eta,\delta)$ *on S is defined as follows:*

$$T(\eta,\delta)(p)=T(\eta(p),\delta(p))$$

for all $p\in S.$

Remark: Instead of T-norm, if we take minimum T-norm in Definition 3.14, T-intersection is known as a intersection of fuzzy sets η and δ.

Theorem 3.15. *Let* η *and* δ *be the fuzzy sets of S. If* η *and* δ *are T-fuzzy right [left] ideals of S, then* $T(\eta,\delta)$ *is a T-fuzzy right [left] ideal of S.*

Proof. Let η and δ be the T-fuzzy right ideals of S and let $p,q\in S.$ Now

$$T(\eta,\delta)(p+q)=T(\eta(p+q),\delta(p+q))$$

$$\geq T(T(\eta(p),\eta(q)),T(\delta(p),\delta(q)))$$
$$= T(\eta(p),T(\eta(q),T(\delta(p),\delta(q))))$$
$$= T(\eta(p),T(T(\eta(q),\delta(p)),\delta(q)))$$
$$= T(\eta(p),T(T(\delta(p),\eta(q)),\delta(q)))$$
$$= T(\eta(p),T(\delta(p),T(\eta(q),\delta(q))))$$
$$= T(T(\eta(p),\delta(p)),T(\eta(q),\delta(q)))$$
$$= T(T(\eta,\delta)(p),T(\eta,\delta)(q)).$$

Therefore $T(\eta,\delta)(p+q) \geq T(T(\eta,\delta)(p),T(\eta,\delta)(q))$ for all $p,q \in S$. Now

$$T(\eta,\delta)(pq) = T(\eta(pq),\delta(pq))$$
$$\geq T(T(\eta(p),\delta(p)))$$
$$= T(T(\eta,\delta)(p)).$$

Therefore $T(\eta,\delta)(pq) \geq T(T(\eta,\delta)(p))$ for all $p,q \in S$. Hence $T(\eta,\delta)$ is a T-fuzzy right ideal of S, Similarly, we prove that if η and δ are T-fuzzy left ideals of S, then $T(\eta,\delta)$ is a T-fuzzy left ideal of S.

Corollary 3.16. *Let η and δ be the fuzzy sets of S. If η and δ are fuzzy right [left] ideals of S, then $\eta \cap \delta$ is a fuzzy right [left] ideal of S.*

Proof. Instead of T-norm, if we take minimum T-norm in Theorem 3.15, we get the result.

Theorem 3.17. *Let η and δ be the fuzzy sets of S. If η and δ are T-fuzzy right [left] h-ideals of S, then $T(\eta,\delta)$ is a T-fuzzy right [left] h-ideal of S.*

Proof. Let η and δ be the T-fuzzy right h-ideals of S. By Theorem 3.15, $T(\eta,\delta)$ is a T-fuzzy right ideal of S. Now $x_1 + a_1 + z_1 = b_1 + z_1$ and $x_1 \in S$ implies

$\delta(x_1) \geq T(\delta(a_1),\delta(b_1))$ and $\eta(x_1) \geq T(\eta(a_1),\eta(b_1))$.
Then

$$T(\eta,\delta)(x_1) = T(\eta(x_1),\delta(x_1))$$
$$\geq T(T(\eta(a_1),\eta(b_1)),T(\delta(a_1),\delta(b_1)))$$
$$= T(\eta(a_1),T(\eta(b_1),T(\delta(a_1),\delta(b_1))))$$
$$= T(\eta(a_1),T(T(\eta(b_1),\delta(a_1)),\delta(b_1)))$$
$$= T(\eta(a_1),T(T(\delta(a_1),\eta(b_1)),\delta(b_1)))$$
$$= T(\eta(a_1),T(\delta(a_1),T(\eta(b_1),\delta(b_1))))$$
$$= T(T(\eta(a_1),\delta(a_1)),T(\eta(b_1),\delta(b_1)))$$
$$= T(T(\eta,\delta)(a_1),T(\eta,\delta)(b_1)).$$

Therefore $x_1 + a_1 + z_1 = b_1 + z_1$ implies

$$T(\eta,\delta)(x_1) \geq T(T(\eta,\delta)(a_1),T(\eta,\delta)(b_1))$$

for $x_1, a_1, b_1, z_1 \in S$.

Hence $T(\eta,\delta)$ is a T-fuzzy right h-ideal of S, Similarly, we prove that if η and δ are T-fuzzy left h-ideals of S, then $T(\eta,\delta)$ is a T-fuzzy left h-ideal of S.

Corollary 3.18. [7] *Let η and δ be the fuzzy sets of S. If η and δ are fuzzy right [left] h-ideals of S, then $\eta \cap \delta$ is a fuzzy right [left] h-ideal of S.*

Proof. Instead of T-norm, if we take minimum T-norm in Theorem 3.17, we get the result.

REFERENCES

[1] P. Dheena and G. Mohanraj, "T-fuzzy ideals in rings," International Journalof Computational Cognition, 9(2), pp. 98-101, 2011.

[2] P. Dheena and G. Mohanraj, "(λ,μ)-fuzzy ideals in Semirings," Advances in Fuzzy Mathematics, 6(2), pp. 183-192, 2011.

[3] P. Dheena and G. Mohanraj, "On Intuitionistic Fuzzy K -ideals of Semirings," International Journal of Computational Cognition, 9(2), pp. 45-50, 2011.

[4] P. Dheena and G. Mohanraj, "On (λ,μ)-Fuzzy Prime ideals of Semirings," The Journal of Fuzzy Mathematics, 20(4), pp. 889-898, 2012.

[5] P. Dheena and G. Mohanraj, "Fuzzy Small Ideals of Ring," Journal of Hyperstructures, 2(1), pp. 8-17, 2013.

[6] J.S. Golan, "Semirings and their applications," Kluwer Academic Publishers, Dordrecht, 1999.

[7] Y.B. Jun, M.A. Ozturk and S.Z. Song, "On fuzzy h-ideals in hemirings," Information Science, 162, pp. 211-226, 2004.

[8] E.P. Klement, R. Mesiar and E. Pap, "Triangular Norms," Kluwer Academic Publishers, Dordrecht, 2000.

[9] D.R. La Torre, "On h-ideals and k-ideals in hemirings," Publ. Math. Debrecen, 12, pp. 219-226, 1965.

[10] G. Mohanraj, R. Hema and E. Prabu, "On various weak fuzzy prime ideals of ordered semigroup", Proceedings of the International Conference on Mathematical Sciences published by Elsevier, pp. 475-479, 2014.

[11] G. Mohanraj and E. Prabu, "Weakly fuzzy prime ideal of hemiring," Proceedings of the International Conference on Mathematical Sciences published by Elsevier, pp. 480-483, 2014.

[12] G. Mohanraj and E. Prabu, "Generalized Fuzzy Right h-Ideals of Hemirings," International Journal of Fuzzy Mathematical Archive," 7(2), pp. 147-155, 2015.

[13] R. Rosenfeld, "Fuzzy groups," Journal of Mathematical Analysis and Applications, 35, pp. 512-517, 1971.

[14] L.A. Zadeh, "Fuzzy sets," Information and Control, 8, pp. 338-353, 1965.

[15] J. Zhan, W.A. Dudek, "Fuzzy h-ideals of hemirings," Information Science, 177, pp. 876-886, 2007.

[16] Xueling Ma, Yunqiang Yin and Jianming Zhana, "Characterizations of h-intra- and h-quasi-hemiregular hemirings" Computers and Mathematics with Applications, 63, pp. 783-793, 2012.

Global Journal of Pure and Applied Mathematics (GJPAM) ISSN 0973-1768 Volume 12,Number 4 (2016)

Stochastic models for a two grade manpower system having thresholds with two components

*K. Parameswari**
Department of Mathematics,
St. Joseph's college of Engineering and Technology,
Thanjavur - 613 001, Tamil Nadu, India.
Email: parameswari.math@gmail.com

A. Srinivasan
PG & Research Department of Mathematics,
Bishop Heber College,
Trichy - 620 017, Tamil Nadu, India.
Email: mathsrinivas@yahoo.co.in

Abstract— **In this paper an organization with two grades is considered in which exit of personnel takes place due to policy decisions announced. In order to avoid the crisis of the organization reaching a breakdown point, a suitable univariate policy of recruitment based on shock model approach is suggested which is used to enable the organization for planning its decision on recruitment. Three mathematical models are constructed and the expected and variance of time for recruitment are obtained when (i) the loss of manpower form a sequence of identically independent distributed random variables and (ii) the threshold for each grade has two components. The influence of the nodal parameters on the system characteristics are studied and relevant conclusions are presented**.

Keywords— **Man power planning; Univariate recruitment policy; Geometric process; correlated random variables; Mean and variance of the time to recruitment; Shock model; Hyper exponential distribution.**

I. INTRODUCTION

Exits of personnel is a common phenomenon in any marketing organization. This leads to reduction in the total strength of marketing personnel and will adversely affect the sales turnover of the organization, if the recruitment is not planned. In fact, frequent recruitment may also be expensive due to the cost of recruitment and training. As the loss of manpower is unpredictable, a suitable recruitment policy has to be designed to overcome this loss. In [1] and [2] several stochastic models for a manpower system with grades are discussed using Markovian and renewal theoretic approach. In [4] the authors have initiated the study on problem of time to recruitment for a single grade manpower system when the inter-decision times are independent and identically distributed random variables using shock model approach. In [8] the authors have studied the work in [4] when the breakdown threshold has a normal component and a component due to frequent breaks. In [5],[6],[7] the authors have obtained the mean and variance of time to recruitment for a two grade manpower system when the threshold for each grade has only the normal component. The present paper studies the results of [5],[6],[7] when the threshold for each grade has two components. This paper is organized as follows: In sections II, III and IV Models 1, 2 and 3 are described and analytical expressions for mean and variance of the time to recruitment are derived. The three models are differ from each other in the context of permitting or not permitting transfer of personnel between two grades and providing a better allowable loss of manpower in the organization. More specifically, in model-1, transfer of personnel between the two grades is not permitted, in Model-2this transfer is permitted. In Model-3 the thresholds for the loss of man-hours in the two grades are combined in order to provide a better allowable loss of man-hours in the organization compared to Models 1 and 2. In section V, the analytical results are numerically illustrated and relevant conclusions are given.

II. MODEL DESCRIPTION AND ANALYSIS FOR MODEL-1

Consider an organization having two grades in which decisions are taken at random epochs in $[0,\infty)$ and at every decision making epoch a random number of persons quit the organization. There is an associated loss of man-hours to the organization, if a person quits and it is linear and cumulative. Let X_i be an exponential random variable with mean 1/c,(c>0) denoting the loss of man-hours in the organization at the i^{th} decision epoch, i=1, 2,3…with probability density function g(.). Let S_n be the cumulative wastage in man-hour, in the first 'n' decisions. Let $U_i, i=1,2,3...$ be the time between i-1^{th} and i^{th} decisions. The best distribution when the inter-decision times have high or low intensity of attrition is the hyper exponential distribution. Let $U_i, i=1,2,3...k$ are independent and identically distributed hyper exponential random variables with distribution (density) function F(.)(f(.)), and high(low) attrition rate $\lambda_h(\lambda_l)$ and p(q) be the proportion of decisions having high (low) attrition rate. Let $F_k(t)$ $(f_k(t))$ be the distribution(probability density) function of $\sum_{i=1}^{k} U_i$. Let T be a continuous random variable denoting the time for recruitment in the organization with probability distribution function (density function) $L(.)(\ell(.))$. Let $l^*(.), g^*(.)$ *and* $f^*(.)$ be the Laplace transform of $\ell(.), g(.)$ *and* $f(.)$ respectively. Let Y be the breakdown threshold for the cumulative loss of manpower in the organization. For grade A(B), let Y_{A1} (Y_{B1}) be the normal exponential threshold for depletion of manpower with positive

*Corresponding author.

This paper was presented by the second author in the National Conference on AMASE-2016 conducted in Department of Mathematics, University College of Engineering Pattukkottai, Thanjavur, Tamil Nadu, India, on 22nd January 2016.

mean $\alpha_{A1}(\alpha_{B1})$ and Y_{A2} (Y_{B2}) be the exponential threshold of frequent breaks of existing workers with positive mean α_{A2} (α_{B2}). In this model, the breakdown threshold for the organization Y is taken as $\min(Y_A,Y_B)$. The loss of man-hours process and the inter-decision time process are statistically independent. The univariate recruitment policy employed in this paper is as follows: ***Recruitment is done as and when the total loss of man-hours in the organization exceeds Y.*** Let $V_k(t)$ be the probability that there are exactly k-decision epochs in (0,t]. Since the number of decisions made in (0,t] form a renewal process, we note that $V_k(t)= F_k(t) - F_{k+1}(t)$, where $F_0(t)=1$. Let E(T) and V(T) be the mean and variance of time for recruitment respectively.

Main results

By definition, $S_{N(t)}$ is the total loss of man-hours in the N(t) decisions taken in (0,t].

Therefore

$$P(T>t)=P(S_{N(t)}<Y) \tag{1}$$

By using laws of probability and on simplification we get

$$\begin{aligned}P(T>t)=&\gamma_1\sum_{k=1}^{\infty}[F_k(t)-F_{k+1}(t)]\left(g^*(\alpha_{A1}+\alpha_{B1})\right)^k+\\&\gamma_2\sum_{n=1}^{k}[F_k(t)-F_{k+1}(t)]\left[g^*(\alpha_{A2}+\alpha_{B2})\right]^{k-1}-\\&\gamma_3\sum_{k=1}^{\infty}[F_k(t)-F_{k+1}(t)]\left[g^*(\alpha_{A1}+\alpha_{B2})\right]^{k-1}-\\&\gamma_4\sum_{k=1}^{\infty}[F_k(t)-F_{k+1}(t)]\left[g^*(\alpha_{A2}+\alpha_{B1})\right]^{k-1}\end{aligned} \tag{2}$$

where $\gamma_1=\frac{\alpha_{A2}\alpha_{B2}}{(\alpha_{A2}-\alpha_{A1})(\alpha_{B2}-\alpha_{B1})},\gamma_2=\frac{\alpha_{A1}\alpha_{B1}}{(\alpha_{A2}-\alpha_{A1})(\alpha_{B2}-\alpha_{B1})},$
$\gamma_3=\frac{\alpha_{A2}\alpha_{B1}}{(\alpha_{A2}-\alpha_{A1})(\alpha_{B2}-\alpha_{B1})}$ and $\gamma_4=\frac{\alpha_{A1}\alpha_{B2}}{(\alpha_{A2}-\alpha_{A1})(\alpha_{B2}-\alpha_{B1})}$

Since $L(t)=1-P(T>t)$

$$\begin{aligned}L(t)=&\gamma_1[1-g^*(\alpha_{A1}+\alpha_{B1})]\sum_{k=1}^{\infty}F_k(t)\left(g^*(\alpha_{A1}+\alpha_{B1})\right)^{k-1}+\\&\gamma_2[1-g^*((\alpha_{A2}+\alpha_{B2}))]\sum_{k=1}^{\infty}F_k(t)\left[g^*(\alpha_{A2}+\alpha_{B2})\right]^{k-1}-\\&\gamma_3[1-g^*(\alpha_{A1}+\alpha_{B2})]\sum_{k=1}^{\infty}F_k(t)\left[g^*(\alpha_{A1}+\alpha_{B2})\right]^{k-1}-\\&\gamma_4[1-g^*(\alpha_{A2}+\alpha_{B1})]\sum_{k=1}^{\infty}F_k(t)\left[g^*(\alpha_{A2}+\alpha_{B1})\right]^{k-1}\end{aligned} \tag{3}$$

From(3) it is found that

$$\begin{aligned}\ell^*(s)=&\gamma_1\frac{\left[1-g^*(\alpha_{A1}+\alpha_{B1})\right]f^*(s)}{1-f^*(s)g^*(\alpha_{A1}+\alpha_{B1})}+\gamma_2\frac{\left[1-g^*(\alpha_{A2}+\alpha_{B2})\right]f^*(s)}{1-f^*(s)g^*(\alpha_{A2}+\alpha_{B2})}\\&-\gamma_3\frac{\left[1-g^*(\alpha_{A1}+\alpha_{B2})\right]f^*(s)}{1-f^*(s)g^*(\alpha_{A1}+\alpha_{B2})}-\gamma_4\frac{\left[1-g^*(\alpha_{A2}+\alpha_{B1})\right]f^*(s)}{1-f^*(s)g^*(\alpha_{A2}+\alpha_{B1})}\end{aligned} \tag{4}$$

It is known that

$$E[T]=-\left.\frac{d(\ell^*(s))}{ds}\right|_{s=0},E[T^2]=\left.\frac{d^2(\ell^*(s))}{ds^2}\right|_{s=0}\text{ and } V[T]=E[T^2]-(E[T])^2 \tag{5}$$

From (4) and (5) it can be shown that

$$E[T]=(M_1)\left[\begin{array}{l}\frac{\gamma_1}{1-g^*(\alpha_{A1}+\alpha_{B1})}+\frac{\gamma_2}{1-g^*(\alpha_{A2}+\alpha_{B2})}-\\ \frac{\gamma_1}{1-g^*(\alpha_{A1}+\alpha_{B2})}-\frac{\gamma_1}{1-g^*(\alpha_{A2}+\alpha_{B1})}\end{array}\right] \tag{6}$$

and

$$\begin{aligned}E[T^2]=&2(M_2)\left[\begin{array}{l}\frac{\gamma_1}{(1-g^*(\alpha_{A1}+\alpha_{B1}))^2}+\frac{\gamma_2}{(1-g^*(\alpha_{A2}+\alpha_{B2}))^2}-\\ \frac{\gamma_1}{(1-g^*(\alpha_{A1}+\alpha_{B2}))^2}-\frac{\gamma_1}{(1-g^*(\alpha_{A2}+\alpha_{B1}))^2}\end{array}\right]-\\&2(M_1)^2\left[\begin{array}{l}\frac{\gamma_1 g^*(\alpha_{A1}+\alpha_{B1})}{(1-g^*(\alpha_{A1}+\alpha_{B1}))}+\frac{\gamma_2 g^*(\alpha_{A2}+\alpha_{B2})}{(1-g^*(\alpha_{A2}+\alpha_{B2}))}-\\ \frac{\gamma_1 g^*(\alpha_{A1}+\alpha_{B2})}{(1-g^*(\alpha_{A1}+\alpha_{B2}))}-\frac{\gamma_1 g^*(\alpha_{A2}+\alpha_{B1})}{(1-g^*(\alpha_{A2}+\alpha_{B1}))}\end{array}\right]\end{aligned} \tag{7}$$

where $M_1=\frac{p\lambda_l+q\lambda_h}{\lambda_h\lambda_l}$ $M_2=\frac{(p\lambda_l+q\lambda_h)^2}{\lambda_h{}^2\lambda_l{}^2}$ and $g^*(\tau)=\frac{c}{c+\tau}$

We shall obtain the E[T] and V[T] by considering different cases on U_i,i=1,2,3…

Note 1.

Assume that the inter-decision times U_i form a geometric process with parameter 'a'.

Since $\{U_i\}$ is a geometric process it is known that

$$f_k^*(s)=\prod_{n=1}^{k}f^*\left(s/_{a^{n-1}}\right) \tag{8}$$

From (2),(5) and (8) we get

$$E[T]=a\,(M_1)\left[\begin{array}{l}\frac{\gamma_1}{a-g^*(\alpha_{A1}+\alpha_{B1})}+\frac{\gamma_2}{a-g^*(\alpha_{A2}+\alpha_{B2})}-\\ \frac{\gamma_3}{a-g^*(\alpha_{A1}+\alpha_{B2})}-\frac{\gamma_4}{a-g^*(\alpha_{A2}+\alpha_{B1})}\end{array}\right] \tag{9}$$

and

$$\begin{aligned}E[T^2]=&\left[a^2M_2\right]\left[\begin{array}{l}\frac{\gamma_1}{a^2-g^*(\alpha_{A1}+\alpha_{B1})}+\frac{\gamma_2}{a^2-g^*(\alpha_{A2}+\alpha_{B2})}-\\ \frac{\gamma_3}{a^2-g^*(\alpha_{A1}+\alpha_{B2})}-\frac{\gamma_4}{a^2-g^*(\alpha_{A2}+\alpha_{B1})}\end{array}\right]-\\&(M_1)^2\left(\sum_{k=0}^{\infty}\left[\left(\sum_{i=1}^{k}\frac{1}{a^{i-1}}\right)^2-\left(\sum_{i=1}^{k+1}\frac{1}{a^{i-1}}\right)^2\right]\right)\times\\&\left(\begin{array}{l}\gamma_1\left(g^*(\alpha_{A1}+\alpha_{B1})\right)^k+\gamma_2\left(g^*(\alpha_{A2}+\alpha_{B2})\right)^k-\\ \gamma_3\left(g^*(\alpha_{A1}+\alpha_{B2})\right)^k-\gamma_2\left(g^*(\alpha_{A2}+\alpha_{B1})\right)^k\end{array}\right)\end{aligned} \tag{10}$$

Global Journal of Pure and Applied Mathematics (GJPAM) ISSN 0973-1768 Volume 12,Number 4 (2016)

Note 2.

Suppose U_i are exchangeable and constantly correlated exponential random variables.

From Gurland [3] $F_k^*(s)$ is given by

$$F_k^*(s) = \frac{m^k}{1+\frac{kR(1-m)}{1-R}} \quad (11)$$

where R is the correlation between U_i and U_j , i # j , v = mean of U_i i=1,2,3… m=1/1+ds and d=v(1-R)

From (11) it is shown that

$$\frac{d}{ds}\left[F_k^*(s)\right] = -kv \quad (12)$$

$$\frac{d^2}{ds^2}\left[F_k^*(s)\right] = k v^2(1-R^2) + k^2 v^2(1+R^2) \quad (13)$$

From (3),(5),(11),(12) and (13) it is shown that

$$E[T] = v\left[\frac{\gamma_1}{1-g^*(\alpha_{A1}+\alpha_{B1})} + \frac{\gamma_2}{1-g^*(\alpha_{A2}+\alpha_{B2})} - \frac{\gamma_3}{1-g^*(\alpha_{A1}+\alpha_{B2})} - \frac{\gamma_1}{1-g^*(\alpha_{A2}+\alpha_{B1})}\right] \quad (14)$$

and

$$E[T^2] = 2\times v^2\left[\frac{\gamma_1(1+R^2)g^*(\alpha_{A1}+\alpha_{B1})}{(1-g^*(\alpha_{A1}+\alpha_{B1}))^2} + \frac{\gamma_2(1+R^2)g^*(\alpha_{A2}+\alpha_{B2})}{(1-g^*(\alpha_{A2}+\alpha_{B2}))^2} - \frac{\gamma_3(1+R^2)g^*(\alpha_{A1}+\alpha_{B2})}{(1-g^*(\alpha_{A1}+\alpha_{B2}))^2} - \frac{\gamma_1(1+R^2)g^*(\alpha_{A2}+\alpha_{B1})}{(1-g^*(\alpha_{A2}+\alpha_{B1}))^2}\right] \quad (15)$$

(15)

III. MODEL DESCRIPTION AND ANALYSIS FOR MODEL-2

For this model, $Y = \max(Y_A, Y_B)$. All the otherassumptions and notations are as in Model-I. In this model it can be shown that

$$P(T>t) = \gamma_3\sum_{k=1}^{\infty}[F_k(t)-F_{k+1}(t)]\left[g^*(\alpha_{A1}+\alpha_{B2})\right]^k + \gamma_5\sum_{k=1}^{\infty}[F_k(t)-F_{k+1}(t)]\left[g^*(\alpha_{A1})\right]^k + \gamma_4\sum_{k=1}^{\infty}[F_k(t)-F_{k+1}(t)]\left[g^*(\alpha_{A2}+\alpha_{B1})\right]^k + \gamma_7\sum_{k=1}^{\infty}[F_k(t)-F_{k+1}(t)]\left[g^*(\alpha_{B1})\right]^k - \gamma_6\sum_{k=1}^{\infty}[F_k(t)-F_{k+1}(t)]\left[g^*(\alpha_{A2})\right]^k - \gamma_8\sum_{k=1}^{\infty}[F_k(t)-F_{k+1}(t)]\left[g^*(\alpha_{B2})\right]^k - \gamma_1\sum_{k=1}^{\infty}[F_k(t)-F_{k+1}(t)]\left(g^*(\alpha_{A1}+\alpha_{B1})\right)^k - \gamma_2\sum_{n=1}^{k}[F_k(t)-F_{k+1}(t)]\left[g^*(\alpha_{A2}+\alpha_{B2})\right]^k \quad (16)$$

where $\gamma_5 = \frac{\alpha_{A2}}{(\alpha_{A2}-\alpha_{A1})}, \gamma_6 = \frac{\alpha_{A1}}{(\alpha_{A2}-\alpha_{A1})}, \gamma_7 = \frac{\alpha_{B2}}{(\alpha_{B2}-\alpha_{B1})}$

and $\gamma_8 = \frac{\alpha_{B1}}{(\alpha_{B2}-\alpha_{B1})}$

Proceeding as in Model-I we get

$$\ell^*(s) = \gamma_3\frac{\left[1-g^*(\alpha_{A1}+\alpha_{B2})\right]f^*(s)}{1-f^*(s)g^*(\alpha_{A1}+\alpha_{B2})} + \gamma_4\frac{\left[1-g^*(\alpha_{A2}+\alpha_{B1})\right]f^*(s)}{1-f^*(s)g^*(\alpha_{A2}+\alpha_{B1})} + \gamma_5\frac{\left[1-g^*(\alpha_{A1})\right]f^*(s)}{1-f^*(s)g^*(\alpha_{A1})} + \gamma_7\frac{\left[1-g^*(\alpha_{B1})\right]f^*(s)}{1-f^*(s)g^*(\alpha_{B1})} - \gamma_6\frac{\left[1-g^*(\alpha_{A2})\right]f^*(s)}{1-f^*(s)g^*(\alpha_{A2})} - \gamma_8\frac{\left[1-g^*(\alpha_{B2})\right]f^*(s)}{1-f^*(s)g^*(\alpha_{B2})} - \gamma_1\frac{\left[1-g^*(\alpha_{A1}+\alpha_{B1})\right]f^*(s)}{1-f^*(s)g^*(\alpha_{A1}+\alpha_{B1})} - \gamma_2\frac{\left[1-g^*(\alpha_{A2}+\alpha_{B2})\right]f^*(s)}{1-f^*(s)g^*(\alpha_{A2}+\alpha_{B2})} \quad (17)$$

From (5) and (17) it can be shown that

$$E[T] = (M_1)\left[\frac{\gamma_3}{1-g^*(\alpha_{A1}+\alpha_{B2})} + \frac{\gamma_4}{1-g^*(\alpha_{A2}+\alpha_{B1})} + \frac{\gamma_5}{1-g^*(\alpha_{A1})} + \frac{\gamma_7}{1-g^*(\alpha_{B1})} - \frac{\gamma_6}{1-g^*(\alpha_{A2})} - \frac{\gamma_8}{1-g^*(\alpha_{B2})} - \frac{\gamma_1}{1-g^*(\alpha_{A1}+\alpha_{B1})} - \frac{\gamma_2}{1-g^*(\alpha_{A2}+\alpha_{B2})}\right] \quad (18)$$

and

$$E[T^2] = 2(M_2)\left[\frac{\gamma_3}{1-g^*(\alpha_{A1}+\alpha_{B2})} + \frac{\gamma_4}{1-g^*(\alpha_{A2}+\alpha_{B1})} + \frac{\gamma_5}{1-g^*(\alpha_{A1})} + \frac{\gamma_7}{1-g^*(\alpha_{B1})} - \frac{\gamma_6}{1-g^*(\alpha_{A2})} - \frac{\gamma_8}{1-g^*(\alpha_{B2})} - \frac{\gamma_1}{1-g^*(\alpha_{A1}+\alpha_{B1})} - \frac{\gamma_2}{1-g^*(\alpha_{A2}+\alpha_{B2})}\right] + 2(M_1)^2\left[\frac{\gamma_3 g^*(\alpha_{A1}+\alpha_{B2})}{(1-g^*(\alpha_{A1}+\alpha_{B2}))^2} + \frac{\gamma_4 g^*(\alpha_{A2}+\alpha_{B1})}{1(-g^*(\alpha_{A2}+\alpha_{B1}))^2} + \frac{\gamma_5 g^*(\alpha_{A1})}{(1-g^*(\alpha_{A1}))^2} + \frac{\gamma_7 g^*(\alpha_{B1})}{(1-g^*(\alpha_{B1}))^2} - \frac{\gamma_6 g^*(\alpha_{A2})}{(1-g^*(\alpha_{A2}))^2} - \frac{\gamma_8 g^*(\alpha_{B2})}{(1-g^*(\alpha_{B2}))^2} - \frac{\gamma_1 g^*(\alpha_{A1}+\alpha_{B1})}{(1-g^*(\alpha_{A1}+\alpha_{B1}))^2} - \frac{\gamma_2 g^*(\alpha_{A2}+\alpha_{B2})}{(1-g^*(\alpha_{A2}+\alpha_{B2}))^2}\right] \quad (19)$$

Note 3.

The inter-decision times U_i form a geometric process with parameter 'a'. Proceeding as in Model-I it is found that

$$E[T] = a\,(M_1)\left[\frac{\gamma_3}{a-g^*(\alpha_{A1}+\alpha_{B2})} + \frac{\gamma_4}{a-g^*(\alpha_{A2}+\alpha_{B1})} + \frac{\gamma_5}{a-g^*(\alpha_{A1})} + \frac{\gamma_7}{a-g^*(\alpha_{B1})} - \frac{\gamma_6}{a-g^*(\alpha_{A2})} - \frac{\gamma_8}{a-g^*(\alpha_{B2})} - \frac{\gamma_1}{a-g^*(\alpha_{A1}+\alpha_{B1})} - \frac{\gamma_2}{a-g^*(\alpha_{A2}+\alpha_{B2})}\right] \quad (20)$$

and

$$E[T^2]=2a^2[M_2]\begin{bmatrix}\frac{\gamma_3}{a^2-g^*(\alpha_{A1}+\alpha_{B2})}+\frac{\gamma_4}{a^2-g^*(\alpha_{A2}+\alpha_{B1})}+\\ \frac{\gamma_5}{a^2-g^*(\alpha_{A1})}+\frac{\gamma_7}{a^2-g^*(\alpha_{B1})}-\\ \frac{\gamma_6}{a^2-g^*(\alpha_{A2})}-\frac{\gamma_8}{a^2-g^*(\alpha_{B2})}-\\ \frac{\gamma_1}{a^2-g^*(\alpha_{A1}+\alpha_{B1})}-\frac{\gamma_2}{a^2-g^*(\alpha_{A2}+\alpha_{B2})}\end{bmatrix}-(M_1)^2\times$$

$$\sum_{k=0}^{\infty}\left[\left(\sum_{i=1}^{k}\frac{1}{a^{i-1}}\right)^2-\left(\sum_{i=1}^{k+1}\frac{1}{a^{i-1}}\right)^2\right]\begin{pmatrix}\gamma_3\left(g^*(\alpha_{A1}+\alpha_{B2})\right)^k+\gamma_5\left(g^*(\alpha_{A1})\right)^k+\\ \gamma_4\left(g^*(\alpha_{A2}+\alpha_{B1})\right)^k+\gamma_7\left(g^*(\alpha_{B1})\right)^k-\\ \gamma_6\left(g^*(\alpha_{A2})\right)^k-\gamma_8\left(g^*(\alpha_{B2})\right)^k-\\ \gamma_1\left(g^*(\alpha_{A1}+\alpha_{B1})\right)^k-\\ \gamma_2\left(g^*(\alpha_{A2}+\alpha_{B2})\right)^k\end{pmatrix} \quad (21)$$

Note 4.

The inter-decision times U_i are exchangeable and constantly correlated exponential random variables.

Proceeding as in Model-I it is shown that

$$E[T]=v\times\begin{bmatrix}\frac{\gamma_3}{1-g^*(\alpha_{A1}+\alpha_{B2})}+\frac{\gamma_4}{1-g^*(\alpha_{A2}+\alpha_{B1})}+\\ \frac{\gamma_5}{1-g^*(\alpha_{A1})}+\frac{\gamma_7}{1-g^*(\alpha_{B1})}-\frac{\gamma_6}{1-g^*(\alpha_{A2})}-\\ \frac{\gamma_8}{1-g^*(\alpha_{B2})}-\frac{\gamma_1}{1-g^*(\alpha_{A1}+\alpha_{B1})}-\frac{\gamma_2}{1-g^*(\alpha_{A2}+\alpha_{B2})}\end{bmatrix} \quad (22)$$

$$E[T^2]=2v^2\begin{bmatrix}\frac{\gamma_3(1+R^2g^*(\alpha_{A1}+\alpha_{B2}))}{\left(1-g^*(\alpha_{A1}+\alpha_{B2})\right)^2}+\frac{\gamma_4(1+R^2g^*(\alpha_{A2}+\alpha_{B1}))}{1-g^*(\alpha_{A2}+\alpha_{B1})}+\\ \frac{\gamma_5(1+R^2g^*(\alpha_{A1}))}{1-g^*(\alpha_{A1})}+\frac{\gamma_7(1+R^2g^*(\alpha_{B1}))}{1-g^*(\alpha_{B1})}-\\ \frac{\gamma(1+R^2g^*(\alpha_{A2}))_6}{1-g^*(\alpha_{A2})}-\frac{\gamma_8(1+R^2g^*(\alpha_{B2}))}{1-g^*(\alpha_{B2})}-\\ \frac{\gamma_1(1+R^2g^*(\alpha_{A1}+\alpha_{B1}))}{1-g^*(\alpha_{A1}+\alpha_{B1})}-\frac{\gamma_2(1+R^2g^*(\alpha_{A2}+\alpha_{B2}))}{1-g^*(\alpha_{A2}+\alpha_{B2})}\end{bmatrix} \quad (23)$$

IV. MODEL DESCRIPTION AND ANALYSIS FOR MODEL-3

For this Model, $Y=Y_A+Y_B$. All the other assumptions and notations are as in Model-I. Proceeding as in Model-I it can be shown that

$$P(T>t)=\gamma_9\sum_{k=1}^{\infty}[F_k(t)-F_{k+1}(t)]\left[g^*(\alpha_{A1})\right]^k+\gamma_{10}\sum_{k=1}^{\infty}[F_k(t)-F_{k+1}(t)]\left[g^*(\alpha_{B1})\right]^k-\gamma_{11}\sum_{k=1}^{\infty}[F_k(t)-F_{k+1}(t)]\left[g^*(\alpha_{A2})\right]^k-\gamma_{12}\sum_{k=1}^{\infty}[F_k(t)-F_{k+1}(t)]\left[g^*(\alpha_{B2})\right]^k \quad (24)$$

where

$$\gamma_9=\frac{\alpha_{A1}\alpha_{A2}\alpha_{B1}\alpha_{B2}}{(\alpha_{A2}-\alpha_{A1})(\alpha_{B1}-\alpha_{A1})(\alpha_{B2}-\alpha_{A1})},\gamma_{10}=\frac{\alpha_{A1}\alpha_{A2}\alpha_{B1}\alpha_{B2}}{(\alpha_{B2}-\alpha_{B1})(\alpha_{B1}-\alpha_{A1})(\alpha_{B1}-\alpha_{A2})},$$

$$\gamma_{11}=\frac{\alpha_{A1}\alpha_{A2}\alpha_{B1}\alpha_{B2}}{(\alpha_{A2}-\alpha_{A1})(\alpha_{B1}-\alpha_{A2})(\alpha_{B2}-\alpha_{A2})}\,and\,\frac{\alpha_{A1}\alpha_{A2}\alpha_{B1}\alpha_{B2}}{(\alpha_{B2}-\alpha_{B1})(\alpha_{B2}-\alpha_{A1})(\alpha_{B2}-\alpha_{A2})}$$

Proceeding as in Model-I we get

$$\ell^*(s)=\gamma_9\frac{\left[1-g^*(\alpha_{A1})\right]f^*(s)}{1-f^*(s)g^*(\alpha_{A1})}+\gamma_{10}\frac{\left[1-g^*(\alpha_{B1})\right]f^*(s)}{1-f^*(s)g^*(\alpha_{B1})}-\gamma_{11}\frac{\left[1-g^*(\alpha_{A2})\right]f^*(s)}{1-f^*(s)g^*(\alpha_{A2})}-\gamma_{12}\frac{\left[1-g^*(\alpha_{B2})\right]f^*(s)}{1-f^*(s)g^*(\alpha_{B2})} \quad (25)$$

From (5) and (25) it can be shown that

$$E[T]=(M_1)\begin{bmatrix}\frac{\gamma_9}{1-g^*(\alpha_{A1})}+\frac{\gamma_{10}}{1-g^*(\alpha_{B1})}-\\ \frac{\gamma_{11}}{1-g^*(\alpha_{A2})}-\frac{\gamma_{12}}{1-g^*(\alpha_{B2})}\end{bmatrix} \quad (26)$$

and

$$E[T^2]=2(M_2)\begin{bmatrix}\frac{\gamma_9}{1-g^*(\alpha_{A1})}+\frac{\gamma_{10}}{1-g^*(\alpha_{B1})}-\\ \frac{\gamma_{11}}{1-g^*(\alpha_{A2})}-\frac{\gamma_{12}}{1-g^*(\alpha_{B2})}\end{bmatrix}-2(M_1)^2\begin{bmatrix}\frac{\gamma_9g^*(\alpha_{A1})}{\left(1-g^*(\alpha_{A1})\right)^2}+\frac{\gamma_{10}g^*(\alpha_{B1})}{\left(1-g^*(\alpha_{B1})\right)^2}-\\ \frac{\gamma_{11}g^*(\alpha_{A2})}{\left(1-g^*(\alpha_{A2})\right)^2}-\frac{\gamma_{12}g^*(\alpha_{B2})}{\left(1-g^*(\alpha_{B2})\right)^2}\end{bmatrix} \quad (27)$$

Note 5.

The inter-decision times U_i form a geometric process with parameter ‘a’. Proceeding as in Model-I it is found that

Proceeding as in Model-I it is found that

$$E[T]=a\,(M_1)\begin{bmatrix}\frac{\gamma_9}{a-g^*(\alpha_{A1})}+\frac{\gamma_{10}}{a-g^*(\alpha_{B1})}+\\ \frac{\gamma_{11}}{a-g^*(\alpha_{A2})}+\frac{\gamma_{12}}{a-g^*(\alpha_{B2})}\end{bmatrix} \quad (28)$$

and

$$E[T^2]=2a^2[M_2]\left[\frac{\gamma_9}{a-g^*(\alpha_{A1})}+\frac{\gamma_{10}}{a-g^*(\alpha_{B1})}+\frac{\gamma_{11}}{a-g^*(\alpha_{A2})}+\frac{\gamma_{12}}{a-g^*(\alpha_{B2})}\right]-(M_1)^2\left(\sum_{k=0}^{\infty}\left[\left(\sum_{i=1}^{k}\frac{1}{a^{i-1}}\right)^2-\left(\sum_{i=1}^{k+1}\frac{1}{a^{i-1}}\right)^2\right]\right)\times\begin{pmatrix}\gamma_9\left(g^*(\alpha_{A1})\right)^k+\gamma_{10}\left(g^*(\alpha_{B1})\right)^k-\\ \gamma_{11}\left(g^*(\alpha_{A2})\right)^k-\gamma_{12}\left(g^*(\alpha_{B2})\right)^{k^k}\end{pmatrix} \quad (29)$$

Note 6.

The inter-decision times U_i are exchangeable and constantly correlated exponential random variables.

Proceeding as in Model-I it is shown that

$$E[T] = v \times \left[\frac{\gamma_9}{1-g^*(\alpha_{A1})} + \frac{\gamma_{10}}{1-g^*(\alpha_{B1})} - \frac{\gamma_{11}}{1-g^*(\alpha_{A2})} - \frac{\gamma_{12}}{1-g^*(\alpha_{B2})} \right] \quad (30)$$

and

$$E[T^2] = 2 \times v^2 \left[\begin{array}{l} \frac{\gamma_9(1+R^2 g^*(\alpha_{A1}))}{1-g^*(\alpha_{A1})} + \frac{\gamma_{10}(1+R^2 g^*(\alpha_{B1}))}{1-g^*(\alpha_{B1})} - \\ \frac{\gamma_{11}(1+R^2 g^*(\alpha_{A2}))}{1-g^*(\alpha_{A2})} - \frac{\gamma_{12}(1+R^2 g^*(\alpha_{B2}))}{1-g^*(\alpha_{B2})} \end{array} \right] \quad (31)$$

V. NUMERICAL ILLUSTRATION

The influence of parameters on the performance measure namely mean and variance of the time for recruitment is studied numerically. In the following table these performance measures are calculated by varying the parameter ‘c’ and keeping the parameters α_{A1}, α_{A2}, α_{B1}, α_{B2} and λ fixed. $\alpha_{A1}=0.2$, $\alpha_{A2}=0.3$, $\alpha_{B1}=0.4$, $\alpha_{B2}=0.5$, k=2and $\lambda=0.75$

c	Model-I		Model-II		Model-III	
	$E(T)$	$V(T)$	$E(T)$	$V(T)$	$E(T)$	$V(T)$
3	3.33	11.11	10	71.56	12.67	96.44
4	4.22	17.83	13.11	121.33	16.67	164
5	5.11	26.12	16.22	184.15	20.67	249.33

Table: Effect of ‘c’ on the performance measures E[T] and V[T]

From the above table the following observation is given: As ‘c’ increases both E(T) and V(T) increases for all the three models.

VI. CONCLUSION

Model-3 is more suitable from the organization point of view as it postponed the time to recruitment compared to Models 1 and 2.

REFERENCES

[1] D.J Bartholomew, “Statistical Models for Social Processes,” John Wiley and Sons, New York, 1973.

[2] D.J. Barthlowmew.D.J, and A.F.Forbes, “Statistical Techniques for Manpower Planning,” 1st Edition, John Wiley and Sons, New York, 1979.

[3] J.Gurland, “Distribution of the maximum of arithmetic mean of correlated random variables,” Applied Mathematical Statistics, Vol.26, 1995, pp. 294-300.

[4] R.Sathiyamoorthi, and R.Elangovan.R, “Shock model approach to determine the expected time for recruitment,” Journal of Decision and Mathematika Sciences, Vol.3(1-3),1998, pp. 67-78.

[5] J.Sridharan,K.Parameswari, and A.Srinivasan, “A stochastic model on time to recruitment in a two grade manpower system based on order statistics,” International Journal of Mathematical Sciences and Engineering Applications, Vol 6(5), 2012, pp. 23-30.

[6] J.Sridharan,K.Parameswari, and A.Srinivasan, “A stochastic model on time to recruitment in a two grade manpower system having correlated wastage,” Bessel Journal of Mathematics,Vol.3(3), 2013, pp. 209-224.

[7] J.Sridharan,K.Parameswari, and A.Srinivasan, “Expected time to recruitment in a two grade manpower syatem,” Intenational Journal of Engineering Research and Applications, Vol.4(2), 2014, pp. 578-592,.

N.Vijayasankar, R.Elangovan, and R.Sathiyamoorthi, “Determination of expected time to recruitment when backup resource of manpower exits,” Ultra Scientist, Vol 25(1) B, 2013,pp. 61-68.

Global Journal of Pure and Applied Mathematics (GJPAM) ISSN 0973-1768 Volume 12,Number 4 (2016)

Λ_δ^s-Separation axioms in bitopological spaces

A. Edward Samuel
Ramanujan Research Centre,
PG & Research Department of Mathematics,
Government Arts College (Autonomous),
Kumbakonam – 612002, Tamil Nadu, India.
Email: aedward74_thrc@yahoo.co.in

*D. Balan**
Ramanujan Research Centre,
PG & Research Department of Mathematics,
Government Arts College (Autonomous),
Kumbakonam – 612002, Tamil Nadu, India.
Email: dh.balan@yahoo.com

Abstract **- The aim of this paper is to introduce the concept of $ij - \Lambda_\delta^s$ open sets and associated closure operator in bitopological spaces and we study some of the fundamental properties of such sets. Also we shall introduce the notions of pairwise $\Lambda_\delta^s - T_i$ and pairwise $\Lambda_\delta^s - R_i$ bitopological spaces for $i = 0, 1, 2$ and investigate their properties.**

Key words: ***ij – δ open set, $ij - \delta$ semi open set, $ij - \Lambda_\delta^s$ open set, pairwise $\Lambda_\delta^s - T_0$, pairwise $\Lambda_\delta^s - T_1$, pairwise $\Lambda_\delta^s - T_2$, pairwise $\Lambda_\delta^s - R_0$, pairwise $\Lambda_\delta^s - R_1$.***

AMS Subject Classification: 54A10, 54A25, 54D10, 54E55.

I. INTRODUCTION

In topology, the class of generalized Λ-sets studied by Maki in [16] and defined the associated closure operator C^Λ. El-Sharkasy [9] studied the concept of $\Lambda_\alpha -$sets and the associated topology T^{Λ_α}. Caldas et al.[4,5] introduced the concept $\Lambda_\delta^s -$ sets (resp. $V_\delta^s -$ sets) in topological spaces, which is the intersection of $\delta -$ semiopen (resp. union of $\delta -$ semiclosed) sets. Khedr and Al-saadi [15] introduced and studied the concept of *ij*-*s*Λ -semi θ-closed and pairwise θ-generalized *s*Λ-set in bitopological spaces, which is an extension of the class of generalized Λ-sets. Ghareeb and Noiri [10] introduced the concept of Λ - Generalized closed sets in bitopological spaces. In 2006, Caldas et al. [6] introduced the notions of $\Lambda_\delta - T_0$, $\Lambda_\delta - T_1$, $\Lambda_\delta - R_0$ and $\Lambda_\delta - R_1$ in bitopological spaces. Quite recently, Edward Samuel and Balan [8] studied the concept of $\Lambda_\delta^s -$ Sets in bitopological spaces.

The purpose of this paper is to continue research along these directions but this time by utilizing $ij - \Lambda_\delta^s$ open sets. In this paper, we introduce $ij - \Lambda_\delta^s$ open sets and associated closure operator in bitopological spaces and we study some of their fundamental properties. Also, we introduce the notions of $\Lambda_\delta^s - T_0$, $\Lambda_\delta^s - T_1$, $\Lambda_\delta^s - T_2$, $\Lambda_\delta^s - R_0$, $\Lambda_\delta^s - R_1$ bitopological spaces and the major properties of this new concept will be studied.

II. PRELIMINARIES

Throughout the present paper, (X, τ_1, τ_2) (or briefly X) always mean a bitopological space. Also $i, j = 1, 2$ and $i \neq j$. Let A be a subset of (X, τ_1, τ_2). By $i - int(A)$ and $i - cl(A)$, we mean respectively the interior and the closure of A in the topological space (X, τ_i) for $i = 1, 2$. A subset A of X is called $ij -$ regular open [12] if $A = i - int[j - cl(A)]$. A point *x* of X is called an $ij - \delta -$ cluster point of A if

$i - Int(j - Cl(U)) \cap A \neq \phi$ for every $\tau_i -$ open set U containing x.

The set of all $ij - \delta -$ cluster points of A is called the $ij - \delta -$ closure of A and is denoted by $ij - \delta Cl(A)$.

Definition 2.1[13] A subset A is said to be $ij - \delta$ closed if $ij - \delta cl(A) = A$. The complement of $ij - \delta$ closed set is said to be $ij - \delta$ open. The set of all $ij - \delta$ open (resp. $ij - \delta$ closed) sets of X will be denoted by $ij - \delta O(X)$(resp. $ij - \delta C(X)$).

Definition 2.2[7] A subset A of a bitopological space (X, τ_1, τ_2) is called $ij - \delta$ semi open if there exists an $ij - \delta$ open set U such that $U \subseteq A \subseteq j - cl(U)$.

Definition 2.3[8] For a subset A of a bitopological space (X, τ_1, τ_2), we define $A^{\delta s \Lambda_{ij}}$ and $A^{\delta s V_{ij}}$ as follows, $A^{\delta s \Lambda_{ij}} = \cap \{U: A \subseteq U, U \in ij - \delta SO(X)\}$ and $A^{\delta s V_{ij}} = \cup \{U: U \subseteq A, U^C \in ij - \delta SO(X)\}$.

Definition 2.4[8] A subset A of a bitopological space (X, τ_1, τ_2) is called,

(a) $ij - \Lambda_\delta^s$ set if $A = A^{\delta s \Lambda_{ij}}$.
(b) $ij - V_\delta^s$ set if $A = A^{\delta s V_{ij}}$.

The family of all $ij - \Lambda_\delta^s$ sets (resp. $ij - V_\delta^s$) is denoted by $ij - \Lambda_\delta^s(X, \tau_1, \tau_2)$ (resp. $ij - V_\delta^s(X, \tau_1, \tau_2)$).

III. $ij - \Lambda_\delta^s$ CLOSURE OPERATOR

Definition 3.1 Let A be a subset of a bitopological space (X, τ_1, τ_2),

(a) A is called a $ij - \Lambda_\delta^s$ closed set if $A = T \cap C$, where T is a $ij - \Lambda_\delta^s$ set and C is a $ji - \delta$ semi closed set. The complement of a $ij - \Lambda_\delta^s$ closed set is called $ij - \Lambda_\delta^s$ open. The family of all $ij - \Lambda_\delta^s$ open sets and $ij - \Lambda_\delta^s$ closed sets are denoted by $ij - \Lambda_\delta^s O(X, \tau_1, \tau_2)$ and $ij - \Lambda_\delta^s C(X, \tau_1, \tau_2)$.

(b) A point $x \in (X, \tau_1, \tau_2)$ is called a $ij - \Lambda_\delta^s$ cluster point of A if for every $ij - \Lambda_\delta^s$ open set U of (X, τ_1, τ_2) containing x, $A \cap U \neq \phi$. The set of all $ij - \Lambda_\delta^s$ cluster points is called the $ij - \Lambda_\delta^s$ closure of A and is denoted by $ij - C^{\Lambda_\delta^s}(A)$.

Theorem 3.2 Let A, B and $\{B_\alpha, \alpha \in J\}$ be subsets of a bitopological space (X, τ_1, τ_2) . For $ij - \Lambda_\delta^s$ closure, the following properties hold,

(a) $A \subseteq ij - C^{\Lambda_\delta^s}(A)$.
(b) $ij - C^{\Lambda_\delta^s}(A) = \{U: A \subseteq U, U \in ij - \Lambda_\delta^s C(X, \tau_1, \tau_2)\}$.
(c) If $A \subseteq B$, then $ij - C^{\Lambda_\delta^s}(A) \subseteq ij - C^{\Lambda_\delta^s}(B)$.

*Corresponding author.

This paper was presented by the second author in the National Conference on AMASE-2016 conducted in Department of Mathematics, University College of Engineering-Pattukkottai, Thanjavur, Tamil Nadu, India, on 22nd January 2016.

(d) A is $ij-\Lambda_\delta^s$ closed if and only if $A = ij - C^{\Lambda_\delta^s}(A)$.
(e) $ij - C^{\Lambda_\delta^s}(A)$ is $ij-\Lambda_\delta^s$ closed.
(f) $\bigcup_{\alpha\in J} ij - C^{\Lambda_\delta^s}(B_\alpha) = ij - C^{\Lambda_\delta^s}(\bigcup_{\alpha\in J} B_\alpha)$.
(g) $ij - C^{\Lambda_\delta^s}[ij - C^{\Lambda_\delta^s}(A)] = ij - C^{\Lambda_\delta^s}(A)$.

Proof. (a), (b), (c), (e) Obvious. From the definition.

(d) Obvious. From (a) and definition.

(f) Suppose that there exists a point x such that $x \notin ij - C^{\Lambda_\delta^s}(\bigcup_{\alpha\in J} B_\alpha)$. Then, there exists a subset $U \in ij - \Lambda_\delta^s(X,\tau_1,\tau_2)$ such that $\bigcup_{\alpha\in J} B_\alpha \subseteq U$ and $x \notin U$. Thus for each $\alpha \in J$, we have $x \notin ij - C^{\Lambda_\delta^s}(B_\alpha)$. Thus implies that $x \notin \bigcup_{\alpha\in J} ij - C^{\Lambda_\delta^s}(B_\alpha)$.

Conversely, we suppose that there exists a point $x \in X$ such that $x \notin \bigcup_{\alpha\in J} ij - C^{\Lambda_\delta^s}(B_\alpha)$. Then, there exist subsets $U_\alpha \in ij - \Lambda_\delta^s(X,\tau_1,\tau_2)$ for each $\alpha \in J$ such that $x \notin U_\alpha$ and $B_\alpha \subseteq U_\alpha$. Let $U = \bigcup_{\alpha\in J} U_\alpha$, we have $x \notin U$, $\bigcup_{\alpha\in J} B_\alpha \subseteq U_\alpha$ and $U \in ij - \Lambda_\delta^s(X,\tau_1,\tau_2)$. Thus $x \notin ij - C^{\Lambda_\delta^s}(\bigcup_{\alpha\in J} B_\alpha)$.

(g) Suppose that there exists a point $x \in X$ such that $x \notin ij - C^{\Lambda_\delta^s}(A)$. Then there exists a subset $U \in ij - \Lambda_\delta^s(X,\tau_1,\tau_2)$ such that $x \notin U$ and $U \supseteq A$. Since $U \in ij - \Lambda_\delta^s(X,\tau_1,\tau_2)$ we have $ij - C^{\Lambda_\delta^s}(A) \subseteq U$. Thus we have $x \notin ij - C^{\Lambda_\delta^s}[ij - C^{\Lambda_\delta^s}(A)]$. Therefore $ij - C^{\Lambda_\delta^s}[ij - C^{\Lambda_\delta^s}(A)] \subseteq ij - C^{\Lambda_\delta^s}(A)$.

Theorem 3.3 Let A be a subset of a bitopological space (X,τ_1,τ_2), then following are hold,

(a) If A_α is $ij-\Lambda_\delta^s$ closed sets for each $\alpha \in J$, then $\bigcap_{\alpha\in J} U_\alpha$ is $ij-\Lambda_\delta^s$ closed.
(b) If A_α is $ij-\Lambda_\delta^s$ open sets for each $\alpha \in J$, then $\bigcup_{\alpha\in J} U_\alpha$ is $ij-\Lambda_\delta^s$ open.

Proof. Obvious.

Definition 3.4 Let A be a subset of a bitopological space (X,τ_1,τ_2), then the $ij-\Lambda_\delta^s$ kernel of A, denoted by $ij-\Lambda_\delta^s\mathrm{Ker}(A)$ is defined to be the set $ij-\Lambda_\delta^s\mathrm{Ker}(A) = \bigcap\{U \in ij-\Lambda_\delta^s O(X,\tau_1,\tau_2) : A \subseteq U\}$.

Theorem 3.5 For any two subsets A and B of a bitopological space (X,τ_1,τ_2),

(a) If $A \subseteq B$, then $ij-\Lambda_\delta^s\mathrm{Ker}(A) \subseteq ij-\Lambda_\delta^s\mathrm{Ker}(A)$.
(b) $ij-\Lambda_\delta^s\mathrm{Ker}[ij-\Lambda_\delta^s\mathrm{Ker}(A)] = ij-\Lambda_\delta^s\mathrm{Ker}(A)$.

Proof. Obvious.

Theorem 3.6 For any two points x and y of a bitopological space (X,τ_1,τ_2), $y \in ij-\Lambda_\delta^s\mathrm{Ker}(\{x\})$ if and only if $x \in ij - C^{\Lambda_\delta^s}(\{y\})$.

Proof. Let $y \notin ij-\Lambda_\delta^s\mathrm{Ker}(\{x\})$. Then there exists a $ij-\Lambda_\delta^s$ open set U containing x such that $y \notin U$. Hence $x \notin ij - C^{\Lambda_\delta^s}(\{y\})$. Similarly the converse is true.

Theorem 3.7 If (X,τ_1,τ_2) be a bitopological space and $A \subset X$, then $ij-\Lambda_\delta^s\mathrm{Ker}(A) = \{x \in X : ij - C^{\Lambda_\delta^s}(\{x\}) \cap A \neq \phi\}$.

Proof. Let $x \in ij-\Lambda_\delta^s\mathrm{Ker}(A)$ and suppose that $ij - C^{\Lambda_\delta^s}(\{x\}) \cap A = \phi$. Then $x \notin X \backslash ij - C^{\Lambda_\delta^s}(\{x\})$ which is a $ij-\Lambda_\delta^s$ open set containing A. This is impossible, since $x \in ij-\Lambda_\delta^s\mathrm{Ker}(A)$. Consequently, $ij - C^{\Lambda_\delta^s}(\{x\}) \cap A \neq \phi$. Next, let $x \in X$ such that $ij - C^{\Lambda_\delta^s}(\{x\}) \cap A \neq \phi$ and suppose that $x \notin ij-\Lambda_\delta^s\mathrm{Ker}(A)$. Then there exists a $ij-\Lambda_\delta^s$ open set U containing A and $x \notin U$. Let $y \in ij - C^{\Lambda_\delta^s}(\{x\}) \cap A$. Hence U is a $ij-\Lambda_\delta^s$ neigbourhood of y which does not contain x. By this contradiction $x \in ij-\Lambda_\delta^s\mathrm{Ker}(A)$.

Definition 3.8 A bitopological space space (X,τ_1,τ_2) is called,

(a) pairwise $\Lambda_\delta^s - T_0$ if for each pair of distinct points in X, there is a $ij-\Lambda_\delta^s$ open set containing one of the points but not the other.

(b) pairwise $\Lambda_\delta^s - T_1$ if for each pair of distinct points x and y in X, there is a $ij-\Lambda_\delta^s$ open U in X containing x but not y and a $ji-\Lambda_\delta^s$ open set V in X containing y but not x.

(c) pairwise $\Lambda_\delta^s - T_2$ if for each pair of distinct points x and y in X, there exist a $ij-\Lambda_\delta^s$ open set U and $ji-\Lambda_\delta^s$ open set V such that $x \in U, y \in V$ and $U \cap V = \phi$.

Remark 3.9 If a bitopological space space (X,τ_1,τ_2) is pairwise $\Lambda_\delta^s - T_i$, then it is pairwise $\Lambda_\delta^s - T_{i-1}$, $i = 1, 2$.

Theorem 3.10 A bitopological space space (X,τ_1,τ_2) is pairwise $\Lambda_\delta^s - T_0$ if and only if for each pair of distinct points x, y of X, $ij - C^{\Lambda_\delta^s}(\{x\}) \neq ji - C^{\Lambda_\delta^s}(\{y\})$.

Proof. Suppose that $x, y \in X$, $x \neq y$ and $ij - C^{\Lambda_\delta^s}(\{x\}) \neq ji - C^{\Lambda_\delta^s}(\{y\})$. Let z be a point of X such that $z \in ij - C^{\Lambda_\delta^s}(\{x\})$ but $z \notin ji - C^{\Lambda_\delta^s}(\{y\})$. We claim that $x \notin ji - C^{\Lambda_\delta^s}(\{y\})$. For it, if $x \in ji - C^{\Lambda_\delta^s}(\{y\})$ then $ij - C^{\Lambda_\delta^s}(\{x\}) \subseteq ji - C^{\Lambda_\delta^s}(\{y\})$ and this contradicts the fact that $z \notin ji - C^{\Lambda_\delta^s}(\{y\})$. Consequently, $x \in ji-\Lambda_\delta^s O(X,\tau_1,\tau_2)$, $[ji - C^{\Lambda_\delta^s}(\{y\})]^C$ to which y does not belong.

Conversely, Let (X,τ_1,τ_2) be a pairwise $\Lambda_\delta^s - T_0$ space and x, y be any two distinct points of X. There exists a $ij-\Lambda_\delta^s$ open set G containing x or y, say x but not y. Then G^C is a $ij-\Lambda_\delta^s$ closed set which does not contain x but contains y. Since $ji - C^{\Lambda_\delta^s}(\{y\})$ is the smallest $ji-\Lambda_\delta^s$ closed set containing y, $ji - C^{\Lambda_\delta^s}(\{y\}) \subseteq G^C$, and so $x \notin ji - C^{\Lambda_\delta^s}(\{y\})$. Consequently, $ij - C^{\Lambda_\delta^s}(\{x\}) \neq ji - C^{\Lambda_\delta^s}(\{y\})$.

Theorem 3.11 A bitopological space (X,τ_1,τ_2) is pairwise $\Lambda_\delta^s - T_1$ if and only if the singletons are $ij-\Lambda_\delta^s$ closed sets.

Proof. Suppose that (X,τ_1,τ_2) is pairwise $\Lambda_\delta^s - T_1$ and x be any point of X. Let $y \in \{x\}^C$. Then $x \neq y$ and so there exists a $ij-\Lambda_\delta^s$ open set U_y such that $y \in U_y$ but $x \notin U_y$. Consequently, $y \in U_y \subseteq \{x\}^C$ i.e., $\{x\}^C = \bigcup\{U_y : y \in \{x\}^C\}$ which is $ij-\Lambda_\delta^s$ open.

Conversely, suppose that $\{p\}$ is $ij-\Lambda_\delta^s$ closed for every $p \in X$. Let $x, y \in X$ with $\neq y$. Now $x \neq y$ implies $y \in \{x\}^C$. Hence $\{x\}^C$ is a $ij-\Lambda_\delta^s$ open set containing y but not containing x. Similarly $\{y\}^C$ is a $ji-\Lambda_\delta^s$ open set containing x but not y. Therefore, (X,τ_1,τ_2) is a pairwise $\Lambda_\delta^s - T_1$ space.

Definition 3.12 A bitopological space (X,τ_1,τ_2) is pairwise $\Lambda_\delta^s -$ symmetric if for x and y in X, $x \in ji - C^{\Lambda_\delta^s}(\{y\})$ implies $y \in ji - C^{\Lambda_\delta^s}(\{x\})$.

Definition 3.13 A subset A of a bitopological space (X,τ_1,τ_2) is called a $ij-\Lambda_\delta^s$ generalized closed set (briefly $ij-\Lambda_\delta^s - g$

closed) if $ji - C^{\Lambda_\delta^s}(A) \subseteq U$ whenever $A \subseteq U$ and U is $ij - \Lambda_\delta^s$ open.

Theorem 3.14 Every $ij - \Lambda_\delta^s$ closed set is $ij - \Lambda_\delta^s - \mathrm{g}$ closed.

Remark 3.15 The converse of above theorem is not true in general.

Theorem 3.16 A bitopological space $(\mathrm{X}, \tau_1, \tau_2)$ is pairwise $\Lambda_\delta^s -$ symmetric if and only if $\{x\}$ is $ij - \Lambda_\delta^s - \mathrm{g}$ closed for each $x \in X$.

Proof. Assume that $x \in ji - C^{\Lambda_\delta^s}(\{y\})$ but $y \notin ij - C^{\Lambda_\delta^s}(\{x\})$. This implies that the $[ij - C^{\Lambda_\delta^s}(\{x\})]^C$ contains y. Therefore, the set $\{y\}$ is a subset of $[ij - C^{\Lambda_\delta^s}(\{x\})]^C$. This implies that $ji - C^{\Lambda_\delta^s}(\{y\})$ is a subset of $[ij - C^{\Lambda_\delta^s}(\{x\})]^C$. Now $[ij - C^{\Lambda_\delta^s}(\{x\})]^C$ contains x which is a contradiction.

Conversely, suppose that $\{x\} \subseteq U \in ij - \Lambda_\delta^s O(\mathrm{X}, \tau_1, \tau_2)$, but $ij - C^{\Lambda_\delta^s}(\{x\})$ is not a subset of U. This means that $ij - C^{\Lambda_\delta^s}(\{x\})$ and U^C are not disjoint. Let $y \in ij - C^{\Lambda_\delta^s}(\{x\}) \cap (X \backslash U)$. Now we have $x \in ji - C^{\Lambda_\delta^s}(\{y\})$ which is a subset of U^C and $x \notin U$. This is a contradiction.

Theorem 3.17 If a bitopological space $(\mathrm{X}, \tau_1, \tau_2)$ is pairwise $\Lambda_\delta^s - \mathrm{T}_1$ space, then it is pairwise

$\Lambda_\delta^s -$ symmetric.

Proof. In a pairwise $\Lambda_\delta^s - \mathrm{T}_1$ space, singleton sets are $ij - \Lambda_\delta^s$ closed and Therefore, $ij - \Lambda_\delta^s - \mathrm{g}$ closed. By theorem 3.16, $(\mathrm{X}, \tau_1, \tau_2)$ is pairwise $\Lambda_\delta^s -$ symmetric.

Theorem 3.18 For a bitopological space $(\mathrm{X}, \tau_1, \tau_2)$ the following are equivalent:

(a) $(\mathrm{X}, \tau_1, \tau_2)$ is pairwise $\Lambda_\delta^s -$ symmetric and pairwise $\Lambda_\delta^s - \mathrm{T}_0$.

(b) $(\mathrm{X}, \tau_1, \tau_2)$ is pairwise $\Lambda_\delta^s - \mathrm{T}_1$.

Proof. (a) $\Longrightarrow$(b) Let $x \neq y$ and by pairwise $\Lambda_\delta^s - \mathrm{T}_0$, by remark 3.9 we may assume that $x \in U_1 \subseteq \{y\}^C$ for some $U_1 \in ij - \Lambda_\delta^s \mathrm{O}(\mathrm{X}, \tau_1, \tau_2)$. Then $x \notin ji - C^{\Lambda_\delta^s}(\{y\})$. Therefore, by the definition of pairwise $\Lambda_\delta^s -$ symmetric, we have $y \notin ij - C^{\Lambda_\delta^s}(\{x\})$. There exists a $U_2 \in ji - \Lambda_\delta^s \mathrm{O}(\mathrm{X}, \tau_1, \tau_2)$ such that $y \in U_2 \subseteq \{x\}^C$. Therefore, $(\mathrm{X}, \tau_1, \tau_2)$ is a pairwise $\Lambda_\delta^s - \mathrm{T}_1$ space.

Theorem 3.19 For a pairwise $\Lambda_\delta^s -$ symmetric space $(\mathrm{X}, \tau_1, \tau_2)$ the following are equivalent:

(1) $(\mathrm{X}, \tau_1, \tau_2)$ is pairwise $\Lambda_\delta^s - \mathrm{T}_0$.

(2) $(\mathrm{X}, \tau_1, \tau_2)$ is pairwise $\Lambda_\delta^s - \mathrm{T}_1$.

Proof. (1) $\Longrightarrow$ (2) Obvious. From theorem 3.18.

(2) $\Longrightarrow$ (1) Obvious. From Remark 3.9.

IV. PAIRWISE $\Lambda_\delta^s - \mathrm{R}_0$ SPACES

Definition 4.1 A bitopological space $(\mathrm{X}, \tau_1, \tau_2)$ is a pairwise $\Lambda_\delta^s - \mathrm{R}_0$ if for each $ij - \Lambda_\delta^s$ open set U, $x \in U$ implies $ji - C^{\Lambda_\delta^s}(\{x\}) \subseteq U$.

Theorem 4.2 In a bitopological space $(\mathrm{X}, \tau_1, \tau_2)$, the following statements are equivalent:

(a) $(\mathrm{X}, \tau_1, \tau_2)$ is pairwise $\Lambda_\delta^s - \mathrm{R}_0$.

(b) for any $ij - \Lambda_\delta^s$ closed set G and a point $x \notin G$, there exists $U \in ji - \Lambda_\delta^s \mathrm{O}(\mathrm{X}, \tau_1, \tau_2)$ such that $x \notin U$ and $G \subseteq U$.

(c) for any $ij - \Lambda_\delta^s$ closed set G and $x \notin G$, then $ji - C^{\Lambda_\delta^s}(\{x\}) \cap G = \phi$.

Proof. (a) $\Longrightarrow$ (b): Let G be a $ij - \Lambda_\delta^s$ closed set and $x \notin G$. Then by (a), $ji - C^{\Lambda_\delta^s}(\{x\}) \subseteq X \backslash G$. Let $U = X \backslash ji - C^{\Lambda_\delta^s}(\{x\})$, then $U \in ji - \Lambda_\delta^s \mathrm{O}(\mathrm{X}, \tau_1, \tau_2)$ and also $G \subseteq U$ and $x \notin U$.

(b) $\Longrightarrow$ (c): Let G be a $ij - \Lambda_\delta^s$ closed set and a point $x \notin G$. Then by (b), there exists $U \in ji - \Lambda_\delta^s \mathrm{O}(\mathrm{X}, \tau_1, \tau_2)$ such that $G \subseteq U$ and $x \notin U$. Since $U \in ji - \Lambda_\delta^s \mathrm{O}(\mathrm{X}, \tau_1, \tau_2)$, $U \cap ji - C^{\Lambda_\delta^s}(\{x\}) = \phi$. Then $\cap\ ji - C^{\Lambda_\delta^s}(\{x\}) = \phi$.

(c) $\Longrightarrow$ (a): Let $G \in ij - \Lambda_\delta^s \mathrm{O}(\mathrm{X}, \tau_1, \tau_2)$ and $x \in G$. Now $X \backslash G$ is $ij - \Lambda_\delta^s$ closed and $x \notin X \backslash G$ x. By (c), $ji - C^{\Lambda_\delta^s}(\{x\}) \cap (X \backslash \mathrm{G}) = \phi$ and hence $ji - C^{\Lambda_\delta^s}(\{x\}) \subseteq G$. Therefore, $(\mathrm{X}, \tau_1, \tau_2)$ is pairwise $\Lambda_\delta^s - \mathrm{R}_0$.

Theorem 4.3 A bitopological space $(\mathrm{X}, \tau_1, \tau_2)$ is pairwise $\Lambda_\delta^s - \mathrm{R}_0$ if and only if for each pair x, y of distinct points in X, $ij - C^{\Lambda_\delta^s}(\{x\}) \cap ji - C^{\Lambda_\delta^s}(\{y\}) = \phi$ or $\{x, y\} \subseteq ij - C^{\Lambda_\delta^s}(\{x\}) \cap ji - C^{\Lambda_\delta^s}(\{y\})$.

Proof. Let $(\mathrm{X}, \tau_1, \tau_2)$ be pairwise $\Lambda_\delta^s - \mathrm{R}_0$. Suppose that $ij - C^{\Lambda_\delta^s}(\{x\}) \cap ji - C^{\Lambda_\delta^s}(\{y\}) \neq \phi$ and $\{x, y\} \nsubseteq ij - C^{\Lambda_\delta^s}(\{x\}) \cap ji - C^{\Lambda_\delta^s}(\{y\})$. Let $p \in ij - C^{\Lambda_\delta^s}(\{x\}) \cap ji - C^{\Lambda_\delta^s}(\{y\})$ and $x \notin ij - C^{\Lambda_\delta^s}(\{x\}) \cap ji - C^{\Lambda_\delta^s}(\{y\})$. Then $x \notin ji - C^{\Lambda_\delta^s}(\{y\})$ and $x \in X \backslash ji - C^{\Lambda_\delta^s}(\{y\}) \in ji - \Lambda_\delta^s \mathrm{O}(\mathrm{X}, \tau_1, \tau_2)$. But $ij - C^{\Lambda_\delta^s}(\{x\})$ is not a subset of $X \backslash ji - C^{\Lambda_\delta^s}(\{y\})$, this is a contradiction. Hence for each pair x, y of distinct points in X, $ij - C^{\Lambda_\delta^s}(\{x\}) \cap ji - C^{\Lambda_\delta^s}(\{y\}) = \phi$ or $\{x, y\} \subseteq ij - C^{\Lambda_\delta^s}(\{x\}) \cap ji - C^{\Lambda_\delta^s}(\{y\})$.

Conversely, let U be a $ij - \Lambda_\delta^s$ open set and $x \in U$. Suppose that $ji - C^{\Lambda_\delta^s}(\{x\})$ is not a subset of U. So there is a point $y \in ji - C^{\Lambda_\delta^s}(\{x\})$ such that $y \notin U$ and $-C^{\Lambda_\delta^s}(\{x\}) \cap U = \phi$. Since $X \backslash U$ is $ij - \Lambda_\delta^s$ closed and $y \in X \backslash U$. Hence $\{x, y\} \nsubseteq ij - C^{\Lambda_\delta^s}(\{x\}) \cap ji - C^{\Lambda_\delta^s}(\{y\})$ and thus $ij - C^{\Lambda_\delta^s}(\{x\}) \cap ji - C^{\Lambda_\delta^s}(\{y\}) \neq \phi$.

Theorem 4.4 In a bitopological space $(\mathrm{X}, \tau_1, \tau_2)$, the following statements are equivalent:

(1) $(\mathrm{X}, \tau_1, \tau_2)$ is pairwise $\Lambda_\delta^s - \mathrm{R}_0$.

(2) For any $x \in X$, $ij - C^{\Lambda_\delta^s}(\{x\}) = ji - \Lambda_\delta^s \mathrm{Ker}(\{x\})$.

(3) For any $x \in X$, $ij - C^{\Lambda_\delta^s}(\{x\}) \subseteq ji - \Lambda_\delta^s \mathrm{Ker}(\{x\})$.

(4) For any $x, y \in X$, $y \in ij - C^{\Lambda_\delta^s}(\{x\})$ if and only if $x \in ji - C^{\Lambda_\delta^s}(\{y\})$.

(5) For any $ij - \Lambda_\delta^s$ closed set F, $F = \cap\{G : G$ is a $ij - \Lambda_\delta^s$ open set and $\mathrm{F} \subseteq \mathrm{G}\}$.

(6) For any $ij - \Lambda_\delta^s$ open set G, $G = \cup\{F : F$ is a $ij - \Lambda_\delta^s$ closed set and $\mathrm{F} \subseteq \mathrm{G}\}$.

(7) For every $A \neq \phi$ and each $G \in ij-\Lambda_\delta^s O(X,\tau_1,\tau_2)$ such that $A \cap G \neq \phi$, there exists a $ji-\Lambda_\delta^s$ closed set F such that $F \subseteq G$ and $A \cap F \neq \phi$.

Proof. (1) ⟹ (2) Let $x, y \in X$. Then by theorem 3.6 and 4.3, $y \in ji-\Lambda_\delta^s \mathrm{Ker}(\{x\})$, implies $x \in ji-C^{\Lambda_\delta^s}(\{y\})$, $y \in ij-C^{\Lambda_\delta^s}(\{x\})$. Hence $ij-C^{\Lambda_\delta^s}(\{x\}) = ji-\Lambda_\delta^s \mathrm{Ker}(\{x\})$.

(2) ⟹ (3) Obvious.

(3) ⟹ (4) For any $x, y \in X$, if $y \in ij-C^{\Lambda_\delta^s}(\{x\})$, then $y \in ji-\Lambda_\delta^s \mathrm{Ker}(\{x\})$ by (3). Then by theorem 3.6, $x \in ji-C^{\Lambda_\delta^s}(\{y\})$. Similarly the converse.

(4) ⟹ (5) Let F be a $ij-\Lambda_\delta^s$ closed set and $H = \cap\{G: G \text{ is a } ji-\Lambda_\delta^s \text{ open set and } F \subseteq G\}$. . Clearly $F \subseteq H$. Let $x \notin F$. Then for any $y \in F$, we have that $ij-C^{\Lambda_\delta^s}(\{y\}) \subseteq F$. Hence follows that $x \notin ij-C^{\Lambda_\delta^s}(\{y\})$. Now by (4), $y \notin ji-C^{\Lambda_\delta^s}(\{x\})$. There exists a $ji-\Lambda_\delta^s$ open set G_y such that $y \in G_y$ and $x \notin G_y$. Let $G = \cup_{y\in F}\{G_y : G_y \text{ is a } ji-\Lambda_\delta^s \text{ open set}, y \in G_y \text{ and } x \notin G_y\}$. Thus, there exists a $ji-\Lambda_\delta^s$ open set G such that $x \notin G$ and $F \subseteq G$. Hence, $x \notin H$. Therefore, $F = H$.

(5) ⟹ (6) Obvious.

(6) ⟹ (7) Let $A \neq \phi$ and G be a $ij-\Lambda_\delta^s$ open set and $x \in A \cap G$. By (6), $G = \cup\{F: F \text{ is a } ij-\Lambda_\delta^s \text{ closed set and } F \subseteq G\}$. It follows that there is a $ij-\Lambda_\delta^s$ closed set F such that $x \in A \subseteq G$. Hence $A \cap F \neq \phi$.

(7) ⟹ (1) Let G be a $ij-\Lambda_\delta^s$ open set and $x \in G$, then $\{x\} \cap G \neq \phi$. Therefore by (7), there exists a $ji-\Lambda_\delta^s$ closed F such that $x \in F \subseteq G$ and $\{x\} \cap F \neq \phi$, which implies $ji-C^{\Lambda_\delta^s}(\{x\}) \subseteq G$. Therefore, (X,τ_1,τ_2) is pairwise $\Lambda_\delta^s-R_0$.

Theorem 4.5 In a bitopological space (X,τ_1,τ_2), the following properties are equivalent:

(1) (X,τ_1,τ_2) is pairwise $\Lambda_\delta^s-R_0$.

(2) For any $ij-\Lambda_\delta^s$ closed set $F \subset X$, $F = ji-\Lambda_\delta^s Ker(F)$.

(3) For any $ij-\Lambda_\delta^s$ closed set $F \subset X$ and $x \in F$, $ji-\Lambda_\delta^s Ker(\{x\}) \subseteq F$.

(4) For any $x \in X$, $ji-\Lambda_\delta^s Ker(\{x\}) \subseteq ij-C^{\Lambda_\delta^s}(\{x\})$.

Proof. (1) ⟹ (2) Let F be $ij-\Lambda_\delta^s$ closed and $x \notin F$. Then $X\backslash F$ is $ij-\Lambda_\delta^s$ open containing x. Since (X,τ_1,τ_2) is pairwise $\Lambda_\delta^s-R_0$, $ji-C^{\Lambda_\delta^s}(\{x\}) \subseteq X\backslash F$. Therefore, $ji-C^{\Lambda_\delta^s}(\{x\}) \cap F = \phi$ and by theorem 3.7, $x \notin ji-\Lambda_\delta^s Ker(F)$. Hence $F = ji-\Lambda_\delta^s Ker(F)$.

(2) ⟹ (3) Let F be a $ij-\Lambda_\delta^s$ closed set containing x. Then $\{x\} \subseteq F$ and $ji-C^{\Lambda_\delta^s}(\{x\}) \subseteq ji-\Lambda_\delta^s Ker(F)$. From (2), it follows that $ji-C^{\Lambda_\delta^s}(\{x\}) \subseteq F$.

(3) ⟹ (4) Since $x \in ij-C^{\Lambda_\delta^s}(\{x\})$ and $ij-C^{\Lambda_\delta^s}(\{x\})$ is $ij-\Lambda_\delta^s$ closed in X, by (3) it follows that $ji-\Lambda_\delta^s Ker(F) \subseteq ij-C^{\Lambda_\delta^s}(\{x\})$.

(4) ⟹ (1) Obvious. Proof follows from theorem 4.4.

Remark 4.6 Let (X,τ_1,τ_2) be a bitopolgical space. Then for each $x \in X$, let $bi-\Lambda_\delta^s(\{x\}) = 12-C^{\Lambda_\delta^s}(\{x\}) \cap 21-C^{\Lambda_\delta^s}(\{x\})$ and $bi-\Lambda_\delta^s \mathrm{Ker}(\{x\}) = 12-\Lambda_\delta^s Ker(\{x\}) \cap 21-\Lambda_\delta^s Ker(\{x\})$.

Theorem 4.7 If a bitopological space (X,τ_1,τ_2) is pairwise $\Lambda_\delta^s-R_0$ then for each pair of distinct points $x, y \in X$, either $bi-\Lambda_\delta^s(\{x\}) = bi-\Lambda_\delta^s(\{y\})$ or $bi-\Lambda_\delta^s(\{x\}) \cap bi-\Lambda_\delta^s(\{y\}) = \phi$.

Proof. Let (X,τ_1,τ_2) be a pairwise $\Lambda_\delta^s-R_0$ space. Suppose that $bi-\Lambda_\delta^s(\{x\}) \neq bi-\Lambda_\delta^s(\{y\})$ and $bi-\Lambda_\delta^s(\{x\}) \cap bi-\Lambda_\delta^s(\{y\}) \neq \phi$. Let $s \in bi-\Lambda_\delta^s(\{x\}) \cap bi-\Lambda_\delta^s(\{y\})$ and $x \notin bi-\Lambda_\delta^s(\{y\}) = 12-C^{\Lambda_\delta^s}(\{y\}) \cap 21-C^{\Lambda_\delta^s}(\{y\})$. Then $x \notin ij-C^{\Lambda_\delta^s}(\{y\})$. And $x \in X\backslash ij-C^{\Lambda_\delta^s}(\{y\}) \in ij-\Lambda_\delta^s O(X,\tau_1,\tau_2)$. But $ji-C^{\Lambda_\delta^s}(\{x\})$ is not a subset of $X\backslash ij-C^{\Lambda_\delta^s}(\{y\})$ since $s \in bi-\Lambda_\delta^s(\{x\}) \cap bi-\Lambda_\delta^s(\{y\})$. Thus (X,τ_1,τ_2) is not a pairwise $\Lambda_\delta^s-R_0$ space which is a contradiction to our assumption. Hence we have either $bi-\Lambda_\delta^s(\{x\}) = bi-\Lambda_\delta^s(\{y\})$ or $bi-\Lambda_\delta^s(\{x\}) \cap bi-\Lambda_\delta^s(\{y\}) = \phi$.

V. PAIRWISE $\Lambda_\delta^s-R_1$ SPACES

Definition 5.1 A bitopological space (X,τ_1,τ_2) is said to be pairwise $\Lambda_\delta^s-R_1$ if for each $x, y \in X$, $ij-C^{\Lambda_\delta^s}(\{x\}) \neq ji-C^{\Lambda_\delta^s}(\{y\})$, there exist disjoint sets $U \in ji-\Lambda_\delta^s O(X,\tau_1,\tau_2)$ and $V \in ij-\Lambda_\delta^s O(X,\tau_1,\tau_2)$ such that $ij-C^{\Lambda_\delta^s}(\{x\}) \subseteq U$ and $ji-C^{\Lambda_\delta^s}(\{y\}) \subseteq V$.

Theorem 5.2 If a bitopological space (X,τ_1,τ_2) is pairwise $\Lambda_\delta^s-R_1$, then it is pairwise $\Lambda_\delta^s-R_0$.

Proof. Suppose that (X,τ_1,τ_2) is pairwise $\Lambda_\delta^s-R_1$. Let U be a $ij-\Lambda_\delta^s$ open set and $x \in U$. Then for each point $y \in X\backslash U$, $ji-C^{\Lambda_\delta^s}(\{x\}) \neq ij-C^{\Lambda_\delta^s}(\{y\})$. Since (X,τ_1,τ_2) is pairwise $\Lambda_\delta^s-R_1$, there exists a $ij-\Lambda_\delta^s$ open set U_y and a $ji-\Lambda_\delta^s$ open set V_y such that $ji-C^{\Lambda_\delta^s}(\{x\}) \subseteq U_y$, $ij-C^{\Lambda_\delta^s}(\{y\}) \subseteq V_y$ and $U_y \cap V_y = \phi$. Let $A = \cup\{V_y: y \in X\backslash U\}$. Then $X\backslash U \subseteq A$, $x \notin A$ and A is a $ji-\Lambda_\delta^s$ open set. Therefore, $ji-C^{\Lambda_\delta^s}(\{x\}) \subseteq X\backslash A \subseteq U$. Hence (X,τ_1,τ_2) is pairwise $\Lambda_\delta^s-R_0$.

Theorem 5.3 A bitopological space (X,τ_1,τ_2) is pairwise $\Lambda_\delta^s-R_1$ if and only if for every pair of points x and y of X such that $ij-C^{\Lambda_\delta^s}(\{x\}) \neq ji-C^{\Lambda_\delta^s}(\{y\})$, there exists a $ij-\Lambda_\delta^s$ open set U and $ji-\Lambda_\delta^s$ open set V such that $x \in V$, $y \in U$ and $U \cap V = \phi$.

Proof. Suppose that (X,τ_1,τ_2) is pairwise $\Lambda_\delta^s-R_1$. Let x, y be points of X such that $ij-C^{\Lambda_\delta^s}(\{x\}) \neq ji-C^{\Lambda_\delta^s}(\{y\})$. Then there exist a $ij-\Lambda_\delta^s$ open set U and a $ji-\Lambda_\delta^s$ open set V such that $x \in ij-C^{\Lambda_\delta^s}(\{x\}) \subseteq V$ and $y \in ji-C^{\Lambda_\delta^s}(\{y\}) \subseteq U$. On the other hand, suppose that there exists a $ij-\Lambda_\delta^s$ open set U and $ji-\Lambda_\delta^s$ open set V such that $x \in V$, $y \in U$ and $U \cap V = \phi$. Since every pairwise $\Lambda_\delta^s-R_1$ space is pairwise $\Lambda_\delta^s-R_0$, $ij-C^{\Lambda_\delta^s}(\{x\}) \subseteq V$ and $ji-C^{\Lambda_\delta^s}(\{y\}) \subseteq U$. This completes the proof.

Theorem 5.4 A pairwise $\Lambda_\delta^s-R_0$ space (X,τ_1,τ_2) is pairwise $\Lambda_\delta^s-R_1$ if for each pair of points x and y of X such that $ij-C^{\Lambda_\delta^s}(\{x\}) \cap ji-C^{\Lambda_\delta^s}(\{y\}) = \phi$, there exist disjoint sets $U \in ij-\Lambda_\delta^s O(X,\tau_1,\tau_2)$ and $V \in ji-\Lambda_\delta^s O(X,\tau_1,\tau_2)$ such that $x \in U$ and $y \in V$.

Proof. It follows directly from definition 4.1 and theorem 4.7.

Theorem 5.5 In a bitopological space (X, τ_1, τ_2), the following statements are equivalent:

(1) (X, τ_1, τ_2) is pairwise $\Lambda_\delta^s - R_1$.

(2) For any two distinct points $x, y \in X$, $ij - C^{\Lambda_\delta^s}(\{x\}) \neq ji - C^{\Lambda_\delta^s}(\{y\})$ implies that there exist a $ij - \Lambda_\delta^s$ closed set F_1 and a $ji - \Lambda_\delta^s$ closed set F_2 such that $x \in F_1$, $y \in F_2$, $x \notin F_2$, $y \notin F_1$ and $X = F_1 \cup F_2$.

Proof. (1) ⟹ (2) Suppose that (X, τ_1, τ_2) is pairwise $\Lambda_\delta^s - R_1$. Let $x, y \in X$ such that $ij - C^{\Lambda_\delta^s}(\{x\}) \neq ji - C^{\Lambda_\delta^s}(\{y\})$. By theorem 5.3, there exist disjoint sets $V \in ij - \Lambda_\delta^s(X, \tau_1, \tau_2)$ and $U \in ji - \Lambda_\delta^s(X, \tau_1, \tau_2)$ such that $x \in U$ and $y \in V$. Then $F_1 = X \backslash V$ is a $ij - \Lambda_\delta^s$ closed set and $F_2 = X \backslash U$ is a $ji - \Lambda_\delta^s$ closed set such that $x \in F_1$, $x \notin F_2$, $y \in F_2$, $y \notin F_1$ and $X = F_1 \cup F_2$.

(2) ⟹ (1) Let $x, y \in X$ such that $ij - C^{\Lambda_\delta^s}(\{x\}) \neq ji - C^{\Lambda_\delta^s}(\{y\})$. Hence for any two distinct points x, y of X, $ij - C^{\Lambda_\delta^s}(\{x\}) \cap ji - C^{\Lambda_\delta^s}(\{y\}) = \phi$. Then by theorem 4.3, (X, τ_1, τ_2) is pairwise $\Lambda_\delta^s - R_0$. By (2), there exists a $ij - \Lambda_\delta^s$ closed set F_1 and a $ji - \Lambda_\delta^s$ closed set F_2 such that $X = F_1 \cup F_2$, $x \in F_1$, $y \in F_2$, $x \notin F_2$, $y \notin F_1$. Therefore, $x \in X \backslash F_2 = U \in ji - \Lambda_\delta^s(X, \tau_1, \tau_2)$ and $y \in X \backslash F_1 = V \in ij - \Lambda_\delta^s(X, \tau_1, \tau_2)$ which implies that $ij - C^{\Lambda_\delta^s}(\{x\}) \subseteq U$, $ji - C^{\Lambda_\delta^s}(\{y\}) \subseteq V$ and $U \cap V = \phi$. Hence (X, τ_1, τ_2) is pairwise $\Lambda_\delta^s - R_0$.

ACKNOWLEDGEMENT

The authors would like to thank the referees for the useful comments and valuable suggestions for improvement of the paper.

REFERENCES

[1] H. M. Abu-Donia, "New types of generalized closed sets in bitopological spaces", Journal of the Egyptian Mathematical Society, *21*, (2013), 318–323.

[2] H. M. Abu Donia, M. A. Abd Allah, A. S. Nawar, "Generalized $\psi^* -$ closed sets in bitopological spaces", Journal of the Egyptian Mathematical Society, 23, (2015), 527–534.

[3] Bishwambhar Roy and M. N. Mukherjee, "A unified theory for R_0, R_1 and certain other separation properties and their variant forms", Bol. Soc. Paran. Mat. (3s.) V.28, 2, (2010), 15–24.

[4] M. Caldas, J. Dontchev, "G. $\Lambda_s -$ sets and G. $V_s -$ sets", Mem. Fac. Sci. Kochi Univ. Math., 21, (2000),21–30.

[5] M. Caldas, M. Ganster, D. N. Georgiou, S. Jafari, and S. P. Moshokoa, "δ – semi open sets in topology", Topology Proc., 29, No. 2, (2005),369-383.

[6] M. Caldas, S. Jafari, S. A. Ponmani and M. L. Thivagar, "On some low separation axioms in bitopological spaces", Bol. Soc. Paran. Mat.,(3s.) V. 24, 1-2, (2006), 69-78.

[7] A. Edward Samuel and D. Balan, "Some aspects of $ij - \delta$ semi open sets in bitopological spaces", Global Journal of Pure and Applied Mathematics, Vol. 11, No. 6, (2015), pp.4879-4898.

[8] A. Edward Samuel and D. Balan, "On $\Lambda_\delta^s -$ Sets in bitopological spaces", General Mathematics Notes, Vol. 32, No. 1, January (2016), pp.21-31

[9] M. M. El-Sharkasy, "On $\Lambda_\alpha -$sets and the associated topology T^{Λ_α}", Journal of the Egyptian Mathematical Society, 23, (2015), 371–376.

[10] A. Ghareeb, T. Noiri, "Λ - Generalized closed sets in bitopological spaces", Journal of the Egyptian Mathematical Society, 19, (2011), 142–145.

[11] M. J. Jeyanthi, A. Kilicman, S. Pious Missier and P. Thangavelu, "$\Lambda_r -$ Sets and separation axioms", Malaysian Journal of Mathematics, 5(1), (2011), 45 – 60.

[12] A. B. Khalaf and A. M. Omer, "$S_i -$ open sets and $S_i -$ continuity in bitopological spaces", Tamkang journal of Mathematics,Vol.43,.No.1, (2012), 81-97.

[13] F. H. Khedr, "Properties of $ij -$ delta open sets", Fasciculi Mathematici, No.52, (2014), 65 - 81.

[14] F. H. Khedr and K. M. Abdelhakiem, "Generalized Λ - sets and λ - sets in bitopological spaces", International Mathematical Forum, 4, No. 15, (2009), 705– 715.

[15] F. H. Khedr and H. S. Al-saadi, "On pairwise θ-semi-generalized closed sets", Far East J. Mathematical Sciences, 28 (2), Feb., (2008), 381–394.

[16] H. Maki, "Generalized Λ - sets and the associated closure operator", The special Issue in commemoration of Prof. Kazuada IKEDA's Retirement, (1986), 139-146.

[17] M. Mirmiran "Weak insertion of a perfectly continuous function between two real-valued functions", Mathematical Sciences And Applications E-Notes, V. 3 No. 1,(2015), 103-107.

[18] M. Pritha, V. Chandrasekar and A. Vadivel, "Some aspects of pairwise fuzzy semi preopen sets in fuzzy bitopological spaces", Gen. Math. Notes, Vol. 26, No. 1, Jan.(2015), 35-45.

Global Journal of Pure and Applied Mathematics (GJPAM) ISSN 0973-1768 Volume 12,Number 4 (2016)
© Research India Publications : http://www.ripublication.com

Properties of (α, β) cut sets of Intuitionistic L-Fuzzy Semi Filter (ILFSF) of lattices

*A. Maheswari**
Department of Mathematics,
Velammal College of Engineering & Technology,
Madurai, Tamil Nadu, India.
Email: sathyapriya1972@gmail.com

S. Karthikeyan
Assistant Professor/Mathematics
Velammal College of Engineering & Technology,
Madurai, Tamil Nadu, India.
Email: karthikeyan19732002@yahoo.com

M. Palanivelrajan
Department of Mathematics
Government Arts College,
Paramakudi, Tamil Nadu, India.
Email: palanivelrajan1975@gmail.com

***Abstract*— By combining the concept of L-fuzzy semi filter and Intuitionistic L-fuzzy sets we developed Intuitionistic L fuzzy Semi filter(ILFSF). As an extension of Intuitionistic L-fuzzy semi filter [3] the notion of (α, β) cut set have been put forward in our work. Some related properties also have been established with proof.**

Keywords*— Fuzzy subset, L-fuzzy subset, Intuitionistic L-fuzzy subset, Intuitionistic L-fuzzy semi filter, Intuitionistic L-fuzzy semi ideal, (α, β) cut sets of ILFSF

I. Introduction

In 1965, Lofti A. Zadeh [9] introduced the notion of a fuzzy subset of a set as a method for representing uncertainty in real physical world. The concept of intuitionistic fuzzy set was introduced by Atanassov.K.T [1] as a generalization of the notion of fuzzy set. Although a lot of studies have been done for fuzzy order structures the lattice-valued sets can be more appropriate to model natural problems. The justification to consider lattice valued fuzzy sets has been widely explained in the literature, since lattices are more richer structure and we can obtain non-comparable values of fuzzy sets. They can be applied, for instance, in image processing. Also the concepts of (α, β) cuts sets play a principal role in the relationship between fuzzy sets and crisp sets. They can be viewed as a bridge by which fuzzy sets and crisp sets are connected.

In the present paper, we have considered finite poset X and complete lattice L. The main purpose of this paper is to analyze the characterization of (α, β) cut sets of Intuitionistic L-fuzzy semi filter (ILFSF) of lattices

II. Preliminaries

In this section, some well-known definitions are recalled. It will be necessary in order to understand the new concepts and theorems introduced in this paper.

A poset is a nonempty set X with a partial order ≤. It is usually denoted as an ordered pair (X, ≤). A sub-poset of (X, ≤) is a subset Y of X in which the order is the one restricted from X, and usually denoted in the same way (≤). A semi filter on a poset X is any sub poset U, satisfying the following: for $x \in U$, $y \in X$, $x \le y$ implies $y \in U$. Dually, a semi ideal on X is any sub-poset D, satisfying: for $x \in D$, $y \in X$, $y \le x$ implies $y \in D$. A lattice is a poset L in which for each pair of elements x, y there is a greatest lower bound (glb, infimum, meet) and a least upper bound (lub, supremum, join), denoted respectively by $x \wedge y$ and $x \vee y$. These are binary operations on L. A non-empty poset L is said to be a complete lattice if infimum and supremum exist for each subset of L. Complete lattice possesses the top (1) and the bottom element (0). On the other hand, a lattice L is distributive, if each operation is distributive with respect to the other.

Definition 2.1. *Let (L,≤) be a complete lattice with least element 0 and greatest element 1 and an involutive order reversing operation $N : L \to L$. Then an Intuitionistic L−fuzzy subset (ILFS) A in a non-empty set X is defined as an object of the form $A = \{< x, \mu_A(x), \nu_A(x)> / x \in X\}$ where $\mu_A : X \to L$ is the degree of membership and $\nu_A : X \to L$ is the degree of non-membership of the element $x \in X$ satisfying $\mu_A(x) \le N(\nu_A(x))$.*

Definition 2.2. *An Intuitionistic L-fuzzy set of a Lattice is called as an Intuitionistic L-fuzzy semi filter whenever $x \le y$, we have $\mu_A(x) \le \mu_A(y)$ and $\nu_A(x) \ge \nu_A(y)$.*

Example 2.3. *Let X: {0,1,2,3} and L = {0,a,b,1}*

Define μ: X → L and ν: X → L as follows:

X	0	1	2	3
μ	a	a	b	1
ν	1	b	a	a

Here
$0 \le 1 \Rightarrow \mu_A(0) \le \mu_A(1)$ & $\nu_A(0) \ge \nu_A(1)$
$0 \le 2 \Rightarrow \mu_A(0) \le \mu_A(2)$ & $\nu_A(0) \ge \nu_A(2)$
$0 \le 3 \Rightarrow \mu_A(0) \le \mu_A(3)$ & $\nu_A(0) \ge \nu_A(3)$
$1 \le 2 \Rightarrow \mu_A(1) \le \mu_A(2)$ & $\nu_A(1) \ge \nu_A(2)$
$1 \le 3 \Rightarrow \mu_A(1) \le \mu_A(3)$ & $\nu_A(1) \ge \nu_A(3)$
$2 \le 3 \Rightarrow \mu_A(2) \le \mu_A(3)$ & $\nu_A(2) \ge \nu_A(3)$

Thus whenever $x \le y$, we have $\mu_A(x) \le \mu_A(y)$ and $\nu_A(x) \ge \nu_A(y)$.

Definition 2.4. An Intuitionistic L-fuzzy set of a Lattice is called as an Intuitionistic L-fuzzy semi ideal whenever $x \le y$, we have $\mu_A(x) \ge \mu_A(y)$ and $\nu_A(x) \le \nu_A(y)$.

*Corresponding author.

This paper was presented by the first author in the National Conference on AMASE-2016 conducted in Department of Mathematics, University College of Engineering-Pattukkottai, Thanjavur, Tamil Nadu, India, on 22nd January 2016.

Definition 2.5. *Let A be an Intuitionistic L-fuzzy semi filter(ideal) on X. Then for α, β∈L, the (α, β) cut set of Intuitionistic L-fuzzy semi filter (ideal) is defined as the set* $A_{(\alpha,\beta)} = \{x \in X \,/\, \mu_A(x) \geq \alpha \text{ and } \nu_A(x) \leq \beta\}$.

Example 2.6.

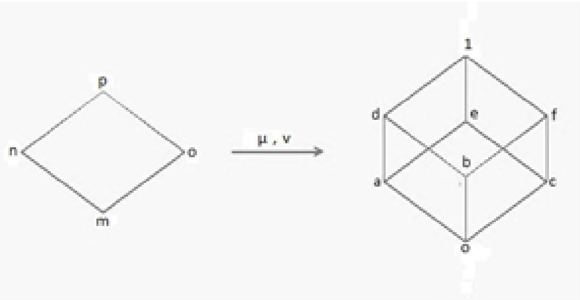

μ	m	n	o	p	ν	m	n	o	p
μ_1	o	b	c	f	ν_1	f	c	b	o
μ_2	o	a	b	d	ν_2	d	b	a	o
μ_3	b	d	f	1	ν_3	1	f	d	b
μ_4	o	a	c	e	ν_4	e	c	a	o

Consider μ_1 and ν_1

If $\alpha \leq \beta$ then	If $\alpha \geq \beta$ then
A_{ob} = {o, p}	A_{bo} = {p}
A_{oc} = {n, p}	A_{co} = {p}
A_{bf} = {n, p}	A_{cb} = {o, p}
A_{cf} = {o, p}	A_{fc} = {p}
A_{of} = {m, n, o, p}	A_{fo} = {p}

Definition 2.7. *Let X and X' be any two sets. Let f: X → X' be any function and A be an Intuitionistic Fuzzy set in X, V be an Intuitionistic Fuzzy set in f(x) = X' defined by* $\mu_v(y) = \sup_{x \in f^{-1}(y)} \mu_A(x)$ *and* $\nu_v(y) = \inf_{x \in f^{-1}(y)} \nu_A(x)$ *for every x∈X and y∈X' then A is called a pre image of V under f and is denoted by* $f^{1}(V)$.

III. Properties of (α, β) Cut Sets

Let A be an Intuitionistic L fuzzy semi filter. Then the union and the intersection of two (α, β) cut sets is again a (α, β) cut set of A. The same can be proved in the case of Intuitionistic L fuzzy semi ideal also.

Proposition 3.1. *Let (X, ≤) be a poset. Let (L, ≤) be a complete lattice and A be an Intuitionistic L fuzzy set on X. Then the following are equivalent*

i) A is an Intuitionistic L-fuzzy semi filter
ii) $A_{(\alpha,\beta)}$ *is a crisp semi filter*

Proof. In the proof of this theorem we have to prove the equivalence among these conditions.
By combining the definition of Intuitionistic L-fuzzy semi filter and classical semi filter we can have the proof for the necessary part.

that is A = {< x, $\mu_A(x)$, $\nu_A(x)$> / x ∈ X} and if $x \leq y$, we have $\mu_A(x) \leq \mu_A(y)$ and $\nu_A(x) \geq \nu_A(y)$.
Also $x \in A_{(\alpha,\beta)} \Rightarrow \mu_A(x) \geq \alpha$ and $\nu_A(x) \leq \beta$.
Hence $\alpha \leq \mu_A(x) \leq \mu_A(y)$ and $\nu_A(y) \geq \nu_A(x) \geq \beta$.
Therefore $x \leq y$ and $y \in X \Rightarrow y \in A_{(\alpha,\beta)}$ which proves $A_{(\alpha,\beta)}$ is a crisp semi filter.

Since the elements of $A_{(\alpha,\beta)}$ are the elements of X we can easily prove the sufficient part.
Considering $\mu_A(x) = \alpha$ and $\nu_A(x) = \beta$ we will have $\mu_A(y) \geq \mu_A(x)$ and $\nu_A(y) \leq \nu_A(x)$.
⇒ whenever $x \leq y$, we have $\mu_A(x) \leq \mu_A(y)$ and $\nu_A(x) \geq \nu_A(y)$.
Thus the proof of this theorem is an immediate consequence of the definitions of (α, β) cut sets and Intuitionistic L-fuzzy semi filter.

Proposition 3.2. *Let A and B are two Intuitionistic L fuzzy semi filters on X. If* $A \subseteq B$ *then* $A_{(\alpha,\beta)} \subseteq B_{(\alpha,\beta)}$.

Proof. Taking an element x in $A_{(\alpha,\beta)}$, we will prove this x always belongs to $B_{(\alpha,\beta)}$. If $A \subseteq B$ then $\mu_A(x) \leq \mu_B(x)$ and $\nu_A(x) \geq \nu_B(x)$. From the definition of Intuitionistic L-fuzzy semi filter we have $x \leq y \Rightarrow \mu_A(x) \leq \mu_A(y)$ and $\nu_A(x) \geq \nu_A(y)$ and $x \in A_{(\alpha,\beta)} \Rightarrow \mu_A(x) \geq \alpha$ and $\nu_A(x) \leq \beta$.
Combining the above we have $\mu_B(x) \geq \alpha$ and $\nu_B(x) \leq \beta$ which implies $x \in B_{(\alpha,\beta)}$. Thus we have the result.

The converse of the above theorem is not true. That is $A_{(\alpha,\beta)} \subseteq B_{(\alpha,\beta)}$ does not imply $A \subseteq B$

Example 3.3.

Consider X = {1,2,3,5,6,10,15,30}.
A = {(1,x,y), (2,0,1), (3,b,e), (5,c,d), (6,0,1), (10,0,1), (15,f,x), (30,0,1)}
B = {(1,0,1), (2,a,f), (3,b,e), (5,c,d), (6,d,c), (10,e,b), (15,f,a), (30,1,0)}

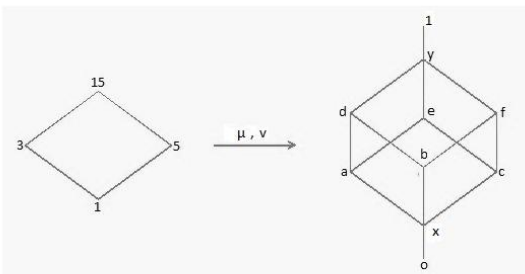

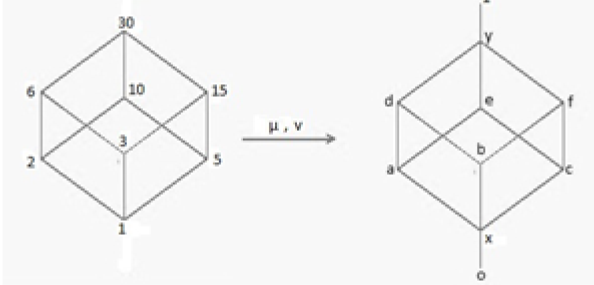

Global Journal of Pure and Applied Mathematics (GJPAM) ISSN 0973-1768 Volume 12,Number 4 (2016)

Here $A_{(b, f)}$ = {3, 15} ana $B_{(b, f)}$ = {3, 6, 10, 15, 30}
clearly $A_{(b, f)} \subseteq B_{(b, f)}$, But $A \not\subset B$

Proposition 3.4. *The homomorpic image of an (α, β) cut set of an ILFSF is again a (α, β) cut set.*

Proof. Considering two lattices L_1 and L_2 and let f : $L_1 \rightarrow L_2$ be a homomorphism. Taking an Intuitionistic L fuzzy semi filter A of L_1 and let B = f(A) of L_2 we have B is an Intuitionistic L fuzzy semi filter of L_2 [3]. From the definition 2.7 if $A_{(\alpha, \beta)}$ is an (α, β) cut set of A, then $\mu_A(x) \geq \alpha$ and $\nu_A(x) \leq \beta$. Also from the definition 2.7 it is clear that $\mu_A(x) = \mu_B(f(x))$ and $\nu_A(x) = \nu_B(f(x))$. Hence $\mu_B(f(x)) \geq \alpha$ and $\nu_B(f(x)) \leq \beta$ which gives the result that $B_{(\alpha\ \beta)}$ is a (α, β) cut set of f(A).

Proposition 3.5. *The collection of all (α, β) cut sets of an Intuitionistic L-fuzzy semi filter is a complete lattice.*

Proof. Considering { $A_{(\alpha_i,\beta_i)}$ } be the family of (α, β) cut sets of an Intuitionistic L-fuzzy semi filter A, we can prove that this family is a complete lattice. First of all let us prove that { $A_{(\alpha_i,\beta_i)}$ } is a poset. For that we choose the partial order as $\subseteq$

i) cleary $A_{(\alpha_i,\beta_i)} \subseteq A_{(\alpha_i,\beta_i)}$ $\forall$i since $\alpha_i \leq \alpha_i$ and $\beta_i \leq \beta_i$ (Reflexivity)

ii) Let $A_{(\alpha_i,\beta_i)} \subseteq A_{(\alpha_j,\beta_j)}$ and $A_{(\alpha_j,\beta_j)} \subseteq A_{(\alpha_i,\beta_i)}$

$\Rightarrow \alpha_j \leq \alpha_i$ & $\beta_j \geq \beta_i$ and $\alpha_i \leq \alpha_j$ & $\beta_i \geq \beta_j$

$\Rightarrow \alpha_j \leq \alpha_i$ & $\alpha_i \leq \alpha_j$ and $\beta_j \geq \beta_i$ & $\beta_i \geq \beta_j$

$\Rightarrow \alpha_i = \alpha_j$ & $\beta_i = \beta_j$

Thus $A_{(\alpha_i,\beta_i)} = A_{(\alpha_j,\beta_j)}$ (Anti symmetry)

iii) Let $A_{(\alpha_i,\beta_i)} \subseteq A_{(\alpha_j,\beta_j)}$ and $A_{(\alpha_j,\beta_j)} \subseteq A_{(\alpha_k,\beta_k)}$

$\Rightarrow \alpha_j \leq \alpha_i$, $\beta_j \geq \beta_i$ and $\alpha_k \leq \alpha_j$ & $\beta_k \geq \beta_j$

$\Rightarrow \alpha_i \geq \alpha_j \geq \alpha_k$ and $\beta_i \leq \beta_i \leq \beta_k$

$\Rightarrow \alpha_i \geq \alpha_k$ and $\beta_i \leq \beta_k$

Thus $A_{(\alpha_i,\beta_i)} \subseteq A_{(\alpha_k,\beta_k)}$ (Transitivity)

Hence { $A_{(\alpha_i,\beta_i)}$ } is poset

To prove: { $A_{(\alpha_i,\beta_i)}$ } is a complete lattice

Here every member of { $A_{(\alpha_i,\beta_i)}$ } is a subset of A formed by an (α, β) cut set

Considering the partial order $\subseteq$, we can have

$A_{(\alpha_i,\beta_i)} \vee A_{(\alpha_j,\beta_j)} = A_{(\alpha_i,\beta_i)} \cup A_{(\alpha_j,\beta_j)}$ and

$A_{(\alpha_i,\beta_i)} \wedge A_{(\alpha_j,\beta_j)} = A_{(\alpha_i,\beta_i)} \cap A_{(\alpha_j,\beta_j)}$

Clearly every 2-element subsets of { $A_{(\alpha_i,\beta_i)}$ } has least upper bound and greatest lower bound.

Hence { $A_{(\alpha_i,\beta_i)}$ } is a lattice.

Moreover every non empty subset of { $A_{(\alpha_i,\beta_i)}$ } also has both lub and glb

Thus { $A_{(\alpha_i,\beta_i)}$ } is a complete lattice.

Remark 3.6

- If the family of (α, β) cut sets is formed by all the classical semi filters of X then the membership and non membership functions μ and ν are order embedding.
- If α ≤ β then all the (α, β) cut sets of A will be the same irrespective of the membership and non membership functions.
- If α ≥ β then also we get the same (α, β) cut sets under any membership and non membership functions.
- It is clear that every $A_{(\alpha, \beta)}$ is closed under intersections and contains X.
- In example 3.3 we have that the family of (α, β) cut sets is formed by the classical semi filter of x. Also when we consider the other μ_i's and νi's there also we get the same sets. Moreover all the (α, β) cut sets are classical semi filters of X

IV. CONCLUSION

In this paper, we have considered the (α, β) cut sets of Intuitionistic L-fuzzy semi filter and investigated some of their useful properties. The relationships between (α, β) cut sets and the classical semi filters are also examined. Moreover, we have established necessary and sufficient conditions under which for a given family of classical semi filters , there exists an (α, β) cut set such that its collection of cuts coincides with the family of classical semi filters. In particular, we have done a deeper study for the Intuitionistic L-fuzzy semi filter such that its family of (α, β) cuts is formed by all the classical semi filters.

ACKNOWLEDGMENT

The authors appreciatively acknowledge the financial support of the Chairman, Velammal Educational Trust, and also acknowledge the Principal, HOD, Supervisor, Joint Supervisor and family for their support in doing research work.

REFERENCES

[1] Atanassov K.T, "Intuitionistic Fuzzy sets", Fuzzy Sets and Systems Vol.20, Issue 1, pages 87 – 96, 1986.

[2] Kog A. and Balkanay E., "θ-Euclidean L-fuzzy ideals of Rings", Turkish journal of mathematics, Vol. 26, pages. 149 – 158, 2002

[3] Maheswari.A, Palanivelrajan.M, "Introduction to Inutitionistic L-fuzzy Semi Filter", ICMLC Vol.5, pages 275–277, 2011.

[4] Maheswari.A, Karthikeyan.S, Palanivelrajan.M, "Characterization of level sets of Iintuitionistic L-fuzzy Semi filter of lattices" Notes on Intuitionistic Fuzzy Sets, Vol. 18, 2012, No. 2, 21–25.

[5] Maheswari.A, Karthikeyan.S, Palanivelrajan.M "Some Operations on Intuitionistic L- fuzzy semi filter" Antartica Journal of Mathematics Vol.11, No.1, 13 – 17, March 2014.

[6] Mohammed M. Atallah, "On the L-fuzzy prime ideal theorem of distributive lattices", The journal of fuzzy Mathematics, Vo.l 9, No. 4, 2001.

[7] Palaniappan .N , Palanivelrajan.M and Arjunan. K "On Intuitionistic L-fuzzy ideal of Lattices", Antarctica J. Math. Vol.5 Issue 2, pages. 53-57, 2008.

[8] Sharma.P.K "(α,β) – Cut of Intuitionistic Fuzzy Groups", International Mathematical Forum, Vol. 6, 2011, no. 53, 2605 – 2614.

[9] Zadeh.L.A, "Fuzzy sets",. Inform.Control. Vol.8, pages.338-353 1965.

[10] Yuan Xue-Hai, Li Hong-xing, "Cut Sets on Interval- valued Intuitionistic Fuzzy Sets", 6th International Conference on Fuzzy Systems and Knowledge Discovery, 2009.

Global Journal of Pure and Applied Mathematics (GJPAM) ISSN 0973-1768 Volume 12,Number 4 (2016)

Review on importance of distance measure in data mining and its application

*E. Kavitha**
University College of Engineering Villupuram,
Villupuram, Tamil Nadu, India
Email: ekavithavrs@gmail.com

R. Tamilarasan
University College of Engineering Pattukottai,
Thanjavur, Tamil Nadu, India.
Email: rrtamilk@yahoo.co.in

***Abstract*— This review paper deals with the importance of Distance Measure in Data Mining. It conjointly expresses the essential of distance measure in mining of knowledge by varied researchers. Here we tend expose the fundamentals of Data Mining techniques, its completely different approaches, difficulties, execs and cons of them. Completely different measures of distance or similarity are convenient for various varieties of analysis. Data Mining is an analytic process to explore information in search of consistent patterns, then to validate the findings by applying the detected patterns to new subsets of data. Retrieval of information, similarities / dissimilarities, finding and implementing the correct measure are at the heart of data mining. Distance measures are mathematical approaches to measure distance between the objects. Practically distance measures helps to compare the objects from three different standpoints such as Similarity, Dissimilarity and Correlation. The work carried out in this paper is based on the study of popular distance measures.**

Keywords*—*Data mining, distance measure, Euclidean distance, Manhattan distance, Correlation distance.

I. INTRODUCTION

Simply saying for easy understanding Data mining refers to extracting or mining knowledge from large amounts of data. Many data mining techniques are based on similarity measures between objects [1]. At heart, the goal of data mining is to extract knowledge from data. Data mining is an interdisciplinary field, whose core is at the intersection of machine learning, statistics, and databases. There are several data mining task, including classification, regression, clustering etc., [2]. Each of these tasks can be regarded as a kind of problem to be solved by a data mining algorithm.

II. DISTANCE MEASURE

Importance of Measurement aims to mine structured data is to discover relationships that exist in the real world – business, physical, conceptual etc. Instead of looking at real world we look at data describing it .Data maps entities in the area of concern to symbolic representation by means of a measurement procedure. Numerical relationships between variables confine relationships between objects. Measurement process is crucial. Similarity metric is the basic measurement and used by a number of data mining algorithms. It measures the similarity or dissimilarity between two data objects which have one or multiple attributes. Informally, the similarity is a numerical measure of the degree to which the two objects are alike. It is usually non-negative and are often between 0 and 1, where 0 means no similarity, and 1 means complete similarity [8]. Considering different data type with a number of attributes, it is important to use the appropriate similarity metric to well measure the proximity between two objects. For example, Euclidean distance and correlation are useful for dense data such as time series or two-dimensional points. Jaccard and cosine similarity measures are useful for sparse data like documents, or binary data.

Proximity is a general term to indicate similarity and dissimilarity [11]. Similarity [4] is a numerical measure of how alike two data objects are. Value is higher when objects are more alike. It often falls in the range [0,1]. Dissimilarity is numerical measure of how different two data objects are. Lower when objects are more alike .Minimum dissimilarity is often 0 and the upper limit varies.

Distance or Metric should satisfy

1. d(i,j) ≥ 0 Positivity

2 d(i,j) = d(j,i) Commutativity

3 d(i,j) < d(i,k)+d(k,j) Triangle Inequality

The different distance measures are

- Euclidean distance
- Manhattan distance
- Correlation distance
- Min- kowski distance

The Minkowski distance is a metric in a normed vector space which can be considered as a generalization of both the Euclidean distance and the Manhattan distance. The Minkowski distance is as follows

$$d(i,j) = \sqrt[q]{(|x_{i1} - x_{j1}|^q + |x_{i2} - x_{j2}|^q + \ldots + |x_{ip} - x_{jp}|^q)}$$

where i = (x_{i1}, x_{i2}, …, x_{ip}) and j = (x_{j1}, x_{j2}, …, x_{jp}) are two p-dimensional data objects, and q is a positive integer .

If q = 1, d is Manhattan distance

$$d(i,j) = |x_{i1} - x_{j1}| + |x_{i2} - x_{j2}| + \ldots + |x_{ip} - x_{jp}|$$

If q = 2, d is Euclidean distance

$$d(i,j) = \sqrt{(|x_{i1} - x_{j1}|^2 + |x_{i2} - x_{j2}|^2 + \ldots + |x_{ip} - x_{jp}|^2)}$$

*Corresponding author.

This paper was presented by the first author in the National Conference on *Advances in Mathematics and its Applications to Science and Engineering* (AMASE-2016) conducted in Department of Mathematics, University College of Engineering-Pattukkottai, Thanjavur, Tamil Nadu, India, on 22nd January 2016.

Euclidean distance [5], [6], [7], [10] is one of the most commonly-used methods to measure the distance between two data objects.

Correlation is often used as a preliminary technique to discover relationships between variables. More precisely, the correlation is a measure of the linear relationship between two variables. The correlation is a measure of how well two sets of data fit on a straight line. Correlation is always in the range -1 to 1. A correlation of 1 (-1) means that x and y have a perfect positive (negative) linear relationship. If the correlation is 0, then there is no linear relationship between the attributes of the two data objects. However, the two data objects might have non-linear relationships. There are different types of correlation and few examples are Pearson Correlation[10] and Jackknife Correlation [6].

Pearson correlation is defined by the following equation. x and y represents two data objects.

$$d_C(x,y) = 1 - \frac{\sum_{i=1}(x_i - \bar{x})(y_i - \bar{y})}{\sqrt{\sum_{i=1}(x_i - \bar{x})^2 \sum_{i=1}(y_i - \bar{y})^2}}.$$

Distance is to indicate dissimilarity. The active use of any of these measures (Table 1) is highly influenced by the number of data records / instances, their dimensionality, the level of precision required and the nature of analysis required.

TABLE I. DIFFERENT DISTANCE MEASURE

Distance measure	**Forms**	**Explanation**
Min-kowski distance	$D_{Mk} = \sqrt[p]{\sum_{i=1}^{d} \lvert X_i - Y_i \rvert^p}$	Metric. Invariant to any translation and rotation only for n = 2 (Euclidean distance). Features with large values and variances tend to dominate over other features.
Euclidean distance	$D_{Euc} = \sqrt{\sum_{i=1}^{d} \lvert X_i - Y_i \rvert^2}$	The most commonly used metric. Special case of Minkowski metric at n = 2. Tends to form hyper-spherical clusters.
City-block distance	$D_C = \sum_{i=1}^{d} \lvert X_i - Y_i \rvert$	Special case of Minkowski metric at n = 1. Tend to form hyper- rectangular clusters.
Sup distance	$D_{Sp} = max \lvert X_i - Y_i \rvert$	Special case of Minkowski metric at n $\rightarrow \infty$.
Mahala-nobis distance	$D_M = (X_i - Y_i)^T S^{-1} (X_i - Y_i)$ where S is within group co-variance matrix.	Invariant to any nonsingular linear transformation. S is calculated based on all objects. Tends to form hyper-ellipsoidal clusters. When features are not correlated, squared Mahalanobis distance is equivalent to squared Euclidean distance. May tend to be computationally expensive.
Pearson correlation	$D_p(X,Y) = \sum_{i=1}^{d} \frac{(X_i - Y_i)^2}{Y_i}$	Not a metric. Derived from correlation coefficient. Unable to detect the magnitude of differences of two variables.

III. DATA MINING

Data mining is abstraction of interesting (non-trivial, implicit, previously unknown and potentially useful) information or patterns from data in large databases. Data mining tasks are classified into two Descriptive data mining and Predictive data mining. Prediction Tasks are used in some variables to predict unknown or future values of other variables whereas Description Tasks used to find human-interpretable patterns that describe the data. Some of the common data mining tasks are Classification [Predictive], Clustering [Descriptive], Association Rule Discovery [Descriptive], Sequential Pattern Discovery [Descriptive], Regression [Predictive], Deviation Detection [Predictive] etc. Commonly clustering is used to find out the similar, dissimilar and outlier items from the databases. The key idea behind the clustering is the distance between the data items. Clustering [12] is the task of discovering groups on the bases of the similarities of data items within the clusters and dissimilarities outside the clusters on the other hand from data set. A cluster is therefore a collection of objects which are “similar” between them and are “dissimilar” to the objects belonging to other clusters. Clustering is a main task of

Explorative data mining, and a common technique for statistical data analysis used in many fields, including machine learning, pattern recognition, image analysis, information retrieval, and bioinformatics. So, the goal of clustering is to determine the intrinsic grouping in a set of unlabeled data.

IV. APPLICATIONS

Data mining is widely used in diverse areas [3]. Most of the application in data mining are Retail, telecommunication, banking, fraud analysis, DNA mining, stock market analysis, Web mining, Weblog analysis, etc.

A. *Fraud Detection*

Predict fraudulent cases in credit card transactions. Use credit card transactions and the information on its account-holder as attributes. When a customer buys, what he buys, how often he pays on time, etc. Label past transactions as fraud or fair transactions. This forms the class attribute. Learn a model for the class of the transactions. Use this model to detect fraud by observing credit card transactions on an account.

B. *Market Segmentation*

Subdivide a market into distinct subsets of customers where any subset may conceivably be selected as a market target to be reached with a distinct marketing mix. Collect different attributes of customers based on their geographical and lifestyle related information. Find clusters of similar customers. Measure the clustering quality by observing buying patterns of customers in same cluster vs. those from different clusters.

C. *Document Clustering*

To find groups of documents that are similar to each other based on the important terms appearing in them. To identify frequently occurring terms in each document. Form a similarity measure based on the frequencies of different terms. Use it to cluster. Information Retrieval can utilize the clusters to relate a new document or search term to clustered documents.

V. CONCLUSION

In this paper we literature several papers to find the importance of distance measure in Data mining. Data mining plays an important role in many fields to retrieve useful information as the need of the customer. In retrieving or grouping of similar information under a common group the distance measure plays a major role. Grouping of similar items into a separate group is called as clustering. There are several papers dealing about the different distance measure and its support according to the nature of applications. The distance measure like Euclidean, Pearson, Jaccard etc are showing their benefits in grouping of similar data objects. They also have their own merits and demerits according to the place of using them.

REFERENCES

[1] David Hand, Heikki Mannila and Padhraic Smyth,. Principles of Data Mining, MIT press, 2002.

[2] U. M. Fayyad, G. Piatetsky-Shapiro, and P. Smyth, "From data mining to knowledge discovery: An overview," in Advances in Knowledge Discovery & Data Mining

[3] J. Han and M. Kamber, Data Mining: Concepts and Techniques. San Mateo, CA: Morgan Kaufmann, 2001.

[4] D. P. Berrar, W. Dubitzky, and M. Granzow, A Practical Approach to Microarray Data Analysis. Norwell, MA: Kluwer, 2003.

[5] Huai-Kuang Tsai, Jinn-Moon Yang, Yuan-Fang Tsai, and Cheng-Yan Kao," An Evolutionary Approach for Gene Expression Patterns,", IEEE Transactions on Information Technology in Biomedicine, VOL. 8, No. 2, June 2004 R. Uthurusamy, Eds. Cambridge, MA: MIT Press, 1996, pp. 1–34.

[6] Daxin Jiang, Chun Tang, and Aidong Zhang , "Cluster Analysis for Gene Expression Data: A Survey," IEEE Transactions on Knowledge and Data Engineering, Vol. 16, NO. 11, November 2004.

[7] http://en.wikipedia.org/wiki/Euclidean_distance

[8] Introduction to Data Mining, Pang-Ning Tan, Michael Steinbach, Vipin Kumar, Published by Addison Wesley

[9] Georgina Stegmayer, Diego H. Milone, Laura Kamenetzky,Mariana G. Lo´ pez, and Fernando Carrari, "A Biologically Inspired Validity Measure for Comparison of Clustering Methods over Metabolic Data Sets," IEEE/ACM Transactions on Computational Biology and Bioinformatics, VOL. 9, NO. 3, MAY/JUNE 2012.

[10] Daxin Jiang, Jian Pei, Member, IEEE Computer Society, and Aidong Zhang, Member, IEEE," An Interactive Approach to Mining Gene Expression Data," IEEE Transactions on Knowledge and Data Engineering, Vol. 17, NO. 10, October 2005.

[11] Pablo A. Jaskowiak, Ricardo J.G.B. Campello, and Ivan G. Costa," Proximity Measures for Clustering Gene Expression Microarray Data: A Validation Methodology and a Comparative Analysis," IEEE/ACM Transactions on Computational Biology and Bioinformatics, Vol. 10, No. 4, July/August 2013.

[12] Deepak Sinwar, Rahul Kaushik,Study of Euclidean and Manhattan Distance Metrics using Simple K-Means Clustering," International Journal For Research in Applied Science and Engineering Technology (I JRAS ET), Vol. 2 Issue V, May 2014.

[13] L. D. Chase, " Euclidean Distance", College of Natural Resources, Colorado State University, Fort Collins, Colorado, USA, 824-146-294, NR 505, December 8, 2008.

Global Journal of Pure and Applied Mathematics (GJPAM) ISSN 0973-1768 Volume 12,Number 4 (2016)
© Research India Publications : http://www.ripublication.com

Extension of TOPSIS model for multi-criteria decision making

*G. Mohanraj**
Department of Mathematics, Annamalai University,
Tamil Nadu, India.
Email: gmohanraaj@gmail.com

S. Azhaguvelavan
Department of Mathematics, Annamalai University,
Tamil Nadu, India.
Email: solaiazhagumaths@gmail.com

***Abstract*— Multi criteria group decision making methods are broadly used in the real-world decision circumstances for homogeneous groups. Decision-making problems often involve a complex decision-making process in which multiple requirements and uncertain conditions have to be taken into consideration simultaneously. In this paper, we consider the ideal solution and the anti-ideal solution and assess each alternative in terms of similarity to the ideal solution and the anti-ideal solution. To minimize the error, the normalization of fuzzy data is carefully avoided. To get greater accuracy in ranking fuzzy rating, we use the latest and advanced similarity measure. The proposed method is more flexible in modeling the decision makers preferences and more appropriate and effective to handle multi-criteria problems of considerable complexity.**

Keywords*— Trapezoidal fuzzy number, Multi criteria group decision making, Similarity measure.

I. INTRODUCTION

In 1981, C. L. Hwang and K. Yoon [13] first developed a **T**echnique for **O**rder **P**erformance by **S**imilarity to the **I**deal **S**olution (TOPSIS) for solving **M**ulti-**C**riteria **D**ecision-**M**aking (MCDM) problems. It helps decision maker(s)(DMs) organize the problems to be solved, and carry out analysis, comparisons and rankings of the alternatives. The basic principle of the TOPSIS is that chosen alternative should have the largest ideal solution from positive ideal solution and least ideal solution from negative ideal solution. In classical methods for multi-criteria decision making problems, the ratings and weights of criteria are known precisely. In the classical TOPSIS method, the ratings of alternatives and the weights of criteria are presented by real values, too. The classical TOPSIS method has been successfully used in different fields [5], [19].

In the past few years, numerous attempts to handle this vagueness, imprecision, and subjectiveness have been carried out to apply fuzzy set theory to multiple criteria evaluation methods [1, 2, 5, 24, 25, 26]. The overall utility of the alternatives with respect to all criteria is often represented by a fuzzy number, which is named the fuzzy utility and is often referred to by fuzzy multi-criteria evaluation methods. The ranking of the alternatives is based on the comparison of their corresponding fuzzy utilities [3, 5, 27, 14]. Multi-criteria evaluation methods are used widely in fields such as information project selection [14, 15], material selection [19], and many other areas of management decision problems [19] and strategy selection problems [4, 7, 9, 21]. Tsaur et al.[20] first convert a fuzzy MCDM problem into a crisp one via centroid defuzzification and then solve the non-fuzzy MCDM problem using the TOPSIS. Hsu and Chen [12] discuss an aggregation of fuzzy opinions under group decision making. Li [18] proposes a simple and efficient fuzzy model to deal with multi-judges/MCDM problems in a fuzzy environment. Liang [17] incorporates fuzzy set theory and the basic concepts of positive ideal and negative ideal points and extends MCDM to a fuzzy environment.

In 2003 Chen.S.J and Chen.S.M.[6] introduced a similarity measure using trapezoidal fuzzy numbers. Hejazi et al.[11] also introduced similarity measure between two trapezoidal fuzzy numbers. In 2010 Xu et al.[23] initiated new similarity measure of trapezoidal fuzzy numbers.

P.Dheena and G.Mohanraj [8] proposes the ideal solution and anti-ideal solution and assess each alternative in terms of distance as well as similarity to the ideal solution and anti-ideal solution.

This paper is organized as follows: The extension of TOPSIS for fuzzy multi-criteria decision making in section3.In section 4; an illustrative numerical example is given to apply the fuzzy multi-criteria method for alternatives of evaluating university faculty for tenure and promotion.

II. PRELIMINARIES

Definition *2.1.* *Let a_1, a_2, a_3, a_4 be any real numbers, such that $-\infty < a_1 \leq a_2 \leq a_3 \leq a_4 \leq \infty$. The membership function of a trapezoidal fuzzy number $\hat{T}$ has of the form is given by*

$$\mu_{\hat{T}}(x) = \begin{cases} 0 & if \ x < a_1 \\ \dfrac{x - a_1}{a_2 - a_1} & if \ a_1 \leq x \leq a_2 \\ 1 & if \ a_2 \leq x \leq a_3 \\ \dfrac{a_4 - x}{a_4 - a_3} & if \ a_3 < x \leq a_4 \\ 0 & if \ x > a_4 \end{cases}$$

Definition *2.2.* *Let a_1,a_2,a_3,a_4 be any real numbers, such that $-\infty < a_1 \leq a_2 \leq a_3 \leq a_4 \leq \infty$ and let w be the weight such that $0 \leq w \leq 1$. Then the membership function is given by*

*Corresponding author.

This paper was presented by the second author in the National Conference on *Advances in Mathematics and its Applications to Science and Engineering* (AMASE-2016) conducted in Department of Mathematics, University College of Engineering-Pattukkottai, Thanjavur, Tamil Nadu, India, on 22nd January 2016.

$$\mu_{\hat{T}}(x)=\begin{cases}0 & if\ x<a_1\\ w\times\left(\dfrac{x-a_1}{a_2-a_1}\right) & if\ a_1\le x\le a_2\\ w & if\ a_2\le x\le a_3\\ w\times\left(\dfrac{a_4-x}{a_4-a_3}\right) & if\ a_3< x\le a_4\\ 0 & if\ x>a_4\end{cases}$$

Similarity measure: *Let* $\hat{A}=(a_1,a_2,a_3,a_4;w_A)$ *and* $\hat{B}=(b_1,b_2,b_3,b_4;w_B)$ *be two generalized trapezoidal fuzzy numbers Xu et al.[23] proposed the similarity measure* $S(\hat{A},\hat{B})$ *that is given by*

$$S(\hat{A},\hat{B})=1-\frac{1}{8}\sum_{i=1}^{4}|a_i-b_i|-\frac{d(\hat{A},\hat{B})}{2} \qquad (2.1)$$

where

$$d(\hat{A},\hat{B})=\sqrt{\frac{(x^*_{\hat{A}}-x^*_{\hat{B}})^2+(y^*_{\hat{A}}-y^*_{\hat{B}})^2}{1.25}}$$

$$y^*_{\hat{A}}=\begin{cases}w_{\hat{A}}\times\dfrac{\left(\dfrac{a_3-a_2}{a_4-a_1}+2\right)}{6} & if\ a_4\ne a_1\\ \dfrac{w_{\hat{A}}}{2} & if\ a_4=a_1\end{cases}$$

$$y^*_{\hat{B}}=\begin{cases}w_{\hat{B}}\times\dfrac{\left(\dfrac{b_3-b_2}{b_4-b_1}+2\right)}{6} & if\ b_4\ne b_1\\ \dfrac{w_{\hat{B}}}{2} & if\ b_4=b_1\end{cases}$$

$$x^*_{\hat{A}}=\begin{cases}\dfrac{y^*_{\hat{A}}\times(a_3+a_2)+(a_4+a_1)\times(w_{\hat{A}}-y^*_{\hat{A}})}{2w_{\hat{A}}}, & if\ w_{\hat{A}}\ne 0;\\ \dfrac{a_4+a_1}{2}\ , & if\ w_{\hat{A}}=0\end{cases}$$

$$x^*_{\hat{B}}=\begin{cases}\dfrac{y^*_{\hat{B}}\times(b_3+b_2)+(b_4+b_1)\times(w_{\hat{B}}-y^*_{\hat{B}})}{2w_{\hat{A}}}, & if\ w_{\hat{B}}\ne 0;\\ \dfrac{a_4+a_1}{2}\ , & if\ w_{\mathbf{\hat{B}}}=0\end{cases}$$

Linguistic variables: *Let* $L^u=(l_0^u,l_1^u,l_2^u,...,l_t^u)$ *be the* u^{th} *pre-established finite and totally ordered linguistic term set* $t=1,2,3,...,t+1,$ *where* l_i^u *be the i-th linguistic term of* L^u *and* $t+1$ *is the cardinality of* L^u, l_i^u *can be approximately expressed as a trapezoidal fuzzy number.The* i^{th} *linguistic variables* l_i^u *is expressed as* $\hat{d}_i^u$ *by a formula[8] given by* $\hat{d}_i^u=(d_i^{u_1},d_i^{u_2},d_i^{u_3},d_i^{u_4})$

$$=\left(\max\left\{\frac{2i-1}{2t+1},0\right\},\frac{2i}{2t+1},\frac{2i+1}{2t+1},\min\left\{\frac{2i+2}{2t+1},1\right\}\right)$$

(2.2)

TABLE 3.1. *The raetings of the three alternatives by decision expertsunder all criteria*

		Decision makers		
Criteria	Alternatives	D_1	D_2	D_3
C_1:Teaching	A_1	MP	F	F
	A_2	F	G	F
	A_3	MP	G	MG
	A_4	VG	GF	VG
	A_5	MG	MG	MG
C_2:Research	A_1	G	MP	VG
	A_2	VG	F	MP
	A_3	MP	G	G
	A_4	MG	MG	MG
	A_5	G	VG	G
C_3:Service	A_1	G	G	VG
	A_2	VG	VG	G
	A_3	VG	MG	F
	A_4	MP	MG	VG
	A_5	MG	F	F

III. Extension of TOPSIS for Fuzzy Multi-Criteria Decision Making

A multi-criteria decision making problem is to select best alternatives from the set of alternatives by consisting set of criteria. The classical TOPSIS method is based on the idea that the best alternative have the largest similarity to the positive ideal solution and least similarity of the negative ideal solution. The positive ideal solution is compose of the best achievable values of local criteria while a negative ideal solution least achievable values of the local criteria.

Suppose multi-criteria decision making problem based on "m" –alternatives and "n"-criteria. There are "k" decision makers now give their ratings and alternative with respect to criteria.

The TOPSIS method consists of the following steps:

Step 1: The set of linguistic variable is given by the Table 3.2 Let $DM_1, DM_2, \ldots, DM_k$, be the k -set of decision makers. Let $l_{ij}^{(u)}$ be the linguistic variable is given by uth decision maker DM_u to the ith alternative A_i with respect to criteria C_j , which is give by the Table 3.1

TABLE 3.2: *LINGUISTIC TERMS AND CORRESPONDING TRAPEZOIDAL FUZZY NUMBERS.*

Linguistic terms	Trapezoidal fuzzy number
Low	(0,0,0.0769,0.1538)
Medium Low	(0.0769,0.1538,0.2308,0.3077)
Medium	(0.2308,0.3077,0.3846,0.4615)
Medium High	(0.3846,0.4615,0.5385,0.6154)
High	(0.5385,0.6154,0.6923,0.7692)
Very High	(0.6923,0.7692,0.8462,0.9231)
Extremely High	(0.8462,0.9231,1,1)

Step 2: The linguistic variables is converted into fuzzy trapezoidal numbers by the Equation 2.2.

Step 3: Let $\hat{r}_{ij}^{u}$ be the fuzzy trapezoidal number which is converted by the Equation 2.2 , corresponding to the linguistic variable $l_{ij}^{(u)}$.

Step 4: The normalized decision matrix

$$\hat{D} = \begin{pmatrix} \hat{v}_{11} & \hat{v}_{12} & . & . & . & \hat{v}_{1n} \\ \hat{v}_{21} & \hat{v}_{22} & . & . & . & \hat{v}_{2n} \\ . & . & . & . & . & . \\ . & . & . & . & . & . \\ . & . & . & . & . & . \\ \hat{v}_{m1} & \hat{v}_{m2} & . & . & . & \hat{v}_{mn} \end{pmatrix}$$

is calculated as follows

$$\hat{v}_{ij} = \sum_{u=1}^{k} r_{ij}^{u} w^{u} \qquad \textbf{(3.3)}$$

where $w^1, w^2, w^3, \ldots, w^k$ is the weight of $DM_1, DM_2, \ldots, DM_k$.

Step 5: Let B be set of the benefit criteria and C be the cost criteria. The positive ideal solution A_j^+ is given by

$$A_j^+ = \begin{cases} (1,1,1,1;1) & if\ i \in B \\ (0,0,0,0;1) & if\ i \in C \end{cases}$$

For all i=1,2,3,…n.

The negative ideal solution A_j^- is given as follows:

$$A_j^- = \begin{cases} (0,0,0,0;1) & if\ i \in B \\ (1,1,1,1;1) & if\ i \in C \end{cases}$$

For all i=1,2,3,…,n.

Step 6: Let S_{ij}^+ and S_{ij}^- be the similarity measures of $S(\hat{v}_{ij}, A_j^+)$ and $S(\hat{v}_{ij}, A_j^-)$ respectively which are calculated by the Equation 2.1

Step 7: The rank of alternative $R(A_i)$ is calculated by the formula

$$\sum_{j=1}^{n} \left(\frac{S_{ij}^+ + 1 - S_{ij}^-}{2} \right) \times w_j \qquad \textbf{(3.4)}$$

Where $w_1, w_2, w_3, \ldots, w_n$ be the weights of $n-$criteria $(C_1, C_2, C_3, \ldots C_n)$.

Step 8: The top rank of alternative is selected to be the best alternative.

IV. Numerical Example

In this section, we work out a numerical example to illustrate the TOPSIS approach for decision making problem with fuzzy data. Here multi-criteria decision making problem of evaluating university faculty for tenure and promotion.

Five faculty candidates are the alternatives denoted by $A = \{A_1, A_2, A_3, A_4, A_5\}$.The criteria are used at university are C_1 : Teaching, C_2 : Research, C_3 : Service and the weight vector $w =$ (0.36; 0.31; 0.33) for criteria (C_1, C_2, C_3). The alternatives $A = \{A_1, A_2, A_3, A_4, A_5\}$ are evaluated using linguistic values by decision makers DM = DM_1, DM_2, DM_3 whose weight vector $\lambda =$ (0.4, 0.5, 0.1) under this criteria. Here all criteria is benefit criteria.

Step 1: Decision maker's rating in linguistic variable is given in the Table 3.2.

Step2: The linguistic variable converted into trapezoidal fuzzy numbers by the Equation 2.2.

Step 3: $\hat{v}_{ij}$ is calculated by the Equation 3.3.

Step 4: Normalized decision matrix is calculated by the Equation 3.3.

Step 5: Positive ideal solution $A_j^+ = (1, 1, 1, 1; 1)$ and negative ideal solution $A_j^- = (0, 0, 0, 0; 1)$.

Step 6: S_{ij}^+ and S_{ij}^- as calculated and tabulated in Table 4.1and 4.2

TABLE 4.1. *SIMILARITY MEASURE FOR POSITIVE IDEAL SOLUTION* S_{ij}^+

	A_1	A_2	A_3	A_4	A_5
C_1	0.284151852	0.474464158	0.434375989	0.559535826	0.474464158
C_2	0.4161558236	0.510643781	0.437234174	0.469298464	0.652830065
C_3	0.612113381	0.710296354	0.562097759	0.391129334	0.391127069

TABLE 4.2. *SIMILARITY MEASURE FOR NEGATIVE IDEAL SOLUTION* S_{ij}^-

	A_1	A_2	A_3	A_4	A_5
C_1	0.652462673	0.474464158	0.514020213	0.380529530	0.47464158
C_2	0.521447474	0.425388402	0.488704536	0.469298464	0.277831249
C_3	0.323034603	0.214650561	0.377677782	0.549442439	0.549439563

Step 7: Rank of each alternatives is calculated and tabulated in Table 5.5.

TABLE 4.3. *RANK OF EACH ALTERNATIVE*

A_i	$R(A_i)$
A_1	0.465081844
A_2	0.594996140
A_3	0.50811543
A_4	0.519145255
A_5	0.532003254

V. CONCLUSION

In this method, normalization is carefully avoided to minimize the error. The alternatives are rankers as $A_2 \succ A_5 \succ A_4 \succ A_3 \succ A_1$.The alternative A_2 is selected to be the best alternative.

REFERENCES

[1] Buckley.J.J, Fuzzy hierarchical analysis. Fuzzy Sets System 17,(1982),233-247.

[2] Carlsson. C, Tackling an MCDM-problem with the help of some results from fuzzy set theory, Eur J Oper Res 10(3),(1982), 270-281.

[3] Chen.M.F and Tzeng.G.H,Combining grey relation and TOPSIS concepts for selecting an expatriate host country,Math Comput Model 40, (2004),1473-1490.

[4] Chen.Y.J, Structured methodology for supplier selection and evaluation in a supply chain,Information Sciences 181, (2011), 1651-1670.

[5] Chen.S.J and Hwang. C.L, Fuzzy multiple attribute decision making methods and applications, Springer, Berlin,(1992).

[6] Chen.S.J and Chen.S.M, Fuzzy risk analysis based on similarity measures of generalized fuzzy numbers, IEEE Trans, Fuzzy Syst, 11,(2003),45-56.

[7] Chiou.H.K, Tzeng.G.H and Cheng.D.C, Evaluating sustainable _shing development strategies using fuzzy MCDM approach, Omega, 33(3),(2005),223-234.

[8] Dheena.P and Mohanraj.G, Multi-criteria decision-making combining fuzzy set theory, ideal and anti-ideal points for location site selection, Expert Systems with Applications, 38,(2011),13260-13265

[9] Ding.J.F and Liang.G.S,Using fuzzy MCDM to select partners of strategic alliances for liner shipping Inf Sci 173(1-3),(2005),197-225.

[10] Fan, Zhi-Ping, Liu and Yang, A method for group decision-making based on multi-granularity uncertain linguistic information, Experts System with Applications, 37, (2010), 4000-4008.

[11] Hejazi.S.R, Doostparast.A and Hosseini.S.M, An improved fuzzy risk analysis based on new similarity measures of generalized fuzzy numbers, Expert Syst. Appl,38,(2011),9179-9185.

[12] Hsu.H.M and Chen.C.T, Aggregation of fuzzy opinions under group decision making. Fuzzy Sets System 79(3),(1996),279-285.

[13] Hwang.C.L and Yoon.K, Multiple Attribute Decision Making Methods and Applications, Springer, Berlin, Heidelberg,(1981).

[14] Lee.J.W and Kim S.H, An integrated approach for interdependent information system project selection. Int J Proj Manag 19(2),(2001), 111-118.

[15] Lee.J.W and Kim.S.H, Using analytic network process and goal programming for interdependent information system project selection, Comput Oper Res 27(4),(2000), 367-382.

[16] Li.R.J,Fuzzy method in group decision making, Comput Math Appl 38(1),(1999),91-101.

[17] Liang.G.S, Fuzzy MCDM based on ideal and anti-ideal concepts, Eur J Oper Res, 112(3),(1999),682-691.

[18] Peng.Y, Wang.G and Wang.H, User preferences based software defect detection algorithms selection using MCDM,Information Sciences 191, (2012), 3-13.

[19] Shanian.A and Savadogo.O,TOPSIS multiple-criteria decision support analysis for material selection of metallic bipolar plates for polymer electrolyte fuel cell,J Power Sources 159(2),(2006), 1095-1104.

[20] Tsaur.H,Chang.T.Y and Yen.C.H,The evaluation of airline service quality by fuzzy MCDM, Tour Manage 23,(2002),107-115.

[21] Wang.J and Lin.Y.T,Fuzzy multi-criteria group decision making approach to select con_guration items for software development, Fuzzy Sets Systems 134(3),(2003),343-363.

[22] Xu.Z, Shang.S, Qjan.W and Shu.W, A method for fuzzy risk analysis based on the new similarity of trapezoidal fuzzy numbers, Experts System with Applications, 37, (2010), 1920-1927.

[23] Xu.Z, Shang.S, Quin.W, and Shu.W, A method for fuzzy risk analysis based on the new similarity of trapezoidal fuzzy numbers, Expert Syst. Appl, 37,(2010),1920-1927.

[24] Zadeh. L.A, The concept of a linguistic variable and its application to approximate reasoning, part 1, Information Sciences 8(3), (1975), 199-249

[25] Zadeh. L.A, The concept of a linguistic variable and its application to approximate reasoning, part 2, Information Sciences 8(4), (1975), 301-357

[26] Zadeh.L.A, The concept of a linguistic variable and its application to approximate reasoning, part3, Information Sciences 9(1), (1985), 43-58.

[27] Zimmermann.H.J, Fuzzy set theory and its applications, Kluwer, Boston,(1996).

Global Journal of Pure and Applied Mathematics (GJPAM) ISSN 0973-1768 Volume 12,Number 4 (2016)

On T-fuzzy lateral ideals of ternary semigroups

*G. Mohanraj**
Department of Mathematics, Annamalai University,
Tamil Nadu, India.
Email: gmohanraaj@gmail.com

M. Vela
Department of Mathematics, Annamalai University,
Tamil Nadu, India.
Email: velamaths@gmail.com

***Abstract*— We introduce the notion of T - fuzzy ternary sub semigroups and T – fuzzy lateral, T - fuzzy right and T - fuzzy left ideals of ternary semigroups. We redefine T - fuzzy ternary subsemigroups and T - fuzzy lateral ideals, T - fuzzy right ideals and T - fuzzy left ideals using fuzzy ternary T - product of ternary semigroups. We introduce the notion of T - intersection of fuzzy sets. We establish that T – intersection of two T - fuzzy lateral ideals of ternary semigroups is again a T fuzzy lateral ideal. We prove that homomorphic pre-image of a T - fuzzy lateral ideal is again a T - fuzzy lateral ideal**

Keywords*— *T-norm, lateral ideal, ternary product, ternary T-product.

I. INTRODUCTION

D.H.Lehmer [11] introduced the notion of ternary algebraic system in 1932. Los. J [12] introduced the notion of ternary semigroups. L.A.Zadeh [16] initiated the concept of fuzzy sets in the year of 1965 and latter it is applied to many branches of mathematics. After the introduction of the concept of fuzzy groups in pioneering paper of Rosenfed [13] started the study of fuzzy algebraic structures. Fuzzy ideals in semigroups was introduced and studied by Kuroki [9] [10]. F.M.Sioson and F.Mideal [15] studied the ideal theory in ternary groups in the year 1965. M.L.Santiago and S.S.Bala [14] had developed the theory of ternary semigroups. Dheena and Mohanraj[2] used the fuzzy algebra in many branches extensively of Triangular norm.

In this paper, we introduce the notions T -fuzzy ternary subsemigroups and T -fuzzy lateral, T -fuzzy right and T -fuzzy left ideals of a ternary semigroup. We redefine T -fuzzy ternary subsemigroups and T -fuzzy lateral , T - fuzzy right ideal and T - fuzzy left ideal using fuzzy ternary T -product of a ternary semigroup.We introduce the notion of T -intersection of fuzzy sets. We establish that T -intersection of two T –fuzzy lateral ideals of ternary semigroup is again a T -fuzzy lateral ideal . We prove that homomorphic pre-image of a T -fuzzy lateral ideal is again a T -fuzzy lateral.

II. PRELIMINARIES

Definition 2.1. *A non-empty set S together with the mapping $S \times S \times S \to S$ which maps $(a,b,c) \to abc$ is called ternary semigroup that satisfies the following condition:*

(i) $abc \in S$ *for all* $a,b,c \in S$

(ii) $ab(cde) = a(bcd)e = (abc)d$ *for all* $a,b.c,d,e \in S$.

Examples:

(1) Let Z^{-} be the set of all non positive integers then with usual ternary Multiplication Z^{-} forms a ternary semi group.

(2) The set of odd permutation of a non empty set X, under ternary composition forms a ternary semigroup.

Definition 2.2. *A non-empty set B of ternary semi group S is called ternary sub semi group if $BBB \subseteq B$.*

Definition 2.3. *A non-empty set B of ternary semigroup S is called ternary lateral [right, left] ideal if $SBS \subseteq B$ [$BSS \subseteq B, SSB \subseteq B$].*

Definition 2.4. *[2] A binary operation T on [0 , 1] is called a triangular norm[T-norm] on [0,1] which satisfies the following conditions:*

$(i) T(x,1) = T(1,x) = x$

$(ii) T(x,y) = T(y,x)$

$(iii) T(x,T(y,z)) = T(T(x,y),z)$

(iv) *If* $x^* \leq x, y^* \leq y$ *then* $T(x^*, y^*) \leq T(x,y)$ *forall* $x,y,z \in [0,1]$

Note 1. *Some other triangular norms [4] are defined as follows:*

(i) Minmum T–norm: $T_M(x,y) = \min\{x,y\}$

(ii)Product T–norm $T_p(x,y) = x \cdot y$

(iii)Lukasiewicz T–norm: $T_L(x,y) = \max\{x+y-1,0\}$

(iv)Drastic product T-norm:

$$T_D(x,y) = \begin{cases} 0 & \text{if } x,y \in [0,1] \\ \min\{x,y\} & \text{is otherwise} \end{cases}$$

(v) *Hamacher -T norms: for any* $\lambda \in [0,\infty)$

$$T_\lambda{}^H(x,y) = \begin{cases} T_D(x,y) & \text{if } \lambda = \infty \\ 0 & \text{if } \lambda = x = y = 0 \\ \dfrac{xy}{\lambda + (1-\lambda)(x+y-xy)} & \text{otherwise} \end{cases}$$

Definition 2.5. [2] *Let f be a function from ternary semigroup S into S' and ξ be a fuzzy set of S. The image of ξ under f denoted by f (ξ) is the fuzzy set on S' that is defined as follows:*

*Corresponding author.

This paper was presented by the second author in the National Conference on *Advances in Mathematics and its Applications to Science and Engineering* (AMASE-2016) conducted in Department of Mathematics, University College of Engineering-Pattukkottai, Thanjavur, Tamil Nadu, India, on 22nd January 2016.

$$(f(\xi))(y)=\begin{cases}\vee\{\xi(x)\mid x\in f^{-1}(y)\} & \text{if } f^{-1}(y)\neq\phi\\ 0 & \text{otherewise}\end{cases}$$

for all $x,y\in S'$

Definition 2.6.*[2] Let* f *be a function from ternary semigroup* S *into* S' *and* ω *be a fuzzy set of* S'*, The pre- image of* ω *under* f *denoted by* $f^{-1}(\omega)$ *is the fuzzy set on* S *, that is defined as follows:*

$$\left(f^{-1}(\omega)\right)(x)=\omega(f(x)) \quad \text{for all } x\in S.$$

Definition 2.7. *Let* ξ *be a fuzzy set of* S*. Then* ξ *is said to be fuzzy ternary subsemigroup of* S *if* $\xi(xyz)\geq\min\{\xi(x),\xi(y),\xi(z)\}$ *for all* $x,y,z\in S$.

.

Definition 2.8. *Let* ξ *be a fuzzy set of* S*. Then* ξ *is said to be fuzzy lateral [right, left] ideals of* S *if* $\xi(xyz)\geq\xi(y)\ [\xi(xyz)\geq\xi(x)\ ;\ \xi(xyz)\geq\xi(z)]$ *for all* $x,y,z\in S$

Remark *``1 " is a fuzzy set on* S *that is defined as* $1(x)=1$ *for all* $x\in S$.

III. Redefined T-fuzzy lateral ideals

Through this paper, unless otherwise specified, S denotes a ternary semigroup and T indicates a triangular norm on [0, 1].

Definition 3.1. *Let* ξ, ω *and* υ *be a fuzzy sets of a ternary semigroup* S *and* T *be the triangular norm on [0, 1]. The ternary* T*-product of* ξ, ω *and* υ *is defined as follows:*

$$(\xi\circ_T\omega\circ_T\upsilon)(x)=\begin{cases}\bigvee\limits_{x=abc}\mathrm{T}(\xi(\mathrm{a}),T(\omega(b),\upsilon(c))) & \text{if } x=abc\\ 0 & \text{if } x \text{ cannot be expressible as } x=abc\end{cases}$$

Note: *[5] By taking* T *-norm as a minimum* T *-norm, then ternary* T *–product becomes fuzzy ternary product of* ξ, ω *and* υ

Definition 3.2. *A fuzzy set* ξ *of* S *is said to be* T *-ternary subsemigroup of* S *if* $\xi(xyz)\geq T(\xi(x),T(\xi(y),\xi(z)))$ *for all* $x,y,z\in S$.

Definition 3.3. *A fuzzy set* ξ *of* S *is said to be* T *-fuzzy lateral [right ,left] ideals of* S *if* $\xi(xyz)\geq\xi(y)\ [\xi(xyz)\geq\xi(x);\xi(xyz)\geq\xi(z)]$ for all $x,y,z\in S$.

Theorem 3.4. *A fuzzy set* ξ *of* S *is a* T *- fuzzy ternary subsemigroup if and only if* $\xi\circ_T\xi\circ_T\xi\subseteq\xi$.

Proof. Let ξ is a T –fuzzy ternary subsemigroup of S. If x can not be expressible as $x=abc$, then $(\xi\circ_T\xi\circ_T\xi)(x)=0\leq\xi(x)$. If $x=abc$, then $T(\xi(a),T(\xi(b),\xi(c)))\leq\xi(x)$ implies

$$\bigvee_{x=abc}T(\xi(a),T(\xi(b),\xi(c)))\leq\xi(x).$$

Therefore

$$(\xi\circ_T\xi\circ_T\xi)(x)=\bigvee_{x=abc}T(\xi(a),T(\xi(b),\xi(c)))\leq\xi(x).$$

Hence $(\xi\circ_T\xi\circ_T\xi)\subseteq\xi$

Conversely, $(\xi\circ_T\xi\circ_T\xi)(x)\leq\xi(x)$ for all $x\in S$. Thus

$$\begin{aligned}\xi(abc)&\geq(\xi\circ_T\xi\circ_T\xi)(abc).\\&=\bigvee_{xyz=abc}T(\xi(x),T(\xi(y),\xi(z)))\\&\geq T(\xi(a),T(\xi(b),\xi(c))).\end{aligned}$$

Thus ξ is a T-fuzzy ternary subsemigroup of S.

Theorem 3.5. *Let* ξ *be a fuzzy set of* S*. Then* ξ *is said to be* T *-fuzzy lateral [right, left] ideals if and only if* $1\circ_T\xi\circ_T1\subseteq\xi[\xi\circ_T1\circ_T1\subseteq\xi,\ 1\circ_T1\circ_T\xi\subseteq\xi]$

Proof. Let ξ be T -fuzzy lateral ideal of S. If x can not be expressible as $x=abc$, then $\xi(x)=\xi(abc)\geq\xi(b)$.

$$\begin{aligned}\xi(x)&=\xi(abc).\\&\geq\xi(b)\\&=T(1,\xi(b))\\&=T(1,\ T(\xi(b),1))\\&=T(1(a),\ T(\xi(b),1(c)))\end{aligned}$$

Thus, $\xi(x)\geq\bigvee\limits_{x=abc}T(1(a),T(\xi(b),1(c)))$

$$=(1\circ_T\xi\circ_T1)(x)$$

Therefore $1\circ_T\xi\circ_T1\subseteq\xi$

Conversely,

$$\begin{aligned}\xi(xyz)&\geq(1\circ_T\xi\circ_T1)(xyz)\\&\geq T(1(x),T(\xi(y),1(z)))\\&=T(1,T(\xi(y))\\&=\xi(y)\end{aligned}$$

Thus $\xi(xyz)\geq\xi(y)$, for all $x,y,z\in S$.

Therefore ξ is a T-fuzzy lateral ideal of S.

Similarly, we prove that ξ is a T-fuzzy right ideal of S if and only if $\xi\circ_T1\circ_T1\subseteq\xi$ and ξ is a T-fuzzy left ideal of S if and only if $1\circ_T1\circ_T\xi\subseteq\xi$ respectively.

Corollary 3.6. [5] *Let* ξ *be a fuzzy set of* S*. Then* *(i) fuzzy ternary subsemigroup of* S *if and only if* $\xi \circ \xi \circ \xi \subseteq \xi$

(ii) fuzzy left ideal of S *if and only if* $1 \circ 1 \circ \xi \subseteq \xi$

(iii)fuzzy lateral ideal of S *if and only if* $1 \circ_T \xi \circ_T 1 \subseteq \xi$

(iv)fuzzy right ideal of S *if and only if* $\xi \circ 1 \circ 1 \subseteq \xi$

Proof. By taking T -norm as a minmum T-norm in Theorem 3.4 and 3.5, we get the result.

IV. T-INTERSECTION OF T-FUZZY LATERAL IDEALS

Definition 4.1. *Let* ξ *and* ω *be a fuzzy sets of* S *and* T *be a triangular norm on [0, 1]. A* T *-intersection of fuzzy sets* ξ *and* ω *is defined as follows:*

$T(\xi,\omega)(x) = T(\xi(x),\omega(x))$ *for all* $x \in S$

Theorem 4.2 *Let* ξ *,* ω *be a fuzzy sets of* S. *If* ξ *and* ω *are* T *-fuzzy lateral ideal of* S*, then* $T(\xi,\omega)$ *is* T *- fuzzy lateral ideal of* S.

Proof: Let ξ and ω be a T - fuzzy lateral ideal of S

$$\begin{aligned} T(\xi,\omega)(xyz) &= T(\xi(xyz),\omega(xyz)) \\ &= T(\xi(y),\omega(y)) \\ &\geq T(\xi,\omega)(y) \end{aligned}$$

Therefore $T(\xi,\omega)(xyz) \geq T(\xi,\omega)(y)$ for all $x,y,z \in S$. Hence $T(\xi,\omega)$ is a T - fuzzy lateral ideal of S.

Similarly, we prove that $T(\xi,\omega)$ is a T-fuzzy right ideal of S if and only if $T(\xi,\omega)(xyz) \geq T(\xi,\omega)(x)$ and $T(\xi,\omega)$ a T-fuzzy left ideal of S if and only if $T(\xi,\omega)(xyz) \geq T(\xi,\omega)(z)$ respectively.

Corollary 4.3. *Let* ξ *and* ω *are fuzzy lateral (right, left) ideal of* S*, then* $\xi \cap \omega$ *is fuzzy lateral (right , left) ideal of* S.

Proof. By taking T -norm as a minimum T -norm in Theorem 4.2 we get the result.

Theorem 4.4. *Let* ξ *and* ω *be a* T *-fuzzy ternary sub semigroup of* S*, then* $T(\xi,\omega)$ *is a* T *-fuzzy ternary sub semigroup.*

Proof. Let ξ and ω be a T -fuzzy ternary sub semigroup of S. Then, $T(\xi,\omega)(xyz) = T(\xi(xyz),\omega(xyz))$

$$\begin{aligned}
&\geq T(T(\xi(x),T(\xi(y),\xi(z))),T(\omega(x),T(\omega(y),\omega(z)))) \\
&= T(T(\xi(x),T(T(\xi(y),\xi(z)),\omega(x))),T(\omega(y),\omega(z))) \\
&= T(T(\xi(x),T(\xi(y),T(\xi(z),\omega(z)))),T(\omega(y),\omega(z))) \\
&= T(T(\xi(x),T(\xi(y),T(\omega(x),\xi(z)))),T(\omega(y),\omega(z))) \\
&= T(T(\xi(x),T(T(\xi(y),\omega(x)),\xi(z))),T(\omega(y),\omega(z))) \\
&= T(T(\xi(x),T(T(\omega(x),\xi(y)),\xi(z))),T(\omega(y),\omega(z))) \\
&= T(T(\xi(x),T(\omega(x),T(\xi(y),\xi(z)))),T(\omega(y),\omega(z))) \\
&= T(T(T(\xi(x),\omega(x)),T(\xi(y),\xi(z))),T(\omega(y),\omega(z))) \\
&= T(T(\xi,\omega)(x),T(T(\xi(y),\xi(z)),T(\omega(y),\omega(z)))) \\
&= T(T(\xi,\omega)(x),T(\xi(y),T(\xi(z),T(\omega(y),\omega(z))))) \\
&= T(T(\xi,\omega)(x),T(\xi(y),T(T(\xi(z),\omega(y)),\omega(z)))) \\
&= T(T(\xi,\omega)(x),T(\xi(y),T(T(\omega(y),\xi(z))\omega(z)))) \\
&= T(T(\xi,\omega)(x),T(\xi(y),T(\omega(y),T(\xi(z),\omega(z))))) \\
&= T(T(\xi,\omega)(x),T(T(\xi(y),\omega(y)),T(\xi(z),\omega(z)))) \\
&= T(T(\xi,\omega)(x),T(T(\xi,\omega)(y),T(\xi,\omega)(z)))
\end{aligned}$$

Therefore

$T(\xi,\omega)(xyz) \geq T(T(\xi,\omega)(x),T(T(\xi,\omega)(y),T(\xi,\omega)(z)))$ for all $x,y,z \in S$.

Hence $T(\xi,\omega)$ is T -fuzzy subsemigroup of S.

Corollary 4.5. *Let* ξ *and* ω *are fuzzy subsemigroup of S. then* $\xi \cap \omega$ *is fuzzy subsemigroup of S.*

Proof. By taking T-norm as a minimum T -norm in Theorem 4.2. we get the result.

V. HOMOMORPHISM AND T-FUZZY LATERAL IDEALS

Definition 5.1. *Let* S *and* S' *be two ternary semigroups. Then mapping* f *from* S *and* S' *is called a homomorphism of* S *and* S' *if* $f(abc) = f(a)f(b)f(c)$*,for all* $x,y,z \in S$.

Theorem 5.2. *Let* $f : S \to S'$ *be a homomorphism and let* ξ *be a* T *-fuzzy set of* S'. *If* ξ *is a* T *-fuzzy lateral (right, left) ideal of* S'*, then* $f^{-1}(\xi)$ *is a* T *-fuzzy lateral (right, left) ideal of* S.

Proof. Let ξ be a T -fuzzy lateral (right, left) ideal of S'. Let $x,y,z \in S$. Now, $(f^{-1}(\xi))(xyz) = \xi(f(xyz))$

$$\begin{aligned} &= \xi(\delta(x)\delta(y)\delta(z)) \\ &\geq \xi(f(y)) \\ &= (f^{-1}(\xi)(y)) \end{aligned}$$

Therefore $(f^{-1}(\xi))(xyz) \geq (f^{-1}(\xi)(y))$ for all $x,y,z \in S$. $f^{-1}(\xi)$ is a T -fuzzy lateral ideal of S.

Similarly, We prove that ξ is a T -fuzzy right ideal of S' if and only if $f^{-1}(\xi)$ is a T -fuzzy right ideal of S and ξ is a T -fuzzy left ideal of S' if and only if $f^{-1}(\xi)$ is a T -fuzzy left ideal of S respectively .

Corollary 5.3. Let $f : S \to S'$ be a homomorphism and let ξ be a fuzzy set of S'. If ξ is fuzzy lateral (right, left) ideal of S', then $f^{-1}(\xi)$ is a fuzzy lateral (right, left) ideal of S.

Proof. By taking T -norm as a minimum T -norm in Theorem 5.2 we get the result.

Theorem 5.4. Let f be a homomorphism from S onto S' and let ξ be a T -fuzzy set of S'. Then ξ is a T -fuzzy lateral (right, left) ideal of S', if and only if $f^{-1}(\xi)$ is a T -fuzzy lateral (right, left) ideal of S.

Proof. Let ξ be a T -fuzzy lateral ideal of S'.Then by Theorem 5.2, $f^{-1}(\xi)$ is T -fuzzy lateral ideal of S.

Conversely, Let $x', y', z' \in S'$, Then there exist $x, y, z \in S$ such that

Now, $\xi(x', y', z') = \xi(f(x), f(y), f(z))$

$$= \xi(f(xyz))$$
$$= (f^{-1}(\xi))(xyz)$$
$$= (f^{-1}(\xi))(y)$$
$$\geq \xi(f(y))$$
$$= \xi(y')$$

Therefore $\xi(x', y', z' \geq \xi(y'))$ for all $x', y', z' \in S'$. Hence ξ is a T -fuzzy lateral ideal of S'.

Similarly, We prove that $f^{-1}(\xi)$ is T -fuzzy right ideal of S if and only if ξ be a T -fuzzy right ideal of S' and $f^{-1}(\xi)$ is T -fuzzy left ideal of S if and only if ξ be a T -fuzzy left ideal of S' respectively.

Corollary 5.5. *Let f be a homomorphism from S onto S' and let ξ be a fuzzy set of S'. Then ξ is a fuzzy lateral (right, left) ideal of S', if and only if $f^{-1}(\xi)$ is a fuzzy lateral (right, left) ideal of S.*

Proof. By taking T -norm as a minimum T -norm in Theorem 5.4 we get the result.

Theorem 5.6. *Let f be a homomorphism from S onto S'. If ξ is a T -fuzzy lateral (right, left) ideal of S, then $f(\xi)$ is a T -fuzzy lateral (right, left) ideal of S'*

Proof. Let ξ be a T -fuzzy lateral ideal of S.For each $x', y', z' \in S'$, there exist $x, y, z \in S$ such that $f(x) = x', f(y) = y', f(z) = z'$. Let $x', y,' z' = a'$

$$(f(\xi))(xyz) = \vee\{\xi(xyz) \mid f(xyz) = a'\}$$
$$= \vee\{\xi(xyz) \mid f(x)f(y)f(z) = a'\}$$
$$= \vee\{\xi(xyz) \mid f(x) = x', f(y) = y', f(z) = z'\}$$
$$= \vee\{\xi(xyz) \mid f(y) = y'\}$$
$$\geq (f(\xi))(y)$$

Therefore $(f(\xi))(xyz) \geq (f(\xi))(y)$ for all $x, y, z \in S$. Hence $f(\xi)$ is a T -fuzzy lateral (right, left) ideal of S'.

Similarly, We prove that ξ is a T -fuzzy right ideal of S if and only if $f(\xi)$ is a T -fuzzy right, ideal of S' and ξ is a T -fuzzy left ideal of S, if and only if $f(\xi)$ is a T -fuzzy left ideal of S' respectively.

Corollary 5.7. Let f be a homomorphism from S onto S' If ξ is a fuzzy lateral (right, left) ideal of S, then $f(\xi)$ is a fuzzy lateral (right, left) ideal of S'.

Proof. By taking T -norm as a minimum T -norm in Theorem 5.2, we get the result.

REFERENCES

[1] Bijan devvaz,Anwar zeb and Asghar Khan, On(α,β) fuzzy ideals of ternary semigroups ,J.Indones.Math.soc.19(2)(2013)123-138.

[2] Dheena.P and Mohanraj.G, T -fuzzy ideals in rings, International Journal of Computational Cognition 9(2)(2011),98-101.

[3] Dixit and sarita dewan, A Note on quasi and bi-ideals in ternary semigroups Internat.J.Math and Math.sci.18(3)(1995)501-508.

[4] Klement.E.P,Mesiar.R,Pap.E, Triangular Norms. Kluwer Academic puplishers, Dordrecht.(2000).

[5] Kar.S,Sarkar.P, Fuzzy ideals of ternary semigroups, Fuzzy Information and Engineering 2(2012),181-193.

[6] Kar.S,Marity.K.B, Congruences on ternary semigroups, Journal of the chungcheong mathematical socity 20(3)2007,191-201.

[7] Mohanraj.G, On intuitionistic -fuzzy ideals of semiring, Annamalai University science journal,46(1)(2010),81-88.

[8] Mohanraj.G,Krishnaswamy.D, and Hema.R, On generalized redened fuzzy prime ideals of ordered semigroups,Annals of Fuzzy Mathematics and Informatics,6(1)(2013),171-179.

[9] Kuroki.N Ideals and fuzzy bi-ideals in semigroups. Fuzzy Sets and System 5(1981),203-215.

[10] Kuroki.N, On fuzzy semigroups. Information Science 3(1991),203-236.

[11] Lehmer.H,A ternary analogue of abelian groups American Journal of mathematics 54(1932),329-338.

[12] Los.J. On the extending of models, Information Fundamenta athematica 42 (1995),38-54.

[13] Rosenfeld. A fuzzy groups, Journal of Mathematical Analysis and Application 35 (1971),512-517.

[14] Santiago.M.L and Bala. S.STernary semigroups ,Semigroups Forum 81(2010),380-388.

[15] Sioson.F.Mideal, Theory in ternary semigroups, Mathematica Japonica 10(1965),63-84.

[16] Zadeh.L.A ,Fuzzy sets, Information and control 8(1965),338-353.

Global Journal of Pure and Applied Mathematics (GJPAM) ISSN 0973-1768 Volume 12,Number 4 (2016)

Adjacent vertex distinguishing total coloring of grid graphs and shadow graphs

S. Sudha
Ramanujan Institute for Advanced Study in Mathematics,
University of Madras, Tamil Nadu, India.
Email: sudhasubramanian1955@gmail.com

*K. Manikandan**
Ramanujan Institute for Advanced Study in Mathematics,
University of Madras, Tamil Nadu, India.
Email: kmanimaths1987@gmail.com

***Abstract*- An adjacent vertex distinguishing total coloring of a graph G is a proper coloring of G in such a way that any pair of adjacent vertices have distinct set of colors. The minimum number of colors needed for an adjacent vertex distinguishing total coloring of G is denoted by $\chi_{at}(G)$. In this paper, we have discussed the adjacent vertex distinguishing total coloring of grid of diamonds, grid of hexagons and shadow graphs of (i) a path and (ii) a cycle. We have also discussed the adjacent vertex distinguishing total coloring of a crown graph.**

Keywords*- *Grid of diamonds; Grid of hexagons; Shadow graph; Path; Cycle; Crown graph; Adjacent vertex distinguishing total coloring and Adjacent vertex distinguishing total chromatic number.

AMS Subject Classification: 05C15

I. INTRODUCTION

If $G=\left(V\left(G\right),E\left(G\right)\right)$ is a graph with the vertex set $V\left(G\right)$ and the edge set $E\left(G\right)$, a proper total coloring of G is an assignment of colors to the vertices and the edges in such a way that

1. no two adjacent vertices are assigned with the same color,
2. no two adjacent edges are assigned with the same color,
3. no edge and its end vertices are assigned with the same color and
4. for every adjacent vertices have distinct set of colors.

*Corresponding author.

This paper was presented by the second author in the National Conference on *Advances in Mathematics and its Applications to Science and Engineering* (AMASE-2016) conducted in Department of Mathematics, University College of Engineering-Pattukkottai, Thanjavur, Tamil Nadu, India, on 22nd January 2016.

Zhang et al. [1] introduced the concept of an adjacent vertex distinguishing total coloring and found the adjacent vertex distinguishing total chromatic number for a cycle, a complete graph, a complete bipartite graph, a wheel and a tree. They have also posed the following conjecture:

For any graph G with order at least 2, we have $\chi_{at}(G)\le(G)+3.$

Chen [2] and Wang [3] confirmed that this conjecture is true for graphs with $\Delta(G)=3$ whereas Hulgan [4] presented a proof for this conjecture for a complete graph and a cycle. Chen et al. [5] have verified this conjecture for a generalized Halin graphs with maximum degree at least 6. Wang et al. [6] have verified this conjecture for planar graphs. Papaioannou et al. [7] have discussed adjacent vertex distinguishing total coloring of 4 - regular graphs. Sudha et al. [8] have discussed and found in general the adjacent vertex distinguishing total coloring of corona product of two paths; two cycles; two complete graphs; a path and a cycle; a cycle and a path; a complete graph and a path; a complete graph and a cycle. Luiz et al. [9] have found the adjacent vertex distinguishing total chromatic number of complete equipartite graph of even order $\Delta(G)+2.$

In this paper, we have obtained the adjacent vertex distinguishing total coloring of grid of diamonds, grid of hexagons and shadow graphs of (i) a path and (ii) a cycle. We have also discussed the adjacent vertex distinguishing total coloring of a crown graph.

II. SUDHA GRID OF DIAMONDS

Definition 2.1. Sudha grid of diamonds $S_d\left(m,n\right)$ is an induced subgraph of the tensor product of two paths P_m and P_n (both m and n odd, $m \geq 3$ and $n \geq 3$) with the vertex set and the edge set given by

$$V(S_d(m,n)) = \left\{ \begin{array}{r} (u_i, v_j) / \, either \; i \equiv 1(\text{mod } 2) \; and \;\; j \equiv 0(\text{mod } 2) \\ or \; i \equiv 0(\text{mod } 2) \; and \;\; j \equiv 1(\text{mod } 2) \end{array} \right\}$$

and

$$E(S_d(m,n)) = \{(u_i, v_j)(u_k, u_l) / u_i u_k \in E(P_m) \, and \, v_j v_l \in E(P_n)\}$$

Illustration 2.2. Consider Sudha grid of diamonds for $m = 5$ and $n = 5$.

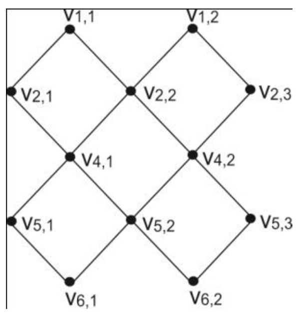

Figure 1: Sudha grid of diamonds $S_d(5,5)$

The above graph is the induced subgraph of the tensor product of two paths P_5 with the vertex set $\{u_i\}$, $1 \leq i \leq 5$ and P_5 with the vertex set $\{v_j\}$, $1 \leq j \leq 5$ as per definition. In the fig.1 the vertices are denoted by $v_{i,j}$ instead of (u_i, v_j) for simplicity.

Theorem 2.3. The adjacent vertex distinguishing total coloring of Sudha grid of diamonds $S_d(m,n)$ is $\Delta(G)+2$ for odd $m \geq 3$ and odd $n \geq 3$.

Proof. Let the vertex set and the edge set of Sudha grid of diamonds $S_d(m,n)$ be given by

$$V(S_d(m,n)) = \{v_{i,j}; 1 \leq \text{i} \leq 2\text{m} + 1, 1 \leq \text{j} \leq \text{n} + 1\}$$

and

$$E(S_d(m,n)) = \{v_{i,j}v_{i+1,j}; 1 \leq i, j \leq m,n\} \cup \{v_{i,j}v_{i+1,j+1}; 1 \leq i, j \leq m,n\} \cup \{v_{i,j}v_{i+1,j-1}; 1 \leq i, j \leq m,n\}$$

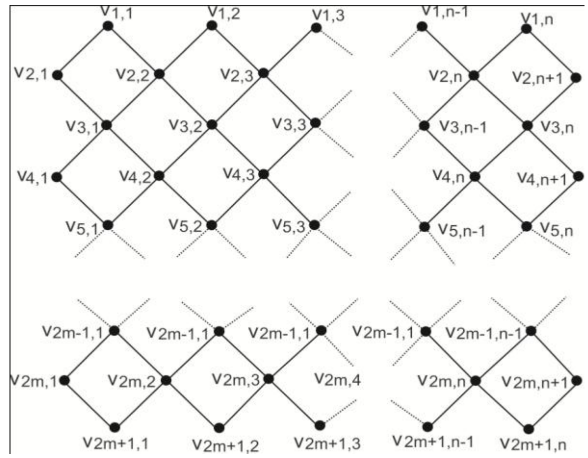

Figure 2: Sudha grid of diamonds $S_d(m,\text{n})$

$S_d(m,n)$ consists of $\left(\dfrac{mn-1}{2}\right)$ vertices and $(m-1)(n-1)$ edges respectively.

Define the function f_1 be a mapping from the vertices to a color set $\{1,2,3,...,k\}$ as

for all $1 \leq i \leq m$, $1 \leq j \leq n$,

$$f_1(v_{i,j}) = \begin{cases} 1, & \text{if } \; i \equiv 1(\text{mod } 2) \\ 2, & \text{otherwise} \end{cases}$$

Define the function f_2 be a mapping from the edges to a color set $\{1,2,3,...,k\}$ as

for all $1 \leq i \leq m$, $1 \leq j \leq n$,

$$f_2(v_{i,j}v_{i+1,j}) = \begin{cases} 3, & \text{if } \; i \equiv 1(\text{mod } 2) \\ 5, & \text{otherwise} \end{cases}$$

and for the remaining edges, there are two cases for f_2 one for odd i and one for even i: for odd i, the function f_2 is defined as

for all $1 \leq i \leq m$, $1 \leq j \leq n$,

$$f_2(v_{i,j}v_{i+1,j+1}) = 4,$$

For even i, the function f_2 is defined as

for all $1 \leq i \leq m$, $1 \leq j \leq n$,

$$f_2(v_{i,j}v_{i+1,j+1}) = 6,$$

The above coloring pattern satisfies the condition of an adjacent vertex distinguishing total coloring and the chromatic number of Sudha grid of diamonds $S_d(m,n)$ is $\Delta(G)+2$.

Illustration 2.4. Consider the Sudha grid of diamonds $S_d(7,5)$

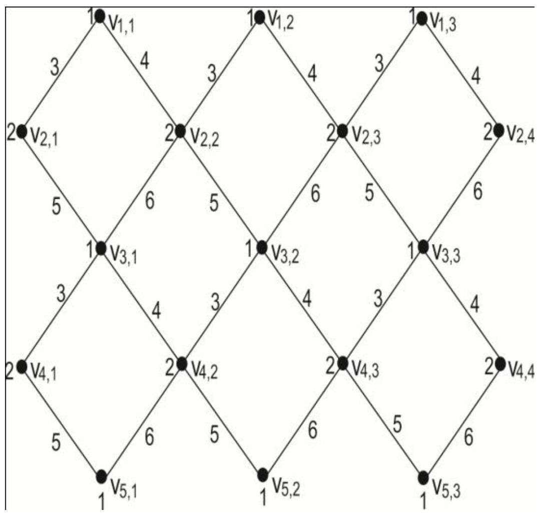

Figure 3: Sudha grid of diamonds $S_d(7,5)$

By using the coloring pattern given in theorem 2.3, the colors $1,2,3,4,5,6$ are assigned to the vertices and the edges are assigned with the colors as shown in fig.3.

The adjacent vertex distinguishing total chromatic number of $S_d(7,5)$ is 6.

III. SUDHA GRID OF HEXAGONS

Definition 3.1. Sudha grid of hexagons $S_h(m,n)$ is an induced subgraph of the strong product of two paths P_m and P_n (m is odd, ≥ 3 and $n \equiv 0(mod 4)$) with the vertex set and the edge set given by

$$V(S_h(m,n)) = \left\{ \begin{matrix} (u_i,v_j)/\, i+j \equiv 1(\bmod 2) \\ \text{and} \quad i+j \equiv 0(\bmod 2) \end{matrix} \right\}$$

and

$$E(S_h(m,n)) = \left\{ \begin{matrix} (u_i,v_j)(u_k,v_l)/\, u_iu_k \in E(P_m) \text{and} \\ v_jv_l \in E(P_n), u_iu_k \in E(P_m) \text{ and } j=l \end{matrix} \right\}$$

Illustration 3.2. Consider the Sudha grid of hexagons $S_h(7,8)$

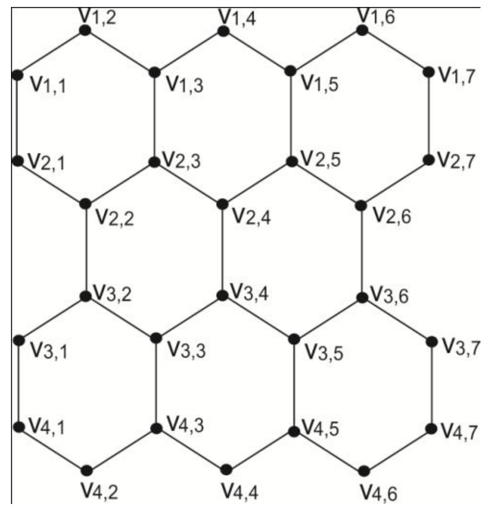

Figure 4: Sudha grid of hexagons $S_h(7,8)$

The graph is the induced subgraph of the strong product of two paths P_7 with the vertex set $\{u_i\}$, $1 \leq i \leq 7$ and P_8 with the vertex set $\{v_j\}$, $1 \leq j \leq 8$.

Theorem 3.3. The adjacent vertex distinguishing total coloring of Sudha grid of hexagons $S_h(m,n)$ is $\Delta(G)+2$ for odd $m \geq 3$ and $n \equiv 0(\bmod 4)$.

Proof. Let the vertex set and the edge set of Sudha grid of hexagons $S_h(m,n)$ be given by

$$V(S_h(m,n)) = \{v_{i,j}; 1 \leq i \leq 2m+1,\ 1 \leq j \leq n+1\}$$

and

$$E(S_d(m,n)) = \{v_{i,j}v_{i,j+1}, 1 \leq i \leq 2m, 1 \leq j \leq n\} \cup \{v_{i,j}v_{i+1,j}, (i+j) \text{ is even}\}$$

$S_h(m,n)$ consists of $\frac{mn}{2}$ vertices and $\frac{mn+2(m-1)(n-1)}{4}$ edges respectively.

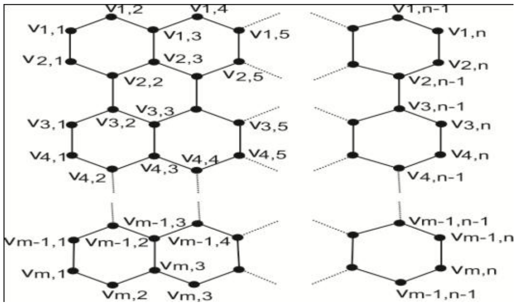

Figure 5: Sudha grid of hexagons $S_h(m,\mathrm{n})$

Define the function f_1 be a mapping from the vertices to a color set $\{1,2,3,...,k\}$ as
for all $1 \le i \le m, 1 \le j \le n$,

$$f_1(v_{i,j}) = \begin{cases} 1, & \text{if } (i+j) \equiv 0 \pmod 2 \\ 2, & \text{otherwise} \end{cases}$$

Define the function f_2 to be the mapping from the edges to a color set $\{1,2,3,...,k\}$ as
for all $1 \le i \le m, 1 \le j \le n$,

$$f_2(v_{i,j}v_{i,j+1}) = \begin{cases} 3, & \text{if } j \equiv 1 \pmod 2 \\ 4, & \text{otherwise} \end{cases}$$

$$f_2(v_{i,j}v_{i+1,j}) = 5, \textit{ if } (i+j) \textit{ is even}.$$

The above coloring pattern satisfies the condition of an adjacent vertex distinguishing total coloring and the chromatic number of Sudha grid of diamonds $S_d(m,n)$ is $\Delta(G)+2$.

Illustration 3.4. Consider the Sudha grid of hexagons $S_h(7,8)$

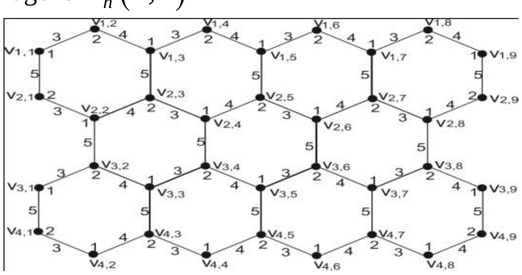

Figure 6: Sudha grid of hexagons $S_h(7,8)$

By using the coloring pattern given in theorem 3.3, the colors $1,2,3,4,5$ to the vertices and the edges are assigned with the colors as shown in fig.6.

The adjacent vertex distinguishing total chromatic number of $S_h(7,8)$ is 5.

IV. CROWN GRAPH

Definition 4.1. The crown graph S_n^0 for an integer $n \ge 2$ is the graph with the vertex set $\{u_1,u_2,...,u_n,v_1,v_2,...,v_n\}$ and the edge set $\{u_iv_j, 1 \le i, j \le n, \text{ where } i \ne j\}$.

The crown graph S_n^0 has $2n$ vertices and $n(n-1)$ edges.

Illustration 4.2. Consider the crown graph S_4^0.

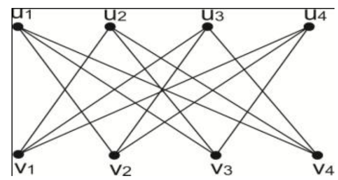

Figure 7: Crown graph S_4^0

The crown graph S_4^0 is shown in fig. 7 with the vertex set $\{u_i\}, 1 \le i \le 4$ and $\{v_j\}, 1 \le j \le 4$.

Theorem 4.3. The adjacent vertex distinguishing total chromatic number of a crown graph S_n^0 is $n+1$ for $n \ge 2$.

Proof. Let the vertex set and the edge set of the crown graph be denoted by

$$V(S_n^0) = \bigcup_{i=1}^{n} \{\{u_i\} \cup \{v_i\}\}$$

and $E(S_n^0) = \bigcup_{i=1}^{n} \{u_iv_j, 1 \le j \le n\}, \text{where } i \ne j$

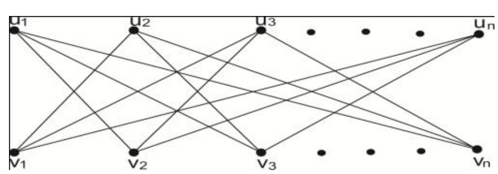

Figure 8: Crown graph S_n^0

Define the functions f_1 and f_2 be the mapping from the vertices and the edges to a color set $\{1,2,3,...,k\}$ as follows:

for all $1 \le i, j \le n$,

$$f_1(u_i) = n+1,$$

$$f_1(v_j) \equiv \begin{cases} 2j(\bmod n), \ if \ 2j \not\equiv 0(\bmod n) \\ n, \text{ otherwise} \end{cases}$$

$$f_2(u_i v_j) \equiv \begin{cases} (i+j)(\bmod n), \ if \ (i+j) \not\equiv 0(\bmod n) \\ n, \text{ otherwise} \end{cases}$$

Depending on the nature of n, if the vertices and the edges are colored, the conditions for total coloring is satisfied and we found that the adjacent vertex distinguishing total chromatic number is $n+1$ for $n \ge 2$.

Illustration 4.4. Consider the crown graph $S_4^0 = 5$.

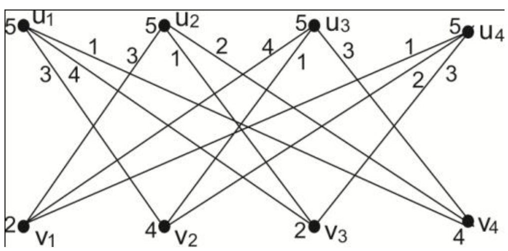

Figure 9: Crown graph S_n^0

The upper vertices denoted by u_1, u_2, u_3 and u_4 are colored with the color 5. The lower vertices v_1, v_2, v_3 and v_4 are colored by the colors $2,4,2$ and 4 respectively. The edges are colored as shown in fig.9. Since only 5 colors are used, the adjacent vertex distinguishing total chromatic number of S_4^0 is 5.

V. SHADOW GRAPHS

Definition 5.1. The Shadow graph $D_2(G)$ of a connected graph G is constructed by taking two copies of G say G' and G''. Join each vertex v' in G' to the neighbours of the corresponding vertex v'' in G''.

Illustration 5.2.

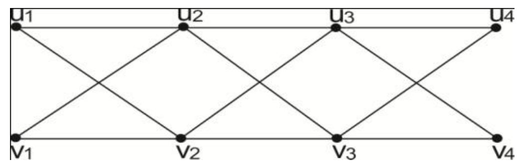

Figure 10: shadow graph of a path $D_2(P_4)$

The shadow graph of the path P_4 is shown in fig.10 with the vertex set $\{u_i\}, 1 \le i \le 4$ and $\{v_j\}, 1 \le j \le 4$.

Theorem 5.3. The adjacent vertex distinguishing total coloring of the shadow graph of a path $D_2(P_n)$ is given by

$$\chi_{at}(D_2(P_n)) = \begin{cases} \Delta(G)+2, & for \quad m > 3 \\ \Delta(G)+1, & for \quad m = 3 \end{cases}$$

Proof. Let the vertex set of the path P_n be $\{v_i, 1 \le i \le n\}$.

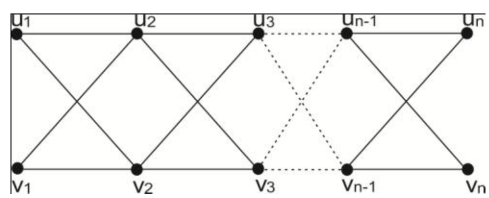

Figure 11: shadow graph of a path $D_2(P_n)$

The vertex set of the shadow graph of the path P_n is

$$V(D_2(P_n)) = \bigcup_{i,j=1}^{n-1} \left\{ \{u_i\} \cup \{v_j\} \right\}$$

and its edge set is

$$E(D_2(P_n)) = \bigcup_{i,j=1}^{n-1} \begin{Bmatrix} \{u_i u_{i+1}\} \cup \{v_j v_{j+1}\} \\ \cup \{u_i v_{j+1}\} \cup \{v_j u_{i+1}\} \end{Bmatrix}$$

Define the functions f_1 and f_2 to be the mapping from the vertices and the edges to a color set $\{1,2,3,...,k\}$ as follows:

for all $1 \le i, j \le n$,

$$f_1(u_i) = \begin{cases} 1, \ if \ \ i \equiv 1(\bmod 2) \\ 2, \text{ otherwise} \end{cases}$$

$$f_1(v_j) = \begin{cases} 1, & if\ \ j \equiv 1 (\text{mod } 2) \\ 2, & \text{otherwise} \end{cases}$$

$$f_2(u_i u_{i+1}) = \begin{cases} 3, & if\ \ i \equiv 1 (\text{mod } 2) \\ 4, & \text{otherwise} \end{cases}$$

$$f_2(v_j v_{j+1}) = \begin{cases} 3, & if\ \ j \equiv 1 (\text{mod } 2) \\ 4, & \text{otherwise} \end{cases}$$

for all $1 \le i, j \le n-1,$

$f_2(u_i v_{j+1}) = 5,\ if\ \ i = j$

$f_2(v_j u_{i+1}) = 6,\ if\ \ i = j.$

Using this general pattern of the coloring, the graph is adjacent vertex distinguishing total colored and the chromatic number is $\Delta(G)+2,$ for $n > 3.$

Remark 5.4. When $n = 3,$ we found that $\chi_{at}(D_2(P_3)) = \Delta(G)+1.$

Illustration 5.5. Consider the shadow graph of a path $D_2(P_4)$.

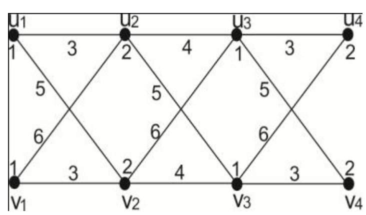

Figure 12: shadow graph of a path $D_2(P_4)$

By using the coloring pattern as given in theorem 5.1, the colors $1,2,3,4,5,6$ are assigned to the vertices and the edges are assigned with the colors as shown in fig.12.
The adjacent vertex distinguishing total chromatic number of $D_2(P_4)$ is $6.$

Theorem 5.6. The adjacent vertex distinguishing total coloring of the shadow graph of a cycle $D_2(C_n)$ is $\Delta(G)+2.$

Proof. Let the vertex set of the path C_n be $\{v_i, 1 \le i \le n\}.$

The vertex set of the shadow graph of the cycle C_n is

$$V(D_2(C_n)) = \bigcup_{i,j=1}^{n} \left\{ \{u_i\} \cup \{v_j\} \right\}$$

and its edge set is

$$E(D_2(C_n)) = \bigcup_{i,j=1}^{n-1} \left\{ \begin{array}{l} \{u_i u_{i+1}\} \cup \{v_j v_{j+1}\} \cup \{u_i v_{j+1}\} \cup \{u_n v_1\} \\ \cup \{v_j u_{i+1}\} \cup \{u_n u_1\} \cup \{v_n v_1\} \cup \{v_n u_1\} \end{array} \right\}$$

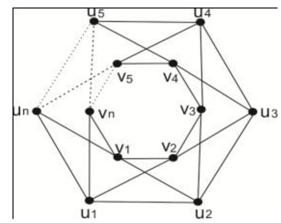

Figure 13: shadow graph of a path $D_2(C_n)$

Define the functions f_1 and f_2 be the mapping from the vertices and the edges to a color set $\{1,2,3,...,k\}$ as follows. There are two cases:

Case 1: Let n be even.

For all $1 \le i, j \le n,$

$$f_1(u_i) = \begin{cases} 1, & if\ \ i \equiv 1 (\text{mod } 2) \\ 2, & \text{otherwise} \end{cases}$$

$$f_1(v_j) = \begin{cases} 1, & if\ \ j \equiv 1 (\text{mod } 2) \\ 2, & \text{otherwise} \end{cases}$$

for all $1 \le i, j \le n-1,$

$$f_2(u_i u_{i+1}) = \begin{cases} 3, & if\ \ i \equiv 1 (\text{mod } 2) \\ 4, & \text{otherwise} \end{cases}$$

$$f_2(v_j v_{j+1}) = \begin{cases} 3, & if\ \ j \equiv 1 (\text{mod } 2) \\ 4, & \text{otherwise} \end{cases}$$

$f_2(u_n u_1) = 3, f_2(v_n v_1) = 4$

for all $1 \le i, j \le n-1,$

$f_2(u_i v_{j+1}) = 5,\ \ if\ \ i = j$

$f_2(v_j u_{i+1}) = 6,\ if\ \ i = j$

$f_2(u_n v_1) = 5\ and\ f_2(v_n u_1) = 6.$

Case 2: Let n be odd.

For all $1 \le i, j \le n-1,$

$$f_1(u_i) = \begin{cases} 1, & if\ \ i \equiv 1 (\text{mod } 2) \\ 2, & \text{otherwise} \end{cases}$$

$$f_1(v_j) = \begin{cases} 1, & if\ \ j \equiv 1 (\text{mod } 2) \\ 2, & \text{otherwise} \end{cases}$$

$f_1(u_n) = f_1(v_n) = 3$

for all $1 \le i,\ j \le n-1,$

$$f_2(u_i u_{i+1}) = \begin{cases} 3, \ if \ \ i \equiv 1 (\text{mod } 2) \\ 4, \ \text{otherwise} \end{cases}$$

$$f_2(v_j v_{j+1}) = \begin{cases} 3, \ if \ \ j \equiv 1 (\text{mod } 2) \\ 4, \ \text{otherwise} \end{cases}$$

$$f_2(u_n u_1) = f_2(v_n v_1) = 2$$

for all $1 \le i,\ j \le n-1,$

$$f_2(u_i v_{j+1}) = 5, if \ i = j$$

$$f_2(v_j u_{i+1}) = 6, \ if \ \ i = j$$

$$f_2(u_n v_1) = 5 \ and \ \ f_2(v_n u_1) = 6.$$

Using this general pattern of coloring, the graph $D_2(C_n)$ is adjacent vertex distinguishing total colored and its chromatic number is $\Delta(G)+2,$ for odd $n.$

Illustration 5.7. Consider the shadow graph of a cycle C_6

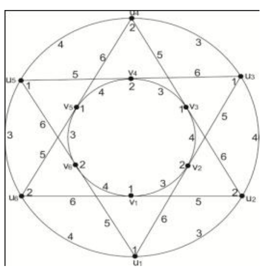

Figure 14: shadow graph of a path $D_2(C_6)$

By using the coloring pattern as given in case 1 of theorem 5.2, the colors $1, 2, 3, 4, 5, 6$ are assigned to the vertices and the edges are assigned with the colors as shown in fig.14.

The adjacent vertex distinguishing total chromatic number of $D_2(C_6)$ is $6.$

Illustration 5.8. Consider the shadow graph of a cycle C_7.

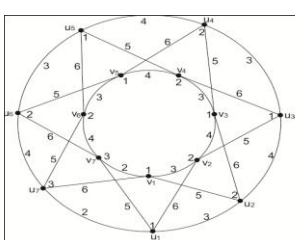

Figure 15: shadow graph of a path $D_2(C_7)$

By using the coloring pattern as given in case 2 of theorem 5.2, the colors $1, 2, 3, 4, 5, 6$ are assigned to the vertices and the edges are assigned with colors as shown in fig.15.

The adjacent vertex distinguishing total chromatic number of $D_2(C_7)$ is $6.$

VI. CONCLUSION

The concept of adjacent vertex distinguishing total chromatic number for the larger graphs obtained from the product of paths are discussed in this paper and found the adjacent vertex distinguishing total chromatic number for Sudha grid of diamonds, Sudha grid of hexagons and shadow graph of (i) a path and (ii) a cycle. We also found the adjacent vertex distinguishing total chromatic number of a crown graph.

REFERENCES

[1] X.Zhang, H.Chen, J.Li, B.Yao, J.Wang,"On adjacent-vertex-distinguishing total coloring of graphs," Sci.China Ser. A 48, 289-299, 2005.

[2] X.Chen, "On the adjacent vertex distinguishing total chromatic numbers of graphs with $\Delta = 3,$ "Discrete. Math., 308, 4003-4007, 2008.

[3] H.Wang, "On the adjacent vertex distinguishing total chromatic numbers of graphs with $\Delta = 3,$" J. Comb.Optim., 14, 87-109, 2007.

[4] J.Hulgan, "Concise proofs for adjacent vertex-distinguishing total colorings", Discrete.Math., 309, 2548-2550, (2009).

[5] X.Chen, Z.Zhang, "AVDTC numbers of generalized Halin graphs with maximum degree at least 6," Acta Math. Appl. Sin. Engl. Ser, 24, 55-58, 2008.

[6] W.Wang . D.Huang, "The adjacent vertex distinguishing total coloring of planar graphs," J Comp.Optim., 27, 379- 396, 2014.

[7] A.Papaioannou, C.Raftopoulou, "On the adjacent vertex distinguishing total coloring of 4-regular graphs," Discrete Math. 330, 20-40, 2014.

[8] S.Sudha, K.Manikandan, "Adjacent vertex distinguishing totoal coloring of corona graphs," Asian Journal of current engineering and Maths, 4, 8-19, 2015.

[9] A.G.Luiz, C.N.Campos, C.P.de Mello, "Adjacent vertex distinguishing total coloring of complete equipartite graphs," Discrete Math.184, 189-195, 2015.

Global Journal of Pure and Applied Mathematics (GJPAM) ISSN 0973-1768 Volume 12,Number 4 (2016)

Segmentation of abdominal organs using min cut/ max flow algorithm–An application of Graph theory

*S.N Kumar**
Department of ECE,
Sathyabama University,
Tamil Nadu, India.
Email: appu123kumar@gmail.com

A. Lenin Fred
Department of CSE,
Mar Ephraem College of Engineering and Technology
Tamil Nadu, India.
Email: leninfred.a@gmail.com

S. Lalitha Kumari
Department of ECE,
Sathyabama University,
Tamil Nadu, India.
Email: lalithavengat@gmail.com

***Abstract*—Medical image processing is the processing of medical images using computer aided algorithms for the analysis of anomalies. The segmentation of abdominal organs like kidney, liver from CT image is used as an effective and accurate indicator for the diagnosis in many clinical situations. The goal of this paper is to accurately segment the abdominal organs from low contrast CT images. The CT images are corrupted by gaussian noise and pre-processing was done by decision based median filter. The decision based median filter will not alter the non-noisy pixels unlike the conventional median filter. The segmentation was done by graph cut min cut /max flow algorithm. The Boykov - Kolmogorov (BK) augmenting path algorithm was used and it yields better results. The algorithms were developed in Matlab 2010 and tested on real time CT data sets. The results closely match with the manual delineation by the expert physician.**

Keywords— Segmentation; Graph cut; Computer Tomography;

I. INTRODUCTION

Medical imaging modalities like CT, MRI and PET have revolutionized the modern medicine. The medical images obtained from acquisition system are analysed for the diagnosis of anomalies like tumor and cyst. Medical image processing is the process of applying computerized algorithms for the analysis of anomalies. In image processing, segmentation is the process of extraction of desired region of interest in the image or it can also be stated as the separation of foreground object from the background. The segmentation algorithms can be broadly classified into three categories supervised, unsupervised and interactive [1] [2] [3]. The thresholding is the simplest technique, however it produce good results for high contrast objects with sharp edges and is sensitive to noise [4]. The watershed algorithm is sensitive to noise and it produce over segmentation in the case of objects with weak boundaries [5]. The active contour methods require crucial selection of the parameters and suffer from time complexity [6] [7]. In the case of neural network, training should be done properly to yield good results and parameters selection also affects the performance [8] [9]. The graph cut segmentation algorithm is an interactive segmentation approach and it is based on the graph theory in mathematics. The main objective of graph cut algorithm is to perform an optimum cut there by separating the object from the background [10] [11]. The graph cut segmentation algorithm yields better results than conventional segmentation algorithms like thresholding, region growing and watershed algorithm. Section 2 describes materials and methods comprising of acquisition protocol and algorithms used. Section 3 describes the results and discussion and finally conclusions are drawn in section 4.

II. MATERIALS AND METHODS

A. *Acquisition Protocol*

The CT images have been acquired on Optima CT machine. Both plain and contrast enhanced CT images were taken with 0.6mm slice thickness. The patient consent was obtained for publishing the images. The abdominal CT images of 9 data sets were used which comprises of three data sets of normal case, three data sets of malignant renal cell tumor (Renal Cell Carcinoma) and three data sets of malignant liver tumor (Hepatic Cellular Carcinoma). The preprocessing along with segmentation algorithms was applied on all the 9 data sets and the result of typical slices are depicted in the results and discussion. The ethics committee for biomedical activities of Mar Ephraem International Center for Medical Image processing and Metro Scans & Laboratory, Thiruvananthapuram approved the study of CT images of human subjects for research work.

B. *Preprocessing*

The median filter is a conventional spatial domain filter in which each pixel is replaced by the median of the gray values in the neighbourhood [12]. Though median filter is simple, it alters the non-noisy pixels also, hence decision based median filter is used in this paper which will not disturb the non-noisy pixels. It comprises of two stages, noise detection, noise filtering and is free from crucial parameter selection unlike progressive switched median filter**.**

C. *Introduction to Graph Theory in Image Segmentation*

A directed weighted graph G=(V,E) consist of a set of nodes V and a set of directed edges E that connect them. With respect to an image, the nodes represent the pixels. The cost function in graph cut algorithm comprises of terms corresponding to regional and boundary properties of the images. Let P represents pixels in a 2D image and 'N' represents neighbourhood system (8 or 24). The binary vector 'S' can be return as follows

$$S = (S1, S2 \ldots.Sp\ldots.SP) \tag{1}$$

*Corresponding author.

This paper was presented by the first author in the National Conference on *Advances in Mathematics and its Applications to Science and Engineering* (AMASE-2016) conducted in Department of Mathematics, University College of Engineering-Pattukkottai, Thanjavur, Tamil Nadu, India, on 22nd January 2016.

The components of the binary vector 'S' can be either "object" or "background". The cost functions E(S) in terms of regional and boundary properties can be written as follows

$$E(S) = \lambda R(S) + B(S) \quad (2)$$

$$R(S) = \sum_{p \varepsilon P} R_S(S_P) \quad (3)$$

$$B(S) = \sum_{\{p,q\} \varepsilon N} B_{\{P,Q\}} \delta(S_P, S_q) \quad (4)$$

$$\delta(S_p, S_q) = \begin{cases} 1 & ; \text{ if } S_p \neq S_q \\ 0 & ; \text{ otherwise} \end{cases} \quad (5)$$

The term R(S) specifies the regional properties and B(S) specifies the boundary properties of segmentation of image 'S'. The term R(S) describes how many pixels belong to object and background. The component B $_{\{p,\, q\}}$ is large when pixels p and q are similar and is close to zero when the pixels are different. A simple 2D segmentation using graph cut is depicted in figure 1. The 'O' represents the seed point for the object and 'B' represents the seed point for the back ground.

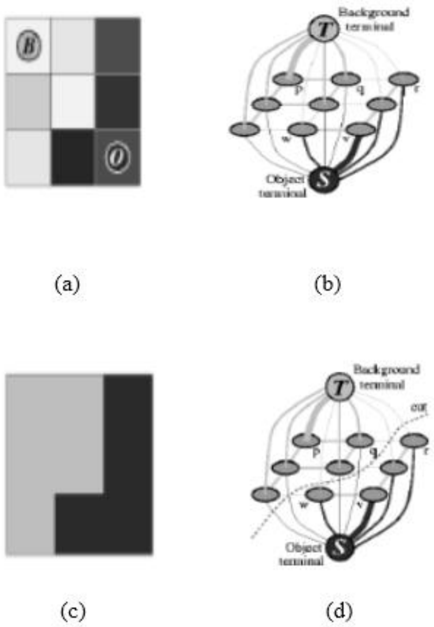

Figure 1: (a) Image with seed points, (b) Graph, (c) Segmentation result, (d) Graph cut

The n-links and t-links represent two types of edges in graph. The t-link connects pixels with terminals and the cost of t-link is defined by the data term R(S) The n-link connects pair of neighbouring pixels or voxels and cost of n link is defined by the interaction term B(S). The segmentation is done by minimizing the energy function by finding a minimum cut using maximum flow algorithm. An s/t cut 'C' on a graph with two terminals can be stated as the portioning of the nodes in the graph into two disjoint subsets 'S' and 'T', such that the source s is in 'S' and the sink t is in 'T'. The cost of a cut C={S, T} is defined as the sum of the cost of the boundary edges (p, q), Where p ε s and q ε T. The minimum cut problem on a graph is to find a cut that has the minimum cost among all cuts. The minimum s/t cut problem can be solved by BK maximum flow algorithm.

D. Boykov- Kolmogorov Algorithm

The basic principle of the Boykov-Kolmogorov (BK) algorithm is to maintain two search tree, one from the source and one from the sink. The trees are updated during the execution of the algorithm. Let 'S' and 'T' represents the two non-overlapping search trees with roots at the source 's' and the sink 't'.

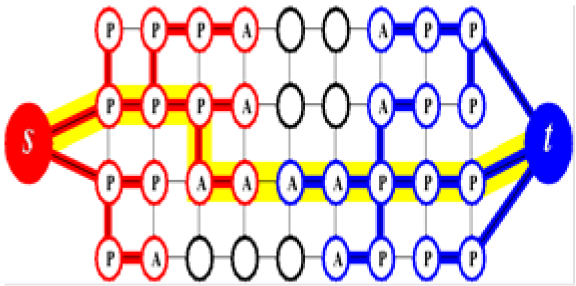

Figure 2: Principle of BK algorithm

All edges form each parent node to child node is non-saturated in 'S' tree, while in 'T' tree edges from child node to parent node are non-saturated. Free nodes are those nodes which are not in 'S' and 'T'. The nodes in search tree 'S' and 'T' can be classified into two types active or passive. The nodes that depicts the outer border in each tree are called active nodes while the internal nodes are called passive nodes. The search tree 'S' and 'T' can grow from active nodes by acquiring new children from a set of free nodes, while the passive nodes cannot grow since it is completely blocked by other nodes from the same trees. When an active node in one of the trees sense a neighbouring node that belong to the other tree, an augmenting path is created. The three stages in BK algorithm are growth stage, augmentation stage and adoption stage. The search trees 'S' and 'T' are depicted as red and blue coloured nodes and the free nodes are depicted in black colour. At the end of growth stage, a path (yellow line) is created from the source's' to the sink 't' and the active and passive nodes are represented by 'A' and 'P'.

1) Growth stage: In this stage, the search trees 'S' and 'T' expand through the active nodes. For each active node, the free nodes which are linked through non-saturated edges are searched. The newly acquired nodes will be the active nodes of the corresponding search tree. The active node will become passive node when all the free nodes are explored. The termination of growth stage occurs when an active node finds an adjacent active node that belongs to the other tree, there by an augmenting path from 'S' and 'T' was found.

2) Augmentation Stage: In this stage augmentation of the path determined at the growth stage takes place. Since the objective is maximum possible flow through the augmenting path, some edges in the path become saturated and the saturated nodes are called orphans. The augmentation stage splits the search trees 'S' and 'T' into forest.

3) Adoption stage **:** In this stage, restoring of single tree takes place and for each orphan generated in the previous stage, the BK algorithm tries to find a new valid parent. If no valid parent is found, the orphan node and its child node become free. The tree rooted in that corresponding orphan is discarded. This stage terminates when all the orphan nodes are connected to a near parent or they are free. Once the adoption stage is completed, the BK algorithm returns to the growth state. The BK algorithm terminates when the search trees 'S' and 'T' cannot grow and the trees are separated by saturated edges that implies maximum flow is achieved.

III. RESULTS AND DISCUSSION

The segmentation algorithm was evaluated on 9 real time CT data sets. Prior to segmentation, the pre-processing was performed by decision based median filter. The algorithms were developed using Matlab 2010 and the BK algorithm code was written in C language. The mex file for the C code was incorporated in Matlab. The algorithms were executed in laptop with specifications of Intel Pentium(R) P6000 processor with 3GB RAM, 64bit windows 7 operating system.

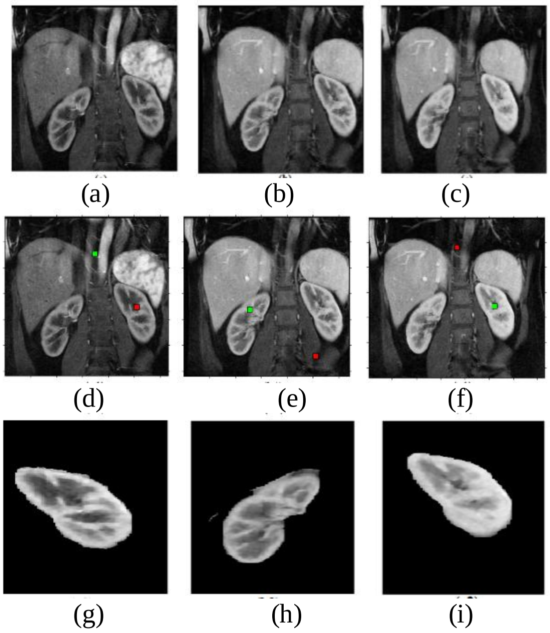

Figure 3: (a, b, c) Input CT image; (d, e, f) Seed point selection; (g, h, i) Kidney segmentation result;

Each data set comprises of 20 axial slice and 20 coronal slice images. The segmentation algorithm was evaluated on all data sets and result of typical slice in each data set is depicted here. The first row of figure 3 depicts the pre-processed input CT images. The second row in figure 3 depicts the seed point selection. The third row in figure 3 depicts the kidney segmentation result without any anomalies. Similarly the figure 4 depicts the kidney tumor segmentation result and figure 6 depicts the liver tumor segmentation result.

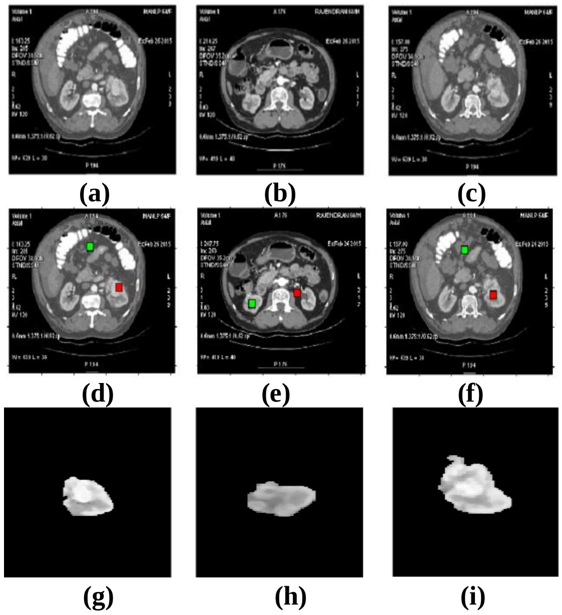

Figure 4: (a, b, c) Input CT image; (d, e, f) Seed point selection; (g, h, i) Kidney tumor Segmentation result;

The performance of graph cut segmentation algorithm was evaluated in terms of dice coefficient. It is a measure to indicate the percentage of spatial overlap between the segmented image and ground truth image. The dice coefficient is given by the equation.

$$D = \frac{2(S \cap G)}{(S \cap G + S \cup G)} \qquad (6)$$

Where S and G are the segmented image and ground truth image.

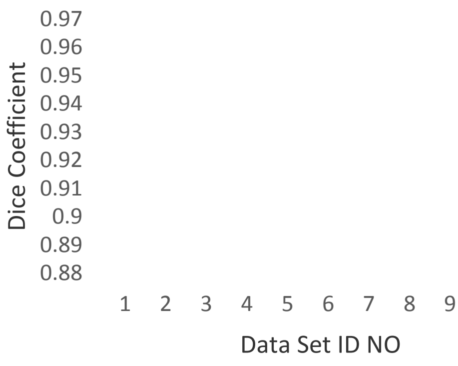

Figure 5: DC plot for data sets

The ground truth image was obtained by the careful delineation of ROI by expert radiologist. The dice coeficient value is 1 for perfect segmentation and the segmentation algorithm result is acceptable if DC $\geq$ 0.9 From the DC plot in figure 5, it is clear that the average value of dice coefficient is 0.94 and hence the graph cut algorithm yields optimum result.

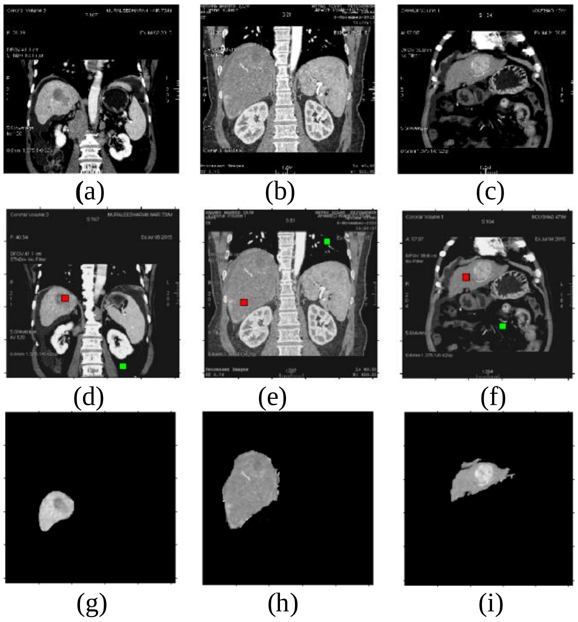

Figure 6: (a, b, c) Input CT image; (d, e, f) Seed point selection; (g, h, i) Liver tumor Segmentation result;

The graph cut segmentation algorithm thus yields good segmentation result for the extraction of abdominal organs in CT images, which was evaluated qualitatively by the radiologist and quantitatively by the performance metric.

IV. CONCLUSION

`In this paper the Min Cut /Max Flow graph cut algorithm is employed for the segmentation of abdominal organs in CT images. The pre-processing of input CT images was performed by decision based median filter. The DC value computed for all the data sets are greater than 0.9 that indicates the efficiency of the graph cut algorithm. The seed point selection is done manually in this paper and it involves human intervention. In future the seed point selection can be made automatic by incorporating neural network in the graph cut algorithm.

ACKNOWLEDGMENT

We thank Dr Sebastian Varghese (Consultant Radiologist, Metro Scans & Laboratory, Trivandrum) for providing the medical CT images, Anchalo Bensiger. S.M (ME: CSE, Mar Ephraem College of Engineering and Technology) and Ajay Kumar H (Department of ECE, Mar Ephraem College of Engineering and Technology for supporting us in the preparation of manuscript.

REFERENCES

[1] Olivier C. Mocquillon, J. J. Rousselle, R. Boné, and H. Cardot, "A supervised texture-based active contour model with linear programming", In Proc. IEEE Int. Conf. Image Processing, pp. 1104–1107, 2008.

[2] M. Schaap, T. van Walsum, L. Neefjes, C. Metz, E. Capuano, M. de Bruijne, and W. Niessen, "Robust shape regression for supervised vessel segmentation and its application to coronary segmentation in CTA", IEEE Trans. Med. Image., Vol. 30, Issue. 11, pp. 1974–1986, 2011.

[3] N. Lee, R. T. Smith, and A. F. Laine. "Interactive segmentation for geographic atrophy in retinal fundus images", In Proc. 42nd Asilomar Conf. Signals, Systems and Computers, pp 655–658, 2008.

[4] P. Karch, I. Zolotova, "An Experimental Comparison of Modern Methods of Segmentation", IEEE 8th International Symposium on SAMI, pp. 247-252, 2010.

[5] Lamia Jaafar Belaid, Walid Mourou, "Image segmentation: A Watershed transformation algorithm", Image Analysis & Stereology, Vol. 28, No 2, 2009.

[6] S. Y. Yeo, X. Xie, I. Sazonov, and P. Nithiarasu. "Geometrically induced force interaction for three-dimensional deformable models", IEEE Trans. Image Process., Vol. 20, Issue 5, pp. 1373–1387, May 2011.

[7] Tsai A, Yezzi A Jr, Wells W, Tempany C,Tucker D, Fan A, Grimson WE and Willsky A, "A shape-based approach to the segmentation of medical imagery using level sets", IEEE Trans Med. Imaging, Vol. 22, Issue 2, pp. 137-54, Feb 2003.

[8] J. Jiang, P. Trundle, J. Ren, "Medical image analysis with artificial neural networks", computerized Medical Imaging and Graphics, pp.617–631, 2010.

[9] M. Egmont-Petersen, D. de Ridder, H. Handels, "Image processing with neural networks a review", Pattern Recognition, Vol. 35, pp.2279–2301, 2002.

[10] Ondrej Danek and Martin Maška, "A Simple Topology Preserving Max-Flow Algorithm for Graph Cut Based Image Segmentation", Sixth Doctoral Workshop on Math. and Eng. Methods in Computer Science (MEMICS'10), pp. 19-25, 2010.

[11] Yuri Y. Boykov Marie-Pierre Jolly, "Interactive Graph Cuts for Optimal Boundary & Region Segmentation of Objects in N-D Images", Proceedings of International Conference on Computer Vision, Vancouver, Canada, vol 1, pp.105-112.2001.

[12] Bhausaheb Shinde, Dnyandeo Mhaske, A.R. Dani, "Study of Noise Detection and Noise Removal Techniques in Medical Images", I.J.Image, Graphics and Signal Processing. Vol. 2(1), pp. 51- 60.2011.

Global Journal of Pure and Applied Mathematics (GJPAM) ISSN 0973-1768 Volume 12,Number 4 (2016)

Base stock policy inventory system with Multiple vacations and Negative customers

*J. Kathiresan**
Department of Mathematics,
Alagappa University, Tamil Nadu, India.
Email: kathiresanmat@gmail.com

N. Anbazhagan
Department of Mathematics,
Alagappa University, Tamil Nadu, India.
Email: anbazhagan_n@yahoo.co.in

***Abstract-* In this paper, we consider a continuous review base stock policy inventory system with multiple vacations and negative customers. The maximum storage capacity is S. The customers arrive according to a Poisson process with finite waiting hall. The customers are of two types : ordinary and negative. An ordinary customer, on arrival, joins the queue and the negative customer does not join the queue and takes away any one of the waiting customers. When the waiting hall is full, arriving primary customer is considered to be lost. The service time and lead time are assumed to have independent exponential distribution. When the inventory becomes empty, the server takes a vacation and the vacation duration is exponentially distributed. We obtained the joint probability distribution of the number of customers in the waiting hall, the inventory level and the server status for the steady state case. Some system performance measures are derived. The long-run total expected cost rate is calculated and numerical study is presented.**

Keywords- Continuous review inventory system, Positive leadtime, Base Stock Policy, Multiple vacations, Negative Customers.

AMS Subject Classification: 90B05, 60J27.

I. INTRODUCTION

Analysis of continuous review perishable inventory systems with positive leadtimes under $(S-1,S)$ policy have been carried out by Schmidt and Nahmias [20], Pal [19], and Kalpakam and Sapna [14, 15]. In all these models, whenever the inventory level drops by one unit, either due to a demand or a failure, an order for one item is placed. Kalpakam and Arivarignan [13] discussed with an $(S-1,S)$ system with renewal demands for non-perishable items. Kalpakam and Shanthi [16] have considered modified base stock policy and random supply quantity. Recently, Gomathi et al. [11] considered a two commodity inventory system for base-stock policy with service facility. They have assumed Poisson arrivals and the life time of each item and service time are assumed to have independent exponential distribution.

Berman et al. [2] have dealt an inventory management system at a service facility which uses one item of inventory for each service provided. Berman and Kim [3] considered a queueing - inventory system with Poisson arrivals, exponential service times and zero lead times. Berman and Sapna [4] studied the concept of queueing - inventory system with service facility. Krishnamoorthy and Anbazhagan [17] analyzed a perishable queueing inventory system with N policy, Poisson arrivals, exponential distributed lead times and service times. The joint probability distributions of the number of customers in the system and the inventory level were obtained in the steady state case. Jeganathan et al. [12] studied a retrial inventory system with non-preemptive priority service.

The concept of negative customer is increasingly considered in queueing systems. The customers who arrive at the service station are classified as ordinary (positive or regular) and negative customers. The arrival of ordinary customers to the service station increases the queue length by one and the arrival of negative customer to the service station causes one ordinary customer to be removed, if any is present. Since the work analysed by Gelenbe [10], the research on queueing systems with negative arrivals has been greatly motivated by some practical applications in computers, neural networks and communication networks etc. For comprehensive literature on queueing networks with negative arrivals, one may refer to Choa et al. [5], and Gelenbe and Pujolle [9]. A recent review can be found in Artalejo [1].

*Corresponding author.

This paper was presented by the first author in the National Conference on *Advances in Mathematics and its Applications to Science and Engineering* (AMASE-2016) conducted in Department of Mathematics, University College of Engineering-Pattukkottai, Thanjavur, Tamil Nadu, India, on 22nd January 2016.

Daniel and Ramanarayanan [6] have first introduced the server vacation in inventory with two servers. Also they have studied an inventory system in which the server takes rest when the level of the inventory is zero in [7]. They assumed that the demands that occurred during stock-out period are assumed to be lost. Narayanan et al. [18] studied on an (s,S) inventory policy with service time, vacation to server and correlated lead time. Sivakumar [21] has considered a retrial inventory system with multiple server vacaion. He has assumed Poisson arrival and exponential service time. Further he assumed that the server takes a vacation of exponential length each time when the inventory level becomes zero.

In this paper we have considered a $(S-1,S)$ policy stochastic inventory system under continuous review at a service facility with a finite waiting hall for customers. The customers arriving to the service station are classified as ordinary and negative customers. The server takes a vacation of exponential length each time when the inventory level becomes empty. When the vacation ends he finds the inventory level is still zero, the server takes another vacation; otherwise, he terminates his vacation, and he is ready to serve any arriving demands. The joint probability distribution of the number of customers in the waiting hall, the inventory level and the server status is obtained for the steady state case. Various system performance measures in the steady state are derived and the long-run total expected cost rate is calculated.

The remainder of this paper is organized as follows. In Section 2, we present the mathematical model and the notations. Analysis of the model and the steady state solution are given in Section 3. In Section 4, we derive various measures of system performance in steady state. In Section 5, The total expected cost rate is calculated and numerical study is presented. The last section is meant for conclusion.

II. MODEL DESCRIPTION

We consider a single server continuous review stochastic inventory system with multiple vacations and negative customers. The maximum inventory level is denoted by S. The primary customers arrive at the system one by one in according to a Poisson stream with arrival rate $\lambda(>0)$. Waiting hall space is limited to accommodate a maximum number M, which includes the customer one who is receiving service. The probability that a customer is an ordinary is p and a negative is $q(=1-p)$. We have assumed that the negative customer removes any one of the ordinary waiting customers from the system including the one at the service point. The service time for each customer follows an exponential distribution with parameter μ. An any arriving primary customer who finds the waiting hall is full is considered to be lost. A one-to-one ordering policy is adopted. According to this policy, orders are placed for one unit as and when the inventory level drops due to a demand. The lead time is exponentially distributed with the rate β. The server leaves for a vacation as soon as the inventory becomes empty. After the vacation, if the inventory level is positive, he begins to serve the customers right away otherwise he takes another vacation. The vacation duration is exponentially distributed with rate θ. We assume that the inter-demand times between primary customers, the lead times, service times and the sever vacation times are mutually independent random variables.

Notations

$[A]_{ij}$: The element / submatrix at (i,j)th position of A.

0 : Zero matrix.

I : Identity matrix.

e : A column vector of 1's of appropriate dimension.

$$\delta_{ij} : \begin{cases} 1, & if \;\; i=j, \\ 0, & otherwise. \end{cases}$$

$$\bar{\delta}_{ij} : 1-\delta_{ij}$$

$$Y(t) : \begin{cases} 0, \text{ if server is on vacation at time } t. \\ 1, \text{if server is not on vacation at time } t. \end{cases}$$

.

III. ANALYSIS

Let $X(t)$, $L(t)$ and $Y(t)$ denote the number of customers in the waiting hall, the inventory level of the commodity and the server status at time t. From the assumptions made on the input and output processes, it can be shown that the triplet $\{(X(t),L(t),Y(t)),t\geq 0\}$ is a continuous time Markov chain with state space given by E.

$E = \{(i,0,0) \ : \ i = 0,1,2,\ldots,M\} \cup \{(i,k,m) \ : \ i = 0,1,2,\ldots,M, \ k = 1,2,\ldots,S, \quad m = 1,0\}$

To determine the infinitesimal generator

$$P = (h((i,k,m),(j,l,n))), \qquad (i,k,m),(j,l,n) \in E$$

of this process we use the following arguments :

Transitions due to the arrival of an ordinary customers:

- $(i,k,m) \to (i+1,k,m)$: the rate is $p\lambda$, for $0 \le i \le M-1$, $1 \le k \le S$, $m = 1,0$.
- $(i,0,0) \to (i+1,0,0)$: the rate is $p\lambda$, for $0 \le i \le M-1$.

Transitions due to the arrival of a negative customers:

- $(i,k,m) \to (i-1,k,m)$: the rate is $q\lambda$, for $1 \le i \le M$, $1 \le k \le S$, $m = 1,0$.
- $(i,0,0) \to (i-1,0,0)$: the rate is $q\lambda$, for $1 \le i \le M$.

Transitions due to service completion in the system:

- $(i,k,1) \to (i-1,k-1,1)$: the rate is μ, for $1 \le i \le M$, $2 \le k \le S$.
- $(i,1,1) \to (i-1,0,0)$: the rate is μ, for $1 \le i \le M$.

Transitions due to replenishments:

- $(i,k,m) \to (i,k+1,m)$: the rate is $(S-k)\beta$, for $0 \le i \le M$, $1 \le k \le S$, $m = 1,0$.
- $(i,0,0) \to (i,1,0)$: the rate is $S\beta$, for $0 \le i \le M$.

Transitions due to vacation completion:

- $(i,k,0) \to (i,k,1)$: the rate is θ, for $0 \le i \le M$, $1 \le k \le S$.

We observe that no transition other than the above is possible.

Denoting $q = ((q,0,0),(q,1,0),(q,1,1),(q,2,0),(q,2,1),\ldots,(q,S,0),(q,S,1))$ for $q = 0,1,\ldots,M$. By ordering states lexicographically, the infinitesimal generator A can be conveniently expressed in a block partitioned matrix with entries

$$[A]_{ij} = \begin{cases} A_2, & j = i, \quad i = M \\ A_1, & j = i, \quad i = 1,2,\ldots,M-1 \\ A_0, & j = i, \quad i = 0 \\ B, & j = i+1, \quad i = 0,1,2,\ldots,M-1 \\ C, & j = i-1, \quad i = 1,2,\ldots,M \\ 0, & \text{otherwise} \end{cases}$$

where

$$[A_0]_{ij} = \begin{cases} G_{S-i}, & j = i, \quad i = S, S-1\ldots,1 \\ G_{01}, & j = 1, \quad i = 0 \\ G_{00}, & j = 0, \quad i = 0 \\ 0, & \text{otherwise} \end{cases}$$

$$[G_{S-i}]_{mn} = \begin{cases} \theta, & n = 1, \quad m = 0 \\ (S-i)\beta, & n = i, \quad m = 1,0 \\ -((S-i)\beta + p\lambda), & n = 1, \quad m = 1 \\ -((S-i)\beta + p\lambda + \theta), & n = 0, \quad m = 0 \\ 0, & \text{otherwise} \end{cases}$$

For $i = S, S-1, \ldots, 1$

$$G_{01} = 0(\;0 \quad \overset{\mathbf{1}\;\; 0}{} \; S\beta), \; G_{00} = \overset{0}{0}(-(S\beta + p\lambda)),$$

$$[A_1]_{ij} = \begin{cases} F_{S-i}, & j = i, \quad i = S, S-1\ldots,1 \\ G_{01}, & j = 1, \quad i = 0 \\ F_{00}, & j = 0, \quad i = 0 \\ 0, & \text{otherwise} \end{cases}$$

$$[F_{S-i}]_{mn} = \begin{cases} \theta, & n = 1, \quad m = 0 \\ (S-i)\beta, & n = i, \quad m = 1,0 \\ -((S-i)\beta + \lambda + \mu), & n = 1, \quad m = 1 \\ -((S-i)\beta + \lambda + \theta), & n = 0, \quad m = 0 \\ 0, & \text{otherwise} \end{cases}$$

For $i = S, S-1, \ldots, 1$

$$F_{00} = \overset{0}{0}(-(S\beta + \lambda)),$$

$$[A_2]_{ij} = \begin{cases} P_{S-i}, & j = i, \quad i = S, S-1\ldots,1 \\ G_{01}, & j = 1, \quad i = 0 \\ P_{00}, & j = 0, \quad i = 0 \\ 0, & \text{otherwise} \end{cases}$$

$$[P_{S-i}]_{mn} = \begin{cases} \theta, & n = 1, \quad m = 0 \\ (S-i)\beta, & n = i, \quad m = 1,0 \\ -((S-i)\beta + q\lambda + \mu), & n = 1, \quad m = 1 \\ -((S-i)\beta + q\lambda + \theta), & n = 0, \quad m = 0 \\ 0, & \text{otherwise} \end{cases}$$

For $i = S, S-1, \ldots, 1$

$$P_{00} = \overset{0}{0}(-(S\beta + q\lambda)),$$

$$B = p\lambda I_{(2S+1)\times(2S+1)}$$
$$C = q\lambda I_{(2S+1)\times(2S+1)}$$

It may be noted that the matrices A_0, A_1, A_2, B and C are square matrices of order $(2S+1)$

3.1 Steady State Analysis

It can be seen from the structure of A that the homogeneous Markov process $\{(X(t), L(t), Y(t)), t \geq 0\}$ on the finite state space E is irreducible. Hence the limiting distribution

$$\pi^{(i,j,k)} = \lim_{t\to\infty} pr\{X(t) = i, L(t) = j, Y(t) = k \mid X(0), L(0), Y(0)\},$$

exists. Let

$$\mathbf{\Pi} = (\Pi^{(0)}, \Pi^{(1)}, \Pi^{(2)}, \ldots, \Pi^{(M)})$$

we partition the vector, $\mathbf{\Pi^{(i)}}$ into as follows:

$$\Pi^{(i)} = (\Pi^{(i,0)}, \Pi^{(i,1)}, \Pi^{(i,2)}, \ldots, \Pi^{(i,S)}),$$
$i = 0, 1, 2, \ldots, M$

which is partitioned as follows:

$$\Pi^{(i,j)} = (\pi^{(i,0,0)})$$

$\Pi^{(i,j)} = (\pi^{(i,j,0)}, \pi^{(i,j,1)})$
for $i = 0,1,2,\ldots,M$, $j = 1,2,\ldots,S$

Then the limiting probability, $\mathbf{\Pi}$ satisfies

$$\mathbf{\Pi}A = 0, \qquad \mathbf{\Pi}e = 1$$

From the structure of A, it is a finite QBD matrix, therefore its steady state vector $\mathbf{\Pi}$ can be computed by using the following algorithm described by Gaver et al. [8].

Algorithm :

1. Determine recursively the matrices

$$F_0 = A_0$$
$$F_i = A_1 + B(-F_{i-1}^{-1})C \text{ , } i = 1,2,\ldots,M-1,$$
$$F_M = A_2 + B(-F_{M-1}^{-1})C \text{ .}$$

2. Compute recursively the vectors $\mathbf{\Pi}^{(i)}$ using

$$\mathbf{\Pi}^{(i)} = \mathbf{\Pi}^{(i+1)}B(-F_i^{-1}) \text{ , } i = 0,1,2,\ldots,M-1$$

3. Solve the system of equations

$$\mathbf{\Pi}^{(M)}F_M = 0 \text{ and } \sum_{i=0}^{M}\mathbf{\Pi}^{(i)}e = 1 \text{ .}$$

From the system of equations $\mathbf{\Pi}^{(M)}F_M = 0$, vector $\mathbf{\Pi}^{(M)}$ could be determined uniquely, upto a multiplicative constant. This constant is decided by $\mathbf{\Pi}^{(i)} = \mathbf{\Pi}^{(i+1)}B(-F_i^{-1})$, $i = 0,1,2,\ldots,M-1$ and $\sum_{i=0}^{M}\mathbf{\Pi}^{(i)}e = 1$.

IV. SYSTEM PERFORMANCE MEASURES

In this section some performance measures of the system under consideration in the steady state are derived.

4.1 Expected inventory level

Let ρ_I denote the mean inventory level in the steady state. Then

$$\rho_I = \sum_{i=0}^{M}\sum_{j=1}^{S} j\left[\pi^{(i,j,1)} + \pi^{(i,j,0)}\right]$$

4.2 Expected reorder rate

Let ρ_R denote the expected reorder rate in the steady state. Then

$$\rho_R = \sum_{i=1}^{M}\sum_{j=1}^{S} \mu\left[\pi^{(i,j,1)}\right]$$

4.3 Expected number of demands in the waiting hall (1)

Let ρ_W denote the expected number of demands in the waiting hall in the steady state. Then

$$\rho_W = \sum_{i=1}^{M}\sum_{j=1}^{S} i\left[\pi^{(i,j,1)} + \pi^{(i,j,0)} + \pi^{(i,0,0)}\right]$$

4.4 Fraction of time server is on vacation

Let ρ_{FV} denote the server is on vacation in the steady state. Then

$$\rho_{FV} = \sum_{i=0}^{M}\sum_{j=0}^{S}\left[\pi^{(i,j,0)}\right]$$

4.5 Expected blocking rate

Let ρ_B denote the expected blocking rate in the steady state. Then

$$\rho_B = \sum_{j=1}^{S} p\lambda\left[\pi^{(M,j,1)} + \pi^{(M,j,0)} + \pi^{(M,0,0)}\right]$$

4.6 Mean rate of arrivals of negative customers

Let ρ_{Ng} denote mean rate of arrivals of negative customers in the steady state. Then

$$\rho_{Ng} = \sum_{i=1}^{M}\sum_{j=1}^{S} q\lambda\left[\pi^{(i,j,1)} + \pi^{(i,j,0)} + \pi^{(i,0,0)}\right]$$

V. *COST ANALYSIS*

The expected total cost per unit time (expected total cost rate) in the steady state for this model is defined to be

c_h : the inventory holding cost per unit item per unit time

c_s : the inventory setup cost per unit item per unit time

c_b : cost per blocking customer

c_w : Waiting cost of a customer in the waiting hall per unit time.

c_n : Cost of loss per unit time due to arrival of a

Global Journal of Pure and Applied Mathematics (GJPAM) ISSN 0973-1768 Volume 12,Number 4 (2016)

negative customer.

The long run total expected cost rate is given by

$$TC(S,M) = c_h\rho_I + c_s\rho_R + c_b\rho_B + c_w\rho_W + c_n\rho_{Ng}$$

Substituting ρ 's into the above equation, we obtain

$$TC(S,M) = c_h\sum_{i=0}^{M}\sum_{j=1}^{S} j\left[\pi^{(i,j,1)} + \pi^{(i,j,0)}\right] + c_s\sum_{i=1}^{M}\sum_{j=1}^{S}\mu\left[\pi^{(i,j,1)}\right] + c_b\sum_{j=1}^{S}p\lambda$$

$$\left[\pi^{(M,j,1)} + \pi^{(M,j,0)} + \pi^{(M,0,0)}\right] + c_w\sum_{i=1}^{M}\sum_{j=1}^{S} i\left[\pi^{(i,j,1)} + \pi^{(i,j,0)} + \pi^{(i,0,0)}\right] +$$

$$c_n\sum_{i=1}^{M}\sum_{j=1}^{S} q\lambda\left[\pi^{(i,j,1)} + \pi^{(i,j,0)} + \pi^{(i,0,0)}\right]$$

5.1 Numerical Examples

Since the total expected cost rate is obtained in a complex form, the convexity of the total expected cost rate cannot be studied by analytical methods. Hence, simple numerical search procedures are used to find the local optimal values for any two of the decision variable (S,M) by considering a small set of integer values for this variable. Table 1 presents the optimal value of the total expected cost rate for various combinations of the primary demand rate λ and the service rate μ. We have assumed constant values for other parameters and costs. Namely, $S=5$, $M=5$ $\theta=0.05$, $\beta=0.7$, $p=0.7$, $q=0.3$, $c_h=0.98$, $c_s=1.2$, $c_w=2.09$, $c_n=0.03$ The optimal value of the total expected cost rate is $TC^*(5,5)$ = 12.659332 for the values of $\lambda=2.3$ and $\mu=0.9$. The value that is shown bold is the least among the values in that column and the value that is shown underlined is the least in that row. Convexity of the total cost for various combinations of λ and μ is given in figure 1.

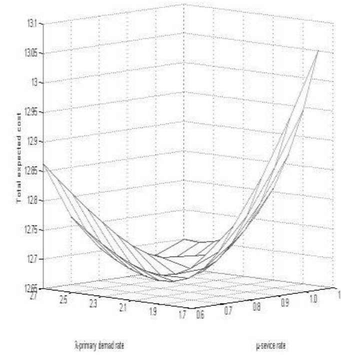

Figure 1: Convexity of the total cost for various combinations of λ and μ

Table 1: Total expected cost rate as a function of λ and μ

μ / λ	0.6	0.7	0.8	0.9	1.0	1.1
1.7	12.733593	12.729977	12.772855	12.848242	12.943846	13.050069
1.8	**12.728964**	**12.703866**	**12.724866**	**12.779530**	**12.856327**	**12.945879**
1.9	12.732824	12.690244	12.693029	12.730161	12.790871	12.866053
2.0	12.742915	**12.686194**	**12.673904**	**12.696304**	**12.743353**	**12.806243**
2.1	12.757527	12.689439	12.664740	12.674827	12.710343	12.762782
2.2	12.775365	12.698203	**12.663342**	**12.663189**	**12.689012**	**12.732606**
2.3	12.795448	12.711102	12.667966	**12.659332**	12.677039	12.713172
2.4	12.817035	12.727060	12.677224	12.661596	**12.672532**	**12.702388**
2.5	12.839564	12.745239	12.690016	12.668646	12.673950	**12.698534**
2.6	12.862613	12.764987	12.705470	12.679410	12.680042	12.700207

VI. CONCLUSION

In this paper, we discussed continuous review inventory system with base stock policy. The customers are of two type : ordinary and negative. Various system performance measures are derived in the steady state. The results are illustrated with numerically. The model discussed here is useful in studying a multiple vacation for the base-stock policy which are slow moving items and the high holding cost.

ACKNOWLEDGEMENT

N. Anbazhagan's research was supported by the University Grants Commission, Government of India through the "Research Award" for the year 2014-16

REFERENCES

[1] G. Artalejo, J. R., *G-networks : A versatile approach for work removal in queueing networks*. European J. Oper. Res., (2000), 126, 233 -249.

[2] Berman, O., Kaplan, E. H. and Shimshak, D. G., *Deterministic approximations for inventory management at service facilities*. IIE Transactions,(1993), 25, 98-104.

[3] Berman, O. and Kim, E., *Stochastic models for inventory management of service facilities*. Stochastic Models, (1999), 15, 695-718.

[4] Berman, O. and Sapna, K.P., *Inventory management at service fa cility for systems with arbitrarily distributed service times*. Communications in Statistics. Stochastic Models, (2000), Vol.16, No.3, 343-360.

[5] Chao, X., Miyazawa, M. and Pinedo, M., *Queueing networks: Customers, Signal and Product Form Solutions*. Wiley, Chichester (1999).

[6] Daniel, J. K. and Ramanarayanan, R., *An inventory system with two servers and rest periods*. Cahiers du C.E.R.O, Universite Libre De Brux- elles, (1987), 29, 95-100.

[7] Daniel, J. K. and Ramanarayanan, R., *An inventory system with rest periods to the server*. Naval Research Logistics, John Wiley and Sons, (1988), 35, 119-123.

[8] Gaver, D.P., Jacobs, P. A. and Latouche, G., *Finite birth-and-death models in randomly changing environments*. Advances in Applied Probability, (1984), 16, 715 - 731.

[9] Gelenbe, E. and Pujolle, G., *Introduction to queueing networks*. Second Edition, Wiley Chichester, (1998).

[10] Gelenbe, E., Production-form queueing networks with negative and positive customers. J.Appl.Prob. (1991), 30, 742 - 748.

[11] Gomathi, D., Jeganathan, K. and Anbazhagan, N., *Two-Commodity Inventory System for Base-Stock Policy with Service Facility*. Global Journal of Science Frontier Research (F), (2012), XII(I), pp. 69-79.

[12] Jeganathan, K. Anbazhagan, N. and Kathiresan, J. *A Retrial Inventory System with Non-preemptive Priority Service*, International Journal of Information and Management Sciences, (2013), 24, 57-77.

[13] Kalpakam, S. and Arivarignan, G., *The (S-1, S) inventory system with lost sales*. Proc. of the Int. Conf. on Math. Mod. Sci. and Tech, (1998), 2, 205-212.

[14] Kalpakam, S. and Sapna, K.P., *(S-1, S) perishable system with stochastic lead times*. Mathl. Comput. Modelling, (1995), 21(6), 95-104.

[15] Kalpakam, S. and Sapna, K.P., *An (S-1, S) perishable inventory system with renewal demands*. Naval Research Logistics, (1996), 43, 129-142.

[16] Kalpakam, S. and Shanthi, S., *A perishable system with modified base stock policy and random supply quantity*. Computers and Mathematics with Applications, (2000), 39, 79-89.

[17] Krishnamoorthy, A. and Anbazhagan, N., *Perishable inventory system at service facility with N policy*. Stochastic Analysis and Applications, (2008), 26, 1-17.

[18] Narayanan, V. C., Deepak, T. G., Krishnamoorthy, A. and Krishnakumar, B., *On an* (s, S) *inventory policy with service time, vacation to server and correlated lead time*. Qualitative Technology and Quantitative Management, (2008), 5(2), 129-143.

[19] Pal, M., The (S-1, S) inventory model for deteriorating items with exponential leadtime. Calcutta Statistical Association Bulletin, (1989), 38, 149-150.

[20] Schmidt, C.P. and Nahmias, S., $(S-1, S)$ *Policies for perishable inventory*. Management Science, (1985), 31, 719-728.

[21] Sivakumar, B., *An inventory system with retrial demands and multiple server vacation*. Quality Technology and Quantitative Management, (2011), 8, pp. 125-146

Global Journal of Pure and Applied Mathematics (GJPAM) ISSN 0973-1768 Volume 12,Number 4 (2016)

Equitable coloring of Sudha gird graohs and Sudha graph

S. Sudha
Ramanujan Institute for Advanced Study in Mathematics, University of Madras,
Chennai, Tamil Nadu, India.
Email: subramaniansudha50@gmail.com

*G. M. Raja**
Ramanujan Institute for Advanced Study in Mathematics
University of Madras
Chennai, Tamil Nadu, India.
Email: rajagopalmalliga@gmail.com

***Abstract*— An equitable coloring of a graph is an assignment of colors to the vertices of the graph, in such a way that no two adjacent vertices have the same color and the number of vertices in any two color classes differ by at most one. Sudha gave the construction of the following graphs:**

(i) Sudha gird of diamonds $S_d(m,n)$,
(ii) Sudha gird of hexagons $S_h(m,n)$ **and**
(iii) Sudha graph $S(n,m)$.

In this paper, we have discussed the equitable coloring of the Sudha gird of diamonds, Sudha gird of hexagons and Sudha graph.

***Keywords*— Sudha gird of diamonds; Sudha gird of hexagons; Sudha graph; Equitable coloring; Color class and Equitable chromatic number.**

AMS Subject Classification : 05C15

I. INTRODUCTION

Mayer [1] introduced the equitable coloring of graphs, Hanna et. al. [2, 3, 4] have discussed about the complexity of equitable vertex coloring of graphs, equitable coloring of some graph products, corona product of graphs and cubic graphs. Hanna [5] also elaborately discussed about the equitable coloring of corona mutiproducts of graphs. Sudha et. al. [6] have discussed about the equitable coloring of prisms and the generalized Petersen graphs. Lih et. al. [7] found the equitable coloring of trees. Dorothee [8] gave the equitable coloring of complete multipartite graph. Sudha et. al. [9] introduced the Sudha graph $S(n,m)$ and found the total coloring of $S(n,m)$ graph.

In this paper, we have discussed the equitable coloring of the Sudha gird of diamonds $S_d(m,n)$, Sudha gird of hexagons $S_h(m,n)$ and $S(n,m)$ graphs. Moreover, we found that the equitable chromatic number of $S_d(m,n)$ is either 2 or 3, the equitable chromatic number of $S_h(m,n)$ is 2 and the equitable chromatic number of $S(m,n)$ is either 3 or 4.

Definition 1.1. *Vertex coloring is the coloring of the vertices of the graph with the minimum number of colors so that no two adjacent vertices have the same color.*

Definition 1.2. *The set of vertices having the same color in the vertex coloring of a graph are said to be in that color class.*

In k-coloring of a graph, there are k color classes. The color classes are represented by $C[1], C[2], \dots,$ if $1, 2, \dots$ represent the colors.

Definition 1.3. *A graph G is said to be equitable k-colorable if its vertex set V can be partitioned into k disjoint subsets $V_1, V_2, \dots, V_k$, satisfy the condition $\big||V_i| - |V_j|\big| \le 1$ for all $1 \le i \le k, 1 \le j \le k$.*

The smallest integer k for which G is equitable k-coloring is known as the equitable chromatic number of G and is denoted by $\chi_= G$.

Definition 1.4. *Sudha grid of diamonds $S_d(m,n)$ is an induced subgraph of the tensor product of two paths P_m with the vertices $u_1, u_2, u_3, \dots, u_m$ for odd $m \ge 3$ and P_n with the vertices $v_1, v_2, v_3, \dots, v_n$ for odd $n \ge 3$ with the vertex set*

$$V(S_d(m,n)) = \left\{u_i v_j \Big/ \begin{matrix} \text{either } i \equiv 1 \ (mod\ 2) \text{ and } j \equiv 0 \ (mod\ 2) \\ \text{or } i \equiv 0 \ (mod\ 2) \text{ and } i \equiv 1 \ (mod\ 2) \end{matrix}\right\}$$

and the edge set

$$E(S_d(m,n)) = \{(u_i v_j)(u_i v_j) / u_i u_k \in E(P_m) \text{ and } v_j v_k \in E(P_n)\}$$

Instead of denoting the vertices as $u_i v_j$, we denoted them as $v_{i,j}$ for simplicity.

Illustration 1.5

$S_d(5,5)$ is a Sudha gird of diamonds with the vertex set $\{v_{1,2}, v_{1,4}, v_{2,1}, v_{2,3}, v_{2,5}, v_{3,2}, v_{3,4}, v_{4,1}, v_{4,3}, v_{4,5}, v_{5,2}, v_{5,4}\}$ as shown in figure 1.

*Corresponding author.
This paper was presented by the second author in the National Conference on *Advances in Mathematics and its Applications to Science and Engineering* (AMASE-2016) conducted in Department of Mathematics, University College of Engineering Pattukkottai, Thanjavur, Tamil Nadu, India, on 22nd January 2016.

Global Journal of Pure and Applied Mathematics (GJPAM) ISSN 0973-1768 Volume 12,Number 4 (2016)

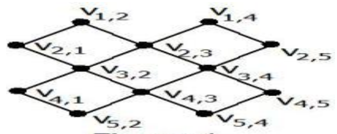

Figure 1

Definition 1.6. *Sudha grid of hexagons $S_h(m,n)$ is an induced subgraph of the strong product of two paths P_m with the vertices $u_1, u_2, u_3, \dots, u_m$ for odd $m \geq 3$ and P_n with the vertices $v_1, v_2, v_3, \dots, v_n$ for $n \equiv 0 \pmod 4$ with the vertex set*

$$V(S_h(m,n)) = \{u_i v_j / \; i+j \equiv 1 \pmod 2 \text{ and } i+j \equiv 0 \pmod 2\}$$

and the edge set

$$E(S_d(m,n)) = \{(u_i v_j)(u_i v_j)/u_i u_k \in E(P_m) \text{ and } v_j v_k \in E(P_n)\}.$$

Illustration 1.7

$S_h(8,7)$ is a Sudha gird of hexagons graph with the vertex set $\{v_{1,2}, v_{1,4}, v_{1,6}, v_{2,1}, v_{2,3}, v_{2,5}, v_{2,7}, v_{2,1}, v_{3,3}, v_{3,5}, v_{3,7}, v_{4,2}, v_{4,4}, v_{4,6}, v_{5,2}, v_{5,4}, v_{5,6}, v_{6,1}, v_{6,3}, v_{6,5}, v_{6,7}, v_{7,1}, v_{7,3}, v_{7,5}, v_{7,7}, v_{8,2}, v_{8,4}, v_{8,6}\}$ as shown in figure 2.

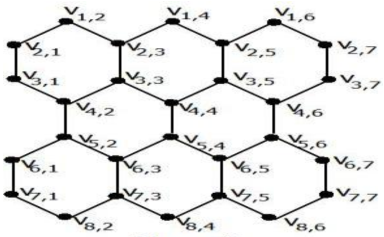

Figure 2

Definition 1.8. *Sudha graph denoted by $S(n,m)$ is defined as the graph with n vertices $\{v_i\}$, $1 \leq i \leq n$ and the following edges for $1 \leq i \leq n$*

(i) v_i is adjacent to v_{i+1} and v_n is adjacent to v_1
(ii) v_i is adjacent to v_{i+m} if $i+m < n$ (iii)
(iii) v_i is adjacent to v_{i+n-m} if $i+m \geq n$.

Illustration 1.9 (iv)

$S(9,2)$ is a Sudha graph with the vertex set $v_1, v_2, v_3, \dots, v_9$ as shown in figure 3.

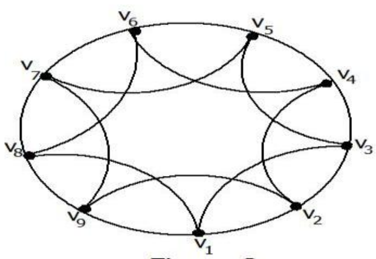

Figure 3.

II. EQUITABLE COLORING OF SUDHA GRID GRAPHS

Thoerem 2.1. *Sudha grid of diamonds $S_d(m,n)$ admit equitable coloring and its chromatic number is either 2 or 3 according to $|m-n| = 0$ (or 2) or $|m-n| > 2$.*

Proof. Sudha grid of diamonds $S_d(m,n)$ is the induced subgraph of the tensor product of the path P_m and the path P_n (for odd $m \geq 3$ and odd $n \geq 3$). The vertices of $S_d(m,n)$ are denoted by $v_{i,j}$, $1 \leq i \leq n, 1 \leq j \leq m$ as shown in figure 4.

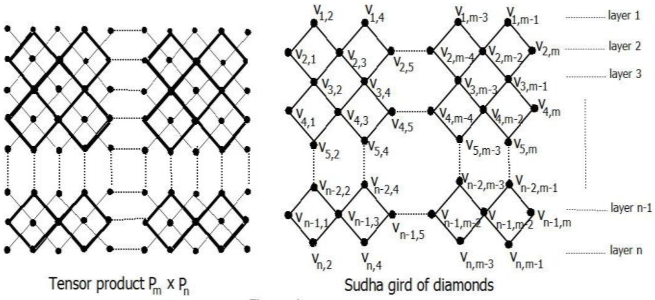

Figure 4

There are two cases :

Case (i) : Let $|m-n| = 0$ or 2.

The function f from the vertex set of $S_d(m,n)$ to the set of colors $\{1,2\}$ is defined as

$$f(v_{i,j}) = \begin{cases} 1, & i \equiv 1 \pmod 2 \\ 2, & i \equiv 0 \pmod 2 \end{cases}$$

The vertices in odd layers are colored with 1 and the even layers are colored with 2 satisfying the condition $||C[1]| - |C[2]|| \leq 1$, since

(i) $|C[1]| = |C[2]| = \frac{mn-1}{4}$ when $m = n$,

(ii) $|C[1]| = \frac{mn+1}{4}$ and $|C[2]| = \frac{mn-3}{4}$ when $m = n-2$,

(iii) $|C[1]| = \frac{mn-3}{4}$ and $|C[2]| = \frac{mn+1}{4}$ when $m = n+2$.

Sudha grid of diamonds $S_d(m,n)$ has equitable coloring with this type of coloring and hence $\chi_=(S_d(m,n)) = 2$ if $|m-n| = 0$ or 2.

Case (ii) : Let $|m-n| > 2$.

There are three types depending on the value of m.

The function f from the vertex set of $S_d(m,n)$ to the set of colors $\{1,2,3\}$ is defined as follows :

Type (a) : Let $m = 1+6j$, $j = 1,2,3,\dots$

The vertices of $S_d(m,n)$ are colored as for i odd, j even,

$$f(v_{i,j}) = \begin{cases} 3, & i \equiv 2 \pmod 6 \\ 1, & i \equiv 4 \pmod 6 \\ 2, & i \equiv 0 \pmod 6 \end{cases}$$

for i even, j odd and $1 < j < m$,

$$f(v_{i,j}) = \begin{cases} 1, & i \equiv 1 \ (mod\ 6) \\ 2, & i \equiv 3 \ (mod\ 6) \\ 3, & i \equiv 5 \ (mod\ 6) \end{cases},$$

$$f(v_{i,1}) = \begin{cases} 1, & i \equiv 2, 0 \ (mod\ 6) \\ 2, & i \equiv 4 \ (mod\ 6) \end{cases}$$

and $$f(v_{i,m}) = \begin{cases} 1, & i \equiv 2, 4 \ (mod\ 6) \\ 2, & i \equiv 0 \ (mod\ 6) \end{cases}$$

The color classes $C[1], C[2]$ and $C[3]$ satisfy the conditions $\big||C[i]| - |C[j]|\big| \leq 1,\ 1 \leq i \leq 3, 1 \leq j \leq 3,$ since

(i) $|C[1]| = |C[2]| = \frac{mn-1}{4}$ when $m = n$,

(ii) $|C[1]| = \frac{mn+1}{4}$ and $|C[2]| = \frac{mn-3}{4}$ when $m = n - 2$,

(iii) $|C[1]| = \frac{mn-3}{4}$ and $|C[2]| = \frac{mn+1}{4}$ when $m = n + 2$.

Sudha grid of diamonds $S_d(m,n)$ has equitable coloring with this type of coloring and hence $\chi_=(S_d(m,n)) = 2$ if $|m - n| = 0$ or 2.

Type (b) : Let $m = 3 + 6j,\ j = 1, 2, 3, \ldots$

The vertices of $S_d(m,n)$ are colored as for i odd, j even,

$$f(v_{i,j}) = \begin{cases} 2, & i \equiv 2 \ (mod\ 6) \\ 1, & i \equiv 4 \ (mod\ 6) \\ 3, & i \equiv 0 \ (mod\ 6) \end{cases}$$

for i even, j odd,

$$f(v_{i,j}) = \begin{cases} 1, & i \equiv 1 \ (mod\ 6) \\ 3, & i \equiv 3 \ (mod\ 6) \\ 2, & i \equiv 5 \ (mod\ 6) \end{cases}$$

The color classes $C[1], C[2]$ and $C[3]$ satisfy the conditions $\big||C[i]| - |C[j]|\big| \leq 1,\ 1 \leq i \leq 3, 1 \leq j \leq 3,$ since $|C[1]| = |C[3]| = \frac{mn-3}{6}$ and $|C[2]| = \frac{mn-3}{6}$.

Sudha grid of diamonds $S_d(m,n)$ has equitable coloring with this type of coloring and hence $\chi_=(S_d(m,n)) = 3$ if $m = 3 + 6j,\ j = 1, 2, 3, \ldots$.

Type (c) : Let $m = 5 + 6j,\ j = 1, 2, 3, \ldots$

The vertices of $S_d(m,n)$ are colored as for i odd, j even,

$$f(v_{i,j}) = \begin{cases} 2, & i \equiv 2 \ (mod\ 6) \\ 3, & i \equiv 4 \ (mod\ 6) \\ 1, & i \equiv 0 \ (mod\ 6) \end{cases}$$

for i even, j odd and $1 < j < m$,

$$f(v_{i,j}) = \begin{cases} 3, & i \equiv 1 \ (mod\ 6) \\ 1, & i \equiv 3 \ (mod\ 6) \\ 2, & i \equiv 5 \ (mod\ 6) \end{cases},$$

$$f(v_{i,1}) = \begin{cases} 3, & i \equiv 2, 0 \ (mod\ 6) \\ 1, & i \equiv 4 \ (mod\ 6) \end{cases},$$

and $$f(v_{i,m}) = \begin{cases} 1, & i \equiv 2 \ (mod\ 6) \\ 2, & i \equiv 4, 0 \ (mod\ 6) \end{cases}.$$

The color classes $C[1], C[2]$ and $C[3]$ satisfy the conditions $\big||C[i]| - |C[j]|\big| \leq 1,\ 1 \leq i \leq 3, 1 \leq j \leq 3$, since

(i) $|C[1]| = |C[2]| = \frac{mn-3}{6}$ and $|C[3]| = \frac{mn+3}{6}$ when $n \equiv 0 \ (mod\ 3)$,

(ii) $|C[1]| = |C[2]| = |C[3]| = \frac{mn-1}{6}$ when $n \equiv 2 \ (mod\ 3)$,

(iii) $|C[1]| = \frac{mn-5}{6}$ and $|C[2]| = |C[3]| = \frac{mn+1}{6}$ when $n \equiv 1 \ (mod\ 3)$.

Sudha grid of diamonds $S_d(m,n)$ has equitable coloring with this type of coloring and hence $\chi_=(S_d(m,n)) = 3$ if $m = 5 + 6j,\ j = 1, 2, 3, \ldots$.

Therefore the equitable chromatic number of $S_d(m,n)$ is either 2 or 3 according to $|m - n| = 0\ (or\ 2)$ or $|m - n| > 2$.

Illustration 2.2.

Consider the graph $S_d(7,5)$. Using theorem 2.1 case (i) we assign the color 1 to the vertices $v_{1,2}, v_{1,4}, v_{1,6}, v_{3,2}, v_{3,4}, v_{3,6}, v_{5,2}, v_{5,4}, v_{5,6}$ and color 2 to the vertices $v_{2,1}, v_{2,3}, v_{2,5}, v_{2,7}, v_{4,1}, v_{4,3}, v_{4,5}, v_{4,7}$ as shown in figure 5.

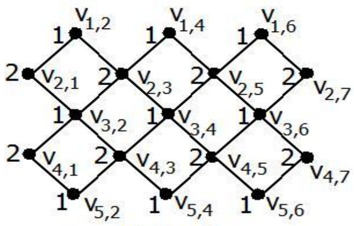

Figure 5

Here $|C[1]| = 9, |C[2]| = 8$ and satisfy the condition $\big||C[1]| - |C[2]|\big| < 1$. This type of coloring on Sudha gird of diamonds $S_d(7,5)$ satisfy the conditions for equitable coloring. Hence $\chi_=(S_d(7,5)) = 2$.

Illustration 2.3

Consider the graph $S_d(13,7)$. Using theorem 2.1 case (ii) type (a) we assign the color 1 to the vertices $v_{1,4}, v_{1,10}, v_{2,1}, v_{2,7}, v_{2,13}, v_{3,4}, v_{3,10}, v_{4,7}, v_{4,13}, v_{5,4}, v_{5,10}, v_{6,1}, v_{6,7}, v_{7,4}, v_{7,10},$ color 2 to the vertices $v_{1,6}, v_{1,12}, v_{2,3}, v_{2,9}, v_{3,6}, v_{3,12}, v_{4,1} v_{4,3}, v_{4,9}, v_{5,6}, v_{5,12}, v_{6,3}, v_{6,9}, v_{7,6}, v_{7,12}$ and color 3 to the vertices $v_{1,1}, v_{1,8}, v_{2,5}, v_{2,11}, v_{3,2}, v_{3,8}, v_{4,5} v_{4,11}, v_{5,2}, v_{5,8}, v_{6,5}, v_{6,11}, v_{6,13}, v_{7,2}, v_{7,8}$ as shown in figure 6.

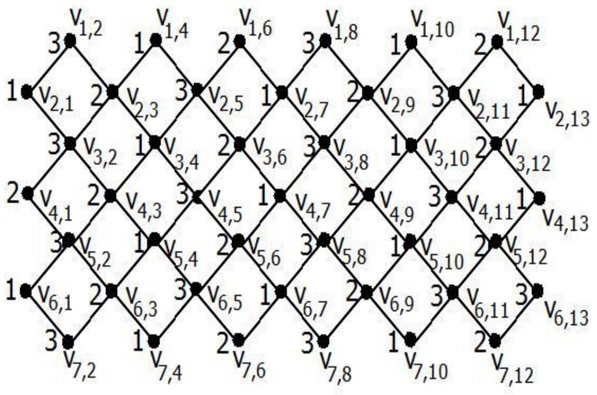

Figure 6

Here $|C[1]| = 15$, $|C[2]| = 15$ and $|C[3]| = 15$, and they satisfy the condition $||C[i]| - |C[j]|| < 1, 1 \le i \le 3$, $1 \le j \le 3$. This type of coloring on Sudha gird of diamond $S_d(13,7)$ satisfy the conditions for equitable coloring. Hence $\chi_=(S_d(13,7)) = 3$.

Theorem 2.4. Sudha grid of hexagons $S_h(m,n)$ admit equitable coloring and its chromatic number is 2.

Proof. Sudha grid of hexagons $S_h(m,n)$ is the induced subgraph of the strong product of the path P_m and the path P_n (for odd $m \ge 3$ and $n \equiv 0\ (mod\ 4)$). The vertices of $S_d(m,n)$ are denoted by $v_{i,j}$, $1 \le i \le n, 1 \le j \le m$ as shown in figure 7.

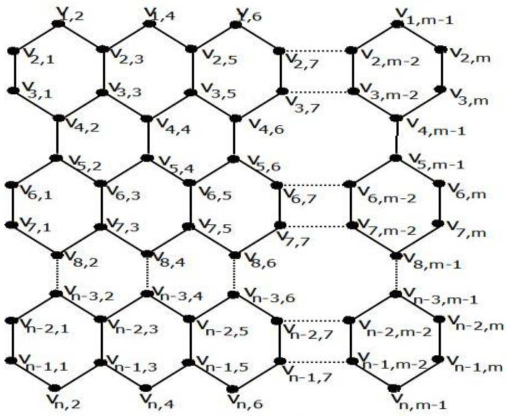

Figure 7

The function f from the vertex set of $S_h(m,n)$ to the set of colors $\{1,2\}$ is defined as

$$f(v_{i,j}) = \begin{cases} 1, & i \equiv 1\ (mod\ 2) \\ 2, & i \equiv 0\ (mod\ 2) \end{cases}$$

The color classes $C[1]$ and $C[2]$ satisfy the condition $||C[1]| - |C[2]|| \le 1$. Sudha grid of hexagons $S_d(m,n)$ has equitable coloring with this type of coloring and hence $\chi_=(S_h(m,n)) = 2$.

Illustration 2.5

Consider the graph $S_h(7,8)$. Using theorem 2.4, we assign the color 1 to the vertices $v_{1,2}, v_{1,4}, v_{1,6}, v_{3,1}, v_{3,3}, v_{3,5}, v_{3,7}, v_{5,2}, v_{5,4}, v_{5,6}, v_{7,1}, v_{7,3}, v_{7,5}, v_{7,7}$ and color 2 to the vertices $v_{2,1}, v_{2,3}, v_{2,5}, v_{2,7}, v_{4,2}, v_{4,4}, v_{4,6}, v_{6,1}, v_{6,3}, v_{6,5}, v_{6,7}, v_{8,2}, v_{8,4}, v_{8,6}$ as shown in figure 8.

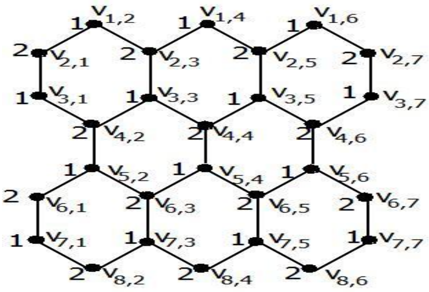

Figure 8

Here $|C[1]| = 14, |C[2]| = 14$ and they satisfy the condition $||C[1]| - |C[2]|| < 1$. This type of coloring on Sudha gird of hexagon $S_h(7,8)$ satisfy the condition for equitable coloring. Hence $\chi_=(S_d(7,8)) = 2$.

III. EQUITABLE COLORING OF SUDHA GRAPH

Theorem 3.1. Sudha graph $S(n,2)$ admits equitable coloring and its chromatic number is either 3 or 4 according to $n \equiv 0\ (mod\ 3)$ or $n \not\equiv 0\ (mod\ 3)$.

Proof. Let $v_1, v_2, v_3, \dots, v_{n-1}, v_n$ be the vertices of the graph $S(n,2)$ and its edges are defined as follows:

for $1 \le i \le n$,

(i) v_i is adjacent to $v_{i+1}$and v_n is adjacent to v_1

(ii) $v_i$is adjacent to v_{i+2} if $i+2 < n$

(iii) v_i is adjacent to v_{i+n-2} if $i+2 \ge n$ as shown in figure 9.

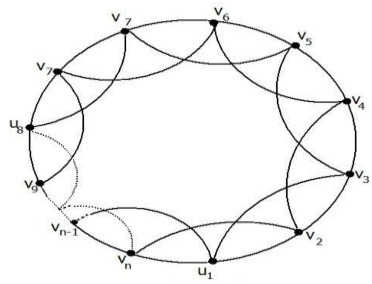

Figure 9

There are three cases :

The function f from the vertex set of $S(n,2)$ to the set of colors $\{1,2,3,4\}$ is defined as follows :

Case (i) : Let $n \equiv 0\ (mod\ 3)$

The vertices of $S(n,2)$ are colored as

$$f(v_i) = \begin{cases} 1, & i \equiv 1\ (mod\ 3) \\ 2, & i \equiv 2\ (mod\ 3) \\ 3, & i \equiv 0\ (mod\ 3) \end{cases}$$

for $1 \le i \le n$

Global Journal of Pure and Applied Mathematics (GJPAM) ISSN 0973-1768 Volume 12,Number 4 (2016)

The color classes $C[1]$, $C[2]$ and $C[3]$ satisfy the condition $||C[i]| - |C[j]|| \leq 1, 1 \leq i \leq 3, 1 \leq j \leq 3,$ since $|C[1]| = |C[2]| = |C[3]| = \frac{n}{3}$.

Sudha graph $S(n,2)$ has equitable coloring with this type of coloring and hence $\chi_{=}(S(n,2)) = 3$ if $n \equiv 0 \ (mod\ 3)$.

Case (ii) : Let n be odd and $n \not\equiv 0 \ (mod\ 3)$

There are two types :

Type (a) : Let $n = 7 + 4j,\ j = 0,1 \ (mod\ 3)$

The vertices of $S(n,2)$ are colored as

$$f(v_i) = \begin{cases} 1, & i \equiv 1 \ (mod\ 4) \\ 2, & i \equiv 2 \ (mod\ 4) \\ 3, & i \equiv 3 \ (mod\ 4) \\ 4, & i \equiv 0 \ (mod\ 4) \end{cases}$$

for $1 \leq i \leq n$.

The color classes $C[1]$, $C[2]$ and $C[3]$ satisfy the condition $||C[i]| - |C[j]|| \leq 1, 1 \leq i \leq 4, 1 \leq j \leq 4,$ since $|C[1]| = |C[2]| = |C[3]| = \frac{n+1}{4}$ and $|C[4]| = \frac{n-3}{4}$

Sudha graph $S(n,2)$ has equitable coloring with this type of coloring and hence $\chi_{=}(S(n,2)) = 4$ if $n = 7 + 4j,\ j = 0,1 \ (mod\ 3)$.

Type (b) : Let $n = 9 + 4j,\ j = 1,2 \ (mod\ 3)$

The vertices of $S(n,2)$ are colored as

$$f(v_i) = \begin{cases} 1, & i \equiv 1 \ (mod\ 4) \\ 2, & i \equiv 2 \ (mod\ 4) \\ 3, & i \equiv 3 \ (mod\ 4) \\ 4, & i \equiv 0 \ (mod\ 4) \end{cases}$$

for $1 \leq i < n - 4$,

$f(v_{n-4}) = 2,$
$f(v_{n-3}) = 3,$
$f(v_{n-2}) = 1,$
$f(v_{n-1}) = 2$
and $f(v_n) = 4$.

The color classes $C[1]$, $C[2]$ and $C[3]$ satisfy the condition $||C[i]| - |C[j]|| \leq 1,\ 1 \leq i \leq 4, 1 \leq j \leq 4,$ since $|C[1]| = |C[3]| = |C[4]| = \frac{n-1}{4}$ and $|C[2]| = \frac{n+3}{4}$.

Sudha graph $S(n,2)$ has equitable coloring with this type of coloring and hence $\chi_{=}(S(n,2)) = 4$ if $n = 9 + 4j,\ j = 1,2 \ (mod\ 3)$.

Case (iii) : Let n be even and $n \not\equiv 0 \ (mod\ 3)$

There are two types :

Type (a) : Let $n = 6 + 4j,\ j = 1,2 \ (mod\ 3)$

The vertices of $S(n,2)$ are colored as

$$f(v_i) = \begin{cases} 1, & i \equiv 1 \ (mod\ 4) \\ 2, & i \equiv 2 \ (mod\ 4) \\ 3, & i \equiv 3 \ (mod\ 4) \\ 4, & i \equiv 0 \ (mod\ 4) \end{cases}$$

for $1 \leq i < n - 1$,

$f(v_{n-1}) = 2$
and $f(v_n) = 3$.

The color classes $C[1]$, $C[2]$ and $C[3]$ satisfy the condition $||C[i]| - |C[j]|| \leq 1,\ 1 \leq i \leq 4, 1 \leq j \leq 4,$ since $|C[1]| = |C[2]| = |C[3]| = |C[4]| = \frac{n}{2}$.

Sudha graph $S(n,m)$ has equitable coloring with this type of coloring and hence $\chi_{=}(S(n,2)) = 4$ if $n = 6 + 4j,\ j = 1,2 \ (mod\ 3)$.

Type (b) : Let $n = 8 + 4j,\ j = 0,2 \ (mod\ 3)$

The vertices of $S(n,2)$ are colored as

$$f(v_i) = \begin{cases} 1, & i \equiv 1 \ (mod\ 4) \\ 2, & i \equiv 2 \ (mod\ 4) \\ 3, & i \equiv 3 \ (mod\ 4) \\ 4, & i \equiv 0 \ (mod\ 4) \end{cases}$$

for $1 \leq i \leq n$.

The color classes $C[1]$, $C[2]$ and $C[3]$ satisfy the condition $||C[i]| - |C[j]|| \leq 1,\ 1 \leq i \leq 4, 1 \leq j \leq 4,$ since $|C[1]| = |C[4]| = \frac{n-2}{4}$ and $|C[2]| = |C[3]| = \frac{n+2}{4}$.

Sudha graph $S(n,2)$ has equitable coloring with this type of coloring and hence $\chi_{=}(S(n,2)) = 4$ if $n = 8 + 4j,\ j = 0,2 \ (mod\ 3)$.

Therefore the equitable chromatic number of $S(n,2)$ is either 3 or 4 according to $n \equiv 0 \ (mod\ 3)$ or $n \not\equiv 0 \ (mod\ 3)$.

Illustration 3.2.

Consider the graph $S(9,2)$. Using theorem 3.1 case (i) we assign the color 1 to the vertices v_1, v_4, v_7, color 2 to the vertices v_2, v_5, v_8 and color 3 to the vertices v_3, v_6, v_9 as shown in figure 10.

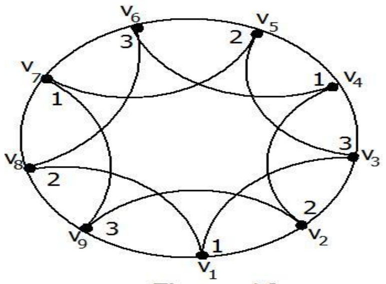

Figure 10

Here $|C[1]| = 3$, $|C[2]| = 3$ and $|C[3]| = 3$. They satisfy the conditions $||C[i]| - |C[j]|| < 1, 1 \leq i \leq 3,$ $1 \leq j \leq 3$. This type of coloring on Sudha graph $S(9,2)$

satisfy the conditions for equitable coloring. Hence $\chi_=(S(9,2)) = 3$.

Illustration 3.3.

Consider the graph $S(17,2)$. Using theorem 3.1 case (ii) type (b), we assign the color 1 to the vertices v_1, v_5, v_9, v_{15} color 2 to the vertices $v_2, v_6, v_{10}, v_{13}, v_{16}$, color 3 to the vertices $v_3, v_7,\ \ v_{11}, v_{14}$ and color 4 for the vertices v_4, v_8, v_{12}, v_{17} as shown in figure 11.

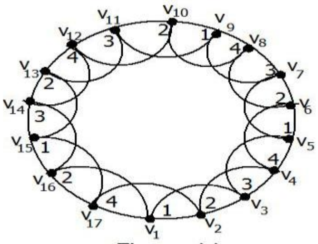

Figure 11

Here $|C[1]| = 4, |C[2]| = 5,\ \ |C[3]| = 4$ and $|C[4]| = 4$. They satisfy the condition $||C[i]| - |C[j]|| < 1, 1 \le i \le 4$, $1 \le j \le 4$. This type of coloring on Sudha graph $S(17,2)$ satisfy the conditions for equitable coloring. Hence $\chi_=(S(17,2)) = 4$.

References

[1] W. Mayer, Equitable coloring, American Mathematical Monthy 80 (1973) P:920-922

[2] Hanna Furmańczyk, Marek Kubale, The Complexity of Equitable Vertex Coloring of Graphs, Journal Of Applied Computer Science Vol. 13. No 2 (2005), P:95-10.

[3] Hanna Furmańczyk, Equitable coloring of graph products, Opuscula Mathematica, Vol. 26, No. 1, 2006.

[4] Hanna Furmanczyk, K. Kaliraj, Marek Kubale, J. Vernold Vivin, Equitable Coloring of Corona Products of Graphs, Advances and Applications in Discrete Mathematics, Vol. 11, No. 2, P:103-120, 2013.

[5] Hanna Furmańczyk, Marek Kubale, Vahan V. Mkrtchyan, Equitable Colorings of Corona Multiproducts of Graphs, arXiv: 1210.6568v1 [cs.DM] 24 Oct 2012.

[6] S. Sudha and G. M. Raja, "Equitable Coloring of Prisms and the Generalized Petersen Graphs," International Journal of Research in Engineering and Technology Vol. 2, 2014, P:105-112 .

[7] Bor. Liang Chen, Ko. Wei Lih, Equitable Coloring of Trees, Journal of Combinatorial Theory, Series B 61, P:83-87 (1994).

[8] Dorothee Blum, Equitable chromatic number of complete multipartite graphs, Millersville University, Millersville, PA 17551.

[9] S. Sudha, K. Manikandan, Total coloring of $S(n,m)$ –graph International Journal of Scientific and Innovative Mathematical Research (IJSIMR) Vol. 2, Issue 1, P:16-22, January – 2014.

Global Journal of Pure and Applied Mathematics (GJPAM) ISSN 0973-1768 Volume 12,Number 4 (2016)

Simulation of two-sided deep cavity flows by lattice Boltzmann Multi-Relaxation-Time Model

D. Arumuga Perumal
Department of Mechanical Engineering,
National Institute of Technology Karnataka,
Surathkal, Mangalore, India – 575 025
Email: perumal@nitk.edu.in

***Abstract*—The present work discusses the characteristics of incompressible viscous flow within a two-sided lid-driven cavity with its two opposite walls moving with a uniform velocity in parallel and antiparallel direction by multi-relaxation-time lattice Boltzmann technique. It is realized that, single-relaxation-time lattice Boltzmann technique have numerous deficiencies. Other than the single-relaxation-time technique, the multi-relaxation-time technique, which has certain points of interest, is additionally utilized. The attributes of the present flow problem are investigated for various Reynolds number furthermore for various aspect ratios. Accurately, the impact of Reynolds number and aspect ratio on the flow pattern and in addition on the strengths of vortices inside the cavity is examined. The Reynolds number effect on the flow structure is virtually manifested with the aid of the streamlines and velocity profiles.**

Keywords— lattice Boltzmann technique; single-relaxation-time; multi-relaxation-time; two-dimensional lid-driven cavity; D2Q9 model.

I. INTRODUCTION

In the area of Computational Fluid Dynamics (CFD), two important approaches to simulate fluids have been developed in the last few decades. First, the classical approach is based on the numerical solutions of the Navier-Stokes equations [1]. Alternatively, Navier-Stokes equation in continuum theory can be derived from the Boltzmann equation in the limit of small Knudsen numbers [2]. Recently, the Lattice Boltzmann technique based on Boltzmann equation has emerged as a new and effective numerical approach of CFD and it has achieved considerable success in simulating fluid flows [3]. Numerous extensions in the past few years have made the lattice Boltzmann technique used for a wide range of problems including thermal flows, porous media, magneto-hydrodynamics, vortex dynamics, turbulent flows, multi-phase flows, free-surface flows, fluid-structure interactions, visco-elastic fluids, particulate suspensions and other complex fluids [4].

Many of the LBM works published so far reveals a plethora of issues concerning single-relaxation-time Lattice Boltzmann technique (LBT-SRT) and its applicability to incompressible viscous flows in particular [5]. It is also known that, the simple and popular incompressible SRT-LBM has few shortcomings. In the LBT-SRT model formulation, both the bulk and shear viscosities are determined by the same relaxation time. Mainly, in LBT-SRT model the relaxation time equal to 0.5 is the critical value for ensuring a non-negative kinematic viscosity. Numerical instability can be expected in LBT-SRT model for relaxation time close to this critical value. It is also known that, the LBT-SRT model can be improved in terms of stability, computational efficiency by using Multi-relaxation-time Lattice Boltzmann technique (LBT-MRT) [6].

Lallemand and Luo [7] showed the robustness of the Multi-Relaxation-Time Lattice Boltzmann method (LBT-MRT) and presented high accuracy results and numerical stability of high Reynolds numbers. They have performed the detailed theoretical analysis on the dispersion, dissipation and stability characteristics of a generalized Lattice Boltzmann Equation model proposed by d'Humieres [8]. It is known that, the flow in a cavity driven by the steady motion of a lid is a classical bench mark problem in fluid mechanics [9]. A few researchers have carried out simulations of the single-sided lid-driven cavity flows using LBT-MRT [10]. Detailed study of two-sided lid-driven deep cavity as to how they grow with increasing Reynolds number has not yet been made by LBT-MRT. Therefore, to demonstrate the ability of the lattice Boltzmann equation with multi-relaxation-time model we simulate the two-dimensional cavity problems such as single-sided lid-driven square cavity flow, two-sided lid-driven square cavity flow and two-sided lid-driven rectangular cavity flow.

The organization of the rest of this paper is as follows. In Section 2, Multi-Relaxation-Time Lattice Boltzmann Method is described in some detail. In Section 3 the two-sided lid-driven cavity problem is described and the results with parallel and antiparallel motion of the walls for different aspect ratios are presented in detail. Concluding remarks are made in Section 4.

This paper was presented by the author in the National Conference on *Advances in Mathematics and its Applications to Science and Engineering* (AMASE-2016) conducted in Department of Mathematics, University College of Engineering Pattukkottai, Thanjavur, Tamil Nadu, India, on 22nd January 2016.

II. LBT MULTI-RELAXATION-TIME

Most of the Lattice Boltzmann technique works published concerning with the Lattice Bhatnagar-Gross-Krook (LBGK) model because of its simplicity [2]. Only a few works used LBT-MRT to predict fluid flow parameters. For simulating 2D flows a D2Q9 square lattice model is used and the discrete particle velocities are represented as $\left\{ \boldsymbol{c_i} \middle| i = 0, 1, ..., N \right\}$ and the particle distribution function is represented as $\left\{ f_i(\mathbf{x}, t) \middle| \; i = 0, 1, ..., N \right\}$. The discretized particle distribution function in a vector space $\underline{R}$ can be written as [10]

$$\left| f_i(\mathbf{x}_i, t_n) \right\rangle = \left\{ f_0(\mathbf{x}_i, t_n),\; f_1(\mathbf{x}_i, t_n), ..., f_N(\mathbf{x}_i, t_n) \right\}^T \quad (1)$$

The Multi-Relaxation-Time Lattice Boltzmann technique (LBT-MRT) evolution equation can be written in discretized form [10]

$$\left| f_i(\mathbf{x}_i + \boldsymbol{c}_i \Delta t, t_n + \Delta t) \right\rangle - \left| f_i(\mathbf{x}_i, t_n) \right\rangle = -M^{-1} \underline{S} \left(\left| m_i(\mathbf{x}_i, t_n) \right\rangle - \left| m_i^{eq}(\mathbf{x}_i, t_n) \right\rangle \right) \quad (2)$$

where $\underline{S}$ is the diagonal matrix, M for the *D2Q9* square lattice model is a 9×9 transformation matrix that linearly transforms the velocity distribution functions f_i to the macroscopic moments. The moments for the two-dimensional *D2Q9* square lattice model are given as $\left| m_i \right\rangle = (\rho, e, \varepsilon, j_x, q_x, j_y, q_y, p_{xx}, p_{xy})^T$. Here ρ is the fluid density, e is the energy, ε is related to square of energy, j_x and j_y are the momentum density (mass flux), q_x and q_y are the energy flux, p_{xx} and p_{xy} correspond to the diagonal and off-diagonal component of the viscous stress tensor. Diagonal matrix ($\underline{S}$) can be written as $\underline{S} = (0, s_2, s_3, 0, s_5, 0, s_7, s_8, s_9)$. It is known that for the LBT-MRT model if we set $s_8 = s_9 = \frac{1}{\tau}$ then we can get same viscosity formula for the LBT-SRT model. In LBT-MRT model it is more flexible to chose the rest of the relaxation parameters such as s_2, s_3, s_5, s_7. In general these parameters can be chosen to be slightly larger than unity. Another important point, is to recover LBT-SRT model results we can set LBT-MRT model parameters such as $s_2, s_3, s_5, s_7, s_8, s_9 = \frac{1}{\tau}$. The transformation matrix M can be written as

$$M = \begin{pmatrix} 1 & 1 & 1 & 1 & 1 & 1 & 1 & 1 & 1 \\ -4 & -1 & 2 & -1 & 2 & -1 & 2 & -1 & 2 \\ 4 & -2 & 1 & -2 & 1 & -2 & 1 & -2 & 1 \\ 0 & 1 & 1 & 0 & -1 & -1 & -1 & 0 & 1 \\ 0 & -2 & 1 & 0 & -1 & 2 & -1 & 0 & 1 \\ 0 & 0 & 1 & 1 & 1 & 0 & -1 & -1 & -1 \\ 0 & 0 & 1 & -2 & 1 & 0 & -1 & 2 & -1 \\ 0 & 1 & 0 & -1 & 0 & 1 & 0 & -1 & 0 \\ 0 & 0 & 1 & 0 & -1 & 0 & 1 & 0 & -1 \end{pmatrix} \quad (3)$$

The present *D2Q9* square lattice model used here has nine discrete particle velocities. Each node of which has eight neighbours connected by eight links and a rest particle at centre as shown in Figure 1. The particle velocities are defined as [11]

$$\begin{aligned} c_i &= 0, \quad i = 0 \\ c_i &= (\cos(\pi/4(i-1)), \sin(\pi/4(i-1))), \quad i = 1, 2, 3, 4 \\ c_i &= \sqrt{2}(\cos(\pi/4(i-1)), \sin(\pi/4(i-1))), \; i = 5, 6, 7, 8. \end{aligned} \quad (4)$$

The macroscopic quantities such as density ρ and momentum density $\rho\boldsymbol{u}$ are defined as velocity moments of the distribution function f_i as follows:

$$\rho = \sum_{i=0}^{N} f_i, \quad (5)$$

$$\rho\boldsymbol{u} = \sum_{i=0}^{N} f_i \boldsymbol{c_i} \quad (6)$$

The density is determined from the particle distribution function. The macroscopic density and the velocities satisfy the Navier-Stokes equations in the low-Mach number limit. This can be demonstrated by using the Chapman-Enskog expansion. In the present nine-speed square lattice model, a suitable equilibrium distribution function that has been proposed is [11]

$$\begin{aligned} f_i^{(0)} &= \rho w_i \left[1 - \frac{3}{2}\boldsymbol{u}^2 \right], \; i = 0 \\ f_i^{(0)} &= \rho w_i \left[1 + 3(\boldsymbol{c_i}.\boldsymbol{u}) + 4.5\,(\boldsymbol{c_i}.\boldsymbol{u})^2 - 1.5\,\boldsymbol{u}^2 \right], \; i = 1, 2, 3, 4 \\ f_i^{(0)} &= \rho w_i \left[1 + 3(\boldsymbol{c_i}.\boldsymbol{u}) + 4.5\,(\boldsymbol{c_i}.\boldsymbol{u})^2 - 1.5\,\boldsymbol{u}^2 \right], \; i = 5, 6, 7, 8 \end{aligned} \quad (7)$$

where the lattice weights are given by $w_0 = 4/9,\; w_1 = w_2 = w_3 = w_4 = 1/9$ and $w_5 = w_6 = w_7 = w_8 = 1/36.$ The relaxation time is related to the viscosity by [11]

$$\tau = \frac{6\upsilon + 1}{2} \quad (8)$$

where υ is the kinematic viscosity measured in lattice units. The implementation of the boundary condition for the LBT-MRT model is the same as the LBT-MRT. At a boundary point, the particle distribution functions along all inward directions are determined by the bounce-back rule. To ensure the no-slip boundary condition ($\boldsymbol{U}$ = 0) on the wall, Yu *et al.* [3] suggested a improved bounce-back boundary condition using a linear interpolation formula

$$f_{\tilde{i}}(\mathbf{x}_w) = f_{\tilde{i}}(\mathbf{x}_w) + \frac{\Delta}{1+\Delta}\left(f_{\tilde{i}}(\mathbf{x}_f + \boldsymbol{c}_i) - f_{\tilde{i}}(\mathbf{x}_w) \right) \quad (9)$$

The above boundary condition is valid for both $\Delta < 0.5$ and $\Delta \geq 0.5$. For a moving wall they added additional momentum [3]

$$f_{\tilde{i}}(\mathbf{x}_W, t+\Delta t) = f_i(\mathbf{x}_\mathbf{W}, t+\Delta t) + 2w_i \rho \frac{3}{c^2} \boldsymbol{c}_i . \boldsymbol{u}_\mathbf{W} \quad (10)$$

where $f_{\tilde{i}}$ indicates post-collision state. For the moving wall, uniform plate velocity $\boldsymbol{U}$ = 0.1, considering the validity of using Lattice Boltzmann technique in simulating incompressible flows. The LBT-MRT is solved in the solution domain subjected to the above initial and boundary conditions on a uniform two-dimensional lattice structure.

A. Code Validation

In order to validate the developed 2D incompressible viscous flow algorithm, the present LBT-MRT code is first applied to the single-sided lid-driven square cavity flow problem. The configuration of single-sided lid-driven cavity flow considered here consists of a two-dimensional square cavity whose top plate moves from left to right with constant velocity U = 0.1, while the other three cavity wall boundaries are fixed. The present simple geometry makes ideal to study and analyze the behaviour of vortices in closed boundary domains. It is known that, the fundamental characteristics of the single-sided lid-driven cavity flow are the emergence of a large primary vortex in the centre of a cavity and of secondary vortices in the lower two bottom cavity corners. The Reynolds number is defined $Re = UL/\nu$ where L is the height or width of the cavity and ν is the kinematic viscosity. In the present work, the lattice size of 181 x 181 is used for Re = 1000. Figure 2 depicts the streamline pattern at Re = 1000 obtained through LBM-MRT code, which closely resembles those given by other researchers [2, 9, 10, 11]. Particularly, an excellent agreement can be found between the present LBT-MRT model and the benchmark results of Ghia *et al.* [12].

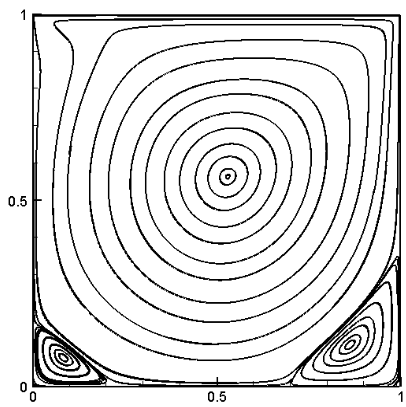

Figure 2: Streamline pattern for the single-sided square cavity flow for Re = 1000.

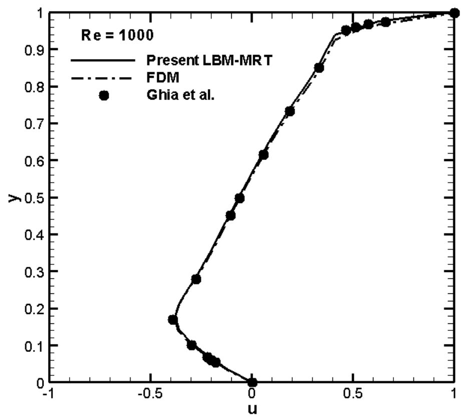

(a)

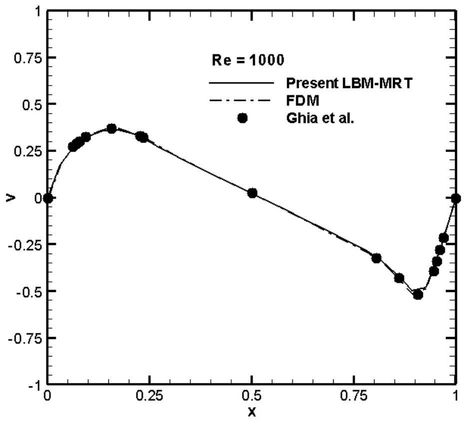

(b)

Figure 3: Code validation: (a) u-velocity along vertical centreline and (b) v-velocity along horizontal centreline for single-sided lid-driven square-cavity (Re = 1000).

Figure 3(a) shows the u-velocity distribution along the vertical centreline, 3(b) shows the v-velocity distribution along the horizontal centreline, compared with Ghia's results [12] and FDM results [1]. It can be seen that the present LBM-MRT model result agrees very well with existing results of Ghia *et al.* [12] and Perumal & Dass [11]. The present results conclude that the present LBT-MRT model can be extended to two-dimensional two-sided incompressible viscous flow without increasing computational efficiency.

III. TWO-SIDED LID-DRIVEN CAVITY FLOW

The classical single-sided lid-driven cavity problem has been extended to two-sided lid-driven cavity problem by two facing walls moving in the same (or) opposite directions [1]. In the parallel wall motion we consider, both the upper and lower facing walls moving from left to right in the x direction with the same velocity of $\boldsymbol{U}$ = 0.1. In the antiparallel wall motion the lower and upper facing walls moving in opposite directions along the x-axis with the same velocity of $\boldsymbol{U}$ = 0.1. All the results presented in the paper are independent of the lattice size and they are substantiated carefully. The boundary conditions for the parallel and antiparallel wall motion are shown in Figures 4 (a) and (b).

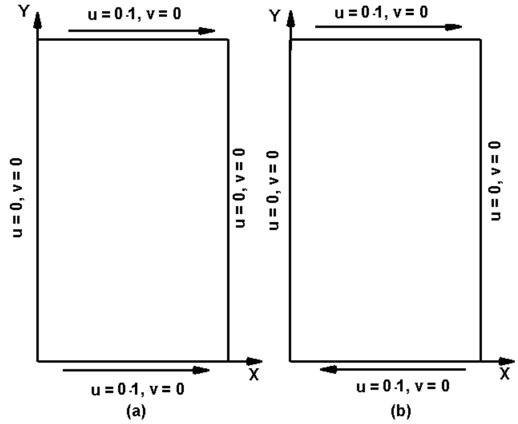

Figure 4: Two-sided lid-driven cavity for (a) parallel wall motion (b) antiparallel wall motion with boundary conditions.

B. Parallel Wall Motion

C. Square Cavity Flow

In the present section, the two-sided lid-driven square cavity for the case of upper and lower facing walls moving in same direction along the *x*-axis with Reynolds number increasing from *Re* = 10 to 1500 using LBT-MRT model on a 161×161 lattice arrangement is studied. Figure 5 shows the streamlines are symmetrical with respect to a line parallel to facing walls and passing through the cavity centre for all Reynolds numbers.

At *Re* = 10, it is observed that a pair of primary re-circulating vortices formed at the lower and upper cavities and form a free shear layer in between. At *Re* = 500, besides the pair of primary vortices, a pair of smaller counter-rotating vortices symmetrically placed about the horizontal centreline near the centre of the right cavity wall. It is also observed that, with the increase in Reynolds number (*Re* = 1500) the primary vortex cores moves towards the centres of the top and bottom halves of the lid-driven cavities and these pair of secondary vortices grow in size.

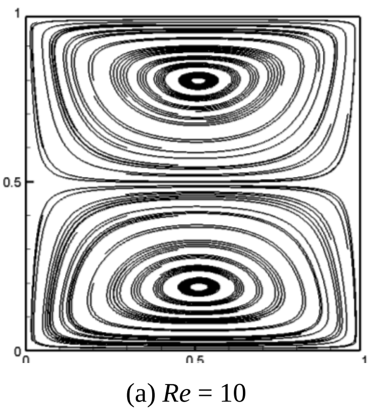

(a) *Re* = 10

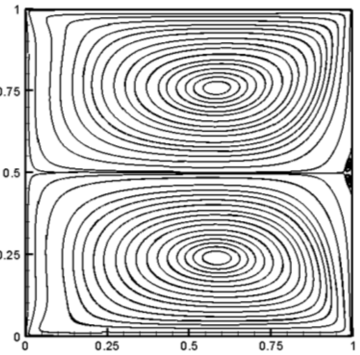

(b) *Re* = 500

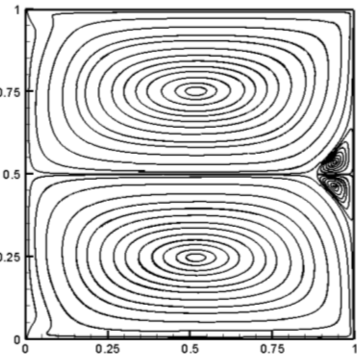

(c) *Re* = 1500

Figure 5: Streamline patterns of double-sided square cavity with parallel wall motion for different Reynolds numbers.

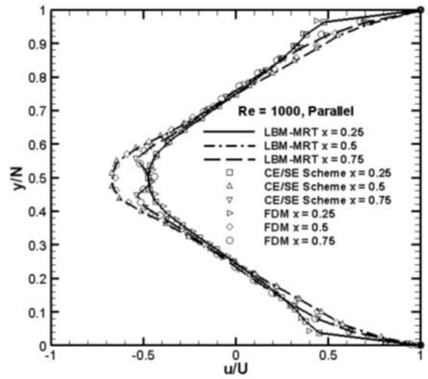

(a)

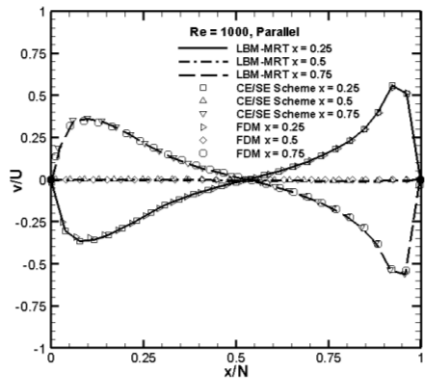

(b)

Figure 6: Parallel wall motion, *Re* = 1000: (a) horizontal velocity *u* along vertical lines (b) vertical velocity *v* along horizontal lines passing through *y* = 0.25, 0.50 and 0.75.

Figures 6 shows the comparison of horizontal velocity profiles along vertical lines and vertical velocity profiles along horizontal lines passing through different points of the two-sided lid-driven square cavity (parallel wall motion) for various Reynolds numbers. Agreement of the velocity profiles given by present LBT-MRT model with those given by the FDM [1] and CE/SE Scheme [13] is excellent. All these results show that the agreement is very good, which further substantiates the accuracy of the present LBT-MRT computations.

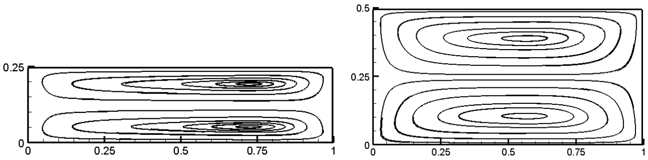

(a) *K* = 0.25 (b) *K* = 0.50

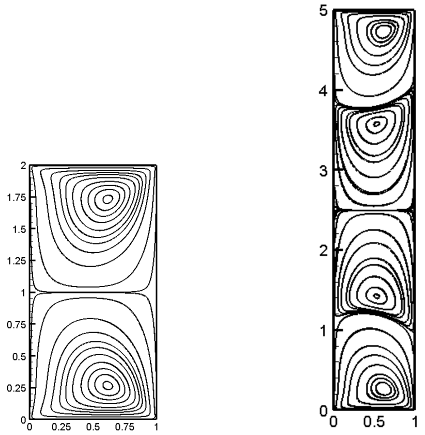

(c) *K* = 2.0 (d) *K* = 5.0

Figure 7: Streamline patterns of *Re* = 10 for double-sided parallel wall motion with different Aspect ratios (a) *K* = 0.25, (b) *K* = 0.50, (c) *K* = 2.0 and (d) *K* = 5.0.

D. Aspect Ratio Effect

To study the aspect ratio effect, low to high aspect ratios of *K* = 0.25, 0.5, 2.0 and 5.0 is considered. It is known that, both walls move in same direction, it can generate their own primary vortex. As aspect ratio *K* increases from 0.25 to 5.0, a sequence of streamline patterns is obtained for Reynolds numbers *Re* = 10, 500 and 1500 as shown in Figures 7-9. Figures 7 (a), (b), (c) and (d) respectively show the streamline patterns of *Re* = 10 where the aspect ratios *K* = 0.25, 0.5, 2.0 and 5.0. At low Reynolds number *Re* = 10 for different aspect ratios *K* the following observations are made. It is seen that, at all aspect ratios the streamlines are symmetrical with respect to a line parallel to facing walls and passing through the cavity centre.

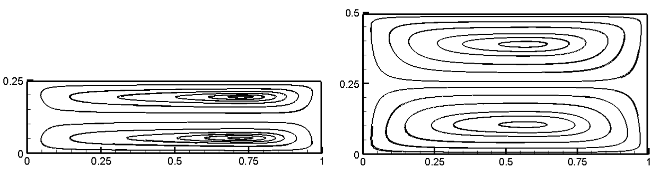

(a) *K* = 0.25 (b) *K* = 0.50

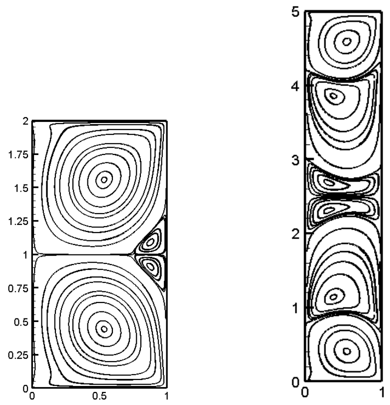

(c) *K* = 2.0 (d) *K* = 5.0

Figure 8: Streamline patterns of *Re* = 500 for double-sided parallel wall motion with different Aspect ratios (a) *K* = 0.25, (b) *K* = 0.50, (c) *K* = 2.0 and (d) *K* = 5.0.

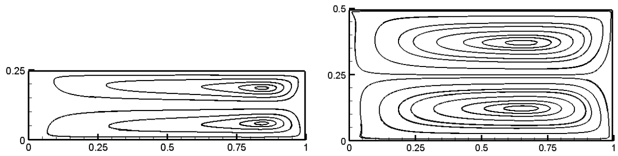

(a) *K* = 0.25 (b) *K* = 0.50

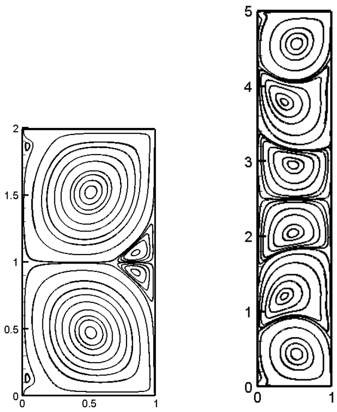

(c) *K* = 2.0 (d) *K* = 5.0

Figure 9: Streamline patterns of *Re* = 1500 for double-sided parallel wall motion with different Aspect ratios (a) *K* = 0.25, (b) *K* = 0.50, (c) *K* = 2.0 and (d) *K* = 5.0.

At *K* = 0.25, two primary vortices appear in the right corner of the cavity. With the increase of aspect ratio from 0.25, the primary vortices centre shifts from the top-right corner towards the geometric centre of the cavity. At high aspect ratio of *K* = 5.0, four primary vortices are generated due to motion of upper and lower facing walls. Figure 8 depicts the moderate Reynolds number of *Re* = 500 for different aspect ratios. Figure 9 depicts the high Reynolds number of *Re* = 1500 for different aspect ratios. As aspect ratio increases the vortices strength also increases.

E. Antiparallel Wall Motion

F. Square Cavity Flow

The streamline patterns for the two-sided lid-driven square cavity for the case of upper and lower facing walls move in the opposite direction with Reynolds number increasing from *Re* = 10 to 1500 using LBT-MRT model on a 161×161 lattice arrangement are shown in Figure 10. From the Figures it is observed that, a single primary vortex centred at the geometric centre of the cavity is formed at low Reynolds numbers. The streamline patterns for *Re* = 1500 are shown in Figures 10(c).

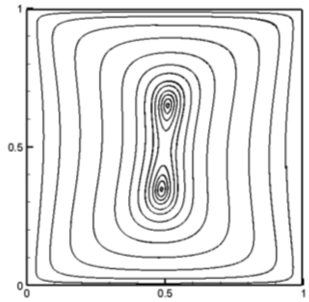

(a) *Re* = 10

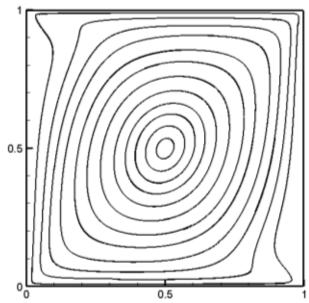

(b) *Re* = 500

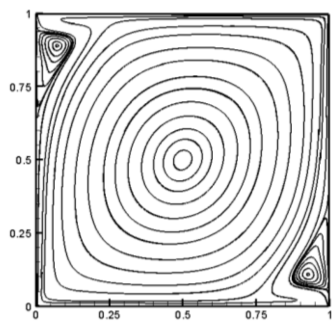

(c) *Re* = 1500

Figure 10: Streamline patterns of two-sided square cavity with antiparallel wall motion for different Reynolds numbers.

The increased Reynolds number results in the appearance of two secondary vortices near the top left and the bottom right corners of the lid-driven cavity and a very small shift of the primary vortex centre from the geometric centre of the cavity. It is also seen that, as the Reynolds number increases, the strength of the two secondary vortices near the top left and the bottom right corners of the cavity also increase in size. Figures 11 shows the comparisons of horizontal velocity profiles along vertical lines and vertical velocity profiles along horizontal lines passing through different points of the double-sided lid-driven square cavity (antiparallel wall motion) for the various Reynolds numbers and the agreement is excellent once again. It is seen that, the LBT-MRT model results given by all the figures and tables are in excellent agreement with those given by the FDM [1] and CE/SE Scheme [13]. This lends credibility to the present LBT-MRT model results for double-sided lid-driven square cavity with antiparallel wall motion problem.

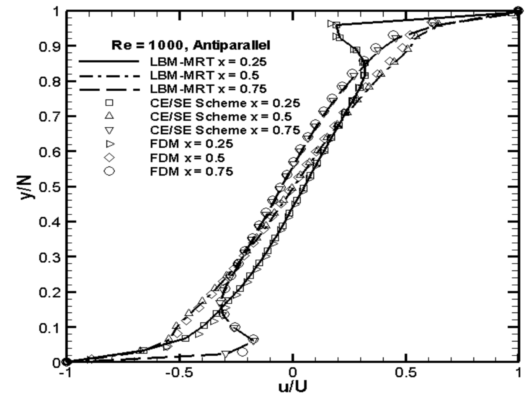

(a)

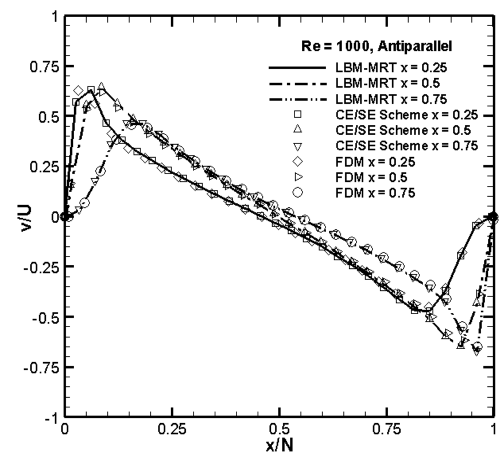

(b)

Figure 11: Antiparallel wall motion, *Re* = 1000: (a) horizontal velocity *u* along vertical lines (b) vertical velocity *v* along horizontal lines passing through *y* = 0.25, 0.50 and 0.75.

G. Aspect Ratio Effect

To study the aspect ratio effect, low to high aspect ratios of *K* = 0.25, 0.5, 2.0 and 5.0 is considered. Figures 12 (a), (b), (c) and (d) respectively show the streamline patterns of *Re* = 10 where the aspect ratios *K* = 0.25, 0.5, 2.0 and 5.0. From Figure 12, it is found that the flow structure inside the cavity changes considerably with the aspect ratio. Here, the near-wall primary vortices have the same sense of rotation and are well-separated as the aspect ratio is large. Figure 13 depicts the moderate Reynolds number of *Re* = 500 for different aspect ratios. Figure 14 depicts the high Reynolds number of *Re* = 1500 for different aspect ratios. It is seen that, as aspect ratio increases the vortices strength also increases.

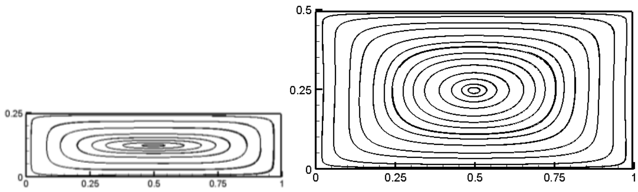

(a) K = 0.25 (b) K = 0.50

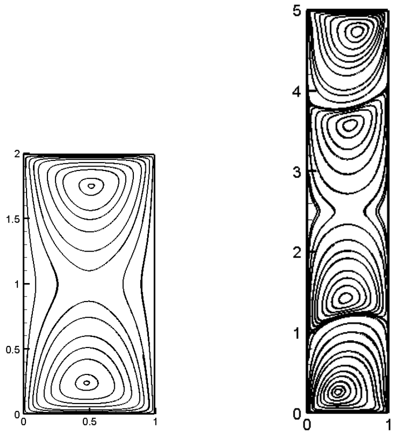

(c) K = 2.0 (d) K = 5.0

Figure 12: Streamline patterns of Re = 10 for two-sided antiparallel wall motion with different Aspect ratios (a) K = 0.25, (b) K = 0.50, (c) K = 1.0, (d) K = 2.0 and (e) K = 5.0.

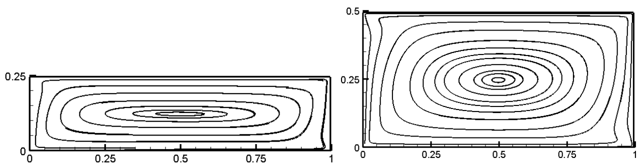

(a) K = 0.25 (b) K = 0.50

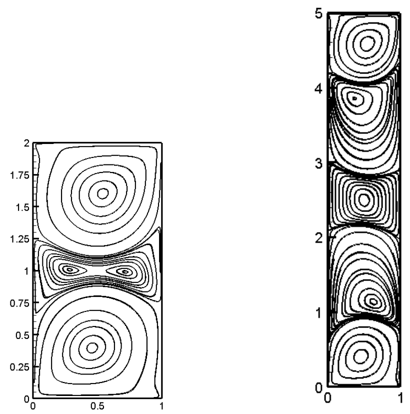

(c) K = 2.0 (d) K = 5.0

Figure 13: Streamline patterns of Re = 500 for two-sided antiparallel wall motion with different Aspect ratios (a) K = 0.25, (b) K = 0.50, (c) K = 1.0, (d) K = 2.0 and (e) K = 5.0.

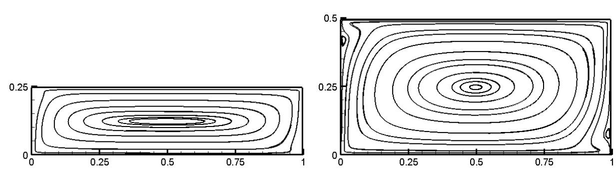

(a) K = 0.25 (b) K = 0.50

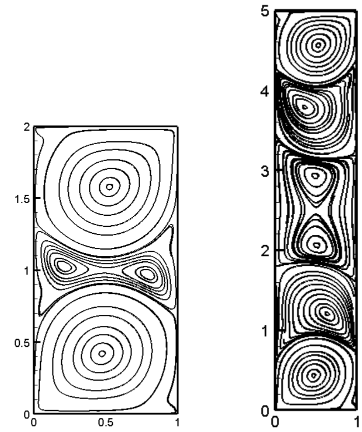

(c) K = 2.0 (d) K = 5.0

Figure 14: Streamline patterns of Re = 1500 for two-sided antiparallel wall motion with different Aspect ratios (a) K = 0.25, (b) K = 0.50, (c) K = 1.0, (d) K = 2.0 and (e) K = 5.0.

All of our computations are carried out on a Pentium 4-based PC with 512 MB RAM.

IV. CONCLUSION

In the present work, the flow in the two-sided lid-driven cavity for the parallel and antiparallel wall motion is numerically investigated using lattice Boltzmann technique with multi-relaxation-time (LBT-MRT) model. For the first geometry, namely, the single-sided lid-driven square cavity, some experimental, numerical and theoretical results exists, by reproducing which with the LBT-MRT model an insight about the appropriateness of the present boundary conditions was gained. This knowledge is then utilized when applying the LBT-MRT model to compute flows in the second geometry, namely, a two-sided lid-driven square cavity flows. The present computations not only confirms the flow features of the problem, but also reveals the effects of Reynolds number and the aspect ratio on the flow structure in the two-sided lid-driven deep cavity in a systematic way. Consequently these results, like those of the single lid-driven deep cavity flow, may be used for validating the algorithms for computing steady flows governed by the two-dimensional incompressible Navier-Stokes equations. To sum up, the present study reveals many interesting features of single-sided and two-sided lid-driven cavity flows and demonstrates the capability of the LBT-MRT model to capture these features.

REFERENCES

[1] D.A. Perumal, and A.K. Dass, "*Simulation of Incompressible flows in two-sided lid-driven square cavities – FDM"*, CFD Letters, Vol. 2(1), pp. 13-24, 2010.

[2] D.A. Perumal, and A.K. Dass, "*Simulation of Incompressible flows in two-sided lid-driven square cavities – LBM"*, CFD Letters, Vol. 2(1), pp. 25-38, 2010.

[3] D. Yu, R. Mei, L.S. Luo and W. Shyy, *"Viscous flow computations with the method of lattice Boltzmann equation"*, Progress in Aerospace Sciences, Vol. 39, pp. 329-367, 2003.

[4] D.A. Perumal, and A.K. Dass., "*Application of Lattice Boltzmann Method for Incompressible viscous flows"*, Applied Mathematical Modelling, Vol. 37(6), pp. 4075-4092, 2013.

[5] P.J. Dellar, "*Incompressible limits of Lattice Boltzmann equations using multiple relaxation times",* Journal of Computational Physics, *Vol.* 190, pp. 351-370, 2003.

[6] R. Du, B. Shi, X. Chen, "*Multi-relaxation-time lattice Boltzmann model incompressible flow",* Physics Letters A, Vol. 359, pp. 564-572, 2006.

[7] P. Lallemand, and L.S. Luo, "*Theory of the lattice Boltzmann method: dispersion, dissipation, isotropy, Galilean invariance, and stability"*, Physical Review E, Vol. 61, pp. 6546-6562, 2000.

[8] D. d'Humieres, "*Generalized lattice Boltzmann equation, in rarefied gas dynamics: theory and simulations"*, Progress in Astronautics and Aeronautics, Edited by B.D. Shizgal and D.P. Weaver, AIAA, D.C. Washington, Vol. 159, pp. 450-458, 1992.

[9] P.N. Shankar, and M.D. Deshpande, "*Fluid mechanics in the driven cavity"*, Annual Review of Fluid Mechanics, Vol. 32, pp. 93-136, 2000.

[10] J.-S. Wu, and Y.-L. Shao, "*Simulation of lid-driven cavity flows by parallel lattice Boltzmann method using multi-relaxation-time scheme",* International Journal of Numerical Methods in Fluids, Vol. 46, pp. 921–937, 2004.

[11] D.A. Perumal, and A.K. Dass, "*Multiplicity of steady solutions in two-dimensional lid-driven cavity flows by lattice Boltzmann method",* Computers & Mathematics with Applications, Vol. 61(12), p. 3711-3721, 2011.

[12] U. Ghia, K.N. Ghia, C.T. Shin, "*High-Re solutions for incompressible flow using Naiver-Stokes equations and a multigrid method"*, Journal of Computational Physics, Vol. 43, pp. 387-441, 1982.

[13] D-X. Yang and Zhang De-Liang, "*Applications of the CE/SE scheme to imcompressible flows in two-sided lid-driven square-cavities"*, Chinese Physics Letters, Vol. 29(8), p. 084717- 1-5, 2012.

Global Journal of Pure and Applied Mathematics (GJPAM) ISSN 0973-1768 Volume 12,Number 4 (2016)

Fatigue behavior of AZ31B Magnesium alloy in FSW joints

R. Manikandan
Department of Mechanical Engineering,
University College of Engineering Pattukkottai
Tamil Nadu, India.
Email: mani131990@gmail.com

*G. Elatharasan**
Department of Mechanical Engineering,
University College of Engineering Pattukkottai,
Tamil Nadu, India.
Email: elatharasan@yahoo.co.in

Abstract- **FSW of a weldment joints often required different structure and assembled structures. FEA model to moderate the experimental structures but it will only base on varies stress states. FEA, now a days most widely used upon a traditional approaches in modern engineering. The main Purpose of this research work is Friction stir welding (FSW) of weldment joints, to investigate the effect of cyclic loading condition and life time feasibility of the AZ31B magnesium alloy with thickness 3 mm. This criteria of fatigue analysis has done by using Finite Element Method. A 3D model plotted in Ansys workbench and design of experiment was carried out and investigate the effect of different parameters such fatigue life, force, stress life etc. Simulation results has a good agreement with the theoretical results for the cyclic loading conditions. This analysis of a model deformation well suited for the fatigue behavior. The fatigue strength of 106 cycles and alternating stress around 160 Mpa for axial loading conditions. The deformation of loading condition on fully reversed state and good relation with the soderberg approaches. Design of experiment has done by the analysis in ansys 14.5. This effect of causes to enhanced with the relationship between the input and output parameters. It can be the results of response surfaces good agreement with the structural results.**

Keywords-Fatigue, FSW, FEM, Soderberg, AZ31B Magnesium

I. INTRODUCTION

Friction stir welding is a solid state welding process and it generate enough yield strength of the various similar and dissimilar alloys [1, 2]. This investigation described the modeling and optimization of a similar alloys as various optimized parameters. Magnesium (AZ31B Mg) is a demand material in engineering materials. It has density of 1.74 g/cm3, lighter than aluminium density of 2.74 g/cm3, and more than four times lighter than steel density of 7.86 g/cm3 [3]. This magnesium alloys has high strength and low weight compare to other than materials. It has good vibrating characteristics and high specific strength, high corrosion resistance, good mechanical properties, and very economically. Now a day's lot of research was done on with magnesium alloys. This measurement of elastic plastic strain to investigate the ductility of the material [4, 5]. Most of the analysis to create a high strength material combinations. Mackenzie, reported as a dynamic and static recrystallization of magnesium alloys [5-7]. Ogarrevic and Stephens have established the fatigue data between the year 1923 and 1990 [8]. These alloys of fatigue behavior to affect the shape and size of the standard size

Specimen. [9-10]. Mechanical properties of AZ31B Mg as shown in table 1.

Yield strength(N/mm^2)	**Ultimate Tensile Strength(N/mm$^{2)}$**	**Elongation (%)**	**Hardness at load 0.05 kg**
212	267	8	77

Table 1. Mechanical properties of AZ31B Mg alloy

Fatigue is an important issue for a subjected to repeat cyclic loading conditions of an indeterminate structures. Any products need a fatigue life, it does a historical primary consideration of the robust designs [12-16]. This type of design to required depending upon the enormous range of limitations as surface finish, size, type of loading, temperature, corrosive, and other aggressive environments, mean stresses, residual stresses, and stress concentrations [11]. Additional factors influencing S-N behavior such as Microstructure, Size Effects, Surface Finish, and Frequency. Simultaneously microstructure includes chemistry, heat treatment, cold working, grain size, anisotropic, inclusions, voids/porosity, and other discontinuities or imperfections. Generally fatigue limits based an alternating stress [17, 18]. This alternating stress may vary as nature of polishing 180 Mpa, axial load 160 Mpa etc. That range from 1 to 70 % does lie in the largest tensile strength. Most of the product life to chosen S-N curve approaches compare to other than two approaches [19, 20]. The mean stress is an essential part of the S-N curve, it may vary fully reversed loading condition, for measuring fatigue life data's.

This paper presents investigation on influence of fatigue failure over an entire cyclic loading conditions. It shows the endurance limit of an AZ31B Magnesium alloys. The standard dimension of the specimen could prepared and life, damage, equivalent alternate stress has done by using finite element method in ANSYS 14.5. Design of experiment was done by the finite element method. The simulation result

*Corresponding author.
This paper was presented by the first author in the National Conference on *Advances in Mathematics and its Applications to Science and Engineering* (AMASE-2016) conducted in Department of Mathematics, University College of Engineering Pattukkottai, Thanjavur, Tamil Nadu, India, on 22nd January 2016.

good agreement with the theoretical results. And also fatigue results using design of experiment to shows the impact and critical damage on the model. This investigation prevents a life of the AZ31B Magnesium alloys.

II. Mathematical Modeling

The static and dynamic load history very typical in engineering situations. Fatigue includes the effect of mean stress amplitude between the ratio of maximum stress and minimum stress. These alternating stress using three more approaches as Soderberg, Goodman and Gerber parabola approaches for the schematic curve representation shows that figure 1.

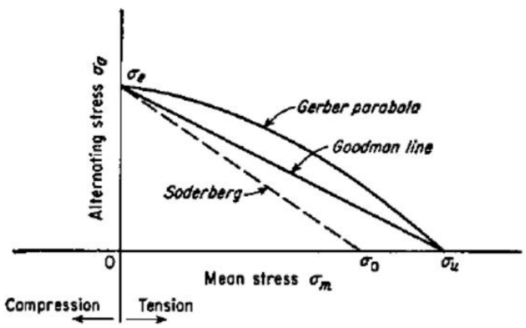

Figure 1. Goodman approach

The straight line to represent the safe zone for the material as a Goodman diagram. The Goodman diagram is typically preferred in engineering design. Actual data can vary around lines by being either concave or convex. Points below Goodman line are considered safe, points above line are considered failed. Most of the fatigue life tested in air environment fully reversed uniaxial fatigue strength or fatigue limits noted upto 106 cycles. For axial loaded unnotched specimen of the nominal stress does not exist, and the average maximum normal stress and mean stress are taken into account. And the following equation is related to fatigue life data.

Soderberg equation

$$\frac{1}{n} = \frac{\sigma_m}{\sigma_y} + K_f \frac{\sigma_s}{\sigma_{-1}} \ldots\ldots\ldots\ldots\ldots (1)$$

Goodman equation

$$\frac{1}{n} = K_t \left[\frac{1}{n} = \frac{\sigma_m}{\sigma_y} + \frac{\sigma_s}{\sigma_{-1}}\right] \ldots\ldots\ldots\ldots\ldots (2)$$

Mean load

$$\sigma_a = \frac{\sigma_{max} + \sigma_{min}}{2} = 0\,N \ldots\ldots\ldots\ldots (3)$$

Variable load

$$\sigma_a = \frac{\sigma_{max} - \sigma_{min}}{2} = 20000\,N$$

Mean stress $\sigma_{m} = 0$ N/mm^2

Most of the applications soderberg equation preferred for the fatigue designs. Endurance limit σ_{-1} to working as a fully reversed cycle can sustain the variable stress for an infinite number of cycles without failure. From the design data approximately the endurance limit of the metal and alloys are $\sigma_{-1} = 0.45\,\sigma_u$. (For tension).

$\sigma_{-1} = 314$ N/mm^2

$$\frac{D}{d} = 1.4 \quad , \frac{r}{d} = 0.3$$

From the design datebook PSGDB

Stress concentration factor (Kt$_)$ = 1.875

Fatigue factor $K_f = 1 + q\,(K_t - 1) = 1.656$

Modified endurance limit $\sigma_{-1m} = \frac{\sigma_{-1} \times K_R}{K_f}$

= 152 N/mm^2

For completely reversed loading condition

$\sigma_{m} = 0$ N/mm^2 $A = \frac{\pi}{4}\,(d^2)$

$A = 153\ mm^2$

Using Soderberg equation

$$\frac{1}{n} = \frac{\sigma_m}{\sigma_y} + K_f \frac{\sigma_s}{\sigma_{-1}}$$

P = σ_a = 23.256 KN

Load for infinite life = 23.256 KN

To increasing load gradually $\sigma_a = 2 \times 152 = 304$ N/mm^2

Endurance strength for N =10^3 cycles = 0.75 σ_u = 200 N/mm^2

Endurance strength for N=10^6 cycles = 152 N/mm^2

N cycles can be found in S-N curve respectively to form a triangle.

Taking logarithmic value for the above load cycles using triangle law to found the value of load cycles.

Log (200) = 2.301, Log (152) = 2.181, Log (153) = 2.48

$$\frac{2.301 - 2.08}{2.301 - 2.181} = \frac{\log N - 3}{6 - 3}$$

N= 36856 cycles.

III. NUMERICAL MODELING

Axial load tensile test strength has improved by the AZ31B Magnesium alloy in the ambient temperature. The same way tensile properties were investigated in numerical modeling of analysis system. It will support a fatigue life over a cyclic loading conditions. This proposal of fatigue data is examined from the axial loading of a structural system as Life, Damage, and Biaxiality Indication, factor of safety, fatigue sensitivity curve. The fatigue strength of 10^6 cycles around 160 Mpa is taken from the datebook. This analysis of two applying fully reversed loading condition for the given input into the tensile specimen as shown in figure 2. S-N curve is based on stress life to update the full life cycles. And more than 10^5 cycles is used compare to strain life, similarly using high fatigue life cycles. This reverse loading condition used to calculate the alternating values and mean stress. This stress variation due acting second load to first load. (Equal and opposite load). This way used to find out the critical fatigue locations. Constant amplitude loading condition for the lowest alternating stress will use minimum life of the tensile specimen. This will helps to adding factor of safety of the material do not exceed the endurance limit.

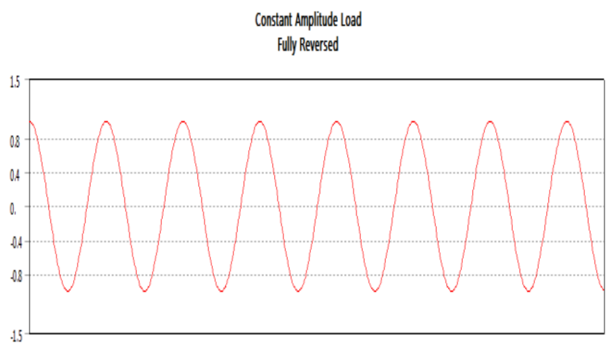

Figure 2. Fully reversed condition

And the soderberg diagram as shown in figure 3. Most of the analysis the engineers using this method for a better capability for the mean stress correction theory.

Figure 3. Soderberg mean correction theory

Stress life based on characterized by a loading type, mean stress effect, multiaxial stress correction and fatigue modification factor. This fully reversed loading condition database based on the alternating stress as shown in the table 2. It is the ratio of difference between the maximum stresses to minimum stress (1 to -1). This approach identifies the critical fatigue locations. From above the soderberg correction theory the value of yield below the triangle material is safe, otherwise it will be some deformation as an unsafe zones. And applying scale factor used to reduce the effect of changing magnitude of loads. Using soderberg equation when the value of infinite life of the AZ31B Magnesium alloy is 23.256 KN. We can avoid the damage to set infinite life of a material alternating stress is beyond the limit of the S-N curve. For higher value of fatigue life will make small damage occur many times.

Table 2. Alternating stress

S.No	Cycles	Alternating Stress (MPa)
1	10	1150
2	20	1050
3	50	950
4	100	850
5	200	730
6	2000	640
7	10000	540
8	20000	450
9	100000	320
10	200000	250
11	1000000	160

The welded specimen could be drawn by using workbench model and the figure as shown in figure 4(a) and (b). The finite element model using triangle mesh the element size 50400 and node 231813 for the purpose of high accuracy. And there is a no mesh failure for the standard specimen for the quality meshes.

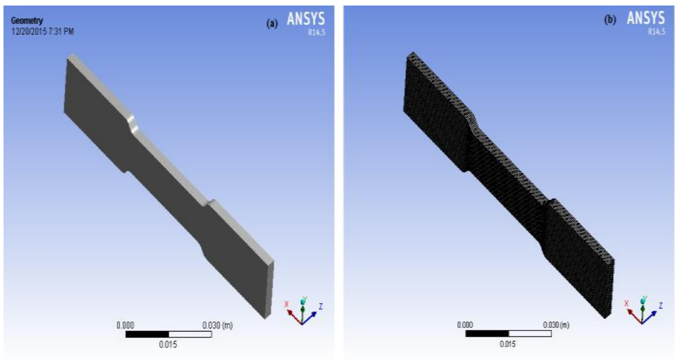

Figure 4. (a) Solid geometry (b) mesh model

IV. DESIGN EXPERIMENT

Design of experiment is a Multiphysics system, it has a different input variable the results amount of output results are predicted and minimize the optimized parameters. In this parameters investigate the optimized key parameters to create a graphical response surfaces. This experiment the force magnitude is an input variable and different outputs are to responses a given fatigue data's. This response surface using central composite design used to derive a various types of design points. This DOE of design points are given an important role. For various output updating the design points are very essential one. The collective design points to show local sensitivity of the life time for the various cyclic loading conditions. Design points has showed in the table 3.The central composite design force magnitude 20000 KN as an input condition and 12 outputs. Central composite design is a five factorial design .There are three types of CCDs that arecommonly used in experiment designs: circumscribed, inscribed, and face-centered CCDs. The five-level coded values of each factor are represented by [-α, -1, 0+1, +α], where [-1, +1] corresponds to the physical lower and upper limit of the explored factor space. It is obvious that [-α, +α] establishes new "extreme" physical lower and upper limits for all factors. The value of [1,-1] varies depending on design property and number of factors in the study. For the circumscribed CCDs, considered to be the original form of Central Composite Designs, the value of +α is greater than 1.

Name	P12	P7	P6	P5	P3	P8	P9	P10	P11
1	20000	0.228928301	22.89209526	394.1078336	893.9555985	8.939851284	78.02220074	12816864.82	0.178979806
2	20000	0.228928301	22.89209526	394.1078336	893.9555985	8.939851284	78.02220074	12816864.82	0.178979806
3	20000	0.228928301	22.89209526	394.1078336	893.9555985	8.939851284	78.02220074	12816864.82	0.178979806
4	20000	0.228928301	22.89209526	394.1078336	893.9555985	8.939851284	78.02220074	12816864.82	0.178979806
5	20000	0.228928301	22.89209526	394.1078336	893.9555985	8.939851284	78.02220074	12816864.82	0.178979806
6	18000	0.206035472	20.60288589	354.6970384	804.5600328	8.045866489	137.8666393	7253386.353	0.198866453
7	22000	0.251821123	25.18130508	433.5185991	983.3511659	9.833836555	39.99465023	25003344.06	0.162708914
8	18373.9321	0.210315652	21.03089011	362.065514	821.2739764	8.213011265	123.938353	8068527.422	0.194819274
9	18373.9321	0.210315652	21.03089011	362.065514	821.2739764	8.213011265	123.938353	8068527.422	0.194819274
10	18373.9321	0.210315652	21.03089011	362.065514	821.2739764	8.213011265	123.938353	8068527.422	0.194819274
11	18373.9321	0.210315652	21.03089011	362.065514	821.2739764	8.213011265	123.938353	8068527.422	0.194819274
12	21626.0679	0.247540947	24.75329977	426.1501235	966.637222	9.666691303	45.00883341	22217860.9	0.165522283
13	21626.0679	0.247540947	24.75329977	426.1501235	966.637222	9.666691303	45.00883341	22217860.9	0.165522283
14	21626.0679	0.247540947	24.75329977	426.1501235	966.637222	9.666691303	45.00883341	22217860.9	0.165522283
15	21626.0679	0.247540947	24.75329977	426.1501235	966.637222	9.666691303	45.00883341	22217860.9	0.165522283

Table 3. Data Points

V. RESULT AND DISCUSSIONS

The mechanical characteristics of AZ31B Magnesium alloy in friction stir welding of a process material in which yield strength, ultimate and fatigue sensitivity in which evaluated by using mathematical and numerical modeling. The boundaries condition was applied same for the experimental rules. Finite element method of investigation was done on with welded specimen. This effect boundaries to causes a nature of stress effects as shown in various figures. The relation between the stress, strain and deformation as shown in figure 5. Structural results for obtained results the load starts from 0 to 20 KN linearly. This static analysis does not change with direction and magnitude of the force vector. As the obtained results good agreement with the design of experiment of a response surfaces.

However the 3D model developed along with the weldment thickness pate 3mm and investigate the mechanical behavior of an AZ31B Magnesium alloys. From the figure 5 value of Total deformation, stress and strain has 0.04379 m, 228.9 N/mm^2 and 8.93 for the force magnitude 20KN. It has a uniform deformation and all the values can obtained below of AZ31 B Magnesium maximum values as an efficiency of ultimate strength has 85.6%. This stress of a maximum limit beyond the limit of the AZ31B Magnesium alloy. Equivalent von-misses stress takes sign of the maximum principle stress. From figure 5 shows the red color mark is a maximum stress limit and blue color is a minimum limit, otherwise enabling the different colors depending upon the stress variation.

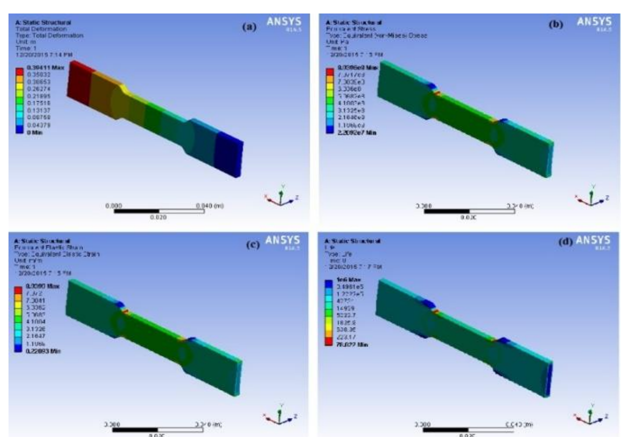

Figure 5. (a) Total deformation (b) Equivalent stress (c) Equivalent strain (d) Life

The fatigue data of the AZ31B Magnesium alloys followed by the date book. This data based calculating alternating stress was acting 106 load cycles. The stress life approach is very difficult compared to the strain life behaviour. The damage was calculated along the fatigue strength factor K_f=1. The fatigue factor does not affect the alternating stress. This loading history of 1 cycle to referred as a 1 day for an every load cycles. S-N curve approaches is important one for using mean stress theory. The fatigue load is applied a fully reversed loading condition the value amplitude is -1. Most of the test procedures using completely reversed loading conditions and strength of axial loading condition based on unnotched specimen was failure upto the range as 10^6 cycles. To finding the nature of stresses are very beneficial in this method for the S-N data as a required alternating stress as shown in figure 6.

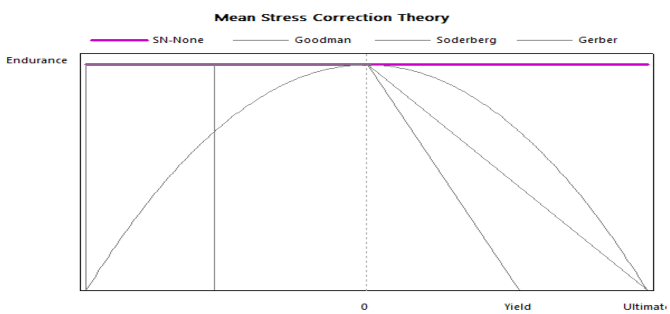

Figure 6. S-N curve approach

The fatigue sensitivity and life, damage, factor of safety, biaxiality indication as shown in figure 7. Constant amplitude loading condition of the minimum value considered as fatigue curve of a last point compared to the non-amplitude loading conditions. The load condition 1 cycle was considered equal to one day over an entire fatigue life of a system. Fatigue damage is a ratio of design life to available life in which the value of damage to reached greater than one the product to indicate the failure before reached the design life. The measurement of factor of safety varied, it belongs to the fatigue failure for the given life. This investigation factor of safety obtained the value of 15 as damage and life has scoped for this analysis. The FOS value less than one to indicate the failure when reached the design life. Generally material characteristics based on biaxiality indication. Biaxiality indication is a type of indicating stress as ratio of minimum principle stress to maximum stress. The value 0 to indicate the uniaxial stress.

Fatigue sensitivity to visualize the fatigue behavior to change the loading on critical location on the model as shown in figure 8. For sensitivity factor using lower deviation 50 % to upper deviation 150 % .It based on life, damage, and factor of safety. As a value of 2.19E+4 is critical location on the model. And equivalent alternating stress used to investigate the effect S-N curve after the cyclic loading conditions. It relate to the fatigue life to stress state. This S-N curve mainly focused on fatigue loading type, mean stress effects, multiaxial effects, and any other factors in the fatigue analysis.

When the stress calculated after the design life determination is possible otherwise it will not suitable for non-constant amplitude loading conditions. The Equivalent alternating stress of maximum value 2.282 pa obtained from the analysis.

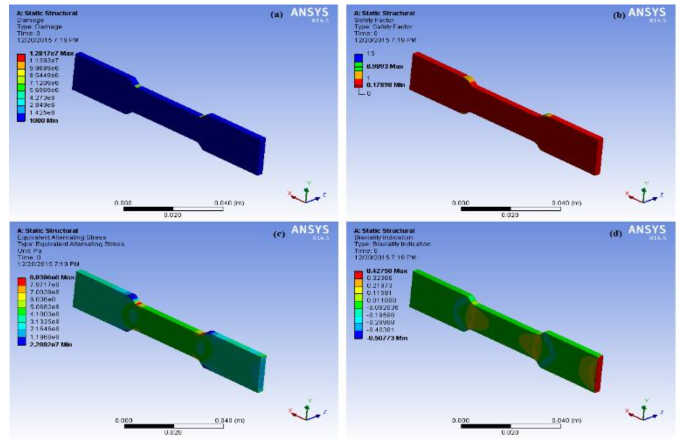

Figure 7. (a) Damage (b) safety factor
(c) Equivalent alternating stress (d) Biaxiality indication

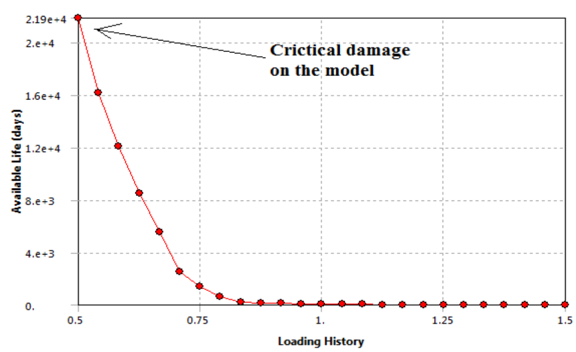

Figure 8. Fatigue sensitivity

Design of experiment of the data has collected from the fatigue behavior of uniaxial loading conditions as 10^6 cycles. This DOE using a single response and to predict various responses of 12 outputs. This design will interpolate the multidimensional space. It can found to visualize the 3D model of a design variable and design performance. For the given response for the design exploration system where created as a collected data points used to a parameters set and to get the output parameters. Using central composite design to update the amount of output parameters. This collection of data points after the updating to relate the other responses for various multi-space dimensions. This analysis basically used 12 parameters for the parallel chart as shown in figure 9.

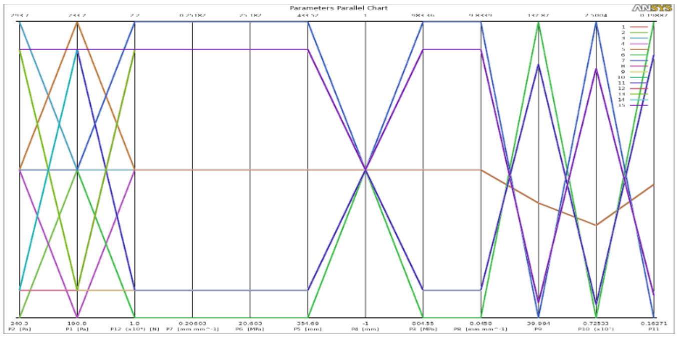

Figure 9. Parameters parallel chart

From the observation of a parameters parallel chart to enabled the different colors in ellipse shape. The goodness for fit using a verification point for whether to checking the response calculating number of verification point chosen 1. This analysis for the goodness for fit curve for various responses as shown in table 3.The next one response surface for the impact of graphical results life, stress, deformation, damage, as shown in figure below 10(a)-10(d).

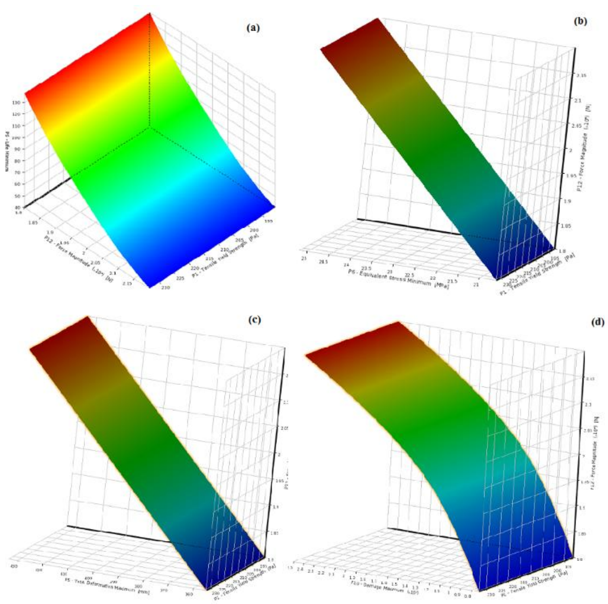

Figure 10. Response surface (a) Life (b) Equivalent stress (c) Total deformation (d) Damage

Figure 10 (a) shows a graphical impact of a life parameters decrease gradually while the effect of force magnitude. Similarly figure 10 (d) shares a maximum life while the effect of force magnitudeand critical load on the model as aresponse point of severe damage is 2.29 in terms of logarithmic values.

Name	P7	P6	P5	P4	P3	P8	P9	P10	P11
Goodness Of Fit									
Coefficient of Determination (Best Value = 1)	1	1	1	1	1	1	1	1	1
Adjusted Coeff of Determination (Best Value = 1)	1	1	1	1	1	1	1	1	1
Maximum Relative Residual (Best Value = 0%)	0	0	0	0	0	0	0	0	0
Root Mean Square Error (Best Value = 0)	4.66E-12	1.52E-07	1.96E-07	0	3.05E-06	3.01E-10	1.07E-06	0.04022	5.40E-10
Relative Root Mean Square Error (Best Value = 0%)	0	0	0	0	0	0	0	0	0
Relative Maximum Absolute Error (Best Value = 0%)	0	0	0	0	0	0	0	0	0
Relative Average Absolute Error (Best Value = 0%)	0	0	0	0	0	0	0	0	0

Table 4. Goodness for fit response

P3 - Equivalent Stress Maximum
P4 - Total Deformation Minimum
P5 - Total Deformation Maximum
P6 - Equivalent Stress Minimum
P7 - Equivalent Elastic Strain Minimum
P8 - Equivalent Elastic Strain Maximum
P9 - Life Minimum
P10 - Damage Maximum
P11 - Safety Factor Minimum

Spider chart once to solve the response surface it will appeared automatically. This chart will show the impact of various output parameters. Once to changing response the output to change a shape and dimensions. The red color to show the response point and various output factor for the spider shows that figure 11(b). Local sensitivity curves the surface parameters are a single sensitivity curves. This curve to calculate the amount of output while changing input as a single parameters curve. The changing output varied for a given inputs, that curve referred as a local sensitivity. And the local sensitivity curve of the figure 11(c)-11(d) shows relation of a life, damage, and stress in figure 13. Above the graph shows different variation of life where occurring damage to decrease gradually. The response point shows life over a 75 cycles to undergoing the damage found in 2.28. This response surface life is a completely reversed loading condition good agreement with the severe damage of red color identification mark. Goodness for fit in table 4 of various output parameters very fit for the best values.

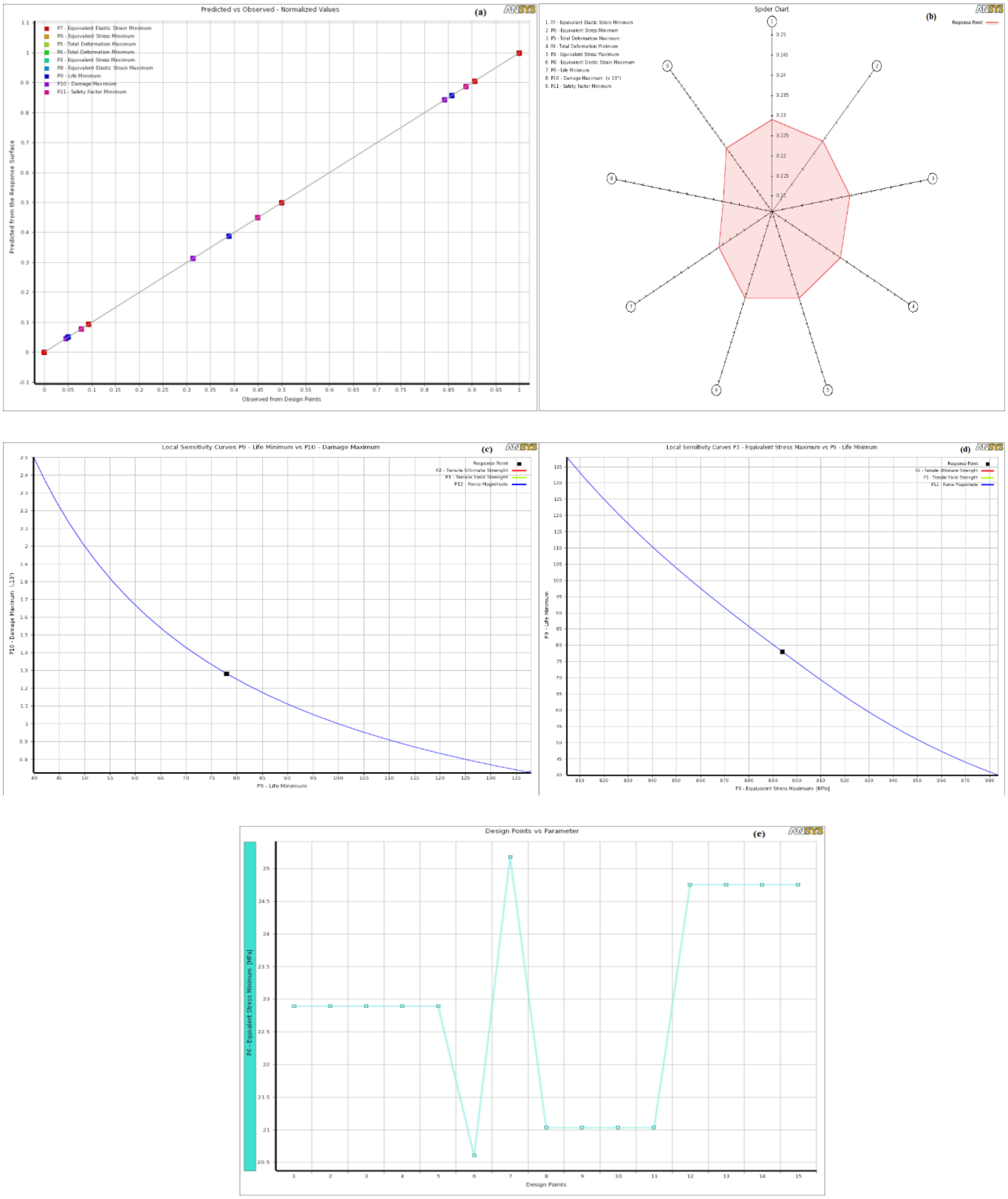

Figure 11.

(a) Goodness for fit
(b) Response surfaces of a spider chart
(c) Local sensitivity curve Life V_s Damage
(d) Local sensitivity curve Life V_s Damage
(e) Design points V_s Equivalent stress

The stress life has constant amplitude reverse loading condition of equivalent alternating stress is lower than the user defined alternating stress in S-N curve that point will be used and also same response point to update the parameters. These all the response surface and local sensivity curves will be formulated by the interpolation equation using log-log, Semi-log, Linear. The interpolation equation to query the S-N curve as data of a stress value not same in the life stress value. It can be used interpolate the appropriate value. And alternating stress calculated by the fatigue strength factor. This factor accounted the differences between the parts from the tested conditions.

VI. CONCLUSION

In this paper, to investigate the fatigue behaviour of a weldment plate as a material of AZ31 B magnesium alloy. Friction stir welding of a weldment joint has a good tensile strength has proved from this analysis. Here optimized parameters like transverse speed, rotational speed, and axial load to provide an important role in friction stir welding. From above the tensile simulation result make sure, it has a good fatigue strength for over 10^6 load cycles as a stress limit of 160 Mpa. The plate thickness 3mm of a deformation of the tensile specimen 0.04379m, equivalent alternate stress 228.9 N/mm^2, strain 8.93 within the limits of AZ31B Magnesium alloys.

The fatigue life of a tensile specimen has to get an expected life over an entire load of 20000 N. This simulation of graphical image to shows the location of various stresses and behavior of plastic deformations. And fatigue sensivity of available life in tensile specimen 2.29E4 to attend the critical damage. Equivalent alternating stress has good loading capacity after the loading histories. It prevent the nature of stress were found after the loading has 228.9 N/mm^2.

Design of experiment of tensile behavior has done by the ANSYS simulation. The above structural results good responses with of a design of experiment. This experiment of a various inputs and outputs to create a large number of data points. This data points responses of a various responses such as parameters parallel chart, goodness for fit, max-min search, and local sensitivity curve and 3D response surfaces. Local sensitivity curve clearly defined life of a welded specimen to lose a life due to increasing damage for a constant loading condition. The graphical view of 3D response surfaces to shows the good impact of outputs for a given input as a force magnitude.

REFERENCES

[1] Elatharasan G, Senthil Kumar V.S mar, Modeling and optimization of friction stir welding parameters of dissimilar alloys using RSM Procedia Engineering 38 (2012) 3477 – 3481.

[2] Elatharasan G, Senthil Kumar V.S Corrosion behaviour of fsw AA7075 alloy by Nano alumina coating.Journal of Chemical and Pharmaceutical Sciences ISSN: 0974-2115.

[3] Mustafa Kemal Kulekci, Magnesium and its alloys application in automotive industry, Int J Adv Manuf Technol (2008) 39:851, DOI 10.1007/s00170-007-1279-2.

[4] Abu-Farha F, Khraisheh M, Deformation characteristics of AZ31 magnesium alloy under various forming temperature and stain rates, in: Proceedings of the English ESAFORM Conference on material forming, Cluj-Napoca Romania, 2005, pp, 627-630.

[5] TsaoL, Wu C,Chuang T Evaluation of superplastic formability of the AZ31 magnesium alloy, Mater.Res.Adv Tech 92(2001) 572-577.

[6] Mackenzie, L. W. F., Lorimer, G. W., Humphreys, F. J. and Wilks. T. Recrystallization Behavior of Two Magnesium Alloys. Mater. Sci. Forum, 2004, 467-482.

[7] Yi, S. B., Zaefferer, S. and Brokmeier, H.- G. Mechanical behavior and microstructural evolution of magnesium alloy AZ31 in tension at different temperatures, Materials Science and Engineering: A, 2006, 275-281, 424.

[8] Del Valle, J. A. and Ruano, O. A. Influence of texture on dynamic recrystallization and deformation mechanisms in rolled or ECAPed AZ31 magnesium alloy, Materials Science and Engineering: A, 2008,473-480, 487.

[9] Tokaji, K., Kamakura, M., Ishiizumi, Y. and Hasegawa, N. Fatigue behavior and fracture mechanism of a rolled AZ31 magnesium alloy, International Journal of Fatigue, 2004, 1217-1224, 26.

[10] Tokaji K, Ogawa T and Kameyama Y., The effects of stress ratio on the growth behaviour of small fatigue cracks in an aluminum alloy 7075-T6 (with special interest in stage I crack growth) fatigue frat Eng Mater Struct; 1990, 411-21, 13.

[11] Tokaji K, goshima Y., Fatigue behaviour of 6063 aluminium alloy in corrosive environments J soc Mater Sci Jpn; 2002,1441-6,51.

[12] Properties and Selection of Metals, Vol 1, Metals Handbook, 8th ed., American Society for Metals, 1961.

[13] Higgins, R.A. Engineering Metallurgy Applied Physical Metallurgy, 6th ed., Arnold, 1993.

[14] Meyers M.A. and. Chawla, K.K MechanicalMetallurgy—Principles and Applications,Prentice-Hall Inc., 1984.

[15] Laird C.M, STP 415, American Society forTesting and Materials, 1966, p 130.

[16] Anderson, T.L. Fracture Mechanics: Fundamentals and Applications, 3rd ed., Taylor& Francis, 2005.

[17] Collins J and Daniewicz, S. FailureConsiderations, Mechanical EngineersHandbook, John Wiley & Sons, Inc.,1998.

[18] Bhandari V.B., Design of Machine Elements (New Delhi, Tata McGraw-Hills, 2009).

[19] Atzori, B. Lazzarin, P. Tovo, R., Fatigue and Fracture of Engineering Materials and Structures, 22 (1999) 369.

[20] Dong P, Hong J. K, International Institute of Welding: IIW Doc. XIII-2036-04/XV-1173-04.

Radaj D. Design and Analysis of Fatigue Resistant Welded Structures, Abington Publishing, Cambridge (1990).

Global Journal of Pure and Applied Mathematics (GJPAM) ISSN 0973-1768 Volume 12,Number 4 (2016)

A Note on Explicit Evaluation of Ramanujan's Cubic Continued Fraction using Theta Function Identities

*Yudhisthira Jamudulia**
Department of Mathematics,
Ramanujan School of Mathematical Sciences,
Puducherry-605014, India.
Email: yudhismath@hotmail.com

Syeda Noor Fathima
Department of Mathematics,
Ramanujan School of Mathematical Sciences,
Puducherry-605014, India.
Email: fathima.mat@pondiuni.edu.in

***Abstract*- In this paper, we derive some general theorems for the explicit evaluation of Ramanujan's cubic continued fraction employing theta function identities.**

***Keywords*- *Theta Functions, Continued Fraction*.**

I. INTRODUCTION

The following beautiful continued fraction, communicated by Ramanujan in his second letter to Hardy

$$G(q) := \frac{q^{1/3}}{1}\,\frac{q+q^2}{+\;1+}\,\frac{q^2+q^4}{1\;+}\,\frac{q^3+q^6}{1\;+\cdots},\quad |q|<1 \qquad (1.1)$$

has recorded on page 366 of his lost notebook [12]. H. H. Chan [6] has discovered many new identities which perhaps are the identities to which Ramanujan vaguely referred. Several new modular equation relating G(q) its explicit evaluations over years are given by several mathematicians. We mention here specially B. C. Berndt, Chan and L-C Zhang [4]. For more works on evaluation of the cubic continued fraction one may see [5], [11], [10], [8], [9] and [7].

Motivated by these works in Section 2 of this paper, we establish some new formulas for evaluating G(q) by employing certain identities found in the works of [2, Entry 62, pp.221] and [3, pp. 127]. As a particular case of our general formulas, we deduce certain known numerical values of G (q).

We conclude this introduction with few customary definition we make use in the sequel. For a and q complex number with $|q|<1$

$$(a)_\infty := (a;q)_\infty = \prod_{n=0}^{\infty}(1-aq^n)$$

and $(a)_n := (a;q)_n = \prod_{k=0}^{n-1}(1-aq^k) = \frac{(a)_\infty}{(aq^n)_\infty}$, n: any integer,

$$f(a,b) = \sum_{n=-\infty}^{\infty} a^{n(n+1)/2} b^{n(n-1)/2},$$

$$= (-a;ab)_\infty(-b;ab)_\infty(ab;ab)_\infty, \qquad |ab|<1.$$

$$f(-q) = f(-q,-q^2) = \sum_{n=-\infty}^{\infty}(-1)^n q^{n(3n-1)/2} = (q;q)_\infty$$

The following identities are quite useful for constructing new theorems ahead

$$e^{-\alpha/24}\sqrt[4]{\alpha}\, f(e^{-\alpha}) = e^{-\beta/24}\sqrt[4]{\beta}\, f(e^{-\beta}),\quad \alpha\beta=\pi^2 \qquad (1.2)$$

If G (q) is defined by (1.1), then

$$\left(27+\frac{f^{12}(-q)}{qf^{12}(-q^3)}\right)^{1/3} = \frac{1}{G(q)} + 4G^2(q)$$

Equations (1.2) and (1.3) are found in [1, Ch. 16, Entry 27, pp. 43] and [1, Ch. 20, Entry 1, pp. 345] respectively.

Along with the identities, the following modular equations are also used to find general theorems.

Theorem 1.1. [2]

If $P=\frac{f(-q)}{q^{1/12}f(-q^3)}$, $Q=\frac{f(-q^5)}{q^{1/12}f(-q^{15})}$, *then*

$$(PQ)^2+5+\frac{9}{(PQ)^2} = \left(\frac{Q}{P}\right)^3 - \left(\frac{P}{Q}\right)^3.$$

For the proof we refer [2, Entry 62, pp.221].

Theorem 1.2. [3]

If $P=\frac{f(-q)}{q^{1/12}f(-q^3)}$, $Q=\frac{f(-q^{11})}{q^{1/12}f(-q^{33})}$, *then*

$$(PQ)^5+\left(\frac{3}{PQ}\right)^5+11\left\{(PQ)^4+\left(\frac{3}{PQ}\right)^4\right\}+66\left\{(PQ)^3+\left(\frac{3}{PQ}\right)^3\right\}+253\left\{(PQ)^2+\left(\frac{3}{PQ}\right)^2\right\}+693\left(PQ+\frac{3}{PQ}\right)+1386=\left(\frac{Q}{P}\right)^6+\left(\frac{P}{Q}\right)^6.$$

For the proof we refer [3, pp. 127]

2. EVALUATION

In this section we present some theorems for explicit evaluation of G (q).

Theorem 2.1.

For $q=e^{-\pi\sqrt{n/3}}$, let

$$J_n = \frac{f(q)}{3^{1/4}q^{1/12}f(q^3)} \qquad (2.1)$$

Then

$$J_nJ_{1/n}=1 \qquad (2.2)$$

$$J_1=1 \qquad (2.3)$$

---

*Corresponding author.

This paper was presented by the first author in the National Conference on *Advances in Mathematics and its Applications to Science and Engineering* (AMASE-2016) conducted in Department of Mathematics, University College of Engineering Pattukkottai, Thanjavur, Tamil Nadu, India, on 22nd January 2016.

Proof. By the definitions of J_n and $J_{1/n}$ as in (2.1) and (1.2), we obtain (2.2). Then setting n=1 in (2.2) we easily obtain (2.3).

Theorem 2.2.

$$3(J_nJ_{25n})^2-5+\frac{3}{(J_nJ_{25n})^2}=\left(\frac{J_{25n}}{J_n}\right)^3-\left(\frac{J_n}{J_{25n}}\right)^3 \qquad (2.4)$$

Proof. Replacing q to –q in Theorem 1.1, we obtain

$$(RS)^2-5+\frac{3}{(RS)^2}=\left(\frac{S}{R}\right)^3-\left(\frac{R}{S}\right)^3 \qquad (2.5)$$

where R= $\frac{f(q)}{q^{1/12}(q^3)}$and S= $\frac{f(q^5)}{q^{5/12}(q^{15})}$. It can be easily seen that R=$3^{1/4}J_n$ and S= $3^{1/4}J_{25n}$. Substituting these R and S in (2.5), we obtain (2.4).

Theorem 2.3.

We have $J_5=\sqrt[6]{\frac{1+\sqrt{5}}{2}}$ and $J_{1/5}=\sqrt[6]{\frac{2}{1+\sqrt{5}}}$.

Proof.

Setting n=1/5 in (2.4) and employing (2.2), we obtain

$$J_5^{12}-J_5^6-1=0.$$

Since $J_n>0$, we obtain by solving the above equation $J_5=\sqrt[6]{\frac{1+\sqrt{5}}{2}}$. Again employing (2.2), we obtain $J_{1/5}=\sqrt[6]{\frac{2}{1+\sqrt{5}}}$.

Theorem 2.4.

We have $J_{25}=\frac{2}{\sqrt{5}-1}$ and $J_{1/25}=\frac{\sqrt{5}-1}{2}$.

Proof. Setting n=1 in (2.4) and observing that J_1 = 1, we have the following quadratic equation $J_{1/25}^2+J_{1/25}-1=0$.
Solving this we obtain $J_{1/25}=\frac{\sqrt{5}-1}{2}$. Using (2.2), we obtain $J_{25}=\frac{2}{\sqrt{5}-1}$.

Theorem 2.5.

$$\left\{\left(3^{1/2}J_nJ_{121n}\right)^5+\left(\frac{3}{3^{1/2}J_nJ_{121n}}\right)^5\right\}-11\left\{\left(3^{1/2}J_nJ_{121n}\right)^4+\left(\frac{3}{3^{1/2}J_nJ_{121n}}\right)^4\right\}+66\left\{\left(3^{1/2}J_nJ_{121n}\right)^3+\left(\frac{3}{3^{1/2}J_nJ_{121n}}\right)^3\right\}-253\left\{\left(3^{1/2}J_nJ_{121n}\right)^2+\left(\frac{3}{3^{1/2}J_nJ_{121n}}\right)^2\right\}+693\left\{3^{1/2}J_nJ_{121n}+\left(\frac{3}{3^{1/2}J_nJ_{121n}}\right)\right\}-1386=\left(\frac{J_{121n}}{J_n}\right)^6+\left(\frac{J_n}{J_{121n}}\right)^6.$$

Proof.

$$\left\{RS^5+\left(\frac{3}{RS}\right)^5\right\}-11\left\{(RS)^4+\left(\frac{3}{RS}\right)^4\right\}+66\left\{(RS)^3+\left(\frac{3}{RS}\right)^3\right\}-253\left\{(RS)^2+\left(\frac{3}{RS}\right)^2\right\}+693\left\{(RS)+\left(\frac{3}{RS}\right)\right\}-1386=\left(\frac{S}{R}\right)^6+\left(\frac{R}{S}\right)^6,$$

where R= $\frac{f(q)}{q^{1/12}(q^3)}$and S= $\frac{f(q^{11})}{q^{11/12}(q^{33})}$. It is easily follows that R= $3^{1/4}J_n$ and S=$3^{1.4}J_{121n}$. Substituting these in (2.7) we obtain (2.6).

Theorem 2.6.

We have$J_{11}=\sqrt[12]{\frac{1+\sqrt{A^2-4}}{2}}andJ_{1/11}=\sqrt[12]{\frac{2}{1+\sqrt{A^2-4}}}$
where A= $1810\sqrt{3}$- 3894.

Proof.

Setting n=1/11 in (2.6) and employing (2.2) we obtain

$$J_{11}^{24}-J_{11}^{12}A+1=0.$$

Solving this equation we obtain $J_{11}=\sqrt[12]{\frac{1+\sqrt{A^2-4}}{2}}$. Again using (2.2) we have $J_{1/11}=\sqrt[12]{\frac{2}{1+\sqrt{A^2-4}}}$.

Theorem 2.7.

$27(1-J_n^{12})=\left(\frac{1}{w}+4w^2\right)^3$ where w= G (-q).

Proof. Replacing q by –q in (1.3) , we have

$$\left(27-\frac{f^{12}(q)}{qf^{12}(q^3)}\right)^{1/3}=\frac{1}{G(-q)}+4G^2(-q).$$

Employing the definition of J_n, we complete the proof of (2.8).

REFERENCE

[1] B. C. Berndt, *Ramanujan's Notebook's Part III*, Springer-Verlag, New York, 1991.
[2] B. C. Berndt, *Ramanujan's Notebook's Part IV*, Springer-Verlag, New York, 1991.
[3] B. C. Berndt, *Ramanujan's Notebook's, Part V*, Springer-Verlag, New York, 1991.
[4] B. C. Berndt, H. H. Chan and L. C. Zhang, *Ramanujan's class invariants and cubic continued fraction*, ActaArithmetica, vol. 73.no.1,pp.76-85,1995C.
[5] Adiga, T. Kim, M. MahadevaNaika and H. S. Madhusudhan, *On Ramanujan's Cubic Continued Fraction and Explicit Evaluations of Theta Function*, Indian J. Pure and App. Math., No. 55, 9(2004), 1047-1062.
[6] H. H. Chan, *On Ramanujan's Cubic Continued Fraction*, ActaArith. 73(1995), 343-355.
[7] J. Yi, Y. Lee and D. H. Paek, *The Explicit Formulas and evaluations of Ramanujan's theta –functions* ψ, J. Math. Anal. Appl., 321(2006), 157-181.
[8] K.G. Ramanathan, *On Ramanujan's cubic continued fraction*, ActaArith., 43(1984), 209-226.
[9] K. R. Vasuki and K. Shivashankara, *On Ramanujan's cubic continued fraction*, Ganita, 53(1)(2002), 81-88.
[10] M. S. MahadevaNaika, *Some theorems on Ramanujan's cubic continued fraction and related identities*, Tamsui Oxford J.Math.Sci.,24(3)(2008),243-256.
[11] N. D. Baruah and NipenSaikia, *Some theorems on the explicit evaluations of Ramanujan's cubic continued fraction*. J.Comp. Appl. Math., 160(2003), 37-51.
[12] S. Ramanujan, *The Lost Notebook and Other Unpublished Papers*, Narosa, New Delhi, 1988.

Global Journal of Pure and Applied Mathematics (GJPAM) ISSN 0973-1768 Volume 12,Number 4 (2016)

IVF-generalized semi-precontinuous mappings

*R. Jeyabalan**
Department of Mathematics,
Alagappa University,
Karaikudi-600 004, Tamil Nadu, India.
Email: jeyram84@gmail.com

K. Arjunan
Department of Mathematics,
H. H. The Rajah's College,
Pudukkottai, Tamilnadu, India.

***Abstract*—In this paper, we introduce interval valued fuzzy(for- ivf) generalized semi-precontinuous mappings. Also we investigate some of their properties.**

***Keywords*—: IVF-set; IVFT-space; IVF-point; IVF-generalized semi-preclosed set.**

2010 AMS Subject Classification: 54A40, 08A72.

I. INTRODUCTION

The concept of fuzzy subset was introduced and studied by L. A. Zadeh [13] in the year 1965. The subsequent research activities in this area and related areas have found applications in many branches of science and engineering. The following papers have motivated us to work on this paper: C. L. Chang [3] introduced and studied fuzzy topological spaces in 1968 as a generalization of topological spaces. Many researchers like this concept and many others have contributed to the development of fuzzy topological spaces. Andrijevic [1] introduced semi-preclosed sets and Dontchev [4] introduced generalized semi-preclosed sets in general topology. After that the set was generalized to fuzzy topological spaces by Saraf and Khanna [12]. Tapas Kumar Mondal and S. K. Samantha [9] introduced the topology of interval valued fuzzy sets. Jeyabalan. R, Arjunan. K, [6] introduced interval valued fuzzy generalaized semi-preclosed sets . In this paper, we introduce that ivf-generalized semi-precontinuous mappings and some properties are investigated.

II. PRELIMINARIES

Definition 2.1. [9] *Let* X *be a non empty set. A mapping* $\overline{A}: X \to D[0,1]$ *is called an interval valued fuzzy set (briefly* $IVFS$ *) on* X *, where* $D[0,1]$ *denotes the family of all closed subintervals of [0,1] and* $\overline{A}(x) = [A^-(x), A^+(x)]$*, for all* $x \in X$ *, where* $A^-(x)$ *and* $A^+(x)$ *are fuzzy sets of* X *such that* $A^-(x) \le A^+(x)$*, for all* $x \in X$ *.*

Thus $\overline{A}(x)$ is an interval (a closed subset of [0,1]) and not a number fom the interval [0,1] as in the case of fuzzy set.Obviously any fuzzy set A on X is an $IVFS$.

Notation 2.2. D^X denotes the set of all IVF-subsets of a non empty set X .

Definition 2.3. [9] *Let* X *be a non empty set. Let* $x_0 \in X$ *and* $\alpha \in D[0,1]$ *be fixed such that* $\alpha \neq [0,0]$*. Then the IVF-subset* $p_{x_0}^{\alpha}$ *is called an IVF-point defined by,*

$$p_{x_0}^{\alpha} = \{\alpha \ x=x\_0 \ \text{if} \ x \ x\_0 \}.$$

Definition 2.4. [9] *Let* $\overline{A}$ *and* $\overline{B}$ *be any two* $IVFS$ *of* X *, that is* $\overline{A} = \{< x, [A^-(x), A^+(x)] >: x \in X\}$, $\overline{B} = \{< x, [B^-(x), B^+(x)] >: x \in X\}$.

We define thefollowing relations and operations:

(i) $\overline{A} \subseteq \overline{B}$ *if and only if* $A^-(x) \le B^-(x)$ *and* $A^+(x) \le B^+(x)$*, for all* $x \in X$ *.*

(ii) $\overline{A} = \overline{B}$ *if and only if* $A^-(x) = B^-(x)$*, and* $A^+(x) = B^+(x)$*, for all* $x \in X$ *.*

(iii) $(\overline{A})^c = \overline{1} - \overline{A} = \{< x, [1 - A^+(x), 1 - A^-(x)] >: x \in X\}$.

(iv) $\overline{A} \cap \overline{B} = \{< x, [\min[A^-(x), B^-(x)], \min[A^+(x), B^+(x)]] >: x \in X\}$.

(v) $\overline{A} \cup \overline{B} = \{< x, [\max[A^-(x), B^-(x)], \max[A^+(x), B^+(x)]] >: x \in X\}$.

We denote by $\overline{0}_X$ and $\overline{1}_X$ for the IVF-sets $\{< x, [0,0] >, \text{ for all } x \in X\}$ and $\{< x, [1,1] >, \text{ for all } x \in X\}$ respectively.

Definition 2.5. [9] *Let* X *be a set and* $\Im$ *be a family of interval vlued fuzzy sets* $(IVFSs)$ *of* X *. The family* $\Im$ *is called an interval valued fuzzy topology* $(IVFT)$ *on* X *if and only if* $\Im$ *satisfies the following axioms:*

(i) $\overline{0}_X, \overline{1}_X \in \Im$,

*Corresponding author.

This paper was presented by the first author in the National Conference on *Advances in Mathematics and its Applications to Science and Engineering* (AMASE-2016) conducted in Department of Mathematics, University College of Engineering Pattukkottai, Thanjavur, Tamil Nadu, India, on 22nd January 2016.

(ii) *If* $\{\overline{A}_i : i \in I\} \subseteq \Im$, *then* $\bigcup_{i \in I} \overline{A}_i \in \Im$,

(iii) *If* $\overline{A}_1, \overline{A}_2, \overline{A}_3, \ldots, \overline{A}_n \in \Im$, *then* $\bigcap_{i=1}^{n} \overline{A}_i \in \Im$.

The pair $(X, \Im)$ is called an IVFT-space $(IVFTS)$. The members of $\Im$ are called interval valued fuzzy open sets $(IVFOS)$ in X.

An interval valued fuzzy set $\overline{A}$ in X is said to be interval valued fuzzy closed set $(IVFCS)$ in X if and only if $(\overline{A})^c$ is an $IVFOS$ in X.

Definition 2.6. [9] *Let* $(X, \Im)$ *be an* $IVFTS$ *and* $\overline{A} = \{< x, [A^-(x), A^+(x)] >: x \in X\}$ *be an* $IVFS$ *in* X. *Then the interval valued fuzzy interior and interval valued fuzzy closure of* $\overline{A}$ *denoted by* $IVFint(\overline{A})$ *and* $IVFcl(\overline{A})$ *are defined by*

$$IVFint(\overline{A}) = \bigcup \{\overline{G} : \overline{G} \text{ is an IVFOS in } X \text{ and } \overline{G} \subseteq \overline{A}\}$$

$$IVFcl(\overline{A}) = \bigcap \{\overline{K} : \overline{K} \text{ is an IVFCS in } X \text{ and } \overline{A} \subseteq \overline{K}\}.$$

For any $IVFS$ $\overline{A}$ in $(X, \Im)$, we have $IVFcl(\overline{A}^c) = (IVFint\ (\overline{A}))^c$ and $IVFint(\overline{A}^c) = (IVFcl(\overline{A}))^c$.

Definition 2.7.
An $IVFS$ $\overline{A} = \{< x, [A^-(x), A^+(x)] >: x \in X\}$ *in an* $IVFTS$ $(X, \Im)$ *is said to be an*

(i) *IVF-regular closed set* $(IVFRCS)$ *if* $\overline{A} = IVFcl(IVFint(\overline{A}))$;

(ii) *IVF-semi closed set* $(IVFSCS)$ *if* $IVFint(IVFcl(\overline{A})) \subseteq \overline{A}$;

(iii) *IVF-preclosed set* $(IVFPCS)$ *if* $IVFcl(IVFint\ (\overline{A})) \subseteq \overline{A}$;

(iv) *IVF-*α *closed set* $(IVF\alpha CS)$ *if* $IVFcl(IVFint\ (IVFcl\ (\overline{A}))) \subseteq \overline{A}$;

(v) *IVF-*β *closed set* $(IVF\beta CS)$ *if* $IVFint(ivfcl\ (ivfint(\overline{A}))) \subseteq \overline{A}$.

Definition 2.8.
An $IVFS$ $\overline{A} = \{< x, [A^-(x), A^+(x)] >: x \in X\}$ *in an* $IVFTS$ $(X, \Im)$ *is said to be an*

(i) *interval valued fuzzy generalized closed set* $(IVFGCS)$ *if* $ivfcl\ (\overline{A}) \subseteq \overline{U}$, *whenever* $\overline{A} \subseteq \overline{U}$ *and* $\overline{U}$ *in an* $IVFOS$;

(ii) *interval valued fuzzy regular generalized closed set* $(IVFRGCS)$ *if* $ivfcl\ (\overline{A}) \subseteq \overline{U}$, *whenever* $\overline{A} \subseteq \overline{U}$ *and* $\overline{U}$ *is an* $IVFROS$.

Definition 2.9.
An $IVFS$ $\overline{A} = \{< x, [A^-(x), A^+(x)] >: x \in X\}$ *in an* $IVFTS$ $(X, \Im)$ *is said to be an*

(i) *interval valued fuzzy semi-preclosed set* $(IVFSPCS)$ *if there exist an* $IVFPCS$ $\overline{B}$, *such that* $ivfint\overline{B} \subseteq \overline{A} \subseteq \overline{B}$;

(ii) *interval valued fuzzy semi-preopen set* $(IVFSPOS)$ *if there exist an* $IVFPOS$ $\overline{B}$, *such that* $\overline{B} \subseteq \overline{A} \subseteq ivfcl(\overline{B})$.

Definition 2.10. *Let* $\overline{A}$ *be an* $IVFS$ *in an* $IVFTS$ $(X, \Im)$. *Then the interval valued fuzzy semi-preinterior of* $\overline{A}$ $(ivfspint(\overline{A}))$ *and the interval valued fuzzy semi-preclosure of* $\overline{A}(ivfspcl(\overline{A}))$ *are defined by*

$$ivfspint(\overline{A}) = \bigcup \{\overline{G} : \overline{G} \text{ is an IVFSPOS in } X \text{ and } \overline{G} \subseteq \overline{A}\},$$

$$ivfspcl(\overline{A}) = \bigcap \{\overline{K} : \overline{K} \text{ is an IVFSPCS in } X \text{ and } \overline{A} \subseteq \overline{K}\}.$$

For any $IVFS$ $\overline{A}$ in $(X, \Im)$, we have $ivfspcl(\overline{A}^c) = (ivfspint(\overline{A}))^c$ and $ivfspint(\overline{A}^c) = (ivfspcl(\overline{A}))^c$.

Definition 2.11. [6] *An* $IVFS$ $\overline{A}$ *in* $IVFTS$ $(X, \Im)$ *is said to be an interval valued fuzzy generalized semi-preclosed set* $(IVFGSPCS)$ *if* $ivfspcl\ (\overline{A}) \subseteq \overline{U}$, *whenever* $\overline{A} \subseteq \overline{U}$ *and* $\overline{U} \in \Im$.

Definition 2.12. [6] *The complement* $\overline{A}^c$ *of an* $IVFGSPCS$ $\overline{A}$ *in an* $IVFTS$ $(X, \Im)$ *is called an interval valued fuzzy generalized semi-preopen set* $(IVFGSPOS)$ *in* X.

Definition 2.13. *An* $IVFTS$ $(X, \Im)$ *is called an interval valued fuzzy* $T_{1/2}$ *space* $(IVFT_{1/2})$ *space if every* $IVFGCS$ *is an* $IVFCS$ *in* X.

Definition 2.14. *An* $IVFTS$ $(X, \Im)$ *is called an interval valued fuzzy semi-pre* $T_{1/2}$ *space* $(IVFSPT_{1/2})$ *space if every* $IVFGSPCS$ *is an* $IVFSPCS$ *in* X.

Definition 2.15. [9] *An* $IVFS$ $\overline{A}$ *of a* $IVFTS$ *of* $(X, \Im)$ *is said to be an interval valued fuzzy neighbourhood(* $IVFN$ *) of an* $IVFP$ $p_{x_0}^{\alpha}$ *if there exists an* $IVFOS$ $\overline{B}$ *in* X *such that* $p_{x_0}^{\alpha} \in \overline{B} \subseteq \overline{A}$.

Definition 2.16. *Let* $(X,\Im)$ *and* (Y,σ) *be* $IVFTSs$. *Then a map* $g: X \to Y$ *is called an*

(i) *interval valued fuzzy continuous* (IVF *continuous mapping) if* $g^{-1}(\overline{B})$ *is* $IVFOS$ *in* X *for all* $\overline{B}$ *in* σ.

(ii) *interval valued fuzzy semi-continuous mapping* ($IVFS$ *-continuous mapping) if* $g^{-1}(\overline{B})$ *is* $IVFSOS$ *in* X *for all* $\overline{B}$ *in* σ.

(iii) *interval valued fuzzy* α *-continuous mapping* ($IVF\alpha$ *-continuous mapping) if* $g^{-1}(\overline{B})$ *is* $IVF\alpha OS$ *in* X *for all* $\overline{B}$ *in* σ.

(iv) *interval valued fuzzy pre-continuous mapping* ($IVFP$ *-continuous mapping) if* $g^{-1}(\overline{B})$ *is* $IVFPOS$ *in* X *for all* $\overline{B}$ *in* σ.

(v) *interval valued fuzzy* β *-continuous mapping* ($IVF\beta$ *-continuous mapping) if* $g^{-1}(\overline{B})$ *is* $IVF\beta OS$ *in* X *for all* $\overline{B}$ *in* σ.

Definition 2.17. *Let* $(X,\Im)$ *and* (Y,σ) *be* $IVFTSs$. *Then a map* $g: X \to Y$ *is called interval valued fuzzy generalized continuous* ($IVFG$ *continuous) mapping if* $g^{-1}(\overline{B})$ *is* $IVFGCS$ *in* X *for all* $\overline{B}$ *in* σ^c.

Definition 2.18. *A mapping* $g:(X,\Im)\to(Y,\sigma)$ *is called an interval valued fuzzy generalized semi-precontinuous* ($IVFGSP$ *continuous) mapping if* $g^{-1}(\overline{V})$ *is an* $IVFGSPCS$ *in* X *for every* $IVFCS$ $\overline{V}$ *in* Y.

Example 2.19. Let $X=\{a,b\}$, $Y=\{u,v\}$ and

$$\overline{K}_1=\{<a,[0.1,0.2]>,<b,[0.3,0.4]>\},$$
$$\overline{L}_1=\{<u,[0.3,0.4]>,<v,[0.4,0.6]>\}.$$

Then $\Im=\{\overline{0}_X,\overline{K}_1,\overline{1}_X\}$ and $\sigma=\{\overline{0}_Y,\overline{L}_1,\overline{1}_Y\}$ are $IVFT$ on X and Y respectively. Define a mapping $g:(X,\Im)\to(Y,\sigma)$ by $g(a)=u$ and $g(b)=v$. Then g is an $IVFGSP$ continuous mapping.

III. Main Results

Theorem 3.1. *Every* IVF *continuous mapping is an* $IVFGSP$ *continuous mapping.*

Proof. Let $g:(X,\Im)\to(Y,\sigma)$ be an IVF continuous mapping. Let $\overline{V}$ be an $IVFCS$ in Y. Then $g^{-1}(\overline{V})$ is an $IVFCS$ in X. Since every $IVFCS$ is an $IVFGSPCS$, $g^{-1}(\overline{V})$ is an $IVFGSPCS$ in X. Hence g is an $IVFGSP$ continuous mapping.

Remark 3.2. The converse of the above theorem 3.1. need not be true from the following example: Let $X=\{a,b\}$, $Y=\{u,v\}$ and

$$\overline{K}_1=\{<a,[0.1,0.2]>,<b,[0.3,0.4]>\},$$
$$\overline{L}_1=\{<u,[0.8,0.9]>,<v,[0.6,0.7]>\}.$$

Then $\Im=\{\overline{0}_X,\overline{K}_1,\overline{1}_X\}$ and $\sigma=\{\overline{0}_Y,\overline{L}_1,\overline{1}_Y\}$ are $IVFTs$ on X and Y respectively. Define a mapping $g:(X,\Im)\to(Y,\sigma)$ by $g(a)=u$ and $g(b)=v$. Then g is an $IVFGSP$ continuous mapping but not an IVF continuous mapping.

Theorem 3.3. *Every* $IVFG$ *continuous mapping is an* $IVFGSP$ *continuous mapping.*

Proof. Let $g:(X,\Im)\to(Y,\sigma)$ be an $IVFG$ continuous mapping. Let $\overline{V}$ be an $IVFCS$ in Y. Then $g^{-1}(\overline{V})$ is an $IVFGCS$ in X. Since every $IVFGCS$ is an $IVFGSPCS$, $g^{-1}(\overline{V})$ is an $IVFGSPCS$ in X. Hence g is an $IVFGSP$ continuous mapping.

Remark 3.4. The converse of the above theorem 3.3. need not be true from the following example: Let $X=\{a,b\}$, $Y=\{u,v\}$ and

$$\overline{K}_1=\{<a,[0.4,0.5]>,<b,[0.6,0.7]>\},$$
$$\overline{L}_1=\{<u,[0.6,0.7]>,<v,[0.7,0.8]>\}.$$

Then $\Im=\{\overline{0}_X,\overline{K}_1,\overline{1}_X\}$ and $\sigma=\{\overline{0}_Y,\overline{L}_1,\overline{1}_Y\}$ are $IVFTs$ on X and Y respectively. Define a mapping $g:(X,\Im)\to(Y,\sigma)$ by $g(a)=u$ and $g(b)=v$. Then g is an $IVFGSP$ continuous mapping but not an $IVFG$ continuous mapping. Since $\overline{L}_1^c$ $=\{<u,[0.3,0.4]>,<v,[0.2,0.3]>\}$ is an $IVFCS$ in Y and $g^{-1}(\overline{L}_1^c)=\{<a,[0.3,0.4]>,<b,[0.2,0.3]>\}\subseteq\overline{K}_1$. But $ivfcl(g^{-1}(\overline{L}_1^c))=\overline{K}_1^c\not\subset\overline{K}_1$. Therefore $g^{-1}(\overline{L}_1^c)$ is not an $IVFGCS$ in X.

Theorem 3.5. *Every* $IVFP$ *continuous mapping is an* $IVFGSP$ *continuous mapping.*

Proof. Let $g:(X,\Im)\to(Y,\sigma)$ be an $IVFP$ continuous mapping. Let $\overline{V}$ be an $IVFCS$ in Y. Then $g^{-1}(\overline{V})$ is an $IVFPCS$ in X. Since every $IVFPCS$ is an $IVFGSPCS$, $g^{-1}(\overline{V})$ is an $IVFGSPCS$ in X. Hence g is an $IVFGSP$ continuous mapping.

Remark 3.6. The converse of the above theorem 3.5 need not be true from the following example: Let $X=\{a,b\}$, $Y=\{u,v\}$ and

$$\overline{K}_1=\{<a,[0.3,0.4]>,<b,[0.4,0.7]>\},$$

$\overline{L}_1 = \{<u,[0.1,0.2]>,<v,[0.3,0.4]>\}$.

Then $\Im = \{\overline{0}_X, \overline{K}_1, \overline{1}_X\}$ and $\sigma = \{\overline{0}_Y, \overline{L}_1, \overline{1}_Y\}$ are *IVFTs* on X and Y respectively. Define a mapping $g:(X,\Im)\to(Y,\sigma)$ by $g(a)=u$ and $g(b)=v$. Then g is an *IVFGSP* continuous mapping but not an *IVFP* continuous mapping. Since $\overline{L}_1^c = \{<u,[0.8,0.9]>,<v,[0.6,0.7]>\}$ is an *IVFCS* in Y and $g^{-1}(\overline{L}_1^c) = \{<a,[0.8,0.9]>,<b,[0.6,0.7]>\}$ is not an *IVFPCS* in X, because $ivfcl(ivfint(g^{-1}(\overline{L}_1^{\,c}))) = ivfcl(\overline{K}_1) = \overline{1}_X \not\subset g^{-1}(\overline{L}_1^c)$.

Theorem 3.7. *Every IVFβ continuous mapping is an IVFGSP continuous mapping.*

Proof. Let $f:(X,\Im)\to(Y,\sigma)$ be an *IVFβ* continuous mapping. Let $\overline{V}$ be an *IVFCS* in Y. Then $g^{-1}(\overline{V})$ is an *IVFβCS* in X. Since every *IVFβCS* is an *IVFGSPCS*, $g^{-1}(\overline{V})$ is an *IVFGSPCS* in X. Hence g is an *IVFGSP* continuous mapping.

Remark 3.8. The converse of the above theorem 3.7. need not be true from the following example: Let $X=\{a,b\}$, $Y=\{u,v\}$ and

$\overline{K}_1 = \{<a,[0.5,0.7]>,<b,[0.3,0.4]>\}$,

$\overline{L}_1 = \{<u,[0.3,0.4]>,<v,[0.4,0.6]>\}$.

Then $\Im = \{\overline{0}_X, \overline{K}_1, \overline{1}_X\}$ and $\sigma = \{\overline{0}_Y, \overline{L}_1, \overline{1}_Y\}$ are *IVFTs* on X and Y respectively. Define a mapping $g:(X,\Im)\to(Y,\sigma)$ by $g(a)=u$ and $g(b)=v$. Then g is an *IVFGSP* continuous mapping but not an *IVFβ* continuous mapping. Since $\overline{L}_1^c = \{<u,[0.6,0.7]>,<v,[0.4,0.6]>\}$ is an *IVFCS* in Y and $g^{-1}(\overline{L}_1^c) = \{<a,[0.6,0.7]>,<b,[0.4,0.6]>\}$ is not an *IVFβCS* in X, because $ivfint(ivfcl(ivfint(g^{-1}(\overline{L}_1^{\,c})))) = ivfint(ivfcl(\overline{K}_1)))$ $= ivfint(\overline{1}_X) = \overline{1}_X \not\subset g^{-1}(\overline{L}_1^c)$

Theorem 3.9. *Every IVFα continuous mapping is an IVFGSP continuous mapping.*

Proof. Let $g:(X,\Im)\to(Y,\sigma)$ be an *IVFα* continuous mapping. Let $\overline{V}$ be an *IVFCS* in Y. Then $g^{-1}(\overline{V})$ is an *IVFαCS* in X. Since every *IVFαCS* is an *IVFGSPCS*, $g^{-1}(\overline{V})$ is an *IVFGSPCS* in X. Hence g is an *IVFGSP* continuous mapping.

Remark 3.10. The converse of the above theorem 3.9. need not be true from the following example: Let $X=\{a,b\}$, $Y=\{u,v\}$ and

$\overline{K}_1 = \{<a,[0.3,0.4]>,<b,[0.4,0.6]>\}$,

$\overline{L}_1 = \{<u,[0.1,0.2]>,<v,[0.3,0.4]>\}$.

Then $\Im = \{\overline{0}_X, \overline{K}_1, \overline{1}_X\}$ and $\sigma = \{\overline{0}_Y, \overline{L}_1, \overline{1}_Y\}$ are *IVFT* on X and Y respectively. Define a mapping $g:(X,\Im)\to(Y,\sigma)$ by $g(a)=u$ and $g(b)=v$. Then g is an *IVFGSP* continuous mapping but not an *IVFα* continuous mapping. Since $\overline{L}_1^c = \{<u,[0.8,0.9]>,<v,[0.6,0.7]>\}$ is an *IVFCS* in Y and $g^{-1}(\overline{L}_1^c) = \{<a,[0.8,0.9]>,<b,[0.6,0.7]>\}$ is not an *IVFαCS* in X, because $ivfcl(ivfint(ivfcl(g^{-1}(\overline{L}_1^{\,c})))) = ivfcl(ivfint(\overline{1}_X))$. $= ivfcl(\overline{1}_X) = \overline{1}_X \not\subset g^{-1}(\overline{L}_1^c)$

Theorem 3.11. *Let $g:(X,\Im)\to(Y,\sigma)$ be a mapping where $g^{-1}(\overline{V})$ is an IVFRCS in X, for every IVFCS $\overline{V}$ in Y. Then g is an IVFGSP continuous mapping.*

Proof. Assume that $g:(X,\Im)\to(Y,\sigma)$ is a mapping. Let $\overline{A}$ be an *IVFCS* in Y. Then $g^{-1}(\overline{V})$ is an *IVFRCS* in X, by hypothesis. Since every *IVFRCS* is an *IVFGSPCS*, $g^{-1}(\overline{V})$ is an *IVFGSPCS* in X. Hence g is an *IVFGSP* continuous mapping.

Remark 3.12. The converse of the above theorem 3.11. need not be true from the following example: Let $X=\{a,b\}$, $Y=\{u,v\}$ and

$\overline{K}_1 = \{<a,[0.3,0.4]>,<b,[0.4,0.7]>\}$,

$\overline{L}_1 = \{<u,[0.1,0.2]>,<v,[0.3,0.4]>\}$.

Then $\Im = \{\overline{0}_X, \overline{K}_1, \overline{1}_X\}$ and $\sigma = \{\overline{0}_Y, \overline{L}_1, \overline{1}_Y\}$ are *IVFT* on X and Y respectively. Define a mapping $g:(X,\Im)\to(Y,\sigma)$ by $g(a)=u$ and $g(b)=v$. Then g is an *IVFGSP* continuous mapping but not a mapping as defined in theorem 3.11., since $\overline{L}_1^c = \{<u,[0.8,0.9]>,<v,[0.6,0.7]>\}$ is an *IVFCS* in Y and $g^{-1}(\overline{L}_1^c) = \{<a,[0.8,0.9]>,<b,[0.6,0.7]>\}$ is not an *IVFRCS* in X, because $ivfcl(ivfint(g^{-1}(\overline{L}_1^{\,c}))) = ivfcl(\overline{K}_1)) = \overline{1}_X \neq g^{-1}(\overline{L}_1^c)$.

Theorem 3.13. *Every IVFS continuous mapping is an IVFGSP continuous mapping.*

Proof. Let $g:(X,\Im)\to(Y,\sigma)$ be an *IVFG* continuous mapping. Let $\overline{V}$ be an *IVFCS* in Y. Then $g^{-1}(\overline{V})$ is an *IVFSCS* in X. Since every *IVFSCS* is an *IVFGSPCS*, $g^{-1}(\overline{V})$ is an *IVFGSPCS* in X. Hence g is an *IVFGSP* continuous mapping.

Theorem 3.14. *Every $IVFSP$ continuous mapping is an $IVFGSP$ continuous mapping.*

Proof. Let $g:(X,\Im)\to(Y,\sigma)$ be an $IVFSP$ continuous mapping. Let $\overline{V}$ be an $IVFCS$ in Y. Then $g^{-1}(\overline{V})$ is an $IVFSPCS$ in X. Since every $IVFSPCS$ is an $IVFGSPCS$, $g^{-1}(\overline{V})$ is an $IVFGSPCS$ in X. Hence g is an $IVFGSP$ continuous mapping.

Theorem 3.15. *Let $g:(X,\Im)\to(Y,\sigma)$ be an $IVFGSP$ continuous mapping, then for each $IVFP$ $p_{x_0}^{\alpha}$ of X and each $\overline{A}\in\sigma$ such that $g(p_{x_0}^{\alpha})\in\overline{A}$, there exist an $IVFGSPOS$ $\overline{B}$ of X such that $p_{x_0}^{\alpha}\in\overline{B}$ and $g(\overline{B})\subseteq\overline{A}$.*

Proof. Let $p_{x_0}^{\alpha}$ be an $IVFP$ of X and $\overline{A}\in\sigma$ such that $g(p_{x_0}^{\alpha})\in\overline{A}$. Put $\overline{B}=g^{-1}(\overline{A})$. Then by hypothesis, $\overline{B}$ is an $IVFGSPOS$ in X such that $p_{x_0}^{\alpha}\in\overline{B}$ and $g(\overline{B})=g(g^{-1}(\overline{A}))\subseteq\overline{A}$.

Theorem 3.16. *Let $g:(X,\Im)\to(Y,\sigma)$ be an $IVFGSP$ continuous mapping. Then g is an $IVFSP$ continuous mapping if X is an $IVFSPT_{1/2}$ space.*

Proof. Let $\overline{V}$ be an $IVFCS$ in Y. Then $g^{-1}(\overline{V})$ is an $IVFGSPCS$ in X, by hypothesis. Since X is an $IVFSPT_{1/2}$ space, $g^{-1}(\overline{V})$ is an $IVFSPCS$ in X. Hence g is an $IVFSP$ continuousmapping.

Theorem 3.17. *Let $g:(X,\Im)\to(Y,\sigma)$ be an $IVFGSP$ continuous mapping andlet $h:(Y,\sigma)\to(Z,\eta)$ be an $IVFG$ continuous mapping where Y is an $IVFT_{1/2}$ space. Then $h\circ g:(X,\Im)\to(Z,\eta)$ is an $IVFGSP$ continuous mapping.*

Proof. Let $\overline{V}$ be an $IVFCS$ in Z. Then $h^{-1}(\overline{V})$ is an $IVFGCS$ in Y, by hypothesis. Since Y is an $IVFT_{1/2}$ space, $h^{-1}(\overline{V})$ is an $IVFCS$ in Y. Therefore $g^{-1}(h^{-1}(\overline{V}))$ is an $IVFGSPCS$ in X, by hypothesis. Hence $h\circ g$ is an $IVFGSP$ continuous mapping.

Theorem 3.18. *For any $IVFS$ $\overline{A}$ in $(X,\Im)$ where X is an $IVFSPT_{1/2}$ space, $\overline{A}\in$ $IVFGSPO(X)$ if and only if for every $IVFP$ $p_{x_0}^{\alpha}\in\overline{A}$, there exists an $IVFGSPOS$ $\overline{B}$ in X such that $p_{x_0}^{\alpha}\in\overline{B}\subseteq\overline{A}$.*

Proof. $Necessity$: If $\overline{A}\in IVFGSPO(X)$, then we can take $\overline{B}=\overline{A}$ so that $p_{x_0}^{\alpha}\in\overline{B}\subseteq\overline{A}$ for every $IVFP$ $p_{x_0}^{\alpha}\in\overline{A}$.

$Sufficiency$: Let $\overline{A}$ be an $IVFS$ in $(X,\Im)$ and assume that there exist an $IVFGSPOS$ $\overline{B}$ in X such that $p_{x_0}^{\alpha}\in\overline{B}\subseteq\overline{A}$. Since X is an $IVFSPT_{1/2}$ space, $\overline{B}$ is an $IVFSPOS$ in X. Then $\overline{A}=\bigcup_{p_{x_0}^{\alpha}\in\overline{A}}\{p_{x_0}^{\alpha}\}\subseteq\bigcup_{p_{x_0}^{\alpha}\in\overline{A}}\overline{B}\subseteq\overline{A}$. Therefore $\overline{A}=\bigcup_{p_{x_0}^{\alpha}\in\overline{A}}\overline{B}$, which is an $IVFSPOS$ in X. Since $IVFSPOS$ is an $IVFGSPOS$. $\overline{A}$ is an $IVFGSPOS$ in $(X,\Im)$.

Theorem 3.19. *Let $g:(X,\Im)\to(Y,\sigma)$ be a mapping from $IVFT$ X into $IVFT$ Y. Then the following statements are equivalent if X and Y are $IVFSPT_{1/2}$ space:*

(i) g is an $IVFGSP$ continuous mapping,

(ii) $g^{-1}(\overline{B})$ is an $IVFGSPOS$ in X for each $IVFOS$ $\overline{B}$ in Y,

(iii) for every $IVFP$ $p_{x_0}^{\alpha}$ in X and for every $IVFOS$ $\overline{B}$ in Y such that $g(p_{x_0}^{\alpha})\in\overline{B}$, there exists an $IVFGSPOS$ $\overline{A}$ in X such that $p_{x_0}^{\alpha}\in\overline{A}$ and $g(\overline{A})\subseteq\overline{B}$.

Proof. $(i)\Leftrightarrow(ii)$ is obvious, since $g^{-1}(\overline{A}^c)=(g^{-1}(\overline{A}))^c$.

$(ii)\Rightarrow(iii)$ Let $\overline{B}$ be any $IVFOS$ in Y and let $p_{x_0}^{\alpha}\in D^X$. Given $g(p_{x_0}^{\alpha})\in\overline{B}$. By hypothesis $g^{-1}(\overline{B})$ is an $IVFGSPOS$ in X. Take $\overline{A}=g^{-1}(\overline{B})$. Now $p_{x_0}^{\alpha}\in g^{-1}(g(p_{x_0}^{\alpha}))$. Therefore $g^{-1}(g(p_{x_0}^{\alpha})\in g^{-1}(\overline{B}))=\overline{A}$. This implies $p_{x_0}^{\alpha}\in\overline{A}$ and $g(\overline{A})=g(g^{-1}(\overline{B}))\subseteq\overline{B}$.

$(iii)\Rightarrow(i)$ Let $\overline{A}$ be an $IVFCS$ in Y. Then its complement, say $\overline{B}=\overline{A}^c$ is an $IVFOS$ in Y. Let $p_{x_0}^{\alpha}\in D^X$ and $g(p_{x_0}^{\alpha})\in\overline{B}$. Then there exists an $IVFGSPOS$, say $\overline{C}$ in X such that $p_{x_0}^{\alpha}\in\overline{C}$ and $g(\overline{C})\subseteq\overline{B}$. Now $\overline{C}\subseteq g^{-1}(g(\overline{C}))\subseteq g^{-1}(\overline{B})$. Thus $p_{x_0}^{\alpha}\in g^{-1}(\overline{B})$. Therefore $g^{-1}(\overline{B})$ is an $IVFGSPOS$ in X, by theorem v. That is $g^{-1}(\overline{A}^c)$ is an $IVFGSPOS$ in

X and hence $g^{-1}(\overline{A})$ is an *IVFGSPCS* in X. Thus g is an *IVFGSP* continuous mapping.

Theorem 3.20. *Let $g:(X,\Im)\to(Y,\sigma)$ be a mapping from IVFT X into IVFT Y. Then the following statements are equivalent if X and Y are $IVFSPT_{1/2}$ space:*

(i) g is an IVFGSP continuous mapping,

(ii) for each IVFP $p_{x_0}^{\alpha}$ in X and for every IVFN $\overline{A}$ of $g(p_{x_0}^{\alpha})$, there exists an IVFGSPOS $\overline{B}$ in X such that $p_{x_0}^{\alpha}\in\overline{B}\subseteq g^{-1}(\overline{A})$,

(iii) for each IVFP $p_{x_0}^{\alpha}$ in X and for every IVFN $\overline{A}$ of $g(p_{x_0}^{\alpha})$, there exists an IVFGSPOS $\overline{B}$ in X such that $p_{x_0}^{\alpha}\in\overline{B}$ and $g(\overline{B})\subseteq\overline{A}$.

Proof. $(i)\Leftrightarrow(ii)$ Let $p_{x_0}^{\alpha}\in X$ and let $\overline{A}$ be an *IVFN* of $g(p_{x_0}^{\alpha})$. Then there exist an *IVFOS* $\overline{C}$ in Y such that $g(p_{x_0}^{\alpha})\in\overline{C}\subseteq\overline{A}$. Since g is an *IVFGSP* continuous mapping, $g^{-1}(\overline{C})=\overline{B}(say)$, is an *IVFGSPOS* in X and $p_{x_0}^{\alpha}\in\overline{B}\subseteq g^{-1}(\overline{A})$

$(ii)\Rightarrow(iii)$ Let $p_{x_0}^{\alpha}\in X$ and let $\overline{A}$ be an *IVFN* of $g(p_{x_0}^{\alpha})$. Then there exist an *IVFGSPOS* $\overline{B}$ in X such that $p_{x_0}^{\alpha}\in\overline{B}\subseteq g^{-1}(\overline{A})$, by hypothesis. Therefore $p_{x_0}^{\alpha}\in\overline{B}$ and $g(\overline{B})\subseteq g(g^{-1}(\overline{B}))\subseteq\overline{A}$.

$(iii)\Rightarrow(i)$ Let $\overline{B}$ be an *IVFOS* in Y and let $p_{x_0}^{\alpha}\in g^{-1}(\overline{B})$. Then $g(p_{x_0}^{\alpha})\in\overline{B}$. Therefore $\overline{B}$ is an *IVFN* of $g(p_{x_0}^{\alpha})$. Since $\overline{B}$ is an *IVFOS*, by hypothesis there exists an *IVFGSPOS* $\overline{A}$ in X such that $p_{x_0}^{\alpha}\in\overline{A}\subseteq g^{-1}(g(\overline{A}))\subseteq g^{-1}(\overline{B})$. Therefore $g^{-1}(\overline{B})$ is an *IVFGSPOS* in X, by theorem 3.18. Hence g is an *IVFGSP* continuous mapping.

References

[1] Andrijevic. D, *Semipreopen Sets*, Mat.Vesnik, 38, (1986), 24-32.

[2] Bin Shahna. A.S, *Mappings in Fuzzy Topological spaces*, Fuzzy sets and Systems., 61, (1994), 209-213.

[3] Chang. C. L., *FTSs*. JI. Math. Anal. Appl., 24(1968), 182-190.

[4] Dontchev. J., *On Generalizing Semipreopen sets*, Mem. Fac. sci. Kochi. Univ. Ser. A, Math.,16, (1995), 35-48.

[5] Ganguly. S and Saha. S, *A Note on fuzzy Semipreopen Sets in Fuzzy Topological Spaces*, Fuzzy Sets and System, 18, (1986), 83-96.

[6] Jeyabalan. R, Arjunan. K, *Notes on interval valued fuzzy generalaized semipreclosed sets*, International Journal of Fuzzy Mathematics and Systems.,Vol .3,No.3(2013), 215-224.

[7] Levine. N, *Generalized Closed Sets in Topology*, Rend. Circ. Math. Palermo,19,(1970),89-96.

[8] Levine. N, *Strong Continuity in Topological Spaces*, Amer. Math. Monthly, 67,(1960), 269.

[9] Mondal. T. K., *Topology of Interval Valued Fuzzy Sets*, Indian J. Pure Appl.Math.30 (1999), No.1, 23-38.

[10] Palaniyappan. N and Rao . K. C., *Regular Generalized Closed Sets*, Kyunpook Math. Jour., 33, (1993), 211-219.

[11] Pu Pao-Ming, J.H. park and Lee. B. Y, *Fuzzy Semipreopensets and Fuzzy semiprecontinuos Mapping*, Fuzzy sets and system, 67, (1994), 359-364.

[12] Saraf. R. K and Khanna. K., *Fuzzy Generalized semipreclosed sets*, Jour.Tripura. Math.Soc.,3, (2001), 59-68.

[13] Zadeh. L. A., *Fuzzy sets*, Information and control, Vol.8 (1965), 338-353.

Mathematical model for the role of fluticasone propionate in asthmatic children

N. Kavitha
Department of Mathematics,
University College of Engineering–Pattukkottai
Thanjavur, Tamil Nadu, India.
Email: kavitha977@yahoo.com.sg

***Abstract*- The purposes of this study are to evaluate the efficacy of fluticasone propionate in asthmatic children by using a Mathematical Model when fluticasone propionate was given as maintenance treatment. Studies of biological objects in reliability deal with their reliability function and steady state probabilities for renewable systems. Nevertheless, because there are no infinitely long living objects and any repair is possible only from the state of partial failure, the modeling of degradation process during life period of an object is an interesting topic. The Mathematical results are useful for medical professionals for their future references.**

Keywords- Childhood Asthma: fluticasone propionate: Birth and Death Process: Transirnt Behaviour.

I. INTRODUCTION

Asthma is the most common chronic illness among children [1]. A heightened airway responsiveness (hyper responsiveness) to a variety of stimuli is considered a hallmark of asthma[2.4]. It is characterized by inflamed airways that result in recurring episodes of breathing difficulties. Symptoms may include coughing, wheezing, shortness of breath and chest-tightness[3]. Inflammation makes the airways sensitive to various allergens and irritants in the environment including dust mites, animal dander, pollen, mold, diesel emissions and tobacco smoke. Stress is our body's reaction to a perceived threat. It is often called the "fight or flight" syndrome. It can weaken our immune system, making it harder to fight off disease[12, 14].

II. APPLICATIONS

A. Childhood Asthma

Asthma is the most common chronic illness among children. A heightened airway responsiveness (hyper responsiveness) to a variety of stimuli is considered a hallmark of asthma[6, 8]. It is characterized by inflamed airways that result in recurring episodes of breathing difficulties. Symptoms may include coughing, wheezing, shortness of breath and chest-tightness[9, 10]. Inflammation makes the airways sensitive to various allergens and irritants in the environment [13].

This paper was presented by the author in the National Conference on *Advances in Mathematics and its Applications to Science and Engineering* (AMASE-2016) conducted in Department of Mathematics, University College of Engineering Pattukkottai, Thanjavur, Tamil Nadu, India, on 22nd January 2016.

B. Methodology

This was a randomized, placebo-controlled, double-blind, parallel-group study[8]. The treatment schedule comprised a 4-week run-in, 12-week treatment phase (visit at weeks 0, 4, 8 and 12) and a follow-up 2 weeks after completion.

Table 1: Patient baseline characteristics

Characteristic	FP (n = 79) N (%)	Placebo (n = 81) N (%)

Inclusion criteria for the run-in period were at least two documented episodes of cough and wheeze or physician-diagnosed asthma with one episode within the previous 4 weeks of Visit 1 and age 12-47 months. Inclusion criteria for randomization at the end of the run-in period were; symptom score of ≥ 1 on at least 21/28 days of run-in symptoms on ≥ 3 days for each of the 4 weeks, a total score of wheeze of ≥ 2 over the 28 days of run-in, at least 80% compliance with reporting symptoms and tolerated a face mask, use of a short-acting β_2-against ≥ 2 times in the last week (prn basis). Symptom score definition; 0= no symptoms; 1=mild symptoms, not troublesome; 2=moderate symptoms; 3=severe, troublesome symptoms[8].

Patients were excluded from the run-in period if they had life-threatening asthma (including hospital admission), had received any corticosteroids within the previous 4 weeks, were unable to change from regularly scheduled β_2- agonists or Patients were excluded if during the run-in they had symptoms that were of concern to parents or investigators or if they had received any corticosteroids, β- adrenergic antagonists (including ophthalmic) or immunosuppressive agents[8]. All patients who required treatment during the study were withdrawn [8].

C. Study Design

160 patients (109 boys, 51 girls) were randomized; 79 patients to the fluticasone propionate (FP) group and 81 patients to the placebo group were selected[8]. Blinded study treatment was FP ($2 \times 50\mu$ bd) or placebo (2 puff bd)

both delivered via Babyhaler spacer device with a facemask. Patients received salbutamol to use on an as required basis for relief of asthma symptoms. Parents were instructed in the correct use of study equipment at Visit 1[8].

The primary endpoint was the percentage of symptom-free 24 hour periods (wheeze, cough and shortness of breath) over the entire treatment period. **Secondary efficacy measures included** percentage 24 hour periods with no cough and percentage 24 hour periods with no wheeze, cough and day- and night- time symptomatic use of salbutamol. Separate scores were recorded for wheeze, cough and shortness of breath. Parents reported their child's day and night time symptom scores either once or twice a day. Parents also recorded the number of occasions that salbutamol was given to relieve asthma symptoms[8].

D. Data

A single venous blood sample (4 mL) was collected at Week 12 from 94 patients whose parents consented at four different time intervals relative to the last morning dose: between 1 hour and immediately prior to morning dose; between 15 min and 1.5 hour post-morning dose; between 3 and 8 hour post-morning dose; and between 9 and 11 hour post-morning dose. Plasma was stored at (-20)°C until assayed for fluticasone propionate by using solid phase extraction in combination with liquid chromatography tandem mass spectrometry[8].

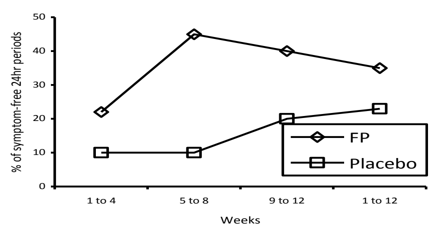

Fig. 1. Effect of FP (100 μg bd) or placebo on % symptom-free 24 hr periods during weeks 1-4, 5-8, 9-12 and 1-12.

III. Mathematical Model

Let us consider a system with only three states, which can be considered as an example, of the aggregated states model, where all states of each group; normal functioning N, degradation D, and failure F are joined into one[5]. Suppose for the simplicity that the failure arise in accordance with the Poissono flow, but the repair times are generally distributed with C.d.f. $B(x)$ and the hazard rate $\beta(x)$. Moreover suppose that the direct transition from normal state into the failure state are also possible with intensity g. The marked transition graph for the process at the Figure 2 is presented.

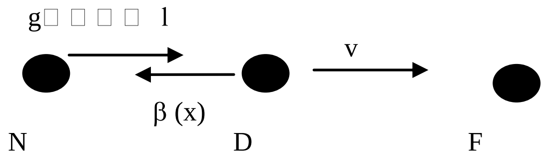

Fig. 2. The Marked Transition Graph of the Process with Aggregated States

In accordance with given transition graph the Kolmogorov's system of differential equations for system states probabilities has the form

Symptoms median (range)				
% Symptom-free 24 h periods	0	(0-24)	0	(0-24)
% Symptom-free 24 h periods of:	4	(0-81)	4	(0-80)
Cough	16	(0-96)	25	(0-93)
Wheeze	1.0	(0-3)	1.0	(0-2)
Day-time symptom scores for:				
Couth	1.0	(0-2)	1.0	(0-2)
Wheeze	1.0	(0-2)	1.0	(0-2)
Shortness of breath	1.0	(0-2)	1.0	(0-2)
Night-time symptom scores for:				
Cough	1.0	(0-2)	1.0	(0-2)
Wheeze	1.0	(0-2)	1.0	(0-2)
Shortness of breath	1.0	(0-2)	0.0	(0-2)
Day-time Ventolin use	1.0	(0-4)	1.0	(0-9)
Night-time Ventolin use	1.0	(0-2)	0.0	(0-3)

$$\begin{cases} \dfrac{d\rho_N(t)}{dt} = -(\lambda+\gamma)\rho_N(t) + \displaystyle\int_0^t \beta(x)\rho_D(t,x)dx \\ \dfrac{\partial\rho_D(t)}{\partial t} + \dfrac{\partial\rho_D(t,x)}{\partial x} = -(v+\beta(x))\rho_D(t,x) \\ \dfrac{d\rho_F(t)}{dt} = \gamma\rho_N(t) + v\rho_D(t,x) \end{cases} \quad \text{... (1)}$$

With the initial and the boundary conditions

$$\begin{cases} \rho_d(t,0) = \lambda\rho_N(t), \\ \rho_N(0) = 1, \rho_D(0,0) = \rho_F(0) = 0. \end{cases} \quad \text{... (2)}$$

The reliability function of the system is

$$R(t) = 1-\rho_F(t) = 1-\int_0^t [\gamma\rho_N(u) + v\rho_D(u)]du. \quad \text{... (3)}$$

where the functions $\rho_N(t)$ and $\rho_D(t,r))$ are the solutions of the two first equations of the system (1) and

$$\rho_D(t) = \int_0^t \rho_D(t,x)dx. \quad \text{... (4)}$$

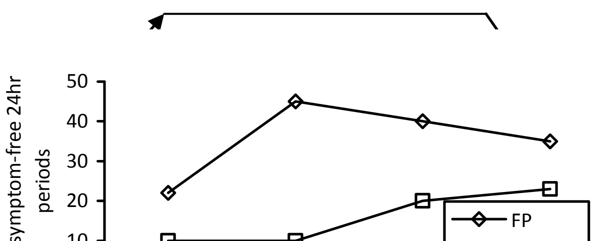

there solution of the second equation from the system (1) accordingly $\rho_i(t,x)=g_i(t-x)$ $(1-A_i(x))(1-B_i(x)), 0\le x\le t<\infty, i\in E$ can be given in the form

$$\rho_D(t,x)=g_D(t-x)e^{-vx}(1-B(x)) \quad \text{... (5)}$$

where the function $g_D(t)$ is determined from the boundary condition (2). It gives

$$\rho_D(t,x)=\lambda\rho_N(t-x)e^{-vx}(1-B(x)).$$

Substitution of this solution into the first equation of the system (1) gives the following equation

$$\frac{d\rho_N(t)}{dt}=-(\lambda+\gamma)\rho_N(t)+\lambda\int_0^t\beta(x)\rho_N(t-x)e^{-vx}\,(1-B(x))dx\cdot \quad \text{... (6)}$$

The best method for its solution is a LT approach. In the terms of LT with the initial condition (2) an equation (6) after the usual order of integration changing takes the form

$$S\hat{\rho}_N(s)-1=-(\lambda+\gamma)\hat{\rho}_N(s)+\lambda\hat{b}(s+v)\hat{\rho}_N(s)$$

Where $\hat{b}(s)=\int_0^\infty e^{-st}b(x)dx$ is a LT of the p.d.f. $b(x)$. It follows from here that the solution of the last equation has a form

$$\hat{\rho}_N(s)=[s+\gamma+\lambda(1-\hat{b}(s+v))]^{-1}. \quad \text{... (7)}$$

Next, the calculation of the LT $\hat{\rho}_D(s)$ of the function $\rho_D(t)$ given by equation (4) after substitution into it of the expression (7) gives

$$\hat{\rho}_D(s)=\int_0^\infty e^{-st}\int_0^t\rho_D(t,x)dxdt=\int_0^\infty e^{-st}\int_0^t\lambda\rho_N(t-x)e^{-vx}(1-b(x))dxdt$$

$$=\frac{\lambda\hat{\rho}_N(s)(1-\hat{b}(s+v))}{s+v}=\frac{\lambda(1-\hat{b}(s+v))}{(s+v)(s+\gamma+\lambda(1-\hat{b}(s+v))}. \quad \text{... (8)}$$

At least for the $LT\hat{\rho}_F(s)$ of the function $\rho_F(t)$ from the last of equations (1) one can find

$$s\hat{\rho}_F(s)=\gamma\hat{\rho}_N(s)+v\hat{\rho}_D(s)=\frac{\gamma(s+v)+\lambda v(1-\hat{b}(s+v))}{(s+v)(s+\gamma+\lambda(1-\hat{b}(s+v)))} \quad \text{... (9)}$$

Therefore, for the LT of the reliability function (3) we get

$$\hat{R}(s)=\frac{1}{s}-\hat{\rho}_F(s)=\frac{1}{s}\left[1=\frac{\gamma(s+v)+\lambda v(1-\hat{b}(s+v))}{(s+v)(s+\gamma+\lambda(1-\hat{b}(s+v)))}\right] \quad \text{... (10)}$$

From the last expression one can find the mean life time of the object

$$m_F=\hat{R}(0)=\frac{v+\lambda(1-\hat{b}(v))}{v(\gamma+\lambda(1-b(v)))}. \quad \text{... (11)}$$

For the calculation of the limiting values of the conditional state probabilities on life period we use the above procedure, which is based on the connection between asymptotic behaviour of the function $\rho_N(t), \rho_D(t), R(t)$ at infinity[11].

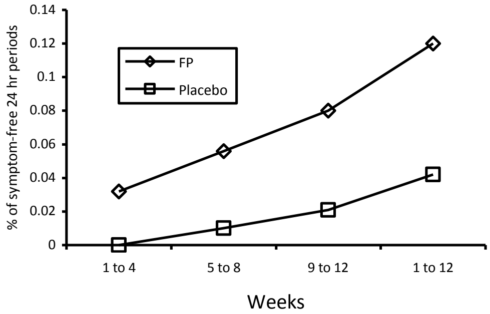

Fig. 3. Effect of FP (100 μg bd) and placebo on LT of $\rho_D(S)$

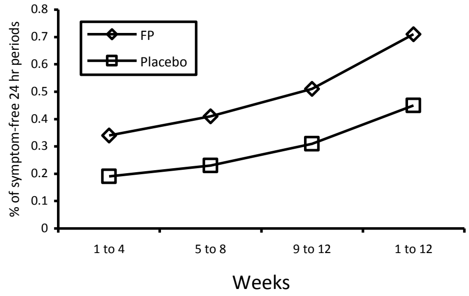

Fig. 4. Effect of FP (100 μg bd) and placebo on LT of $\rho_N(S)$

E. Asymptotic Behaviour

(i) Therefore, when $\gamma\ge v$ the maximal root of the equation $\hat{b}(s+v)=1+\frac{s+\gamma}{\lambda}$ is $-v$ and therefore,

$$\hat{\rho}_N=\lim_{t\to\infty}\hat{\rho}_N(t)=\lim_{t\to\infty}\frac{\rho_N(t)}{R(t)}=\lim_{s\to -v}\frac{\hat{\rho}_N(s)}{\hat{R}(s)}$$

$$=\lim_{s\to -v}\frac{v+s}{s+v+\lambda(1-\hat{b}(s+v))}=\frac{1}{1+\lambda m_B};$$

$$\hat{\rho}_D=\lim_{t\to\infty}\hat{\rho}_D(t)=\lim_{t\to\infty}\frac{\rho_D(t)}{R(t)}=\lim_{s\to -v}\frac{\hat{\rho}_D(s)}{\hat{R}(s)}$$

$$=\lim_{s\to -v}\frac{\lambda(1-\hat{b}(s+v)}{s+v+\lambda(1-\hat{b}(s+v))}=\frac{\lambda m_B}{1+\lambda m_B}. \quad \text{... (12)}$$

that is, if the death intensity from the normal state is grater than the death intensity resulting by degradation then the limiting distribution of the conditional state probabilities is determined by the parameter $\pi = \lambda mB.$

(ii) From another side, under condition $\lambda = v$ the greatest root of the characteristic equation $\Delta(s) = (s+v)(s+\gamma+\lambda(1-\hat{b}(s+v))) = 0$ is the of the equation $\hat{b}(s+v) = 1+\frac{s+\gamma}{\lambda}$, and consequently.

$$\hat{\rho}_N = \lim_{t\to\infty}\hat{\rho}_N(t) = \lim_{t\to\infty}\frac{\rho_N(t)}{R(t)} = \lim_{s\to s_t}\frac{\hat{\rho}_N(s)}{\hat{R}(s)}$$

$$= \lim_{s\to s_1}\frac{v+s}{s+v+\lambda(1-\hat{b}(s+v))} = \frac{s_1+v}{s_1+v+\lambda(1-\hat{b}(s_1+v))};$$

$$\hat{\rho}_D = \lim_{t\to\infty}\hat{\rho}_D(t) = \lim_{t\to\infty}\frac{\rho_D(t)}{R(t)} = \lim_{s\to s_t}\frac{\hat{\rho}_D(s)}{\hat{R}(s)}$$

$$= \lim_{s\to s_t}\frac{\lambda(1-\hat{b}(s+v))}{s+v+\lambda(1-\hat{b}(s+v))} = \frac{\lambda(1-\hat{b}(s_1+v))}{s_1+v+\lambda(1-\hat{b}(s_1-v))}. \quad \text{... (13)}$$

Therefore, if the death intensity from the normal state is less than the same as a degradation result, then the limiting distribution of the conditional probabilities is strongly depend on the value s_1 of the equation. Note that in the case if direct transitions from the normal state to the failure state are impossible, that is when $\gamma = 0$ the second case takes place.

IV. Mathematical Result

This study aimed to evaluate the efficacy of fluticasone propionate (FP) in asthmatic children by using the Mathematical modeling. Generalized Birth and Death Processes, which are the special case of Semi-Markov Processes, are introduced for modeling the degradation processes. The special parameterization of the process allows to give more convenient presentation of the results. The special attention was focused to the conditional state probabilities, which are the mostly interesting for the degradation processes. Figure 3 and 4 showed the greatest response to fluticasone propionate treatment as fluticasone propionate patients had a significantly higher values in the upper curves.

References

[1] American Thoracic Society 1999, 'Recommendation for standardized procedures for the Online and Offline measurement of Exhaled lower respiratory Nitric Oxide and Nasal Nitric Oxide in Adults and Children', American Journal of Respiratory and Critical Care Medicine, vol. 160, pp. 2104-2117.

[2] Arnetz, BB, Wasserman, J, Petrini, B, Brenner, SO, Levi, L, Eneroth, P, Salovaara, H, Hjelm, R, Sallovaara, L & Theorell, T 1987, 'Immune function in unemployed women', Psychosomatic Medicine, vol. 49, pp. 3-12.

[3] Ayres, JG & Clark, TJH 1983, 'Alcoholic drinks and asthma: a survey', British Journal of Diseases of the Chest, vol. 77, pp. 370-375.

[4] Boner, AL & Martinati, LC 1997, 'Diagnosis of asthma in children and adolescents', European Respiratory Review, vol. 7, pp. 3-7.

[5] Dimitrov, B., V.Rykov and P. Stanhev, (2002), On Multi-State Reliability Systems, In: Proceedings MMR 2002, Troudhelin (Norway) June 17-21, 2002.

[6] International consensus report on diagnosis and treatment of asthma, National Heart, Lung and Blood Institute, National Institutes of Health Bethesda 1992, European Respiratory of Journal, vol. 5, pp. 601-641.

[7] Karin, C., Lodrup Carlsen, Steve Stick, Wolfgang Kamin, leva Cirule, Sara Hughes and Claire Wixon, (2005), "The efficacy and safty of fluticasone propionate in very young children with persistent asthma symptoms", *Respiratory Medicine*, **99**:1393-1402.

[8] Kay, AB 1991, 'Asthma and inflammation', Journal of Allergy and Clinical Immunology, vol. 87, pp. 893-911.

[9] Koh, YY, Lim, HS, Min, KU & Kim, YY 1996, 'Maximal airway narrowing on the dose-response curve to methacholine is increased after exercise-induced bronchoconstriction', Journal of Asthma, vol. 33, pp. 55-65.

[10] Lisniansky, A. and G.Levitin, (2003), Multi-State System Reliability, Assessment, *Optimization and Application,* World Scientific, New Jersey, London, Singapore, Hong Kong, 358.

[11] McDonald, D., (1978), On semi-Markov and Semi-Regenerative Process I, II/Z. Fur Wahrach, Verw. Geb., **42**(2): 261-377; *Ann of Prob.*, **6**(6):995-1014.

[12] Perreault, T & Gutkowska, J 1995, 'State of the art. Role of atrial natriuretic factor in lung physiology and pathology', American Journal of Respiratory and Critical Care Medicine, vol. 151, pp. 226-242.

[13] Schoenwetter, WF 2000, 'Allergic Vhinitis: epidemiology and natural history', Allergy and Asthma Proceedings, vol. 21, pp. 1-6.

[14] Stenton, SC, Avery, AJ, Walters, EH & Hendrick, DJ 1994, 'Statistical approaches to the identification of late asthmatic reactions', European Respiratory Journal, vol. 7, pp. 806-812.

Global Journal of Pure and Applied Mathematics (GJPAM) ISSN 0973-1768 Volume 12,Number 4 (2016)

A study on Q-intuitionistic L-fuzzy subsemiring of a semiring

*S. Sampathu**
Department of Mathematics,
Sri Muthukumaran College of Education,
Chennai, Tamil Nadu, India.
Email: sampathugokul@yahoo.in

S. Anita Shanthi
Department of Mathematics,
Annamalai University,
Tamil Nadu, India.
Email: shanthi.Anita@yahoo.com

A. Praveen Prakash
Department of Mathematics,
Hindustan University,
Chennai, Tamil Nadu, India.
Email: apraveenprakash@gmail.com

***Abstract*— In this paper, we made an attempt to study the algebraic nature of Q-intuitionistic L-fuzzy subsemiring of a semiring.**

Keywords- fuzzy subset, (Q, L)-fuzzy subset, (Q,L)-fuzzy subsemiring, Q-intuitionistic L-fuzzy subset, Q-intuitionistic L-fuzzy subsemiring, Q-intuitionistic L-fuzzy relation, Product of Q-intuitionistic L-fuzzy subsets.

2000 AMS Subject classification: 03F55, 06D72, 08A72.

I. INTRODUCTION

After the introduction of fuzzy sets by L.A.Zadeh [25], several researchers explored on the generalization of the concept of fuzzy sets. The concept of intuitionistic fuzzy subset was introduced by K.T.Atanassov [5, 6], as a generalization of the notion of fuzzy set. The notion of fuzzy subnearrings and ideals was introduced by S.Abou Zaid [1]. A.Solairaju and R.Nagarajan [21, 22] have introduced and defined a new algebraic structure called Q-fuzzy subgroups. In this paper, we introduce the some theorems in Q-intuitionistic L-fuzzy subsemiring of a semiring and established some results.

II. PRELIMINARIES

Definition 2.1. [25] Let X be a non–empty set. A fuzzy subset A of X is a function A: $X \to [0, 1]$.

Definition 2.2. [21,22] *Let X be a non-empty set and L= (L, ≤) be a lattice with least element 0 and greatest element 1 and Q be a non-empty set. A (Q, L)-fuzzy subset A of X is a function A: $X\times Q \to L$.*

Definition 2.3. [18] *Let (R, +, ·) be a semiring and Q be a non empty set. A (Q, L)- fuzzy subset A of R is said to be a (Q, L)-fuzzy subsemiring (QLFSSR) of R if the following conditions are satisfied:*

(i) $A(x+y, q) \geq A(x, q) \wedge A(y, q)$,

(ii) $A(xy, q) \geq A(x, q) \wedge A(y, q)$, for all x and y in R and q in Q.

Example 2.4. Let (N , + , •) be a semiring and Q={p}, Then the (Q, L)-Fuzzy Set □ of N is defined by

$$A(x) = \begin{cases} 0.63 & \text{if x is even} \\ 0.27 & \text{if x is odd.} \end{cases}$$

Clearly A is an (Q, L)-Fuzzy subsemiring.

Definition 2.5. [5,6] *An intuitionistic fuzzy subset (IFS) A in X is defined as an object of the form $A = \{\langle x, \mu_A(x), \nu_A(x)\rangle / x \in X\}$, where $\mu_A : X \to [0,1]$ and $\nu_A : X \to [0,1]$ define the degree of membership and the degree of non-membership of the element $x \in X$ respectively and for every $x \in X$ satisfying $0 \leq \mu_A(x) + \nu_A(x) \leq 1$.*

Definition 2.6. *Let (L, ≤) be a complete lattice with an involutive order reversing operation N: $L \to L$ and Q be a nonempty set. A Q-intuitionistic L-fuzzy subset (QILFS) A in X is defined as an object of the form $A=\{< (x, q), \mu_A(x, q), \nu_A(x, q) > / x$ in X and q in Q$\}$, where $\mu_A : X\times Q \to L$ and $\nu_A : X\times Q \to L$ define the degree of membership and the degree of non-membership of the element $x \in X$ respectively and for every $x \in X$ satisfying $\mu_A(x) \leq N(\nu_A(x))$.*

Definition 2.7. *Let A and B be any two Q-intuitionistic L-fuzzy subsets of a set X. We define the following operations:*

i) $(A \cap B = \{ \langle x, \mu_A(x,q) \wedge \mu_B(x,q), \nu_A(x,q) \vee \nu_B(x,q) \rangle \}$, for all $x \in X$ and q in Q. (ii) $A \cup B = \{ \langle x, \mu_A(x,q) \vee \mu_B(x,q), \nu_A(x,q) \wedge \nu_B(x,q) \rangle \}$, for all $x \in X$ and q in Q. (iii) □A= $\{ \langle x, \mu_A(x,q), 1 - \mu_A(x,q) \rangle / x \in X \}$, for all x in X and q in Q. (iv) ◊A = $\{ \langle x, 1 - \nu_A(x,q), \nu_A(x,q) \rangle / x \in X \}$, for all x in X and q in Q.

Definition 2.8. *Let R be a semiring. A Q-intuitionistic L-fuzzy subset A of R is said to be a Q-intuitionistic L-fuzzy subsemiring (QILFSSR) of R if it satisfies the following conditions:*

(i)$\mu_A(x + y,q) \geq \mu_A(x,q) \wedge \mu_A(y,q)$, (ii)$\mu_A(xy,q) \geq \mu_A(x,q) \wedge \mu_A(y,q)$,(iii)$\nu_A(x + y,q) \leq \nu_A(x,q) \vee \nu_A(y,q)$,(iv)$\nu_A(xy,q) \leq \nu_A(x,q) \vee \nu_A(y,q)$, for all x and y in R and q in Q.

Definition 2.9. Let A and B be any two Q-intuitionistic L-fuzzy subsemiring of a semiring G and H, respectively. The

*Corresponding author.

This paper was presented by the first author in the National Conference on *Advances in Mathematics and its Applications to Science and Engineering* (AMASE-2016) conducted in Department of Mathematics, University College of Engineering Pattukkottai, Thanjavur, Tamil Nadu, India, on 22nd January 2016.

Global Journal of Pure and Applied Mathematics (GJPAM) ISSN 0973-1768 Volume 12,Number 4 (2016)

product of A and B, denoted by A×B, is defined as A×B = { ⟨ (x,y),q), $\mu_{A\times B}((x,y),q)$, $\nu_{A\times B}((x,y),q)$ ⟩ / for all x in G and y in H and q in Q }, where $\mu_{A\times B}((x,y),q) = \mu_A(x,q) \wedge \mu_B(y,q)$ and $\nu_{A\times B}((x,y),q) = \nu_A(x,q) \vee \nu_B(y,q)$.

Definition 2.10. *Let A be an Q-intuitionistic L-fuzzy subset in a set S, the strongest Q-intuitionistic L-fuzzy relation on S, that is a Q-intuitionistic L-fuzzy relation on A is V given by* $\mu_V((x,y),q) = \mu_A(x,q) \wedge \mu_A(y,q)$ *and* $\nu_V((x,y),q) = \nu_A(x,q) \vee \nu_A(y,q)$*, for all x and y in S and q in Q.*

Definition 2.11. *Let (R, +, •) and (R', +, •) be any two semirings. Let* $f : R \rightarrow R'$ *be any function and A be an Q-intuitionistic L-fuzzy subsemiring in R, V be an Q-intuitionistic L-fuzzy subsemiring in f(R) = R', defined by* $\mu_v(y,q) = \sup_{x\in f^{-1}(y)} \mu_A(x,q)$ *and* $\nu_V(y,q) = \inf_{x \in f^{-1}(y)} \nu_A(x,q)$*, for all x in R and y in R'. Then A is called a preimage of V under f and is denoted by* $f^{-1}(V)$.

Definition 2.12. *Let A be an Q-intuitionistic L-fuzzy subsemiring of a semiring (R, +, •) and a in R. Then the pseudo Q-intuitionistic L-fuzzy coset* $(aA)^p$ *is defined by* $((a\mu_A)^p)(x,q) = p(a)\mu_A(x,q)$ *and* $((a\nu_A)^p)(x,q) = p(a)\nu_A(x,q)$*, for every x in R and for some p in P and q in Q.*

III. PROPERTIES OF Q-INTUITIONISTIC L-FUZZY SUBSEMIRING OF A SEMIRING R

Theorem 3.1. *Intersection of any two Q-intuitionistic L-fuzzy subsemiring of a semiring R is a Q-intuitionistic L-fuzzy subsemiring of R.*

Proof. *Let A and B be any two Q-intuitionistic L-fuzzy subsemirings of a semiring R and x and y in R and q in Q. Let* $A=\{(x,q),\mu_A(x,q),\nu_A(x,q))/ x\in R$ *and q in Q} and* $B=\{(x,q),\mu_B(x,q),\nu_B(x,q))/x\in R$ *and q in Q} and also let* $C=A\cap B=\{(x,q),\mu_C(x,q), \nu_C(x,q))/x\in R$ *and q in Q},where* $\mu_A(x,q)\wedge\mu_B(x,q)=\mu_C(x,q)$ *and* $\nu_A(x,q)\vee\nu_B(x,q)= \nu_C(x,q)$. *Now,*$\mu_C(x+y,q)=\mu_A(x+y,q)\wedge\mu_B(x+y,q)\geq\{\mu_A(x,q)\wedge\mu_A(y,q)\}\wedge\{\mu_B(x,q)\wedge\mu_B(y,q)\}=\{\mu_A(x,q)\wedge\mu_B(x,q)\}\wedge\{\mu_A(y,q)\wedge\mu_B(y,q)\}=\mu_C(x,q)\wedge\mu_C(y,q)$.*Therefore,* $\mu_C(x+y,q) \geq \mu_C(x,q)\wedge\mu_C(y,q)$, *for all x and y in R and q in Q. And,* $\mu_C(xy,q) = \mu_A(xy,q)\wedge\mu_B(xy,q)\geq\{\mu_A(x,q)\wedge\mu_A(y,q)\}\wedge\{\mu_B(x,q)\wedge\mu_B(y,q)\}=\{\mu_A(x,q)\wedge\mu_B(x,q)\}\wedge\{\mu_A(y,q)\wedge\mu_B(y,q)\}\}=\mu_C(x,q)\wedge\mu_C(y,q)$. *Therefore,* $\mu_C(xy,q)\geq\mu_C(x,q)\wedge\mu_C(y,q)$, *for all x and y in R and q in Q. Now,* $\nu_C(x+y,q)=\nu_A(x+y,q)\vee\nu_B(x+y,q)\leq\{\nu_A(x,q)\vee\nu_A(y,q)\}\vee\{\nu_B(x,q)\vee\nu_B(y,q)\}=\{\nu_A(x,q)\vee\nu_B(x,q)\}\vee\{\nu_A(y,q)\vee\nu_B(y,q)\}=\nu_C(x,q)\vee\nu_C(y,q)$. *Therefore,* $\nu_C(x+y,q)\leq\nu_C(x,q)\vee \nu_C(y,q)$, *for all x and y in R and q in Q. And,* $\nu_C(xy,q)=\nu_A(xy,q)\vee\nu_B(xy,q)\leq \{\nu_A(x,q)\vee\nu_A(y,q)\}\vee\{\nu_B(x,q)\vee \nu_B(y,q)\}\}=\{\nu_A(x,q)\vee \nu_B(x,q) \}\vee \{ \nu_A(y,q)\vee \nu_B(y,q)\}\} = \nu_C(x,q)\vee \nu_C(y,q)$ *.Therefore,* $\nu_C(xy,q) \leq\nu_C(x,q)\vee \nu_C(y,q)$ *, for all x and y in R and q in Q. Therefore C is a Q-intuitionistic L-fuzzy subsemiring of R. Hence the Q-intersection of any two Q-intuitionistic L-fuzzy subsemirings of a semiring R is an Q-intuitionistic L-fuzzy subsemiring of R.*

Theorem 3.2. *The intersection of a family of Q-intuitionistic L-fuzzy subsemirings of semiring R is a Q-intuitionistic L-fuzzy subsemiring of R.*

Proof. Let $\{V_i : i\in I\}$ be a family of Q-intuitionistic L-fuzzy subsemirings of a semiring R and let $A= \bigcap_{i\in I} V_i$. Let x and y in R and q in Q. Then, $\mu(x+y)= \inf_{i \in I} \mu_{Vi}(x+y) \geq \inf_{i \in I} \{\mu_{Vi}(x)\wedge\mu_{Vi}(y)\}= \inf_{i \in I} \mu_{Vi}(x)\wedge \inf_{i \in I} \mu_{Vi}(y) =\mu_A(x)\wedge\mu_A(y)$. Therefore, $\mu_A(x+y)\geq \mu_A(x) \wedge\mu_A(y)$, for all x and y in R and q in Q. And, $\mu_A(xy)= \inf_{i \in I} \mu_{Vi}(xy)\geq \inf_{i \in I} \{\mu_{Vi}(x)\wedge\mu_{Vi}(y)\}= \inf_{i \in I} \mu_{Vi}(x)\wedge \inf_{i \in I} \mu_{Vi}(y)=\mu_A(x)\wedge\mu_A(y)$. Therefore, $\mu_A(xy)\geq\mu_A(x)\wedge\mu_A(y)$, for all x and y in R and q in Q. Now, $\nu_A(x+y)= \sup_{i \in I} \nu_{Vi}(x+y)\leq \sup_{i \in I} \{\nu_{Vi}(x)\vee\nu_{Vi}(y)\}= \sup_{i \in I} \nu_{Vi}(x)\vee \sup_{i \in I} \nu_{Vi}(y)=\nu_A(x)\vee\nu_A(y)$. Therefore, $\nu_A(x+y)\leq\nu_A(x)\vee\nu_A(y)$, for all x and y in R and q in Q. And, $\nu_A(xy)= \sup_{i \in I} \nu_{Vi}(xy)\leq \sup_{i \in I} \{\nu_{Vi}(x)\vee\nu_{Vi}(y)\}= \sup_{i \in I} \nu_{Vi}(x)\vee \sup_{i \in I} \nu_{Vi}(y)=\nu_A(x)\vee\nu_A(y)$. Therefore, $\nu_A(xy)\leq \nu_A(x)\vee\nu_A(y)$, for all x and y in R. That is, A is a Q-intuitionistic L-fuzzy subsemiring of a semiring R. Hence, the Q-intersection of a family of Q-intuitionistic L-fuzzy subsemirings of R is a Q-intuitionistic L-fuzzy subsemiring of R.

Theorem 3.3. *If A and B are any two Q-intuitionistic L-fuzzy subsemirings of the semirings* R_1 *and* R_2 *respectively, then A×B is a Q-intuitionistic L-fuzzy subsemiring of* $R_1\times R_2$.

Proof. Let A and B be two Q-intuitionistic L-fuzzy subsemirings of the semirings R_1 and R_2 respectively. Let x_1 and x_2 be in R_1, y_1 and y_2 be in R_2 and q in Q. Then (x_1,y_1) and (x_2,y_2) are in $R_1\times R_2$. Now, $\mu_{A\times B}[((x_1,y_1)+(x_2,y_2)),q]=\mu_{A\times B}((x_1+x_2,y_1+y_2),q)=\mu_A((x_1+x_2),q)\wedge \mu_B((y_1+y_2),q)\geq\{\{\mu_A(x_1,q)\wedge\mu_A(x_2,q)\}\wedge\{\mu_B(y_1,q)\wedge\mu_B(y_2,q)\}\} =\{\{\mu_A(x_1,q)\wedge\mu_B(y_1,q)\}\wedge\{\mu_A(x_2,q)\wedge\mu_B(y_2,q)\}\}=\mu_{A\times B}((x_1,y_1),q)\wedge \mu_{A\times B}((x_2,y_2),q)$.Therefore,$\mu_{A\times B}[((x_1,y_1)+(x_2,y_2)),q]\geq\mu_{A\times B}((x_1,y_1),q)\wedge\mu_{A\times B}((x_2,y_2),q)$.Also,$\mu_{A\times B}[((x_1,y_1)(x_2,y_2)),q)]=\mu_{A\times B}((x_1x_2,y_1y_2),q)=\mu_A(x_1x_2,q)\wedge\mu_B(y_1y_2,q)\geq\{\{\mu_A(x_1,q)\wedge\mu_A(x_2,q)\}\wedge\{\mu_B(y_1,q)\wedge\mu_B(y_2,q)\}\}=\{\{\mu_A(x_1,q)\wedge\mu_B(y_1,q)\}\wedge\{\mu_A(x_2,q)\wedge\mu_B(y_2,q)\}\} =\mu_{A\times B}((x_1,y_1),q)\wedge\mu_{A\times B}((x_2,y_2),q)$.Therefore,$\mu_{A\times B}[((x_1,y_1)(x_2,y_2)),q]\geq\mu_{A\times B}((x_1,y_1),q)\wedge\mu_{A\times B}((x_2,y_2),q)$.
Now,$\nu_{A\times B}[((x_1,y_1)+(x_2,y_2),q)]=\nu_{A\times B}((x_1+x_2,y_1+y_2),q)= \nu_A((x_1+x_2),q)\vee\nu_B((y_1+y_2),q)\leq\{\{\nu_A(x_1,q)\vee\nu_A(x_2,q)\}\vee\{\nu_B(y_1,q)\vee \nu_B(y_2,q)\}\}=\{\{\nu_A(x_1,q)\vee\nu_B(y_1,q)\}\vee\{\nu_A(x_2,q)\vee\nu_B(y_2,q)\}\} =\nu_{A\times B}((x_1,y_1),q)\vee\nu_{A\times B}((x_2,y_2),q)$.Therefore, $\nu_{A\times B}[((x_1,y_1)+(x_2,y_2),q)]\leq\nu_{A\times B}((x_1,y_1),q)\vee\nu_{A\times B}((x_2,y_2),q)$.
Also,$\nu_{A\times B}[(x_1,y_1)(x_2,y_2),q]=\nu_{A\times B}((x_1x_2,q)(y_1y_2,q))=\nu_A(x_1x_2,q)\vee \nu_B(y_1y_2,q)\leq\{\nu_A(x_1,q)\vee\nu_A(x_2,q)\}\vee\{\nu_B(y_1,q)\vee\nu_B(y2,q)\}\} =\{\{\nu_A(x_1,q)\vee\nu_B(y_1,q)\}\vee\{\nu_A(x_2,q)\vee\nu_B(y_2,q)\}= \nu_{A\times B}((x_1,y_1),q)\vee \nu_{A\times B}((x_2,y_2),q)$. Therefore, $\nu_{A\times B}[((x_1,y_1)(x_2,y_2)),q]\leq \nu_{A\times B}((x_1, y_1), q) \vee \nu_{A\times B}((x_2, y_2),q)$. Hence A×B is a Q-intuitionistic L-fuzzy subsemiring of semiring of $R_1\times R_2$.

Theorem 3.4. *Let A be a Q-intuitionistic L-fuzzy subset of a semiring R and V be the strongest Q-intuitionistic L-fuzzy relation of R. Then A is a Q-intuitionistic L-fuzzy subsemiring of R if and only if V is a Q-intuitionistic L-fuzzy subsemiring of R×R.*

Proof. Suppose that A is a Q-intuitionistic L-fuzzy subsemiring of a semiring R. Then for any $x=(x_1,x_2)$ and $y=(y_1,y_2)$ are in R×R and q in Q . We have, $\mu_V((x+y),q) =\mu_V[((x_1,x_2)+(y_1,y_2)),q)]=\mu_V((x_1+y_1,x_2+y_2),q)=\mu_A((x_1+y_1),q)\wedge \mu_A((x_2+y_2),q)\geq\{\{\mu_A(x_1,q)\wedge\mu_A(y_1,q)\}\wedge\{\mu_A(x_2,q)\wedge\mu_A(y_2,q)\}\}= \{\{\mu_A(x_1,q)\wedge\mu_A(x_2,q)\}\wedge\{\mu_A(y_1,q)\wedge\mu_A(y_2,q)\}\}= \mu_V((x_1,x_2),q)\wedge\mu_V((y_1, y_2),q)=\mu_V(x,q)\wedge\mu_V(y,q)$. Therefore, $\mu_V((x+y),q)\geq\mu_V(x,q)\wedge\mu_V(y,q)$, for all x and y in R×R and q in Q.And,$\mu_V(xy,q)=\mu_V[((x_1,x_2)(y_1,y_2),q)]=\mu_V((x_1y_1,x_2y_2),q)= \mu_A(x_1y_1,q)\wedge\mu_A(x_2y_2,q)\geq\{\{\mu_A(x_1,q)\wedge\mu_A(y_1,q)\}\wedge\{\mu_A(x_2,q)\wedge \mu_A(y_2,q)\}\}=\{\{\mu_A(x_1,q)\wedge\mu_A(x_2,q)\}\wedge\{\mu_A(y_1,q)\wedge\mu_A(y_2,q)\}\}= \{\mu_V((x_1,x_2),q)\wedge\mu_V((y_1,y_2),q)\}=\{\mu_V(x,q)\wedge\mu_V(y,q)\}$.Therefore, $\mu_V(xy,q)\geq\mu_V(x,q)\wedge\mu_V(y,q)$, for all x and y in R×R and q in Q.

Wehave,$\nu_V((x+y),q)=\nu_V[((x_1,x_2)+(y_1,y_2),q)]=\nu_V((x_1+y_1, x_2+y_2),q)=\nu_A((x_1+y_1),q)\vee\nu_A((x_2+y_2),q)\}\leq\{\{\nu_A(x_1,q)\vee\nu_A(y_1,q)\}\vee\{\nu_A(x_2,q)\vee\nu_A(y_2,q)\}\}=\{\{\nu_A(x_1,q)\vee\nu_A(x_2,q)\}\vee\{\nu_A(y_1,q)\vee\nu_A(y_2,q)\}\}=\{\nu_V((x_1,x_2),q)\vee\nu_V((y_1,y_2),q)\}=\nu_V(x,q)\vee\nu_V(y,q)$.Therefore, $\nu_V((x+y),q)\leq\nu_V(x,q)\vee\nu_V(y,q)$, for all x and y in R×R and q in Q.And, $\nu_V(xy,q)=\nu_V[((x_1,x_2)(y_1,y_2),q)]=\nu_V((x_1y_1,x_2y_2),q)=\nu_A(x_1y_1,q)\vee\nu_A(x_2y_2,q)\leq\{\{\nu_A(x_1,q)\vee\nu_A(y_1,q)\}\vee\{\nu_A(x_2,q),\nu_A(y_2,q)\}\}=\{\{\nu_A(x_1,q)\vee\nu_A(x_2,q)\}\vee\{\nu_A(y_1,q)\vee\nu_A(y_2,q)\}\}=\nu_V((x_1,x_2),q)\vee\nu_V((y_1,y_2),q)=\nu_V(x,q)\vee\nu_V(y,q)$. Therefore, $\nu_V(xy,q)\leq\nu_V(x,q)\vee\nu_V(y,q)$, for all x and y in R×R and q in Q. This proves that V is a Q-intuitionistic L-fuzzy subsemiring of R×R. Conversely assume that V is a Q-intuitionistic L-fuzzy subsemiring of R×R, then for any $x=(x_1,x_2)$ and $y=(y_1,y_2)$ are in R×R and q in Q , we have $\mu_A((x_1+y_1),q)\wedge\mu_A((x_2+y_2),q)=\mu_V((x_1+y_1,x_2+y_2),q)=\mu_V[((x_1,x_2),q)+((y_1,y_2),q)]=\mu_V((x+y),q)\geq\mu_V(x,q)\wedge\mu_V(y,q)=\mu_V((x_1,x_2),q)\wedge\mu_V((y_1,y_2),q)=\{\{\mu_A(x_1,q)\wedge\mu_A(x_2,q)\}\wedge\{\mu_A(y_1,q),\mu_A(y_2,q)\}\}$. If $\mu_A((x_1+y_1),q)\leq\mu_A((x_2+y_2),q)$, $\mu_A(x_1,q)\leq\mu_A(x_2,q)$, $\mu_A(y_1,q)\leq\mu_A(y_2,q)$, we get, $\mu_A((x_1+y_1),q)\geq\mu_A(x_1,q)\wedge\mu_A(y_1,q)$, for all x_1 and y_1 in R and q in Q. And, $\mu_A(x_1y_1),q)\wedge\mu_A(x_2y_2),q)\}=\mu_V((x_1y_1,x_2y_2),q)=\mu_V[((x_1,x_2)(y_1,y_2),q)]=\mu_V(xy,q)\geq\mu_V(x,q)\wedge\mu_V(y,q)=\mu_V((x_1,x_2),q)\wedge\mu_V((y_1,y_2),q)\}=\{\{\mu_A(x_1,q)\wedge\mu_A(x_2,q)\}\wedge\{\mu_A(y_1,q)\wedge\mu_A(y_2,q)\}\}$. If $\mu_A(x_1y_1,q)\leq\mu_A(x_2y_2,q)$, $\mu_A(x_1,q)\leq\mu_A(x_2,q)$, $\mu_A(y_1,q)\leq\mu_A(y_2,q)$, we get $\mu_A(x_1y_1,q)\geq\mu_A(x_1,q)\wedge\mu_A(y_1,q)$, for all x_1 and y_1 in R and q in Q. We have $\nu_A((x_1+y_1),q)\vee\nu_A((x_2+y_2),q)=\nu_V((x_1+y_1,x_2+y_2),q)=\nu_V[((x_1,x_2)+(y_1,y_2),q)]=\nu_V(x+y,q)\leq\nu_V(x,q)\vee\nu_V(y,q)=\nu_V((x_1,x_2),q)\vee\nu_V((y_1,y_2),q)=\{\{\nu_A(x_1,q)\vee\nu_A(x_2,q)\}\vee\{\nu_A(y_1,q)\vee\nu_A(y_2,q)\}\}$.If$\nu_A(x_1+y_1,q)\geq\nu_A(x_2+y_2,q)$,$\nu_A(x_1,q)\geq\nu_A(x_2,q)$,$\nu_A(y_1,q)\geq\nu_A(y_2,q)$,weget, $\nu_A(x_1+y_1,q)\leq\nu_A(x_1,q)\vee\nu_A(y_1,q)$, for all x_1 and y_1 in R and q in Q. And, $\nu_A(x_1y_1,q)\vee\nu_A(x_2y_2,q)=\nu_V((x_1y_1,x_2y_2),q)=\nu_V[((x_1,x_2),(y_1,y_2)),q)]=\nu_V(xy,q)\leq\nu_V(x,q)\vee\nu_V(y,q)=\nu_V((x_1,x_2),q)\vee\nu_V((y_1,y_2),q)=\{\{\nu_A(x_1,q)\vee\nu_A(x_2,q)\}\vee\{\nu_A(y_1,q),\nu_A(y_2,q)\}\}$. If $\nu_A(x_1y_1,q)\geq\nu_A(x_2y_2,q)$, $\nu_A(x_1,q)\geq\nu_A(x_2,q)$, $\nu_A(y_1,q)\geq\nu_A(y_2,q)$, we get $\nu_A(x_1y_1,q)\leq\nu_A(x_1,q)\vee\nu_A(y_1,q)$, for all x_1 and y_1 in R and q in Q. Therefore A is a Q-intuitionistic L-fuzzy subsemiring of R.

Theorem 3.5. *If A is a Q-intuitionistic L-fuzzy subsemiring of a semiring (R, +,•), then H={x/x∈R: $\mu_A(x,q)=1,\nu_A(x,q)=0$} is either empty or is a subsemiring of R.*

Proof. If no element satisfies this condition, then H is empty. If x and y in H and q in Q, then $\mu_A(x+y,q)\geq\mu_A(x,q)\wedge\mu_A(y,q)=1\wedge1=1$. Therefore, $\mu_A(x+y,q)=1$. And $\mu_A(xy,q)\geq\mu_A(x,q)\wedge\mu_A(y,q)=1\wedge1=1$. Therefore, $\mu_A(xy,q)=1$. Now, $\nu_A(x+y,q)\leq\nu_A(x,q)\vee\nu_A(y,q)=0\vee0=0$.Therefore,$\nu_A(x+y,q)=0$.And$\nu_A(xy,q)\leq\nu_A(x,q)\vee\nu_A(y,q)=0\vee0=0$. Therefore, $\nu_A(xy,q)=0$. We get x+y, xy in H. Therefore, H is a subsemiring of R. Hence H is either empty or is a subsemiring of R.

Theorem 3.6. *If A be a Q-intuitionistic L-fuzzy subsemiring of a semiring (R, +, •), then (i) if $\mu_A(x+y,q)=0$, then either $\mu_A(x,q)=0$ or $\mu_A(y,q)=0$, for all x and y in R and q in Q. (ii) if $\mu_A(x+y,q)=1$, then either $\mu_A(x,q)=1$ or $\mu_A(y,q)=1$, for all x and y in R and q in Q.*

Proof. Let x and y in R and q in Q. (i) By the definition $\mu_A(x+y,q)\geq\mu_A(x)\wedge\mu_A(y)$, which implies that $0\geq\mu_A(x,q)\wedge\mu_A(y,q)$. Therefore, either $\mu_A(x,q)=0$ or $\mu_A(y,q)=0$.(ii) By the definition $\mu_A(x+y,q)\leq\mu_A(x,q)\vee\mu_A(y,q)$, which implies that $1\leq\mu_A(x,q)\vee\mu_A(y,q)$. Therefore, either $\mu_A(x,q)=1$ or $\mu_A(y,q)=1$.

Theorem 3.7. *If A is a Q-intuitionistic L-fuzzy subsemiring of a semiring (R, +, •), then H={⟨(x,q),$\mu_A(x,q)$⟩:0<$\mu_A(x,q)\leq1$and $\nu_A(x,q)=0$} is either empty or is a subsemiring of R.*

Proof. If no element satisfies this condition, then H is empty. If x and y satisfies this condition, then $\nu_A(x+y,q)\leq\nu_A(x,q)\vee\nu_A(y,q)=0\vee0=0$. Therefore, $\nu_A(x+y,q)=0$, for all x and y in R and q in Q. And, $\nu_A(xy,q)\leq\nu_A(x,q)\vee\nu_A(y,q)=0\vee0=0$. Therefore, $\nu_A(xy,q)=0$, for all x and y in R and q in Q. And, $\mu_A(x+y,q)\geq\mu_A(x,q)\wedge\mu_A(y,q)$.Therefore,$\mu_A(x+y,q)\geq\mu_A(x,q)\wedge\mu_A(y,q)$, for all x and y in R and q in Q. And, $\mu_A(xy,q)\geq\mu_A(x,q)\wedge\mu_A(y,q)$. Therefore, $\mu_A(xy,q)\geq\mu_A(x,q)\wedge\mu_A(y,q)$, for all x and y in R and q in Q. Hence H is a fuzzy subsemiring of R. Therefore, H is either empty or is a subsemiring of R.

Theorem 3.8. *If A is a Q-intuitionistic L-fuzzy subsemiring of a semiring (R, +, •) then H={⟨(x,q),$\mu_A(x,q)$⟩:0<$\mu_A(x,q)\leq1$} is either empty or an fuzzy subsemiring of R.*

Proof. *If no element satisfies this condition, then H is empty. If x and y satisfies this condition, then $\mu_A(x+y,q)\geq\mu_A(x,q)\wedge\mu_A(y,q)$.*

Therefore, $\mu_A(x+y,q)\geq\mu_A(x,q)\wedge\mu_A(y,q)$, for all x and y in R and q in Q . And $\mu_A(xy,q)\geq\mu_A(x,q)\wedge\mu_A(y,q)$. Therefore, $\mu_A(xy,q)\geq\mu_A(x,q)\wedge\mu_A(y,q)$, for all x and y in R and q in Q. Therefore, H is either empty or is a subsemiring of R.

Theorem 3.9. *If A is a Q-intuitionistic L-fuzzy subsemiring of a semiring (R, +, •), then H={⟨(x,q),$\nu_A(x,q)$⟩ :0<$\nu_A(x,q)\leq1$} is either empty or is a subsemiring of R.*

Proof. If no element satisfies this condition, then H is empty. If x and y satisfies this condition, then $\nu_A(x+y,q)\leq\nu_A(x,q)\vee\nu_A(y,q)$.

Therefore, $\nu_A(x+y,q)\leq\nu_A(x,q)\vee\nu_A(y,q)$, for all x and y in R and q in Q. And $\nu_A(xy,q)\leq\nu_A(x,q)\vee\nu_A(y,q)$. Therefore, $\nu_A(xy,q)\leq\nu_A(x,q)\vee\nu_A(y,q)$, for all x and y in R and q in Q. Hence H is either empty or is a subsemiring of R.

Theorem 3.10. *If A is a Q-intuitionistic L-fuzzy subsemiring of a semiring (R, +,•), then A is a Q-intuitionistic L-fuzzy subsemiring of R.*

Proof. Let A be a Q-intuitionistic L-fuzzy subsemiring of a semiring R. Consider A={⟨(x,q),$\mu_A(x,q)$,$\nu_A(x,q)$⟩}, for all x in R and q in Q, we take □A=B={⟨(x,q), $\mu_B(x,q)$,$\nu_B(x,q)$⟩}, where $\mu_B(x,q)=\mu_A(x,q)$, $\nu_B(x,q)=1-\mu_A(x,q)$. Clearly, $\mu_B(x+y,q)\geq\mu_B(x,q)\wedge\mu_B(y,q)$, for all x and y in R and q in Q. Also $\mu_B(xy,q)\geq\mu_B(x,q)\wedge\mu_B(y,q)$, for all x and y in R. Since A is an Q-intuitionistic L-fuzzy subsemiring of R, we have $\mu_A(x+y,q)\geq\mu_A(x,q)\wedge\mu_A(y,q)$, for all x and y in R, which implies that $1-\nu_B(x+y,q)\geq\{(1-\nu_B(x,q))\wedge(1-\nu_B(y,q))\}$, which implies that $\nu_B(x+y,q)\leq1-\{(1-\nu_B(x,q))\wedge(1-\nu_B(y,q))\}=\nu_B(x,q)\vee\nu_B(y,q)$. Therefore, $\nu_B(x+y,q)\leq\nu_B(x,q)\vee\nu_B(y,q)$, **f**or all x and y in R and q in Q. And $\mu_A(xy,q)\geq\mu_A(x,q)\wedge\mu_A(y,q)$, for all x and y in R and q in Q, which implies that $1-\nu_B(xy,q)\geq\{(1-\nu_B(x,q))\wedge(1-\nu_B(y,q))\}$which implies that $\nu_B(xy,q)\leq1-\{(1-\nu_B(x,q))\wedge(1-\nu_B(y,q))\}=\nu_B(x,q)\vee\nu_B(y,q)$. Therefore,$\nu_B(xy,q)\leq\nu_B(x,q)\vee\nu_B(y,q)$, for all x and y in R and q in Q. Hence B=□A is a Q-intuitionistic L-fuzzy subsemiring of a semiring R.

Theorem 3.11. *If A is a Q-intuitionistic L-fuzzy subsemiring of a semiring (R, +, •), then ◊A is a Q-intuitionistic L-fuzzy subsemiring of R.*

Proof. Let A be a Q-intuitionistic L-fuzzy subsemiring of a semiring R. That is $A=\{\langle(x,q),\mu_A(x,q),\nu_A(x,q)\rangle\}$, for all x in R and q in Q. Let $\Diamond A=B=\{\langle(x,q),\mu_B(x,q),\ \nu_B(x,q)\rangle\}$, where $\mu_B(x,q)=1-\nu_A(x,q),\nu_B(x,q)=\nu_A(x,q)$.

Clearly $\nu_B(x+y,q)\leq\nu_B(x)\vee\nu_B(y)$, for all x and y in R and $\nu_B(xy,q)\leq\nu_B(x,q)\vee\nu_B(y,q)$, for all x and y in R and q in Q. Since A is a Q-intuitionistic L-fuzzy subsemiring of R, we have $\nu_A(x+y,q)\leq \nu_A(x,q)\vee \nu_A(y,q)$, for all x and y in R and q in Q, which implies that $1-\mu_B(x+y,q)\leq\{(1-\mu_B(x,q))\vee(1-\mu_B(y,q))\}$,which implies that $\mu_B(x+y,q)\geq1-\{(1-\mu_B(x,q))\vee(1-\mu_B(y,q))\}=\mu_B(x,q)\wedge\mu_B(y,q)$.Therefore, $\mu_B(x+y,q)\geq\mu_B(x,q)\wedge\mu_B(y,q)$, for all x and y in R. And $\nu_A(xy,q)\leq \nu_A(x,q)\vee\nu_A(y,q)$, for all x and y in R and q in Q, which implies that $1-\mu_B(xy,q)\leq\{(1-\mu_B(x,q))\vee(1-\mu_B(y,q))\}$, which implies that $\mu_B(xy,q)\geq1-\{(1-\mu_B(x,q))\vee(1-\mu_B(y,q))\}=\mu_B(x,q)\wedge\mu_B(y,q)$.
Therefore,$\mu_B(xy,q)\geq\mu_B(x,q)\wedge\mu_B(y,q)$, for all x and y in R and q in Q. Hence $B = \Diamond A$ is a Q-intuitionistic L-fuzzy subsemiring of a semiring R.

Theorem 3.12. Let A be a Q-intuitionistic L-fuzzy subsemiring of a semiring H and f is an isomorphism from a semiring R onto H. Then $A\circ f$ is a Q-intuitionistic L-fuzzy subsemiring of R.

Proof. Let x and y in R and q in Q, A be a Q-intuitionistic L-fuzzy subsemiring of a semiring H. Then we have, $(\mu_A\circ f)(x+y,q)=\mu_A(f(x+y),q)=\mu_A(f(x,q)+f(y,q))\geq\mu_A(f(x,q))\wedge\mu_A(f(y,q))\geq(\mu_A\circ f)(x,q)\wedge(\mu_A\circ f)(y,q)$, which implies that

$(\mu_A\circ f)(x+y,q)\geq(\mu_A\circ f)(x,q)\wedge(\mu_A\circ f)(y,q)$.
And$(\mu_A\circ f)(xy,q)=\mu_A(f(xy,q))=\mu_A(f(x,q)f(y,q))\geq\mu_A(f(x,q))\wedge\mu_A(f(y,q))\geq(\mu_A\circ f)(x,q)\wedge(\mu_A\circ f)(y,q)$,which implies that $(\mu_A\circ f)(xy,q)\geq(\mu_A\circ f)(x,q)\wedge(\mu_A\circ f)(y,q)$. Then we have, $(\nu_A\circ f)(x+y,q)=\nu_A(f(x+y,q))=\nu_A(f(x,q)+f(y,q))\leq\nu_A(f(x,q))\vee\nu_A(f(y,q)) \leq (\nu_A\circ f)(x,q)\vee(\nu_A\circ f)(y,q)$, which implies that $(\nu_A\circ f)(x+y,q)\leq(\nu_A\circ f)(x,q)\vee (\nu_A\circ f)(y,q)$.
And$(\nu_A\circ f)(xy,q)=\nu_A(f(xy,q))=\nu_A(f(x,q)f(y,q))\leq\nu_A(f(x,q))\vee\nu_A(f(y,q)) \leq (\nu_A\circ f)(x,q) \vee(\nu_A\circ f)(y,q)$, which implies that $(\nu_A\circ f)(xy,q)\leq(\nu_A\circ f)(x,q)\vee(\nu_A\circ f)(y,q)$. Therefore $(A\circ f)$ is a Q-intuitionistic L-fuzzy subsemiring of a semiring R.

Theorem 3.13. *Let A be a Q-intuitionistic L-fuzzy subsemiring of a semiring (R, +, •), then the pseudo Q-intuitionistic L-fuzzy coset $(aA)^p$ is a Q-intuitionistic L- fuzzy subsemiring of a semiring R, for every a in R.*

Proof. Let A be a Q-intuitionistic L-fuzzy subsemiring of a semiring R. For every x and y in R and q in Q, we have, $((a\mu_A)^p)(x+y,q)=p(a)\mu_A(x+y,q)\geq p(a)\{(\mu_A(x,q)\wedge\mu_A(y,q)\}=p(a)\mu_A(x,q)\wedge p(a)\mu_A(y,q)=((a\mu_A)^p)(x,q)\wedge((a\mu_A)^p)(y,q)$.Therefore, $((a\mu_A)^p)(x+y,q)\geq((a\mu_A)^p)(x,q)\wedge((a\mu_A)^p)(y,q)$.Now,$((a\mu_A)^p)(xy,q)=p(a)\mu_A(xy,q)\geq p(a)\{\mu_A(x,q)\wedge\mu_A(y,q)\}=p(a)\mu_A(x,q)\wedge p(a)\mu_A(y,q)=((a\mu_A)^p)(x,q)\wedge((a\mu_A)^p)(y,q)$.Therefore, $((a\mu_A)^p)(xy,q)\geq((a\mu_A)^p)(x,q)\wedge((a\mu_A)^p)(y,q)$. For every x and y in R and q in Q, we have, $((a\nu_A)^p)(x+y,q) = p(a)\nu_A(x+y,q) \leq p(a)\{(\nu_A(x,q)\vee\nu_A(y,q)\}=p(a)\nu_A(x,q)\vee p(a)\nu_A(y,q)=((a\nu_A)^p)(x,q)\vee((a\nu_A)^p)(y,q)$.Therefore,$((a\nu_A)^p)(x+y,q)\leq((a\nu_A)^p)(x,q)\vee((a\nu_A)^p)(y,q)$.Now,$((a\nu_A)^p)(xy,q)=p(a)\nu_A(xy,q)\leq p(a)\{\nu_A(x,q)\vee\nu_A(y,q)\}=p(a)\nu_A(x,q)\vee p(a)\nu_A(y,q)=((a\nu_A)^p)(x,q)\vee((a\nu_A)^p)(y,q)$.
Therefore,$((a\nu_A)^p)(xy,q)\leq((a\nu_A)^p)(x,q)\vee((a\nu_A)^p)(y,q)$.
Hence $(aA)^p$ is a Q-intuitionistic L-fuzzy subsemiring of a semiring R.

REFERENCES

[1] Abou Zaid. S, On fuzzy subnear rings and ideals, fuzzy sets and systems, 44(1991),139-146.

[2] Akram.M and Dar.K.H, On fuzzy d-algebras, Punjab university journal of mathematics, 37(2005), 61-76.

[3] Akram.M and Dar.K.H, Fuzzy left *h*-ideals in hemirings with respect to a *s*-norm, International Journal of Computational and Applied Mathematics, Volume 2 Number 1 (2007), pp. 7–14

[4] Asok Kumer Ray, On product of fuzzy subgroups, fuzzy sets and systems, 105, 181-183 (1999).

[5] Atanassov.K.T., Intuitionistic fuzzy sets, fuzzy sets and systems, 20(1), 87-96 (1986).

[6] Atanassov.K.T., Intuitionistic fuzzy sets theory and applications, Physica- Verlag, A Springer-Verlag company, April 1999, Bulgaria.

[7] Banerjee.B and D.K.Basnet, Intuitionistic fuzzy subrings and ideals, J.Fuzzy Math.11, no.1, 139-155 (2003).

[8] Chakrabarty, K., Biswas, R., Nanda, A note on union and intersection of Intuitionistic fuzzy sets , Notes on Intuitionistic Fuzzy Sets , 3(4), (1997).

[9] Choudhury.F.P. and Chakraborty.A.B. and Khare.S.S. , A note on fuzzy subgroups and fuzzy homomorphism, Journal of mathematical analysis and applications, 131,537 -553 (1988).

[10] Davvaz.B and Wieslaw.A.Dudek, Fuzzy n-ary groups as a generalization of rosenfeld fuzzy groups, ARXIV-0710.3884VI (MATH.RA) 20 OCT 2007, 1-16.

[11] De, K., Biswas, R, Roy, A.R, On intuitionistic fuzzy sets, Notes on Intuitionistic Fuzzy Sets, 3(4), (1997).

[12] De, K., Biswas, R, Roy, A.R, On intuitionistic fuzzy sets, Notes on Intuitionistic Fuzzy Sets, 4(2), (1998).

[13] Dixit.V.N., Rajesh Kumar, Naseem Ajmal., Level subgroups and union of fuzzy subgroups, Fuzzy sets and systems, 37, 359-371 (1990).

[14] Hur.K, Kang.H.W and H.K.Song, Intuitionistic fuzzy subgroups and subrings, Honam Math. J. 25 no.1,19-41 (2003).

[15] Kim.K.H., On intuitionistic Q-fuzzy semi prime ideals in semi groups, Advances in fuzzy mathematics,1(1),15-21 (2006).

[16] Palaniappan.N & Arjunan.K, Operation on fuzzy and anti fuzzy ideals, Antartica J. Math., 4(1) (2007), 59-64.

[17] Rajesh Kumar, Fuzzy Algebra, Volume 1, University of Delhi Publication Division, July -1993.

[18] Sampathu.S, Anita Shanthi .S, and Praveen Prakash.A, A Study on (Q,L)-fuzzy Subsemiring of a Semiring, General. Math. Notes, Vol.28, No.2, 55-63(2015).

[19] Sampathu.S, Anita Shanthi .S, and Praveen Prakash.A, A Study on (Q,L)-fuzzy Normal Subsemiring of a Semiring, American Journal of Applied Mathematics,3(4),185-188(2015).

[20] Sivaramakrishna das.P, Fuzzy groups and level subgroups, Journal of mathematical analysis and applications, 84, 264-269 (1981).

[21] Solairaju.A and Nagarajan.R, A New Structure and Construction of Q-Fuzzy Groups, Advances in fuzzy mathematics, Volume 4, Number 1 (2009), 23-29.

[22] Solairaju.A and Nagarajan.R, Q-fuzzy left R-subgroups of near rings w.r.t T- norms, Antarctica journal of mathematics, Volume 5 (2008),1-2.

[23] Tang J, Zhang X (2001). Product Operations in the Category of L –fuzzy groups. J. Fuzzy Math., 9:1-10.

[24] Vasantha kandasamy.W.B, Smarandache fuzzy algebra, American research press, Rehoboth -2003.

[25] Zadeh.L.A. Fuzzy sets , Information and control, Vol.8, 338-353 (1965).

Global Journal of Pure and Applied Mathematics (GJPAM) ISSN 0973-1768 Volume 12,Number 4 (2016)
© Research India Publications : http://www.ripublication.com

Review on controller for flow control applications

*T. M. Hariguru**
Department of Electronics and Instrumentation Engineering,
Valliammai Engineering College,
SRM Nagar, Kattankulathur - 603 203,
Kancheepuram, Tamil Nadu, India.
Email-id: harigurutm@gmail.com

K. Ayyar
Department of Electronics and Instrumentation Engineering,
Valliammai Engineering College,
SRM Nagar, Kattankulathur - 603 203,
Kancheepuram, Tamil Nadu, India.
Email-id: drkayyar@gmail.com

***Abstract*— Flow control is important in industrial applications such as chemical reactors, heat exchangers and distillation columns. Many industrial process can limit the performance of conventional PID controller scheme because of inherit dead time and nonlinearities. The objective is to defeat the problems such as handling unpredictable disturbance, unmeasurable noise and it can improve the transient state and steady state response performance. The proposed control scheme is implemented in Flow Control and Calibration of Pilot Plant. The design is done using MATLAB software package and directly it is connected to the Pilot Plant through by DAQ card. Simulation and implementation result of PID controller will gives less overshoot, good control performance, better disturbance handling ability and it is more flexible and intuitive to tune. It is expected that this advanced controller (like plc,scada,dcs) can improves efficiency and production rate in industrial process through by handling of any disturbance.**

Keywords—Software package, Pilot Plant, Flow Control

I. INTRODUCTION

A flow control valve regulates the flow or pressure of a fluid. Control valves normally respond to signals generated by independent devices such as flow meters or temperature gauges. Control valves are normally fitted with actuators and positioners. Pneumatically-actuated globe valves and Diaphragm Valves are widely used for control purposes in many industries, although quarter-turn types such as ball, gate and butterfly valves are also used. Control valves can also work with hydraulic actuators (also known as hydraulic pilots).These types of valves are also known as Automatic Control Valves. The hydraulic actuators will respond to changes of pressure or flow and will open or close the valve. Automatic Control Valves do not require an external power source because fluid pressure is enough to open and close the valve. Automatic control valves. include pressure reducing valves, flow control valve, back-pressure sustaining valves, altitude valves, and relief valves.

To reduce the effect of these load disturbances, sensors and transmitters collect information about the process variable and its relationship to some desired set point. When all the measuring, comparing, and calculating the process. Final control element must implement the strategy selected by the controller. The most common final control element in the process control industries is the control valve. The control valve manipulates a flowing fluid (such as gas, steam, water, or chemical compounds) to compensate for the load disturbance and keep the regulated process variable as close as possible to the desired set point.

II. PID CONTROLLER

In general PID controller is the combination of P-proportional, I-integral, D-derivative controllers. The values of these three parameters are interpreted in terms of time, where, 'P' depends on the present error, 'I' on the accumulation of past errors and 'D' is a prediction of future errors, based on current rate of change. By tuning the three parameters, PID controller can provide control action designed for specific process requirements. The proportional, integral and derivative terms are summed to calculate the output of the PID controller equation and final output [3] defined by u (t) and it given (1) by

$$u(t)=k_p\, e(t) + k_i \int_0^t e(t)\,dt + k_d \left(\frac{de(t)}{dt}\right) \quad (1)$$

Most of the industrial processes are pneumatic valve with PID controller. In industrial PID controller contain box, not an algorithm, Auto-tuning functionality of both pre-tune and self-tune, Manual or cascade mode switch, Bump less transfer between

*Corresponding author.
This paper was presented by the first author in the National Conference on *Advances in Mathematics and its Applications to Science and Engineering* (AMASE-2016) conducted in Department of Mathematics, University College of Engineering Pattukkottai, Thanjavur, Tamil Nadu, India, on 22nd January 2016.

different modes, set point ramp, Loop alarms, Networked or serial port would give a simple model design of PID controller. Model-based tuning is Look at the closed-loop poles and Numerical optimization of the performance index over the PID controller. Basically PID controllers are used in Cohen coon method or Zeigler-Nichols method for tuning purpose.

A. Ziegler–Nichols method

Ziegler-Nichols proposed rules for determining the values of the proportional gain K_p, integral time K_i and derivative time K_d based on the transient – response characteristics of a given plant. PID controller is implemented in plant and it can be transfer function to oscillate and then stabilize of output. In the Ziegler-Nichols method is used in plant and it can be neither integrators nor dominant complex conjugate poles. The conventional PID controller gives some overshoot, large amount of settling time and rise time. But in Ziegler Nichols method the overshoot is completely eliminated but rises time and settling time is greater than the conventional PID. In general, Ziegler Nichols methods have provided starting point and tuning is necessary to get the appropriate value. After tuning of the PID controller both the rise time and settling time will be reduced in large amount and there is some overshoot but anyway it is very less compare to conventional PID controller. Ziegler-Nichols method table [6] is shown in Table.1

Table.1 Ziegler Nichols Method

Control Type	K_p	K_i	K_d
P	0.5 *K_u	-	-
PI	0.45*K_u	1.2*K_p/T_u	-
PID	0.60*K_u	2*K_p/T_u	K_p*T_u/8

The response of the PID controller can be described in terms of the responsiveness of the controller to an error, the degree to which the PID controller overshoots the set point and the degree of system oscillation. It should be noted that the use of the PID algorithm for control and it guarantee optimal control of the system or system stability. The Conventional PID controller and its output to a step input response as achieved with some particular control parameter values.

PID Controller is used in the areas like mechanical, hydraulic, pneumatic techniques. Basically controller is a device. Recently PID controller is used in form of software package like MATLAB. Typical applications of controllers are used to hold settings for temperature, pressure, flow or speed. A system can either be described as a multiple inputs and multiple outputs system (MIMO). MIMO system is requiring more than one controller. In case of single input and single output (SISO) system, it is required only a single controller. Depending on the set-up of the physical (or non-physical) system, adjusting the system input variable will affect the operating parameter; otherwise, it is taken as the controlled output variable. Upon receiving the error signal that marks the disparity between the desired value (set point) and the actual output value, the controller will then attempt to regulate controlled output behavior. The controller achieves by either attenuating or amplifying the input signal to the plant so that the output is returned to the set point.

III. EXPERIMENTAL SETUP DIAGRAM

Controller techniques are directly connected to the plant through Daq card and the matlab software is used to control the entire plant [2]. Data from Pilot Plant are in 4-20mA and converted to 1-5V using series 250 Ohm resistors. Data acquisition is the process of sampling signals and it measures real world physical conditions.so that it converts the resulting samples into digital numeric values that can be manipulated by a computer [1]. Set up is shown in figure.1

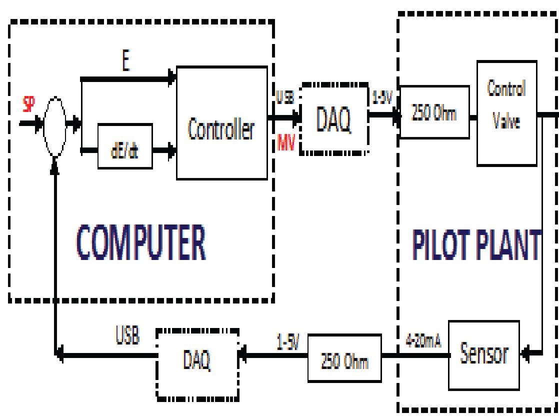

Fig.1 Setup Diagram

IV. PILOT PLANT SETUP

The Pilot plant is simply two series tanks with the objective of transferring the fluid from Buffer Tank to Calibration Tank; while controlling the fluid flow rate between the two tanks. Two pumps are used to circulate the fluid between the two tanks. Computer controls the flow rate by controlling the opening of the Control Valve, and measurements are obtained via Coriolis flow transmitter. The plant is composed by two water tanks, T1 and T2, interconnected via a system of pipes enabling liquid flow between the tanks. The plant works so that one can transfer the liquid from T1 to T2 and from T2 to T1.The flow from T1 to T2 occurs by gravity, since T1 is positioned above T2, through a valve V1. The flow from T2 to T1 requires the action of a centrifugal pump to raise the liquid level, through a valve V2.pilot plant setup diagram is shown in figure.2

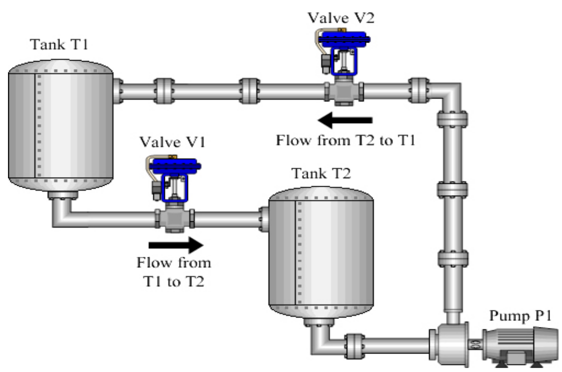

Fig.2 Pilot Plant Setup Diagram

V. RESULT AND DISCUSSION

The simulation of PID and fuzzy logic controller (2) are based on FODT model in equation [5]

$$G(s) = \frac{Ke^{-\tau_d s}}{\tau s+1} \quad (2)$$

The result of empirical modelling of pilot plant (3) is in form of FODT.

$$G(s) = \frac{0.7e^{-0.63s}}{0.17s+1} \quad (3)$$

A. Simulation of PID Controller

The output of PID controller simulation result obtained with the help of MATLAB. Simulation of PID [4] controller has step input with transfer function as well as tuning of PID controller gives output in steady state performance with some oscillations and it can be directly measured by water tank is shown in figure.3

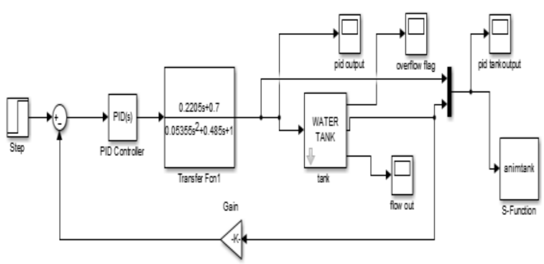

Fig.3 Simulation of PID controller

B. output of PID Controller

The output of PID controller has minimum

overshoot and fastest response is required. A PID controller has been used for industrial purpose due to their simplicity, easy designing method, low cost and effectiveness. In conventional PID controller contains some overshoot but steady state control performance at the output is shown in figure.4

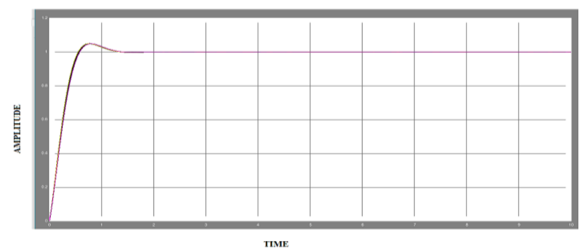

Fig.4 Output of PID controller

VI. CONCLUSION

Controller has various types like PID, fuzzy logic. Plant is to test the performance in cascade system and to tune the according to PID controller. The steady state of output value is one for PID controller. Pilot plant can able to control with the PID controller. The performance of PID controller is to tune and optimize according to pilot plant. It is expected that the designed PID controller into other processes (such as temperature and pressure) can able to measure and control. The various types of controllers (like neuro fuzzy, neural network, fuzzy PID, plc)can able to control this processor at final stage.

REFERENCES

[1] Tareq Aziz Hasan AL-Qutami, Rosdiazli Ibrahim, "Design of a Fuzzy Logic Process Controller for Flow Applications and Implementation in Series Tanks Pilot Plant" IEEE 2015 International Conference on Industrial Instrumentation and Control (ICIC), May 28-30,2015.

[2] E. Pathmanathan and R. Ibrahim, "Development and implementation of Fuzzy Logic Controller for Flow Control Application," in Intelligent and Advanced Systems (ICIAS),2010 International Conference on, 2010, pp. 1-6.

[3] G. Zaidner, S. Korotkin, E. Shteimberg, A. Ellenbogen, M.Arad, and Y. Cohen, "Non linear PID and its application in process control," in Electrical and Electronics Engineers in Israel (IEEEI), 2010 IEEE 26th Convention of, 2010, pp.000574-000577.

[4] Ritu Shakya1, Kritika Rajanwal2, Sanskriti Patel3 and Smita Dinkar (2014), “Design and Simulation of PD, PID and Fuzzy Logic Controller for Industrial Application” International Journal of Information and Computation Technology. ISSN 0974-2239 Volume 4, Number 4, pp. 363-368.

[5] M. Yukitomo, Y. Baba, T. Shigemasa, M. Ogawa, K.Akamatsu, and S. Amano, "A model driven PID control system and its application to chemical processes," in SICE 2002. Proceedings of the 41st SICE Annual Conference,2002, pp. 2656-2660 vol.4.

[6] J. Jantzen, "Tuning Of Fuzzy PID Controllers," Technical University of Denmark, Lyngby, 1998.

Global Journal of Pure and Applied Mathematics (GJPAM) ISSN 0973-1768 Volume 12,Number 4 (2016)

Global behavior of certain types of neutral delay difference equations

*G. Gomathi Jawahar**
Department of Mathematics,
Karunya University, Coimbatore,
Tamil Nadu, India.

M. Chithra
Department of Mathematics,
Karunya University, Coimbatore,
Tamil Nadu, India.

***Abstract*— The aim of this paper is to investigate the global behavior of neutral delay difference equations of the first and third order. Examples are provided to prove the results.**

Keywords—Neutral, Delay, Oscillation, Non Oscillation, Solution.

I. INTRODUCTION

First order Neutral Delay Difference Equation is gaining interest because they are the discrete analogue of differential Equations. In recent years, several papers on oscillation of solutions of Neutral Delay Difference Equations have appeared. [2]John R.Graef, R.Savithri, E.Thandapani (John R. Graef, 2004) have analyzed the non oscillatory solutions of first order Neutral Delay Differential Equations with positive coefficient in the Neutral term. [3] Xi-lan Liu and yang-yang dong provided some oscillatory solutions of third order Neutral Delay Differential Equations .

[1]Ozkan Ocalan extensively discusses the problem of Oscillation of neutral differential equation with positive and negative coefficients, J. Math.Anal.Appl. 33(1), 2007, 644-654. [9]Tanaka, S. (2002) discussed the various Solutions of Oscillation First order Neutral Delay Differential Equations.

Here some oscillation results in difference equations based on the existence results of differential equations are provided. Examples are provided to illustrate the results.

II. MAIN RESULTS

Theorem 2.1. If $\sum_{s=N_0}^{n} \rho_s q_s f(1-p_{s-m}) = \infty$ then, every solution of the equation $\Delta(x_n + p_n x_{n-l}) + q_n f(x_{n-m}) = 0,$

is oscillatory, for some $\rho_n, p_n > 0, f_{nm} > f_n f_m, N_0 > 0, l, m > 0.$

Proof. Suppose x_n be a non oscillatory solution of

$$\Delta(x_n + p_n x_{n-l}) + q_n f(x_{n-m}) = 0. \qquad (1.1)$$

Without loss of generality let us assume that x_n is eventually positive solution. Let $z_n = x_n + p_n x_{n-l}$. Obviously,

$$\Delta(x_n + p_n x_{n-l}) + q_n f(x_{n-m}) = \Delta z_n + q_n f(z_{n-m} - p_{n-m} x_{n-m-l}) = 0. \qquad (1.2)$$

$$\Delta z_n + q_n f(z_{n-m}) f(1-p_{n-m}) < 0 \qquad (1.3)$$

Define

$$w_n = \frac{\rho_n \Delta z_n}{f(z_{n-m})} \text{ then } w_n > 0.$$

(1.3) becomes,

$$\frac{w_n f(z_{n-m})}{\rho_n} < -q_n f(z_{n-m}) f(1-p_{n-m})$$

$$w_n < -\rho_n q_n f(1-p_{n-m})$$

Therefore, $\rho_n q_n f(1-p_{n-m}) < -w_n$.

$$\text{Generlazing, } \sum_{s=N_0}^{n} \rho_s q_s f(1-p_{s-m}) < \infty,$$

for $n \geq N_0$. This contradicts the given condition of the theorem. Hence every solution of the equation (1.1) is oscillatory.

Theorem 2.2. Let x_n be a non oscillatory solution of the equation (1.1) and if the following assumptions holds,

$$A_1 : \frac{f(u)}{u} > \gamma > 0, 0 < p_n \leq 1.$$

$$A_2 : Q_s = \sum_{s=N_0}^{n} \gamma q_s (1-p_{s-m}) < \infty,$$

*Corresponding author.

This paper was presented by the first author in the National Conference on *Advances in Mathematics and its Applications to Science and Engineering* (AMASE-2016) conducted in Department of Mathematics, University College of Engineering Pattukkottai, Thanjavur, Tamil Nadu, India, on 22nd January 2016.

then $V_{N_0} \geq Q_s + \sum_{s=N_0}^{n} Q_s V_{N_0}$.

Proof.

Let x_n be a non oscillatory solution of the equation (1.1) and without loss of generality, assume that $x_n > 0$. Let $z_n = x_n + p_n x_{n-l}$, $\Delta z_n = -q_n f(z_{n-m} - p_{n-m} x_{n-m-l})$. From A_1 : $\Delta z_n + \gamma q_n f(z_{n-m} - p_{n-m} x_{n-m-l}) \leq 0,$ since $z_n > x_n$,

$$\Delta z_n + \gamma q_n z_{n-m}(q_n - p_{n-m}) \leq 0, \quad (1.4)$$

Define $v_n = \frac{z_n}{z_{n-m}}$, $\Delta v_n = \frac{z_{n-m}\Delta z_n - z_n \Delta z_{n-m}}{z_{n-m} z_{n-m+1}}$

$$\frac{\Delta v_n z_{n-m} z_{n-m+1} + z_n \Delta z_{n-m}}{z_{n-m}} = \Delta z_n$$

From(1.4)

$$\frac{\Delta v_n z_{n-m} z_{n-m+1} + z_n \Delta z_{n-m}}{z_{n-m}} = -\gamma q_n z_{n-m}(1 - p_{n-m})$$

$$\Delta v_n z_{n-m+1} + \frac{z_n \Delta z_{n-m}}{z_{n-m}} = -\gamma q_n z_{n-m}(1 - p_{n-m})$$

$$\Delta v_n \leq -\gamma q_n z_{n-m}(1 - p_{n-m}).$$

$$\Delta v_n \leq -\gamma q_n z_{n-m}(1 - p_{n-m}) - v_n^{\,2}$$

taking summation from s = N to n,

$$\sum_{s=N_0}^{n} v_{s+1} - v_s \leq -\sum_{s=N_0}^{n} \gamma q_s (1 - p_{s-m}) - \sum_{s=N_0}^{n} v_s^{\,2}$$

$$v_{n+1} - v_{N_0} \leq -Q_s - \sum_{s=N_0}^{n} v_s^{\,2}$$

$$-v_{N_0} \leq -Q_s - \sum_{s=N_0}^{n} v_s^{\,2} \quad \text{Since } v_{N_0} \geq Q_s \quad \_\_$$

$$v_{N_0} \geq Q_s + \sum_{s=N_0}^{n} Q_s v_{N_0}.$$

This completes the theorem.

Example 2.3. Consider the first order neutral delay difference equation $\Delta(x_n + n^2 x_{n-1}) + (2n^2 + 2n - 1)x_{n-1}^{\;3} = 0 \quad (1.5)$

Equation (1.5) satisfies all conditions of theorem 1.1 and hence all its solutions are oscillatory. One such solution is $x_n = (-1)^n$.

Example 2.4. Consider the first order neutral delay difference equation,

$$\Delta(x_n + \frac{1}{n-2} x_{n-1}) + (\frac{2n^2 - 8n + 7}{(n-1)(n-2)}) x_{n-1}^{\;2} = 0, n > 1,2 \quad (1.6)$$

Equation (1.6) satisfies all conditions of theorem 1.1 and hence all its solutions are oscillatory. One such solution is $x_n = (-1)^n$.

Theorem 2.5. If y_n is an eventually positive solution of equation $\Delta(a_n \Delta b_n (\Delta(y_n + p_n y_{n-k}))) + q_n f(y_{n-l}) = 0 \quad (1.7)$ and $z_n = y_n + p_n y_{n-k}$ then for sufficiently large n, the following condition exists.

$$z_n > 0, \Delta z_n > 0, \Delta(b_n \Delta z_n) > 0.$$

Proof. Let y_n be an eventually positive solution of equation (1.7). Then there exists $n_1 \geq n_0$ such that $y_{n-k} > 0$, $y_{n-l} > 0$ for $n \geq n_1$.

From the definition of z_n, it is clear that $z_n > 0$ and $\Delta(a_n \Delta b_n \Delta z_n) \leq 0, n \geq n_1$.

We claim that

$$\Delta(b_n \Delta z_n) > 0, \quad \text{for } n \geq n_2.$$

Suppose $\Delta(b_n \Delta z_n) \leq 0., forn \geq n_2$.

Since $a_n > 0$, we claim $a_n \Delta(b_n \Delta z_n) < 0$, for $n \geq n_3$.

Then for $a_n \Delta(b_n \Delta z_n) < 0$, for $n \geq n_3$, we get

$$a_n \Delta b_n \Delta z_n \leq a_{n_3} \Delta b_{n_3} \Delta z_{n_3} \leq 0. \quad (1.8)$$

Dividing (1.8) by a_n, we get

$$\Delta b_n \Delta z_n \leq (a_{n_3} \Delta b_{n_3} \Delta z_{n_3}) \frac{1}{a_n} \leq 0.$$

Taking summation from n_3 to n, we obtain

$$\sum_{n_3}^{n}(b_{n+1}-b_n)\Delta z_n \le a_{n_3}\Delta(b_{n_3}\Delta z_{n_3})\sum_{n_3}^{n}\frac{1}{a_n}$$

$$(b_{n_3+1}-b_{n_3})\Delta z_{n_3}+(b_{n_3+2}-b_{n_{33}+1})\Delta z_{n_3+1}+$$

$$(b_{n_3+3}-b_{n_3+2})\Delta z_{n_3+2}+.....+(b_{n+1}-b_n)\Delta z_n \le$$

$$a_{n_3}\Delta(b_{n_3}\Delta z_{n_3})(\frac{1}{a_{n_3}}+\frac{1}{a_{n_3+1}}+.....\frac{1}{a_n})$$

We have, $b_n\Delta z_n \to -\infty,\ \ n\to\infty$.

Hence there exists $n_4 \ge n_3$, such that

$$b_n\Delta z_n \le b_{n_4} < 0, \qquad (1.9)$$

for $n \ge n_4$.

Dividing equation (1.9) by b_n , $\Delta z_n \le b_{n_4}\Delta z_{n_4}\frac{1}{b_n}$.

Taking summation from n_4 to n,

$$\sum_{n_4}^{n}(z_{n+1} - z_n) \le b_{n_4}\Delta z_{n_4}\frac{1}{b_n}$$

$$z_n \to -\infty, n\to\infty.$$

which contradicts the statement of theorem 2.5.

Hence we have $\Delta(b_n\Delta z_n) > 0$ for all n.

References

[1] Ozkan ocalan, oscillation of neutral differential equation with positive andNegative coefficients, j.Math.Anal.Appl.331(1)(2007),644-654.

[2] John R.Graef,R.S.(2004). Oscillation of First order Neutral Delay DifferentialEquations. Electronic journal of Qualitative of differential Equation,proc.7thcoll.QTDE,NO.12,1-11.

[3] Xi-Lan Liu and Yang-yang Dong, oscillatory Behavior of Third orderdifference equations , International journal of difference equations ISSN 0973-6069, volume 9,Number 2, pp223-231(2014).

[4] Tanaka, S.(2002). Oscillation of solution of First order Neutral DelayDifferential Equations.Hiloshima Mathematical Journal,32,73-85.

Global Journal of Pure and Applied Mathematics (GJPAM) ISSN 0973-1768 Volume 12,Number 4 (2016)

Localization techniques for wireless sensor networks

*M. G. Kavitha**
Department of CSE,
University College of Engineering Pattukkottai,
Thanjavur, Tamil Nadu, India.
Email: mgkavi@gmail.com

S. Sendhilnathan
Department of Physics,
University College of Engineering Pattukkottai,
Thanjavur, Tamil Nadu, India.
Email: sendhil29@yahoo.co.in

***Abstract*— Nowadays wireless sensor networks are used in variety of applications such as military surveillance, healthcare monitoring, environmental sensing, industrial monitoring. In all these applications it is required to know the location of sensors that send the sensed data to the base station for further processing of the data. In this paper different techniques used for finding the location of sensors in wireless sensor network are discussed. And also the challenges related with these techniques are also presented here.**

***Keywords*— Trilateration; localization; anchor nodes; TOA; RSS.**

I. INTRODUCTION

A wireless sensor network (WSN) provides a bridge between the real physical and virtual worlds. It is composed of *n* nodes with a communication range of *r*, distributed in a two dimensional squared sensor field $Q = [0,s] \times [0,s]$. For any two nodes *u* and *v*, *u* reaches *v* if and only if *v* reaches *u* and with the same signal strength *w* [1]. We represent the network by the Euclidean graph $G = (V, E)$ with the following properties:

- $V = \{v1, v2, vn\}$ is the set of sensor nodes.
- $\langle i, j\rangle \in E$ if v_i reaches v_j; that is, the distance between v_i and v_j is less than *r*.
- $w(e) \leq r$ is the weight of edge $e = \langle i, j\rangle$, the distance between v_i and v_j.

The architectural diagram of a WSN is given below.

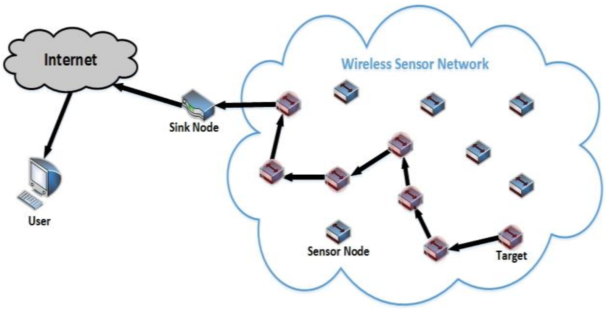

Fig. 1. Wireless sensor network architecture

A. Applications

Wireless sensor networks have a wide range of potential applications to industry, science, transportation, civil infrastructure, and security. Some of the sample applications of WSNs are:

- Seismic Monitoring
- Civil Structural Health Monitoring
- Habitat and Ecosystem Monitoring
- Monitoring Groundwater Contamination
- Rapid Emergency Response
- Industrial Process Monitoring
- Perimeter Security and Surveillance
- Automated Building Climate Control

B. Components

The main components of a WSN node are controller, communication device(s), sensors/actuators, memory and power supply which are specified using the following diagram.

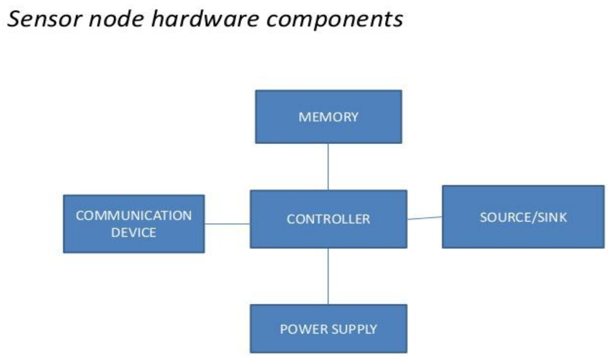

Fig. 2. Components of a sensor node

II. LOCALIZATION

Localization in sensor network estimates the locations of sensors with initially unknown location information by using knowledge of the absolute positions of a few sensors and inter-sensor measurements such as distance and bearing measurements. Sensors with known location information are called *anchors* and their locations can be obtained by using a global positioning system (GPS), or by installing anchors at points with known coordinates. In applications requiring a global coordinate system, these anchors will determine the location of the sensor network in the global coordinate system. The sensors with unknown

*Corresponding author.

This paper was presented by the first author in the National Conference on *Advances in Mathematics and its Applications to Science and Engineering* (AMASE-2016) conducted in Department of Mathematics, University College of Engineering Pattukkottai, Thanjavur, Tamil Nadu, India, on 22nd January 2016.

location information are called *non-anchor* nodes and their coordinates will be estimated by sensor network localization algorithm [2]. Patwari *et al.* described some general signal processing tools that are useful in cooperative WSN localization algorithms [3] with a focus on computing the Cram´er-Rao bounds for localization using a variety of different types of measurements.

In applications such as habitat monitoring, smart building failure detection and reporting, and target tracking, it is necessary to accurately orient the nodes with respect to a global coordinate system in order to report data that is geographically meaningful. Basic middleware services such as routing often rely on location information (e.g., geographic routing).

Ad hoc sensor networks present novel tradeoffs in system design. On the one hand, the low cost of the nodes facilitates massive scale and highly parallel computation. On the other hand, each node is likely to have limited power, limited reliability, and only local communication with a modest number of neighbors. These application contexts and potential massive scale make it unrealistic to rely on careful placement or uniform arrangement of sensors. Rather than use globally accessible beacons or expensive GPS to localize each sensor, it is preferable for the sensors to self-organize a coordinate system.

A. Localization Hardware

The localization problem gives rise to two important hardware problems. The first, the problem of defining a coordinate system and the second, which is the more technically challenging, is the problem of calculating the distance between sensors (the ranging problem).

- *Anchor/Beacon nodes*

Beacon nodes (also frequently called anchor nodes) are a necessary prerequisite to localizing a network in a global coordinate system. Beacon nodes are simply ordinary sensor nodes that know their global coordinates a priori using GPS. At a minimum, three non-collinear beacon nodes are required to define a global coordinate system in two dimensions. If three dimensional coordinates are required, then at least four non-coplanar beacons must be present. Localization accuracy improves if beacons are placed in a convex hull around the network. Locating additional beacons in the center of the network is also helpful. In any event, there is considerable evidence that real improvements in localization can be obtained by planning beacon layout in the network. GPS receivers consume significant battery power, which can be a problem for power-constrained sensor nodes. Beacons are necessary for localization, but their use does not come without cost.

- *Received Signal Strength Indication (RSSI)*

The energy of a radio signal diminishes with the square of the distance from the signal's source. As a result, a node listening to a radio transmission should be able to use the strength of the received signal to calculate its distance from the transmitter.

- *Radio Hop Count*

The local connectivity information provided by the radio defines an unweighted graph, where the vertices are sensor nodes, and edges represent direct radio links between nodes. The hop count hij between sensor nodes si and sj is then defined as the length of the shortest path in the graph between si and sj. y, If the hop count between si and sj is hij then the distance between si and sj , dij , is less than R∗hij , where R is again the maximum radio range.

- *Time Difference of Arrival (TDoA)*

In TDoA schemes, each node is equipped with a speaker and a microphone. Some systems use ultrasound while others use audible fre-quencies. However, the general mathematical technique is independent of particular hardware. In TDoA, the transmitter first sends a radio message. It waits some fixed interval of time, tdelay (which might be zero), and then produces a fixed pattern of "chirps" on its speaker. When listening nodes hear the radio signal, they note the current time, tradio, then turn on their microphones. When their microphones detect the chirp pattern, they again note the current time, tsound. Once they have tradio, tsound, and tdelay, the listeners can compute the distance d between themselves and the transmitter using the fact that radio waves travel substantially faster than sound in air.

$$d = (sradio - ssound) * (tsound - tradio - tdelay)$$

TDOA methods perform best in areas that are free of echoes, and when the speakers and microphones are calibrated to each other.

- *Angle of Arrival (AoA)*

In these methods, several (3-4) spatially separated microphones hear a single transmitted signal. By analyzing the phase or time difference between the signal's arrival at different microphones, it is possible to discover the angle of arrival of the signal.

Angle of Arrival hardware is sometimes augmented with digital compasses. A digital compass simply indicates the global orientation of its node, which can be quite useful in conjunction with AoA information.

III. LOCALIZATION TECHNIQUES

Localization is performed through communication between localized node and unlocalized node for determining their geometrical placement or position. Location is estimated using distance and angle between nodes. The following are the concepts used in localization:

1) Lateration occurs when distance between nodes is measured to estimate location.

2) Angulation occurs when angle between nodes is measured to estimate location.

3) Trilateration Location of node is estimated through distance measurement from three nodes. In this concept, intersection of three circles is calculated, which gives a single point which is a position of unlocalized node.

4) *Multilateration* In this concept, more than three nodes are used in location estimation.

5) *Triangulation* In this mechanism, at least two angles of an unlocalized node from two localized nodes are measured to estimate its position. Trigonometric laws, law of sines and cosines are used to estimate node position.

Localization schemes are classified as anchor based or anchor free, centralized or distributed, GPS based or GPS free, fine grained or coarse grained, stationary or mobile sensor nodes, and range based or range free.

- *Anchor Based and Anchor Free*

Positions of few nodes are known in anchor-based mechanisms. Nodes that do not know their location are localized using these known nodes positions. Accuracy is highly depending on the number of anchor nodes. Anchor-free algorithms estimate relative positions of nodes instead of computing absolute node positions [6].

- *Centralized and Distributed*

In centralized schemes, all information is passed to one central point or node which is usually called "sink node or base station". Sink node computes position of nodes and forwards information to respected nodes. Computation cost of centralized algorithm is decreased, and it takes less energy as compared with computation at individual node. In distributed schemes, sensors calculate and estimate their positions individually and directly communicate with anchor nodes. There is no clustering in distributed schemes, and every node estimates its own position [7-9].

- *GPS Based and GPS Free*

GPS-based schemes are very costly because GPS receiver has to be put on every node. Localization accuracy is very high as well. GPS-free algorithms do not use GPS, and they calculate the distance between the nodes relative to local network and are less costly as compared with GPS-based schemes [11,12]. Some nodes need to be localized through GPS which are called anchor or beacon nodes that initiate the localization process [6].

- *Coarse Grained and Fine Grained*

Fine-grained localization schemes result when localization methods use features of received signal strength, while coarse-grained localization schemes result without using received signal strength.

- *Stationary and Mobile Sensor Nodes*

Localization algorithms are also designed according to field of sensor nodes in which they are deployed. Some nodes are static in nature and are fixed at one place, and the majority applications use static nodes.

- *Range-Free and Range-Based Localization*

1) Range-Free Methods

Range-free methods are distance vector (DV) hop, hop terrain, centroid system, APIT, and gradient algorithm. Range-free methods use radio connectivity to communicate between nodes to infer their location. In range-free schemes, distance measurement, angle of arrival, and special hardware are not used [11,12].

a) DV Hop

DV hop estimates range between nodes using hop count. At least three anchor nodes broadcast coordinates with hop count across the network. The information propagates across the network from neighbor to neighbor node. When neighbor node receives such information, hop count is incremented by one [12]. In this way, unlocalized node can find number of hops away from anchor node [7]. All anchor nodes calculate shortest path from other nodes, and unlocalized nodes also calculate shortest path from all anchor nodes [13]. Average hop distance formula is calculated as follows: distance between two nodes/number of hops [6].

Unknown nodes use triangulation method to estimate their positions from three or more anchor nodes using hop count to measure shortest distance [14].

b) Hop Terrain

Hop terrain is similar to DV hop method in finding the distance between anchor node and unlocalized node. There are two parts in the method. In the first part, unlocalized node estimates its position from anchor node by using average hop distance formula which is distance between two nodes/total number of hops. This is initial position estimation. After initial position estimation, the second part executes, in which initial estimated position is broadcast to neighbor nodes. Neighbor nodes receive this information with distance information. A node refines its position until final position is met by using least square method [13].

c) Centroid System

Centroid system uses proximity-based grained localization algorithm that uses multiple anchor nodes, which broadcast their locations with coordinates. After receiving information, unlocalized nodes estimate their positions [12]. Anchor nodes are randomly deployed in the network area, and they localize themselves through GPS receiver [6]. Node localizes itself after receiving anchor node beacon signals using the following formula [13]:where and are the estimated locations of unlocalized node.

d) APIT

In APIT (approximate point in triangulation) scheme, anchor nodes get location information from GPS or transmitters. Unlocalized node gets location information from overlapping triangles. The area is divided into overlapping triangles [13]. In APIT, the following four steps are included.(i)Unlocalized nodes maintain table after receiving beacon messages from anchor nodes. The table contains information of anchor ID, location, and signal strength [13].(ii)Unlocalized nodes select any three anchor nodes from area and check whether they are in triangle form. This test is called PIT (point in triangulation) test.(iii)PIT test continue until accuracy of unlocalized node location is found by combination of any three anchor nodes.(iv)At the end, center of gravity (COG) is calculated, which is intersection of all triangles where an unlocalized node is placed to find its estimated position [13].

e) Gradient Algorithm

In gradient algorithm, multilateration is used by unlocalized node to get its location. Gradient starts by anchor nodes and helps unlocalized nodes to estimate their positions from three anchor nodes by using multilateration [6]. It also uses hop count value which is initially set to 0 and incremented when it propagates to other neighboring nodes [6]. Every sensor node takes information of the shortest path from anchor nodes. Gradient algorithm follows fes steps such as the following:(i)In the first step, anchor node broadcasts beacon message containing its coordinate and hop count value.(ii)In the second step, unlocalized node calculates shortest path between itself and the anchor node from which it receives beacon signals [14]. To calculate estimated distance between anchor node and unlocalized node, the following mathematical equation is used [14]: where is the estimated distance covered by one hop.(iii)In the third step, error equation is used to get minimum error in which node calculates its coordinate by using multilateration [6] as follows: where is the estimated distance computed through gradient propagation.

2) Range-Based Localization

Range-based schemes are distance-estimation- and angle-estimation-based techniques. Important techniques used in range-based localization are received signal strength indication (RSSI), angle of arrival (AOA), time difference of arrival (TDOA), and time of arrival (TOA) [11-14].

a) Received Signal Strength Indication (RSSI)

In RSSI, distance between transmitter and receiver is estimated by measuring signal strength at the receiver [7]. Propagation loss is also calculated, and it is converted into distance estimation. As the distance between transmitter and receiver is increased, power of signal strength is decreased. This is measured by RSSI using the following equation [6]:where = transmitted power, = transmitter antenna gain, = receiver antenna gain, and = wavelength of the transmitter signal in meters.

b) Angle of Arrival (AOA)

Unlocalized node location can be estimated using angle of two anchors signals. These are the angles at which the anchors signals are received by the unlocalized nodes [13]. Unlocalized nodes use triangulation method to estimate their locations [6].

c) Time Difference of Arrival (TDOA)

In this technique, the time difference of arrival radio and ultrasound signal is used. Each node is equipped with microphone and speaker [35]. Anchor node sends signals and waits for some fixed amount of time which is , then it generates “chirps” with the help of speaker. These signals are received by unlocalized node at time. When unlocalized node receives anchor’s radio signals, it turns on microphone. When microphone detects chirps sent by anchor node, unlocalized node saves the time [14].

d) Time of Arrival (TOA)

In TOA, speed of wavelength and time of radio signals travelling between anchor node and unlocalized node is measured to estimate the location of unlocalized node [6]. GPS uses TOA, and it is a highly accurate technique; however, it requires high processing capability.

GPS-based localization mechanisms are less energy efficient while RSSI-based mechanisms are highly energy efficient.

IV. CONCLUSION

In this paper, different localization techniques are discussed in detail. Localization is a mechanism in which nodes are located. There are many approaches for localization; such approaches are desirable which are capable to take care of limited resources of sensor nodes.

REFERENCES

[1] Horacio A. B. F. Oliveira and Eduardo F. Nakamura, “Localization systems for wireless sensor networks”.

[2] Guoqiang Mao, Barıs, “Wireless sensor network localization techniques”.

N. Patwari, J. Ash, S. Kyperountas, “Locating the nodes: cooperative localization in wireless sensor networks,” IEEE Signal Processing Magazine, vol. 22, no. 4, pp. 54–69, 2005.

[3] Jonathan Bachrach and Christopher Taylor, “Localization in sensor networks”

[4] Y. Kwon, K. Mechitov, S. Sundresh, W. Kim, and G. Agha. “Resilient localization for sensor networks in outdoor environments”, Technical Report UIUCDCS-R-2004-2449, University of Illinois at Urbana-Champaign, June 2004.

[5] R. Manzoor, “Energy efficient localization in wireless sensor networks using noisy measurements” [M.S. thesis], 2010.

[6] L. E. W. Van Hoesel, L. Dal Pont, and P. J. M. Havinga, “Design of an Autonomous Decentralized MAC Protocol for Wireless Sensor Networks”, Centre for Telematics and Information Technology, University of Twente, Enschede, The Netherlands.

[7] A. Youssef and M. Youssef, “A taxonomy of localization schemes for wireless sensor networks”, in Proceedings of the International Conference on Wireless Networks (ICWN '07), pp. 444–450, Las Vegas, Nev, USA, 2007.

[8] D. Moore, J. Leonard, D. Rus, and S. Teller, “Robust distributed network localization with noisy range measurements”, in Proceedings of the 2nd International Conference on Embedded Networked Sensor Systems (SenSys '04), pp. 50–61, November 2004.

[9] J. Liu, Y. Zhang, and F. Zao, “Robust distributed node localization with error management”, in Proceeding of the 7th ACM International Symposium on Mobile Ad-Hoc Networking and Computing (MobiHoc '06), pp. 250–261, Florence, Italy, May 2006.

[10] S. Qureshi, A. Asar, A. Rehman, and A. Baseer, “Swarm intelligence based detection of malicious beacon node for secure localization in wireless sensor networks”, Journal of Emerging Trends in Engineering and Applied Sciences, vol. 2, no. 4, pp. 664–672, 2011.

[11] N. Bulusu, J. Heidemann, and D. Estrin, “GPS-less low-cost outdoor localization for very small devices”, IEEE Personal Communications Magazine, vol. 7, no. 5, pp. 28–34, 2000.

[12] E. Kim and K. Kim, “Distance estimation with weighted least squares for mobile beacon-based localization in wireless sensor networks”, IEEE Signal Processing Letters, vol. 7, no. 6, pp. 559–562, 2010.

[13] T. He, C. Huang, B. M. Blum, J. A. Stankovic, and T. Abdelzaher, “Range-free localization schemes for large scale sensor networks”, in Proceedings of the 9th ACM Annual International Conference on Mobile Computing and Networking (MobiCom '03), pp. 81–95, September 2003.

[14] J. Bachrach and C. Taylor, “Localization in Sensor Networks”, Massachusetts Institute of Technology, Cambridge, Mass, USA, 2004.

[15] S. Tanvir, “Energy efficient localization for wireless sensor network” [Ph.D. thesis], 2010.

[16] Nabil Ali Alrajeh, Maryam Bashir, and Bilal Shams, “Localization Techniques in Wireless Sensor Networks”, International Journal of Distributed Sensor Networks, Volume 2013 (2013).

Global Journal of Pure and Applied Mathematics (GJPAM) ISSN 0973-1768 Volume 12,Number 4 (2016)

On the homogeneous biquadratic equation with 5 unknowns $x^4 - y^4 = 145 (z^2 - w^2) R^2$

P. Jayakumar
Department of Mathematics,
Periyar Maniammai University,
Vallam, Thanjavur - 613403,
Tamil Nadu, India.

*R.Venkatraman**
Department of Mathematics,
Faculty of Engineering and Technology,
SRM University,
Vadapalani, Chennai-600026,
Tamil Nadu, India.
Email: venkarmeeraj@gmail.com

***Abstract*—The Homogenous biquadratic equation with five unknowns given by $x^4 – y^4 = 145(z^2 – w^2) R^2$ is considered and analyzed for finding its non zero distinct integral solutions. Introducing the linear transformations x = u + v, y = u –v, z =2uv+1, w=2uv-1 and employing the method of factorization different patterns of non-zero distinct integer solutions of the equation under the above equation are obtained. A few interesting relations between the integral solutions and the special numbers namely Polygonal numbers, Pyramidal numbers, Centered Polygonal numbers, Centered Pyramidal numbers, Thabit-ibn-Kurrah number, Star number, Carolnumber, woodall number, kyneanumber, pentatopenumber, stellaoctangula number, octahedral number, Mersenne number are exhibited.**

Keywords*— Homogeneous equation, Integral solutions, Polygonal numbers, Pyramidal numbers and special number.

Notations:

- $T_{m,n}$ - Polygonal number of rank n with size m
- P_n^m - Pyramidal number of rank n with size m
- g_n - Gnomonic number of rank n
- Pr_n - Pronic number of rank n
- $Ct_{16,n}$- Centered hexadecagonal pyramidal number of rank n
- OH_n -Octahedral number of rank n
- SO_n - Stella octangular number of rank n
- ky_n - kynea number
- $carl_n$ -carol number

I. INTRODUCTION

The theory of Diophantine equations offers a richvariety of fascinating problems. In particular biquadratic Diophantine equations, homogeneous and non-homogeneous have aroused the interest of numerous mathematicians since antiquity [1-12]. In this context one may refer [4-10] for various problems on the biquadratic Diophantine equations. However, often we come across non-homogeneous biquadratic equations and as such one may require its integral solution in its most general form. This paper concern with the homogeneous biquadratic equation with five unknowns $x^4 – y^4 = 145(z^2 – w^2) R^2$ for determining its infinitely many non-zero integral solutions. Also a few interesting properties among the solutions are presented.

*Corresponding author.

This paper was presented by the second author in the National Conference on *Advances in Mathematics and its Applications to Science and Engineering* (AMASE-2016) conducted in Department of Mathematics, University College of Engineering Pattukkottai, Thanjavur, Tamil Nadu, India, on 22nd January 2016.

II. METHOD OF ANALYSIS

The biquadratic equation with five unknowns to be solved for its non-zero distinct integral solution is

$$x^4 - y^4 = 145 (z^2 - w^2) R^2 \qquad (1)$$

Consider the transformations

$$\left.\begin{aligned} x &= u + v \\ y &= u - v \\ z &= 2uv + 1 \\ w &= 2uv - 1 \end{aligned}\right\} \qquad (2)$$

On substituting (2) in (1), we get

$$u^2 + v^2 = 145R^2 \qquad (3)$$

2.1. Pattern I

Assume $145 = (12+i) (12 – i)$ (4)

and $R= a^2 + b^2 = (a + ib) (a – ib)$ (5)

Using (4) and (5) in (3) and employing the method of factorization we get.

$$(u + iv)\ (u – iv) = (12+i) (12 – i)\ (a +ib)^2 (a – ib)^2$$

On equating the positive and negative factors,

we have,

$$(u + iv) = (12 +i)\ (a +ib)^2$$
$$(u + iv) = (12 –i)\ (a – ib)^2$$

On equating real and imaginary parts, we get

$$u = u (a, b) = 12a^2 – 12b^2 –2ab$$

$v = v(a, b) = a^2 – b^2 + 24ab$.

On substituting u and v in (2) we get the values of x, y, z and w. The non-zero distinct integrals values of x, y, z, w and R satisfying (1) are given by

$x = x(a, b) = 13a^2 – 13b^2 + 22ab$

$y = y(a, b) = 11a^2 – 11b^2 – 26ab$

$z = z(a, b) = 2(12a^4 + 12b^4 – 72a^2 b^2 + 286a^3b – 286ab^3) +1$

$w = w(a, b) = 2(12a^4 + 12b^4 – 72a^2 b^2 + 286a^3b – 286ab^3) – 1$

$R = R(a, b) = a^2 + b^2$.

Properties

1. $11x[a, a(2a^2-1)] - 13y[a, a(2a^2-1)] - 580\, SO_a = 0.$
2. $z(a,1) - w(a,1) \equiv 0 \pmod 2.$
3. $11x[(2a-1)^2, 1] - 13y[(2a-1)^2, 1] - 580(G_a)^2 = 0.$
4. $R[(a+1),(a+1)] - 2T_{4,a} - G_{2a} \equiv 0 \pmod 3.$
5. $R(2a, 2a) - 8T_{4,a} = 0.$
6. $x(1,1) - y(1,1) + R(1,1) - P_4^6 = 0.$
7. $11x[a,(2a^2+1)] - 13y[a,(2a^2+1)] - 17400\, OH_a = 0.$
8. $y(a, 2a-1) - ct_{16,a} + 93T_{4,a} - G_{31,a}$ *is a Jacobsthal number.*

2.2. Pattern II

Also 145 can be written in equation (3) as

$$145 = (1 +12i)(1 – 12i) \quad (6)$$

Using (5) and (6) in equation (3) it is written in factorizable form as $(u +iv)(u – iv) = (1 +12i)(1 – 12i)(a +ib)^2 (a – ib)^2$

On equating the positive and negative factors, we get,

$$(u + iv) = (1 +12i)(a +ib)^2$$

$$(u – iv) = (1 -12i)(a –ib)^2$$

On equating real and imaginary parts, we have

$$u = u(a, b) = a^2 – b^2 – 24ab$$
$$v = v(a, b) = 12a^2 – 12b^2 + 2ab.$$

Substituting the values of u and v in (2), the non-zero distinct values of x, y, z, w and R Satisfying (1) are given by

$x = x(a, b) = 13a^2 – 13b^2 – 22ab$

$y = y(a, b) = – 11a^2 +11b^2 – 26ab$

$z = z(a, b) = 2(12a^4 + 12b^4 – 72a^2 b^2 - 286a^3b + 286ab^3) +1$

$w = w(a, b) = 2(12a^4 + 12b^4 – 72a^2 b^2 - 286a^3b +286ab^3) – 1$

$R = R(a, b) = a^2 + b^2$.

Properties

1. $11x[a(a+1), 1] + 13y[a(a+1), 1] + 96P_a = 0.$
2. $R(3,3) - P_3^5 = 0.$
3. $11x(2,a) + 13y(2,a) \equiv 0 \pmod 2.$
4. $x(1,1) - y(1,1)$ *is a Perfect square.*
5. $11x[a, 2a^2+1] + 13y[a, 2a^2+1] - 1740OH_a = 0.$
6. $x(a+1, a+1) + y(a+1, a+1) + 48T_{4,a} + G_{43,a} + P_4^6 =$ *Woodall number.*
7. $y(a, a+1) - S_a + 32T_{4,a} - G_a - P_3^6 = 0.$

2.3. Pattern III

Rewrite (3) as

$$1 * u^2 = 145R^2 – v^2 \quad (7)$$

Assume

$$u = 145a - b = (\sqrt{145}\,a + b)(\sqrt{145}\,a - b) \quad (8)$$

Write 1 as,

$$1 = (\sqrt{68}+1)(\sqrt{68}-1) \quad (9)$$

Using (8) and (9) in (7) it is written in factorizable from as,

$$(\sqrt{65}+8)(65-8)(\sqrt{65}a+b)^2(\sqrt{65}a-b)^2 = (\sqrt{65}R+V)(\sqrt{65}R-V) \quad (10)$$

On equating the rational and irrational parts, we get

$$(\sqrt{65}+8)(\sqrt{65}a+b)^2 = \sqrt{65}R+V$$

$$(\sqrt{65}-8)(\sqrt{65}a-b)^2 = \sqrt{65}R-V$$

On equating the real and imaginary parts, we get

$$R = R(a, b) = 145a^2 + b^2 + 24ab$$
$$V = v(a, b) = 1740a^2 + 12b^2 + 290ab$$

Substituting the values of u and v in (2), the non–zero distinct integral values of x, y, z, R and w satisfying (1) are given by

$x = x(a, b) = 1885a^2 + 11b^2 + 290ab$

$y = y(a, b) = –1595a^2 – 13b^2 – 290ab$

$z=z(a, b)= 2(252300a^4 – 12b^4 +42050ab^3 – 290a^3b) + 1$

$w=w(a,b)=2(252300a^4–12b^4+42050ab^3 – 290a^3b) -1$

$R = R(a, b) = 145a^2 + b^2 + 24ab$.

Properties

1. $1595x[(a+1),1]+1885y[(a+1),1]+G_{42050a} \equiv 41 \pmod{2221}$.
2. $R(1,1)+40$ *is a Nasty number*.
3. $w(1,1)+z(1,1) \equiv 0 \pmod 2$
4. $13x[1,a(a+1)]+11y[1,a(a+1)]-580P_a - T_{13,36} =$ *Nasty number*.
5. $x[a(2a-1),1]+y[a(2a-1),1]-290(SOa)+$ *Jacobsthal – lucas number* $=0$.

2.4. Pattern IV

Rewrite (3) as $1 * v^2 = 65R^2 - u^2$ (11)

Write 1 as $1=(\sqrt{65}+1)(\sqrt{65}-1)/64$ (12)

Assume

$v = 65a^2 - b^2 = (\sqrt{65}\,a - b)(\sqrt{65}\,a + b)$ (13)

Using (12) and (13) in (11), it is written in factorizable from as,

$$\frac{(\sqrt{65}+1)(\sqrt{65}-1)}{64}(\sqrt{65}a+b)^2(\sqrt{65}a-b)$$

$$= (\sqrt{65}R - u)(\sqrt{65}R + u). \quad (14)$$

On equating the rational and irrational factors we get,

$$\left.\begin{aligned} R = R(a,b) &= \frac{1}{8}(65a^2+b^2+2ab) \\ u = u(a,b) &= \frac{1}{8}(65a^2+b^2+130ab) \end{aligned}\right\} \quad (15)$$

Replacing ‘a’ by 8A and ‘b’ by 8B in the above equations (13) and (15), we get

$R = R(A, B) = 1740A^2 + 12B^2 + 24AB$

$u = u(A, B) = 1740A^2 + 12B^2 + 3480AB$

$v = v(A, B) = 20880A^2 - 144B^2$.

On substituting the values of u and v in (2), the non–zero distinct integrals values of x, y, z, w and R satisfying (1) are given by

$x = x(A, B) = 22620A^2 - 132B^2 + 3480AB$

$y = y(A, B) = -19140A^2 + 156B^2 + 3480AB$

$z = z(A, B) = 2(36331200A^4 - 1728B^4 + 72662400A^3B - 501120AB^3) + 1$

$w = w(A, B) = 2(36331200A^4 - 1728B^4 + 72662400A^3B - 501120AB^3) - 1$

$R = R(A, B) = 1740A^2 + 12B^2 + 24AB$.

Properties

1. $\frac{1}{327}.[x(1,1)+y(1,1)] \equiv 0 \pmod 2$.
2. $19140x[(a+1),a]+22620y[(a+1),a]-1002240T_{4,a} \equiv 29 \pmod{5011200}$.
3. $156x[1,a(a+1)]+132[1,a(a+1)]-1002240(P_a) \equiv 29 \pmod{345600}$.
4. $19140x[2a^2+1,a]+22620y[2a^2+1,a]-1002240T_{4,a} - 435974400\,OH_a = 0$.
5. $\frac{1}{768}[x(1,1)-y(1,1)]$ *is a cubic* integer

2.5. Pattern V

Write (3) as $u^2 - R^2 = 64R^2 - v^2$

$(u+R)(u-R) = (8R+v)(8R-v)$ (16)

Which is expressed in the form of ratio as ,

$$\frac{u+R}{8R+v} = \frac{8R-v}{u-R} = \frac{A}{B}, \quad B \neq 0 \quad (17)$$

This is equivalent to the following two equations,

$-uA + R(8B+A) - VB = 0$

$uB + R(B-8A) - VA = 0$

on solving the above equations by the method of cross multiplication we get,

$u = u(A, B) = -A^2 - B^2 - 16AB$

$R = R(A, B) = -A^2 - B^2$

$v = v(A, B) = 8A^2 - 8B^2 - 2AB$

Substituting the values of u and v in (2), the non – zero distinct integral values of x, y, z, w and R satisfying (1) are given by,

$x = x(A, B) = 11A^2 - 11B^2 - 26AB$

$y = y(A, B) = -13A^2 + 13B^2 - 22AB$

$z = z(A, B) = 2[-12A^4 - 12B^4 + 60A^2B^2 - 286A^3B + 286AB^3] + 1$

$w = w(A, B) = 2[-12A^4 - 12B^4 + 60A^2B^2 - 286A^3B + 286AB^3] - 1$

$R = R(A, B) = -A^2 - B^2$.

Properties

1. $13x[2a^2-1,a]+11y[2a^2-1,a]-580SO_a = 0.$
2. $x(a+1,a+2)+26T_{4,a}+G_{50_a} \equiv 0 \pmod 2.$
3. $y(a,2a^2-1)-2496DF_a+22SO_a = 0.$
4. $13x[a(a+1),1]+11y[a(a+1),1]+580T_{4,a}+G_{290a}$ $= Carol\ number$
5. $x(1,1)+y(1,1)-T_{17,3}=0.$

III. CONCLUSION

It is worth to note that in (2), the transformations for z and w may be considered as z= 2u+v and w =2u –v. for this case, the values of x, y and R are the same as above where as the values of z and w changes for every pattern. To conclude one may consider biquadratic equations with multivariable's ($\geq$5) and search for their non-zero distinct integer solutions along with their corresponding properties.

REFERENCES

[1] Dickson, L.E., History of theory of numbers, Vol.11, Chelsea publishing company, New –York (1952).

[2] Mordell, L.J., Diophantine equation, Academic press, London (1969) Journal of Science and Research, Vol (3) Issue 12, 20-22 (December-14)

[3] Jayakumar. P, Sangeetha, K "Lattice points on the cone $x^2+9y^2=50z^2$" International Journal of Science and Research, Vol (3), Issue 12, 20-22 (December -2014).

[4] Jayakumar P, Kanaga Dhurga, C," On Quadratic Diopphantine equation $x^2+16y^2 = 20z^2$" Galois J. Maths, 1(1) (2014), 17-23.

[5] Jayakumar. P, Kanaga Dhurga. C, "Lattice points on the cone $x^2+9y^2=50z^2$" Diophantus J. Math, 3(2) (2014), 61-71.

[6] Jayakumar. P, Prabha. S "On Ternary Quadratic Diophantine equation $x^2+15y^2=14z^2$" Archimedes J. Math., 4(3) (2014), 159-164

[7] Jayakumar, P, Meena, J "Integral solutions of the Ternary Quadratic Diophantine equation: $x^2+7y^2 = 16z^2$" International Journal of Science and Technology, Vol.4, Issue 4, 1-4, Dec 2014.

[8] Jayakumar. P, Shankarakalidoss, G "Lattice points on Homogenous cone $x^2+9y^2=50z^2$" International journal of Science and Research, Vol (4), Issue 1, 2053-2055, January -2015.

[9] Jayakumar. P, Shankarakalidoss. G "Integral points on the Homogenous cone $x^2+y^2=10z^2$" International Journal for Scienctific Research and Development, Vol (2), Issue 11, 234-235, January -2015.

[10] Jayakumar.P, Prapha.S "Integral points on the cone $x^2+25y^2=17z^2$" International Journal of Science and Research Vol(4), Issue 1, 2050-2052, January-2015.

[11] Jayakumar.P, Prabha. S, "Laattice points on the cone $x^2+9y^2=26z2$ "International Journal of Science and Research Vol (4), Issue 1, 2050-2052, January -2015.

[12] Jayakumar. P, Sangeetha. K, "Integral solution of the Homogeneous Biquadratic Diophantine equation with six unknowns: $(x^3-y^3)z=(W^2-P^2)R^4$ "International Journal of Science and Research, Vol(3), Issue 12, 1021-1023 (December-2014).